T

Taylor Expansion (TE)

▸ Node-Dependent Kinematics, Multilayered Beam, Plate, and Shell Elements

Taylor, Geoffrey Ingram

Holm Altenbach[1] and Otto T. Bruhns[2]
[1]Lehrstuhl Technische Mechanik, Institut für Mechanik, Fakultät für Maschinenbau, Otto-von-Guericke-Universität Magdeburg, Magdeburg, Germany
[2]Institute of Mechanics, Ruhr-University Bochum, Bochum, Germany

Geoffrey Ingram Taylor (*March 7th, 1886 in St. John's Wood, England; †June 27th, 1975 in Cambridge, England, UK) was a physicist and mathematician with main contributions to fluid dynamics and wave theory.

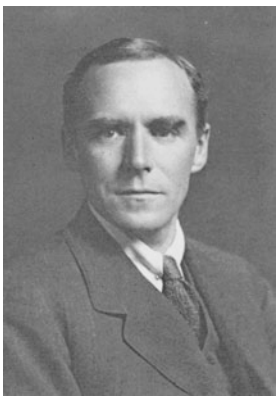

Geoffrey Ingram Taylor

Early Life and Education

His father, Edward Ingram Taylor, was an artist, and his mother, Margaret Boole, came from a family of mathematicians (his aunt was Alicia Boole Stott introducing the term polytope for a convex solid in four or more dimensions, and his grandfather was George Boole working in the field of algebraic logic). It was not surprising that the young Geoffrey Ingram Taylor was fascinated by natural sciences and mathematics after attending the Royal Institution Christmas Lectures. He entered the university college in 1899, and, after winning a scholarship, he moved to Trinity College, Cambridge, in 1905 (up to 1908). He started with studies in mathematics; later his focus was on physics. He won the Smith's prize with a work on shock waves and continued his career at Cambridge.

Professional Career

From 1910, he was a Fellow of Trinity College. His research focus was on turbulence and

H. Altenbach, A. Öchsner (eds.), *Encyclopedia of Continuum Mechanics*,
https://doi.org/10.1007/978-3-662-55771-6

accepted the position of a reader in the field of dynamical meteorology. In 1915, he got for his scientific results the Adams' prize. After World War I, he was appointed as a lecturer at Trinity College, and from 1923, he was nominated as a Royal Society Research Professor. From this time, his focus was on research. In 1952, he retired, but he continued research up to 1972.

Scientific Achievements

Many scientific achievements were made in fluid and solid mechanics, among them are results on the deformation of crystalline materials and on turbulent flow, where he introduced a new approach through a statistical study of velocity fluctuations. In 1934, Taylor, roughly contemporarily with Michael Polanyi and Egon Orowan, realized that the plastic deformation of ductile materials could be explained in terms of the theory of dislocations developed by Vito Volterra in 1905.

Honors

In 1919 he was elected as a Fellow of the Royal Society; in 1925, corresponding member of the Göttingen Academy of Sciences; in 1945, member of the National Academy of Sciences (USA); in 1955, member of the American Philosophical Society; and in 1956, member of the American Academy of Arts and Science. He was also a member of the Academy of Sciences (Soviet Union) and Royal Dutch Academy of Sciences. He was awarded by the following medals: 1933, Royal Medal; 1944, Copley Medal; 1954, Wilhelm Exner Medal; 1958, Timoshenko Medal; 1962, Franklin Medal; 1965, James Watt Medal; and 1969, Theodore von Kármán Medal. In 1972, he was the first recipient of the Theodore von Kármán Prize.

To his honor, the G. I. Taylor Medal of Society of Engineering was established in 1984.

Cross-References

- History of Plasticity
- Orowan, Egon
- Polanyi, Mihály (Michael)

Temperature and Entropy Introduction

- Truesdell's and Zhilin's Approaches: Derivation of Constitutive Equations

Temporal Discretization Methods; Temporal Integration Methods; Time Marching Methods

- Discrete Element and Particle Methods

Tension Field Theory

- Shear Web Theory

Tensor Integral Theorems

- Integration Formulas for Vectors and Tensors

Tensor Notation

- Beams, Plates, and Shells
- Continuum Mechanics Basics, Introduction and Notations

Tensor Random Fields in Continuum Mechanics

Anatoliy Malyarenko[1] and
Martin Ostoja-Starzewski[2]
[1]Division of Applied Mathematics, Mälardalen University, Västerås, Sweden
[2]Department of Mechanical Science and Engineering, Institute for Condensed Matter Theory, and Beckman Institute, University of Illinois at Urbana-Champaign, Urbana, IL, USA

Synonyms

Conductivity; Elasticity; Random fields; Stochastics; Uncertainty quantification

Definition

Let $(\Omega, \mathfrak{F}, \mathsf{P})$ be a probability space, i.e., Ω is a set, $\mathfrak{F}$ is a σ-field of subsets of Ω, and P is a probability measure on $\mathfrak{F}$. Let V be a finite-dimensional linear space consisting of tensors, and let $\mathfrak{B}(\mathsf{V})$ be the σ-field of Borel sets of V. A mapping $\mathsf{T}\colon \Omega \to \mathsf{V}$ is called a *random tensor* if it is measurable, i.e., for any Borel set B we have $\mathsf{T}^{-1}(B) \in \mathfrak{F}$. If V consists of scalars, the term *random variable* is then used instead of random scalar. A tensor *random field* on a real finite-dimensional affine space E is a function of two variables $\mathsf{T}\colon E \times \Omega \to \mathsf{V}$ such that for any $A \in E$ the function $\mathsf{T}(A, \omega)$ is a random tensor.

Why Tensor Random Fields in Continuum Mechanics?

In this article, by continuum physics we understand continuum mechanics and other classical (non-quantum, nonrelativistic) field theoretic models such as continuum thermomechanics (e.g., thermal conductivity, thermoelasticity, thermodiffusion), electromagnetism, and electromagnetic interactions in deformable media (e.g., piezoelectricity). Most tensor fields appearing in these models fall into two categories: fields of dependent quantities (displacement, velocity, deformation, rotation, stress,...) and constitutive responses (conductivity, stiffness, permeability,...). All of these fields are tensors of first or higher rank and, generally, of random nature (i.e., displaying spatially inhomogeneous, random character), indicating that the well-developed theory of scalar random fields has to be generalized to tensor random fields (TRFs).

In deterministic theories of continuum physics, we typically have an equation of the form

$$\mathscr{L}\mathbf{u} = \mathbf{f},$$

defined on some subset $\mathscr{D}$ of the d-dimensional affine Euclidean space $\mathbb{E}^d$, where $\mathscr{L}$ is a differential operator, f is a source or forcing function, and $\mathbf{u}$ is a solution field. This needs to be accompanied by appropriate boundary and/or initial conditions. [We use the symbolic $(\mathbf{u})$ or, equivalently, the subscript $(u_i \ldots)$ notations for tensors, as the need arises; also an overdot will mean the derivative with respect to time, d/dt.]

A field theory is stochastic if either the operator $\mathscr{L}$ is random, or there appears an apparent randomness of $\mathbf{u}$ due to an inherent nonlinearity of $\mathscr{L}$, or the forcing and/or boundary/initial conditions are random. While various combinations of these basic cases are possible, in this paper we focus on the first and second cases; the first case is typically due to the presence of a spatially random material microstructure, e.g., Ostoja-Starzewski (2008). For example, the coefficients of $\mathscr{L}(\omega)$, such as the elastic moduli C, form a tensor-valued random field, and the stochastic equation

$$\mathscr{L}(\omega)\,\mathbf{u} = \mathbf{f}$$

governs the response of a *random medium* $\mathscr{B}$. The second case is exemplified by solutions of the Navier–Stokes equation, which become so irregular in turbulence as to be treated in a stochastic way (Batchelor 1951; Monin and Yaglom 2007a,b; Frisch 1995). In both cases $\mathscr{B}$ is taken as

a set of all the realizations $\mathscr{B}(\omega)$ parameterized by sample events ω of the Ω space

$$\mathscr{B} = \{B(\omega) : \omega \in \Omega\}. \tag{1}$$

In principle, each of the realizations follows deterministic laws of classical mechanics; probability is introduced to deal with the set (1). The ensemble picture is termed stochastic continuum mechanics/physics. Formally speaking, we have a triple $(\Omega, \mathfrak{F}, \mathsf{P})$, where Ω is the space of elementary events, $\mathscr{F}$ is the σ-field, and P is the probability measure defined on it.

Going back to the first case, the stochastic continuum physics was necessary to replace the deterministic picture in problems of stochastic wave propagation: elastic, acoustic, and electromagnetic. A paradigm of wave propagation in random media is offered by the wave equation for a scalar field φ in a domain $\mathscr{D}$

$$\nabla^2 u = \frac{1}{c^2(\omega, \mathbf{x})} \frac{\partial^2 u}{\partial t^2}, \qquad \omega \in \Omega, \quad \mathbf{x} \in \mathscr{D}.$$

Here c is the wave speed in a linear elastic, isotropic medium, so that, effectively, $\mathscr{B}$ is described by a random field $\{c(\omega, \mathbf{x}) : \omega \in \Omega, \mathbf{x} \in \mathscr{D}\}$. Given that we simply have a Laplacian on the left-hand side, this model accounts for spatial randomness in mass density ρ only.

In order to also account for randomness in the elastic response, we could consider this partial differential equation

$$\nabla \cdot [C(\mathbf{x}, \omega) \nabla u] = \rho(\omega, \mathbf{x}) \frac{\partial^2 u}{\partial t^2}, \quad \omega \in \Omega, \quad \mathbf{x} \in \mathscr{D}. \tag{2}$$

Clearly, we now deal with two scalar random fields: C and ρ. This model's drawback, however, is the assumption of an inhomogeneous but locally isotropic second-rank stiffness tensor field $\mathbf{C} = C\mathbf{I}$ instead of $\mathbf{C}$ $(= C_{ij}\mathbf{e}_i \otimes \mathbf{e}_j)$ with full anisotropy. In fact, extensive studies on upscaling of various mechanical and physical phenomena have shown (Ostoja-Starzewski et al. 2016) that the local anisotropy goes hand in hand with randomness: as the smoothing scale (i.e., scale on which the continuum is set up) increases, the anisotropy and random fluctuations in material properties jointly go to zero. Thus, (2) should be replaced by

$$\nabla \cdot (\mathbf{C}(\mathbf{x}, \omega) \cdot \nabla u) = \frac{\partial^2 u}{\partial t^2}, \qquad \omega \in \Omega, \quad \mathbf{x} \in \mathscr{D}, \tag{3}$$

where $\mathbf{C}$ is the second-rank tensor random field.

The same arguments apply to a diffusion equation of, say, heat conduction

$$\nabla \cdot (\mathbf{K}(\mathbf{x}, \omega) \cdot \nabla T) = C_\epsilon(\omega, \mathbf{x}) \rho(\omega, \mathbf{x}) \frac{\partial T}{\partial t}, \quad \omega \in \Omega, \quad \mathbf{x} \in \mathscr{D},$$

in which $\mathbf{K}$ is the thermal conductivity tensor (again with anisotropy present), while the specific heat (in reference state) C_ϵ and mass density ρ jointly premultiply the first derivative of temperature T on the right-hand side.

This line of reasoning also applies to elliptic problems: consider Fig. 1 showing a planar Voronoi tessellation of $\mathbb{E}^2$ which serves as a planar geometric model of a polycrystal (although the same arguments apply in $\mathbb{E}^3$); each cell may be occupied by a differently oriented crystal, with all the crystals belonging to any specific crystal class. Examples of the latter include:

- transverse isotropy modelling, say, sedimentary rocks at long wavelengths;
- tetragonal modelling, say, wulfenite ($PbMoO_4$);
- trigonal modelling, say, dolomite ($CaMg(CO_3)_2$);
- orthotropic modelling, say, wood;
- triclinic modelling, say, microcline feldspar.

Thus, we need to be able to model fourth-rank tensor random fields, point-wise taking values in any crystal class. While the crystal orientations from grain to grain are random, they are not spatially independent of each other – the assignment of crystal properties over the tessellation is not a white noise. This is precisely where the two-point characterization of the random field of elasticity tensor is needed. While the simplest correlation structure to admit would be white noise,

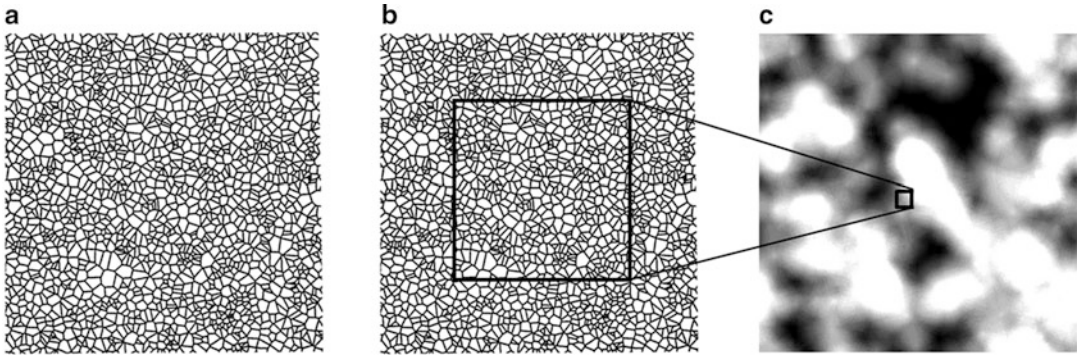

Fig. 1 (**a**) A realization of a Voronoi tesselation (or mosaic); (**b**) placing a mesoscale window leads, via upscaling, to a mesoscale random continuum approximation in (**c**)

a (much) more realistic model would account for any mathematically admissible correlation structures as dictated by the statistically wide-sense homogeneous and isotropic assumption. A specific correlation can then be fitted to physical measurements.

Note that it may also be of interest to work with a mesoscale random continuum approximation defined by placing a mesoscale window at any spatial position as shown in Fig. 1b. Clearly, the larger is the mesoscale window, the weaker are the random fluctuations in the mesoscale elasticity tensor: this is the trend to homogenize the material when upscaling from a statistical volume element (SVE) to a representative volume element (RVE). A simple paradigm of this upscaling, albeit only in terms of a scalar random field, is the opacity of a sheet of paper held against light: the further away is the sheet from our eyes, the more homogeneous it appears. Similarly, in the case of upscaling of elastic properties, on any finite scale, there is (almost surely) an anisotropy, and this anisotropy, with mesoscale increasing, tends to zero hand in hand with the fluctuations, and it is in the infinite mesoscale limit (i.e., RVE) that material isotropy is obtained as a consequence of the statistical isotropy.

Another motivation for development of TRF models is to have a realistic input of elasticity random fields into stochastic field equations such as stochastic partial differential equations (SPDE) and stochastic finite elements (SFE). The classical paradigm of SPDE can be written in terms of the anti-plane elastostatics (with $u = u_3$) as Eq. (2) with zero on the right-hand side. Such an equation is well justified for a piecewise-constant description of realizations of a random medium such as a multiphase composite made of locally isotropic grains. However, in the case of an elliptic boundary value problem set up on coarser (i.e., mesoscales) scales, having continuous realizations of properties, a second-rank tensor random field (TRF) of material properties would be much more appropriate, Fig. 1b. The field equation should then read as (3) where $\mathbf{C}$ is the second-rank tensor random field.

Moving to the in-plane or 3D elasticity, the starting point is the Navier equation of motion [written in symbolic and tensor notations]

$$\mu\nabla^2\mathbf{u} + (\lambda+\mu)\,\boldsymbol{\nabla}\,(\boldsymbol{\nabla}\cdot\mathbf{u}) = \rho\ddot{\mathbf{u}} \quad \text{or}$$
$$\mu u_{i,jj} + (\lambda+\mu)\,u_{j,ji} = \rho\ddot{u}_i. \tag{4}$$

Here $\mathbf{u}$ is the displacement field, λ and μ are two Lamé constants, and ρ is the mass density. This equation is often (e.g., in stochastic wave propagation) used as an Ansatz, typically with the pair (λ, μ) taken ad hoc as a "vector" random field with some simple correlation structure for both components. However, in order to properly introduce the smooth randomness in λ and μ, one has to go one step back in the derivation of (4) and write

$$\begin{aligned}&\mu\nabla^2\mathbf{u} + (\lambda+\mu)\,\boldsymbol{\nabla}\,(\boldsymbol{\nabla}\cdot\mathbf{u})\\ &+\boldsymbol{\nabla}\mu\left(\boldsymbol{\nabla}\mathbf{u} + (\boldsymbol{\nabla}\mathbf{u})^{\top}\right) + \boldsymbol{\nabla}\lambda\boldsymbol{\nabla}\cdot\mathbf{u} = \rho\ddot{\mathbf{u}}\\ &\text{or}\\ &\mu u_{i,jj} + (\lambda+\mu)\,u_{j,ji} + \mu_{,j}\left(u_{j,i} + u_{i,j}\right)\\ &+\lambda_{,i}\,u_{j,j} = \rho\ddot{u}_i.\end{aligned} \tag{5}$$

T

While two extra terms are now correctly present on the left-hand side, this equation still suffers from the drawback (just as (2)) of local isotropy so that, again by micromechanics upscaling arguments, it should be replaced by

$$\nabla\cdot\left(\mathsf{C}\nabla\cdot\mathbf{u}\right)^{\top}=\rho\ddot{\mathbf{u}}\quad\text{or}\quad\left(C_{ijkl}u_{(k,l)}\right),_{j}=\rho\ddot{u}_{i}. \tag{6}$$

Here C $(=C_{ijkl}\mathbf{e}_i\otimes\mathbf{e}_j\otimes\mathbf{e}_k\otimes\mathbf{e}_l)$, which, at any scale finitely larger than the microstructural scale, is almost surely anisotropic. Clearly, instead of (5) one should work with this SPDE (6) for $\mathbf{u}$.

The foregoing arguments outline the setting of TRFs: to obtain explicit representations of correlation functions of TRFs of ranks 1 through 4 so as to enable their simulation, subject to the restrictions imposed by the field equations dictated by physics. Briefly, in the case of dependent TRFs, we have, say, the linear momentum equation restricting the Cauchy stress or the angular momentum equation restricting the Cauchy and couple stresses. In the case of material property fields (elasticity, diffusion, permeability,...), there are conditions of positiveness of either the energy density or the entropy production, as the case may be. In turn, any such conditions lead to restrictions on the respective correlation functions.

Representations of Rank 1 and Rank 2 TRFs

We begin with V, a finite-dimensional real Hilbert space with norm $\|\cdot\|$. Then, we let $\mathsf{T}(\mathbf{x})$, $\mathbf{x}\in\mathbb{R}^3$ be a random field taking values in (a subset of) V: there is a probability space $(\Omega,\mathfrak{F},\mathsf{P})$, and T is a function of two variables

$$\mathsf{T}(\mathbf{x},\omega)\colon V\times\Omega\to V,$$

such that for any fixed $\mathbf{x}_0\in V$ the function $\mathsf{T}(\mathbf{x}_0,\omega)\colon\Omega\to V$ is measurable. We assume that $\mathsf{E}[\|\mathsf{T}(\mathbf{x})\|^2]<\infty$ and $\mathsf{T}(\mathbf{x})$ is mean-square continuous, i.e.,

$$\lim_{\|\mathbf{x}-\mathbf{x}_0\|\to 0}\mathsf{E}[\|\mathsf{T}(\mathbf{x})-\mathsf{T}(\mathbf{x}_0)\|^2]=0\quad\forall\mathbf{x}_0\in\mathbb{R}^3.$$

Next, we let $E(\mathbf{x})=\mathsf{E}[\mathsf{T}(\mathbf{x})]$ be the expectation of the field and let $B(\mathbf{x},\mathbf{y})=\mathsf{E}[\mathsf{T}(\mathbf{x})\otimes\mathsf{T}(\mathbf{y})]$ be the two-point correlation function of the random field $\mathsf{T}(\mathbf{x})$. The group $\mathbb{R}^3$ acts on itself by translations. Assume that the above functions are invariant with respect to this action, i.e., for all $\mathbf{x},\mathbf{y},\mathbf{z}\in\mathbb{R}^3$,

$$\begin{aligned}E(\mathbf{x}+\mathbf{z})&=E(\mathbf{x}),\\ B(\mathbf{x}+\mathbf{z},\mathbf{y}+\mathbf{z})&=B(\mathbf{x},\mathbf{y}).\end{aligned}\qquad\forall\mathbf{x},\mathbf{y},\mathbf{z}\in\mathbb{R}^3.$$

It follows that $E(\mathbf{x})=\mathbf{E}\in V$ is constant, while $B(\mathbf{x},\mathbf{y})\in V\otimes V$ depends only on the difference $\mathbf{x}-\mathbf{y}$.

Let $K=O(3)$ be the group of rotations and reflections in $\mathbb{R}^3$, and let (V,γ) be an orthogonal representation of K. Suppose that for all $k\in K$ and for all $\mathbf{x}\in\mathbb{R}^3$ we have

$$\begin{aligned}E(k\mathbf{x})&=\gamma(k)E(\mathbf{x}),\\ B(k\mathbf{x})&=\gamma(k)B(\mathbf{x})\gamma^{-1}(k).\end{aligned}$$

Our first objective is to find a general form for the expectation and two-point correlation function of such a field. We now consider two particular cases:

Rank 1 TRF

V has dimension 3, $\gamma(k)=k$. Then $E(\mathbf{x})=\mathbf{0}$ and

$$B_{ij}(\mathbf{x},\mathbf{y}):=\mathsf{E}\left\{[T_i(\mathbf{x})-\langle T_i(\mathbf{x})\rangle]\left[T_j(\mathbf{y})-\langle T_j(\mathbf{x})\rangle\right]\right\}$$

is represented in terms of two continuous functions $K_0,K_2\colon[0,\infty)\to\mathbb{R}$ with $K_2(0)=0$, such that

$$B_{ij}(\mathbf{x})=\delta_{ij}K_0(\|\mathbf{x}\|)+x_ix_jK_2(\|\mathbf{x}\|). \tag{7}$$

This representation has been known since the classical paper by Robertson (1940), where it was proved using the invariants. This line of research goes back to Sir Geoffrey Ingram Taylor (1935).

Rank 2 TRF

V is the space of all symmetric second rank tensors over $\mathbb{R}^3$, and the representation is $\gamma(k)\mathbf{T} = k\mathbf{T}k^{-1}$. Then $E_{ij}(\mathbf{x}) = C\delta_{ij}$ with $C \in \mathbb{R}$. Using the theory of invariants (e.g., Spencer 1971), Lomakin (1964) proved that

$$B_{ijlm}(\mathbf{x},\mathbf{y}) := \mathsf{E}\{\left[T_{ij}(\mathbf{x}) - \langle T_{ij}(\mathbf{x})\rangle\right] [T_{lm}(\mathbf{y}) - \langle T_{lm}(\mathbf{x})\rangle]\}$$

is represented in terms of five continuous functions $K_1, \ldots, K_5$: $[0,\infty) \to \mathbb{R}$ with $K_3(0) = K_4(0) = K_5(0) = 0$, such that

$$B_{ij\ell m}(\mathbf{x}) = \sum_{n=1}^{5} L^n_{ij\ell m}(\mathbf{x}) K_n(\|\mathbf{x}\|). \tag{8}$$

Here

$$\begin{aligned}
L^1_{ij\ell m}(\mathbf{x}) &= \delta_{ij}\delta_{\ell m},\\
L^2_{ij\ell m}(\mathbf{x}) &= \delta_{i\ell}\delta_{jm} + \delta_{im}\delta_{jl},\\
L^3_{ij\ell m}(\mathbf{x}) &= \frac{x_j x_\ell}{\|\mathbf{x}\|^2}\delta_{im} + \frac{x_i x_m}{\|\mathbf{x}\|^2}\delta_{j\ell}\\
&\quad + \frac{x_i x_\ell}{\|\mathbf{x}\|^2}\delta_{jm} + \frac{x_j x_m}{\|\mathbf{x}\|^2}\delta_{i\ell},\\
L^4_{ij\ell m}(\mathbf{x}) &= \frac{x_i x_j}{\|\mathbf{x}\|^2}\delta_{\ell m} + \frac{x_\ell x_m}{\|\mathbf{x}\|^2}\delta_{ij},\\
L^5_{ij\ell m}(\mathbf{x}) &= \frac{x_i x_j x_\ell x_m}{\|\mathbf{x}\|^4}.
\end{aligned} \tag{9}$$

Malyarenko and Ostoja-Starzewski (2014b) found five functions $M^1_{ij\ell m}(\mathbf{x})$ such that

$$\begin{aligned}
M^1_{ij\ell m}(\mathbf{x}) &= \frac{1}{3}L^1_{ij\ell m}(\mathbf{x}),\\
M^2_{ij\ell m}(\mathbf{x}) &= -\frac{1}{3\sqrt{5}}L^1_{ij\ell m}(\mathbf{x})\\
&\quad + \frac{1}{2\sqrt{5}}L^2_{ij\ell m}(\mathbf{x}),\\
M^3_{ij\ell m}(\mathbf{x}) &= -\frac{1}{3}L^1_{ij\ell m}(\mathbf{x}) + \frac{1}{2}L^4_{ij\ell m}(\mathbf{x}),\\
M^4_{ij\ell m}(\mathbf{x}) &= \frac{2\sqrt{2}}{3\sqrt{7}}L^1_{ij\ell m}(\mathbf{x}) - \frac{1}{\sqrt{14}}L^2_{ij\ell m}(\mathbf{x})\\
&\quad + \frac{3}{2\sqrt{14}}L^3_{ij\ell m}(\mathbf{x}) - \frac{\sqrt{2}}{\sqrt{7}}L^4_{ij\ell m}(\mathbf{x}),
\end{aligned}$$

$$\begin{aligned}
M^5_{ij\ell m}(\mathbf{x}) &= \frac{1}{2\sqrt{70}}L^1_{ij\ell m}(\mathbf{x}) + \frac{1}{2\sqrt{70}}L^2_{ij\ell m}(\mathbf{x})\\
&\quad - \frac{\sqrt{5}}{2\sqrt{14}}L^3_{ij\ell m}(\mathbf{x})\\
&\quad - \frac{\sqrt{5}}{2\sqrt{14}}L^4_{ij\ell m}(\mathbf{x}) + \frac{\sqrt{35}}{2\sqrt{2}}L^5_{ij\ell m}(\mathbf{x}).
\end{aligned} \tag{10}$$

and the representation

$$B_{ij\ell m}(\mathbf{x}) = \sum_{n=1}^{5} M^n_{ij\ell m}(\mathbf{x}) K_n(\|\mathbf{x}\|). \tag{11}$$

It has been proved in the aforementioned reference that the representation (11) is equivalent to (8), according to the transformation (10).

Note: On the one hand, Lomakin's functions (9) are simpler than functions (10). On the other hand, (9) lead to spectral expansions (Malyarenko and Ostoja-Starzewski 2016) of tensor-valued homogeneous and isotropic random fields similar to those in Yaglom (1957).

Note: Given that T has diagonal and off-diagonal components, there are five special cases of B_{ijkl} which shed light on the physical meaning of K_n's:

1. $\mathsf{E}[T_{ij}(\mathbf{0})T_{kl}(\mathbf{x})]|_{i=j=k=l}$; i.e., auto-correlations of diagonal terms:

$$\mathsf{E}[T_{11}(\mathbf{0})T_{11}(\mathbf{x})] = K_1 + 2K_2 + 2x_1^2K_3 + 4x_1^2K_4 + x_1^4K_5$$

and then $\mathsf{E}[T_{22}(\mathbf{0})T_{22}(\mathbf{x})]$ and $\mathsf{E}[T_{33}(\mathbf{0})T_{33}(\mathbf{x})]$ by cyclic permutations $1 \to 2 \to 3$.

2. $\mathsf{E}[T_{ij}(\mathbf{0})T_{kl}(\mathbf{x})]|_{i=j\neq k=l}$; i.e., cross-correlations of diagonal terms:

$$\mathsf{E}[T_{11}(\mathbf{0})T_{22}(\mathbf{x})] = K_1 + \left(x_2^2 + x_1^2\right)K_3 + x_2^2x_1^2K_5$$

and then $\mathsf{E}[T_{22}(\mathbf{0})T_{33}(\mathbf{x})]$ and $\mathsf{E}[T_{33}(\mathbf{0})T_{11}(\mathbf{x})]$ by cyclic permutations $1 \to 2 \to 3$.

3. $\mathsf{E}[T_{ij}(\mathbf{0})T_{kl}(\mathbf{x})]|_{i=k\neq j=l}$; i.e., auto-correlations of off-diagonal terms:

$$\mathsf{E}[T_{12}(\mathbf{0})T_{12}(\mathbf{x})] = K_2 + \left(x_1^2 + x_2^2\right) K_4 + x_1^2 x_2^2 K_5$$

and then $\mathsf{E}[T_{23}(\mathbf{0})T_{23}(\mathbf{x})]$ and $\mathsf{E}[T_{31}(\mathbf{0})T_{31}(\mathbf{x})]$ by cyclic permutations $1 \to 2 \to 3$.

4. $\mathsf{E}[T_{ij}(\mathbf{0})T_{kl}(\mathbf{x})]|_{j\neq i=k\neq l\neq j}$; i.e., cross-correlations of off-diagonal terms:

$$\mathsf{E}[T_{12}(\mathbf{0})T_{13}(\mathbf{x})] = x_2 x_3 K_4 + x_1^2 x_2 x_3 K_5$$

and then $\mathsf{E}[T_{13}(\mathbf{0})T_{32}(\mathbf{x})]$ and $\mathsf{E}[T_{32}(\mathbf{0})T_{12}(\mathbf{x})]$ by cyclic permutations $1 \to 2 \to 3$.

5. $\mathsf{E}[T_{ij}(\mathbf{0})T_{kl}(\mathbf{x})]|_{i=j=k\neq l\neq j}$; i.e., cross-correlations of diagonal with off-diagonal terms, such as

$$\mathsf{E}[T_{11}(\mathbf{0})T_{12}(\mathbf{x})] = x_1 x_2 \left(K_3 + 2K_4\right) + x_1 x_2^3 K_5$$

and

$$\mathsf{E}[T_{12}(\mathbf{0})T_{13}(\mathbf{x})] = x_2 x_3 K_3 + x_1^2 x_2 x_3 K_5$$

and the other ones by cyclic permutations $1 \to 2 \to 3$.

In principle, we can determine these five correlations for a specific physical situation. For example, when T is the anti-plane elasticity tensor for a given resolution (or mesoscale), we can use micromechanics or experiments (Ostoja-Starzewski 2008; Sena et al. 2013) and then determine the best fits of K_n $(n = 1, \ldots, 5)$ coefficients.

Spectral Expansions of Homogeneous and Isotropic TRFs

In a line of research different from that introduced above, Yaglom (1957) proved that the correlation tensor (2) has the following spectral expansion:

$$R_{ij}(\boldsymbol{\xi}) = \int_0^\infty \left[\frac{j_1(\lambda\rho)}{\lambda\rho}\delta_{ij} - j_2(\lambda\rho)\frac{\xi_i\xi_j}{\rho^2}\right] \mathrm{d}\Phi_1(\lambda) + \int_0^\infty \left[\left(j_0(\lambda\rho) - \frac{j_1(\lambda\rho)}{\lambda\rho}\right)\delta_{ij} + j_2(\lambda\rho)\frac{\xi_i\xi_j}{\rho^2}\right] \mathrm{d}\Phi_2(\lambda), \tag{12}$$

where Φ_1 and Φ_2 are two finite measures on $[0, \infty)$ with $\Phi_1(\{0\}) = \Phi_2(\{0\})$ and where $j_i(t)$ are spherical Bessel functions. In particular, Robertson's functions $A(\rho)$ and $B(\rho)$ [i.e., our K_0 and K_2 in (7)] have the form

$$A(\rho) = \tfrac{1}{\rho^2}\left(\int_0^\infty j_2(\lambda\rho)\,\mathrm{d}\Phi_2(\lambda) - \int_0^\infty j_1(\lambda\rho)\,\mathrm{d}\Phi_1(\lambda)\right),$$
$$B(\rho) = \int_0^\infty \tfrac{j_1(\lambda\rho)}{\lambda\rho}\,\mathrm{d}\Phi_1(\lambda) + \int_0^\infty \left(j_0(\lambda\rho) - \tfrac{j_1(\lambda\rho)}{\lambda\rho}\right)\mathrm{d}\Phi_2(\lambda).$$

In Malyarenko and Ostoja-Starzewski (2016) we have established spectral expansions of homogeneous and isotropic random fields taking values in the three -dimensional Euclidean space $\mathbb{R}^3$ and in the space $\mathsf{S}^2(\mathbb{R}^3)$ of symmetric rank 2 tensors over $\mathbb{R}^3$, whereby we found a link between the theory of random fields and the theory of finite-dimensional convex compacta.

The Spectral Expansion of the Elasticity Random Field

Here we consider planar classical elasticity. Let $E = \mathbb{R}^2$ be a *two*-dimensional Euclidean space with an inner product $(\cdot, \cdot)$ (the space domain). The Hooke law in the theory of elasticity says that $\sigma(\mathbf{x}) = \mathsf{H}(\mathbf{x})\varepsilon(\mathbf{x})$, where $\sigma(\mathbf{x})$ is the stress tensor of a deformable body and $\varepsilon(\mathbf{x})$ its strain tensor and where $\mathsf{H}(\mathbf{x})$ is a symmetric linear operator on the space $\mathsf{S}^2(E)$ of the symmetric rank 2 tensors over E called the elasticity (or stiffness) tensor. It is taken as a random field: there is a probability space $(\Omega, \mathfrak{F}, \mathsf{P})$, and H is a function of two variables

$$\mathsf{H}(\mathbf{x}, \omega)\colon E \times \Omega \to \mathsf{S}^2(\mathsf{S}^2(E)),$$

such that for any fixed $\mathbf{x}_0 \in E$, the function $\mathsf{H}(\mathbf{x}_0, \omega)\colon \Omega \to \mathsf{S}^2(\mathsf{S}^2(E))$ is measurable. In Malyarenko and Ostoja-Starzewski (2014a) we have reported two results:

1. The expected value of the elasticity random field $\mathsf{H}(\mathbf{x})$ is

$$E_{ij\ell m}(\mathbf{x}) = C_1\delta_{ij}\delta_{\ell m} + C_2(\delta_{i\ell}\delta_{jm} + \delta_{im}\delta_{j\ell}),$$
$$C_1, C_2 \in \mathbf{R},$$

where C_1 and C_2 are recognized as the Lamé constants λ and μ, respectively. The correlation tensor of the above field has the form

$$R_{i\cdots m'}(\rho, \varphi_{\mathbf{r}}) = \sum_{t=1}^{2}\int_0^\infty \sum_{n=0}^{4} \mathrm{i}^{2n} J_{2n}(\lambda\rho) \sum_{q=1}^{m_{2n}} N_{2n,q,t}(\lambda) M^{2n,q}_{i\cdots m'}(\varphi_{\mathbf{r}})\, \mathrm{d}\Phi_t(\lambda),$$

where Φ_1 and Φ_2 are two finite measures on $[0, \infty)$ satisfying the condition

$$\Phi_1(\{0\}) \geq 2\Phi_2(\{0\}).$$

Here $J_{2n}(\lambda\rho)$ are the Bessel functions of the first kind of order $2n$, $m_0 = 5$; $m_2 = m_4 = 3$, $m_6 = M_8 = 1$, and $N_{2n,q,t}(\lambda)$ $(0 \leq n \leq 4,\ 1 \leq q \leq m_{2n},\ t = 1, 2)$ are the functions given in Table 2 in Malyarenko and Ostoja-Starzewski (2014a); and $M^{2n,q}_{i\cdots m'}(\varphi_{\mathbf{r}})$ are tensor-valued functions similar to (10).

2. The elasticity random field $\mathsf{H}(\mathbf{x})$ has the spectral expansion

$$H_{ij\ell m}(\rho, \varphi_{\mathbf{r}}) = C_1\delta_{ij}\delta_{\ell m} + C_2(\delta_{i\ell}\delta_{jm} + \delta_{im}\delta_{j\ell})$$
$$+ \sum_{n=0}^{4}\sum_{q=1}^{m_{2n}}\sum_{s=0}^{\infty}\sum_{t=1}^{2}\left(\int_0^\infty \sqrt{N_{2n,q,t}(\lambda)}\, J_s(\lambda\rho)\sin(2s\varphi_{\mathbf{r}})\, \mathrm{d}Z^{nqst-}_{ij\ell m}(\lambda)\right.$$
$$\left. + \int_0^\infty \sqrt{N_{2n,q,t}(\lambda)}\, J_s(\lambda\rho)\cos(2s\varphi_{\mathbf{r}})\, \mathrm{d}Z^{nqst+}_{ij\ell m}(\lambda)\right),$$

where the centered scattered random measures $Z^{nqst\pm}_{ij\ell m}$ are defined by

$$Z^{nqst\pm}_{ij\ell m}(A) = \sum_{(i'j'\ell'm'n'q's'\pm')\leq(ij\ell mnqs\pm)} (\mathbf{L}_t)^{i'j'\ell'm'n'q's'\pm'}_{ij\ell mnqs\pm} W^{nqst\pm}_{ij\ell m}(A),$$

and where $W_{ij\ell m}^{nqst\pm}$ is the sequence of *uncorrelated* scattered random measures with Φ_t as their control measures, i.e.,

$$\mathsf{E}[W_{ij\ell m}^{nqst\pm}(A)W_{ij\ell m}^{nqst\pm}(B)] = \Phi_t(A \cap B).$$

TRFs Dependent Fields

Having explicit representations of correlation functions of TRFs, one can turn to applications in specific physical settings, assuming they are wide-sense homogeneous and isotropic and possess generally anisotropic realizations. Two basic research directions are (i) material property fields such as conductivity or elasticity and (ii) dependent fields such displacement, velocity, stress, strain, rotation, etc. With reference to physics and the discussion in the first section, the direction (i) requires imposition of a positive definiteness property on tensors of second or fourth rank. Another approach to the construction of random elasticity tensor fields, with special attention to information-theory methodology, is given in Guilleminot and Soize (2019).

The direction (ii) requires imposition of a governing equation relevant for a particular physics, such as first done in terms of a zero-divergence condition for incompressible turbulent fluids (Batchelor 1951). That line of research was continued in Lomakin (1964), Shermergor (1971) and Ostoja-Starzewski et al. (2015). Working within the constraints of small strains, attention is given to anti-plane elasticity, thermal conductivity, classical elasticity, and micropolar elasticity, all in quasi-static setting albeit without making any specific statements about the Fourier and Hooke laws. The field equations (such as linear and angular momentum balances and strain-displacement relations) lead to consequences for the respective dependent fields involved. In effect, these consequences are restrictions on the admissible forms of the correlation functions describing the TRFs. The derivations have not involved the Fourier and Hooke laws, so that those restrictions may also apply to other constitutive behaviors providing they involve small gradients and strains.

Cross-References

- Elastic Waves in Microstructured Solids
- Micromechanics
- Non-Gaussian Random Fields in Multiscale Mechanics of Heterogeneous Materials
- Random Fields with Fractal and Hurst Effects in Mechanics
- Scaling Function in Mechanics of Random Materials

Acknowledgements The work of the second author was supported by the National Science Foundation under Grant Number (Grant CMMI-1462749). Any opinions, findings, and conclusions or recommendations expressed in this material are those of the author (MO-S) and do not necessarily reflect the views of the National Science Foundation.

References

Batchelor GK (1951) Note on a class of solutions of the Navier–Stokes equations representing steady rotationally-symmetric flow. Q J Mech Appl Math 4:29–41

Frisch U (1995) Turbulence. The legacy of A. N. Kolmogorov. Cambridge University Press, Cambridge

Guilleminot J, Soize C (2019) Non-Gaussian random fields in multiscale mechanics of heterogeneous materials. In: Encyclopedia of continuum mechanics, 1st edn. Springer, Berlin/Heidelberg, p 10

Lomakin VA (1964) Statistical description of the stressed state of a body under deformation. Dokl Akad Nauk SSSR 155:1274–1277

Malyarenko A, Ostoja-Starzewski M (2014a) The spectral expansion of the elasticity random field. AIP Conf Proc 1637(1):647–655

Malyarenko A, Ostoja-Starzewski M (2014b) Statistically isotropic tensor random fields: correlation structures. Math Mech Complex Syst 2(2):209–231

Malyarenko A, Ostoja-Starzewski M (2016) Spectral expansions of homogeneous and isotropic tensor-valued random fields. Z Angew Math Phys 67(3):Article 59, 20

Monin AS, Yaglom AM (2007a) Statistical fluid mechanics: mechanics of turbulence, vol I. Dover Publications, Inc., Mineola. Translated from the 1965 Russian original, Edited and with a preface by John L. Lumley,

English edition updated, augmented and revised by the authors, Reprinted from the 1971 edition
Monin AS, Yaglom AM (2007b) Statistical fluid mechanics: mechanics of turbulence, vol II. Dover Publications, Inc., Mineola. Translated from the 1965 Russian original, Edited and with a preface by John L. Lumley, English edition updated, augmented and revised by the authors, Reprinted from the 1975 edition
Ostoja-Starzewski M (2008) Microstructural randomness and scaling in mechanics of materials. CRC series: modern mechanics and mathematics. Chapman & Hall/CRC, Boca Raton
Ostoja-Starzewski M, Shen L, Malyarenko A (2015) Tensor random fields in conductivity and classical or microcontinuum theories. Math Mech Solids 20(4):418–432
Ostoja-Starzewski M, Kale S, Karimi P, Malyarenko A, Raghavan B, Ranganathan S, Zhang J (2016) Scaling to RVE in random media. In: Bordas SP, Balint DS (eds) Advances in applied mechanics, vol 49. Elsevier BV, pp 111–211
Robertson HP (1940) The invariant theory of isotropic turbulence. Proc Camb Philos Soc 36:209–223
Sena MP, Ostoja-Starzewski M, Costa L (2013) Stiffness tensor random fields through upscaling of planar random materials. Probab Eng Mech 34:131–156
Shermergor T (1971) Relations between the components of the correlation functions of an elastic field. J Appl Math Mech 35(3):392–397
Spencer A (1971) Part III – theory of invariants. In: Eringen AC (ed) Continuum physics. Volume 1 – mathematics. Academic Press, pp 239–353
Taylor GI (1935) Statistical theory of turbulence. Proc R Soc Lond A Math Phys Eng Sci 151(873):421–444
Yaglom AM (1957) Certain types of random fields in n-dimensional space similar to stationary stochastic processes. Teor Veroyatnost i Primenen 2:292–338

Tensors

Leonid P. Lebedev[1] and Michael J. Cloud[2]
[1]Universidad Nacional de Colombia, Bogotá, D.C., Colombia
[2]Department of Electrical and Computer Engineering, Lawrence Technological University, Southfield, MI, USA

Synonyms

Coordinate-independent quantities; Dyadics; Elements of tensor spaces

Definition

Tensor analysis is a branch of mathematics concerned with entities that remain invariant under change of basis, their properties, and the transformation laws satisfied by their components under change of basis. The entities are called tensors; they include scalar quantities as zero-order tensors, vector quantities as first-order tensors, linear transformations on n-dimensional vector spaces as second-order tensors, and various other quantities important in mechanics.

Originating in mechanics with the vectorial laws for force resultants (Simon Stevin, 1548–1620), tensor analysis was extended to the elements of general linear spaces and their linear transformations. The introduction of the inertia tensor for a solid and of the Cauchy stress and strain tensors $\boldsymbol{\sigma}$ and $\boldsymbol{\epsilon}$ in elasticity, which turned out to be of the same mathematical nature as linear transformations, prompted consideration of nth-order tensors. In particular, the elastic properties of linearly elastic bodies are described by a fourth-order tensor.

The tensor concept finds extensive application in many areas of natural science including mechanics, electromagnetism, relativity, and crystallography.

Second-Order Tensors

This article features tensors of order two, although the method of constructing tensors of higher order is analogous. Just as vectors are objective quantities independent of the basis, so are the linear mappings (transformations, operators) of the vectors, provided the image of any vector $\mathbf{x}$ is required to be a vector $\mathbf{y}$ that is independent of the basis as well. Linear algebra uses column vectors containing the components of vectors and square matrices to represent linear transformations; the result of a transformation is given by the product of a matrix and a column vector. If one changes the basis for representing $\mathbf{x}$, the matrix is also subject to certain transformation rules to

guarantee that the same $\mathbf{y}$ is produced. The set of second-order tensors introduced below is such that, like vectors, they can be represented in terms of components relative to a basis in the initial space of $\mathbf{x}$. As in the article on vectors, the discussion is mostly restricted to $\mathbb{R}^3$. In this case the components of a linear transformation can be exhibited in a 3×3 matrix. Moreover, if one adheres to a canonical basis, the tensorial transformation rules again manifest as matrix multiplication (the matrix of tensor components premultiplying a column vector). Linear transformations are quite important in physics but are not the only objects describable by second-order tensors: many quantities of mechanics and physics in general, by their nature being invariant quantities specified by 3×3 matrices, are also second-order tensors. Examples are the stress and strain tensors specifying the elastic states of a deformable body and the inertia tensor for a rigid body. The process of introducing second-order tensors (or second-rank tensors, as they are sometimes called) starts with the dyad concept.

Dyads

It bears emphasis that many statements pertaining to tensors in $\mathbb{R}^3$ can be extended to tensors in $\mathbb{R}^n$ for any positive integer n. Still, the present discussion will use $\mathbb{R}^3$ as the context. For vectors $\mathbf{a}, \mathbf{b} \in \mathbb{R}^3$, the *tensor product*

$$\mathbf{a} \otimes \mathbf{b}$$

is known as a *dyad*. The symbol $\otimes$ will be retained in this article but is often omitted for brevity (yielding simply $\mathbf{ab}$). If $\mathbf{a} \neq \mathbf{b}$ then

$$\mathbf{a} \otimes \mathbf{b} \neq \mathbf{b} \otimes \mathbf{a}\,;$$

i.e., the tensor product is not commutative. Using the set of all possible dyads, rules for actions with dyads are introduced in such a way that a linear space is produced. This space, denoted as $\mathbb{R}^3 \otimes \mathbb{R}^3$, has elements called second-order tensors. The rules are summarized next.

The concept of linear space requires notions of addition and multiplication of elements by scalars. Here scalars will be denoted by Greek letters α, β, etc. The product of a dyad $\mathbf{a} \otimes \mathbf{b}$ and a scalar α, written as $\alpha\mathbf{a} \otimes \mathbf{b}$, is posited to satisfy

$$(\alpha + \beta)\mathbf{a} \otimes \mathbf{b} = \alpha\mathbf{a} \otimes \mathbf{b} + \beta\mathbf{a} \otimes \mathbf{b}, \tag{1}$$

$$0\mathbf{a} \otimes \mathbf{b} = \mathbf{0} \otimes \mathbf{b} = \mathbf{a} \otimes \mathbf{0} = \mathbf{0} \otimes \mathbf{0}, \tag{2}$$

where $\mathbf{0}$ is the zero vector of $\mathbb{R}^3$ and $\mathbf{0} \otimes \mathbf{0}$ is the *zero dyad*. For the dyad product, we also require that

$$(\mathbf{a} + \mathbf{b}) \otimes \mathbf{c} = \mathbf{a} \otimes \mathbf{c} + \mathbf{b} \otimes \mathbf{c}, \tag{3}$$

$$\mathbf{a} \otimes (\mathbf{b} + \mathbf{c}) = \mathbf{a} \otimes \mathbf{b} + \mathbf{a} \otimes \mathbf{c}. \tag{4}$$

Finally, to establish $\mathbb{R}^3 \otimes \mathbb{R}^3$ as a linear space, linear combinations of dyads such as $\alpha\mathbf{a} \otimes \mathbf{b} + \beta\mathbf{c} \otimes \mathbf{d}$ must be considered. These entail the additional properties

$$\alpha\mathbf{a} \otimes \mathbf{b} + \beta\mathbf{c} \otimes \mathbf{d} = \beta\mathbf{c} \otimes \mathbf{d} + \alpha\mathbf{a} \otimes \mathbf{b}, \tag{5}$$

$$\alpha(\mathbf{a} \otimes \mathbf{b} + \mathbf{c} \otimes \mathbf{d}) = \alpha\mathbf{a} \otimes \mathbf{b} + \alpha\mathbf{c} \otimes \mathbf{d}, \tag{6}$$

$$(\alpha + \beta)(\mathbf{a} \otimes \mathbf{b} + \mathbf{c} \otimes \mathbf{d}) = \alpha(\mathbf{a} \otimes \mathbf{b} + \mathbf{c} \otimes \mathbf{d}) + \beta(\mathbf{a} \otimes \mathbf{b} + \mathbf{c} \otimes \mathbf{d}). \tag{7}$$

The space $\mathbb{R}^3 \otimes \mathbb{R}^3$ is required to contain all linear combinations of dyads. It is easily shown that the set of all dyads having the above properties and containing the zero dyad constitutes a linear space. As mentioned above, the elements of $\mathbb{R}^3 \otimes \mathbb{R}^3$ are called second-order tensors. In this article they will be mostly denoted by bold uppercase letters ($\mathbf{A}$, $\mathbf{B}$, and so on); however, some tensors (such as the strain and stress tensors of elasticity) are denoted otherwise.

Components of a Second-Order Tensor

Let $\mathbf{e}_i$ be a basis of $\mathbb{R}^3$ and let $\mathbf{e}^j$ be its reciprocal basis. Using the above properties of the dyads and spans of the vectors, the dyad $\mathbf{a} \otimes \mathbf{b}$ can be spanned in four forms:

$$\mathbf{a} \otimes \mathbf{b} = a^i\, b^j\, \mathbf{e}_i \otimes \mathbf{e}_j = a_i\, b_j\, \mathbf{e}^i \otimes \mathbf{e}^j = a^i\, b_j\, \mathbf{e}_i \otimes \mathbf{e}^j = a_i\, b^j\, \mathbf{e}^i \otimes \mathbf{e}_j\,. \tag{8}$$

As this can be done for any dyad, any second-order tensor is representable through nine dyads of each of the four sets

$$\mathbf{e}_i \otimes \mathbf{e}_j, \qquad \mathbf{e}^i \otimes \mathbf{e}^j, \qquad \mathbf{e}_i \otimes \mathbf{e}^j, \qquad \mathbf{e}^i \otimes \mathbf{e}_j,$$

which constitute bases of the space of second-order tensors. Any second-order tensor $\mathbf{A}$ can be represented in four ways,

$$\begin{aligned}\mathbf{A} &= a^{ij}\,\mathbf{e}_i \otimes \mathbf{e}_j = a_{ij}\,\mathbf{e}^i \otimes \mathbf{e}^j \\ &= a^{i\cdot}_{\cdot j}\,\mathbf{e}_i \otimes \mathbf{e}^j = a_{i\cdot}^{\cdot j}\,\mathbf{e}^i \otimes \mathbf{e}_j, \end{aligned} \tag{9}$$

with uniquely defined components. The components a^{ij} are said to be *contravariant*, the components a_{ij} are *covariant*, and the remaining components $a^{i\cdot}_{\cdot j}$ and $a_{i\cdot}^{\cdot j}$ are *mixed*. (The position-holding dots in the mixed components are included to clarify the order of the indices when one index is a superscript and the other is a subscript.) It is clear that the components of $\mathbf{A}$ relative to a given basis can fill a 3×3 matrix. This matrix, denoted $[\mathbf{A}]$, will be called the *representative matrix* of $\mathbf{A}$ in the given basis. Although there are infinitely many representative matrices for $\mathbf{A}$, the representative matrix relative to a given, fixed basis is unique.

The various components of $\mathbf{A}$ are interrelated. The chain of equations

$$\begin{aligned}\mathbf{A} &= a^{ij}\,\mathbf{e}_i \otimes \mathbf{e}_j \\ &= a^{ij}\,g_{ik}\,\mathbf{e}^k \otimes \mathbf{e}_j = a_{k\cdot}^{\cdot j}\,\mathbf{e}^k \otimes \mathbf{e}_j \\ &= a^{ij}\,g_{ik}\,\mathbf{e}^k \otimes g_{mj}\,\mathbf{e}^m = a_{km}\,\mathbf{e}^k \otimes \mathbf{e}^m \\ &= a^{ij}\,\mathbf{e}_i \otimes g_{mj}\,\mathbf{e}^m = a^{i\cdot}_{\cdot m}\,\mathbf{e}_i \otimes \mathbf{e}^m \end{aligned}$$

implies that

$$\begin{aligned} a_{k\cdot}^{\cdot j} &= a^{ij}\,g_{ik}, \\ a_{km} &= a^{ij}\,g_{ik}\,g_{jm}, \\ a^{i\cdot}_{\cdot m} &= a^{ij}\,g_{jm}. \end{aligned}$$

Similarly, $a^{ij} = a_{km}\,g^{ki}\,g^{mj}$, etc. This procedure is called the *raising and lowering* of indices.

Dot Product of a Second-Order Tensor by a Vector

The dot product is a key operation used to relate tensors and vectors with the well-known actions in vector spaces that involve matrix operations. The dot products of a dyad $\mathbf{a} \otimes \mathbf{b}$ with a vector $\mathbf{x}$ are defined as follows:

$$(\mathbf{a} \otimes \mathbf{b}) \cdot \mathbf{x} = \mathbf{a}(\mathbf{b} \cdot \mathbf{x}), \tag{10}$$

$$\mathbf{x} \cdot (\mathbf{a} \otimes \mathbf{b}) = (\mathbf{x} \cdot \mathbf{a})\mathbf{b}. \tag{11}$$

So $\mathbf{x}$ is dotted with the nearest vector of the dyad. Extension to linear combinations of dyads is straightforward:

$$\left(\sum_i c_i \mathbf{a}_i \otimes \mathbf{b}_i\right) \cdot \mathbf{x} = \sum_i c_i (\mathbf{b}_i \cdot \mathbf{x})\mathbf{a}_i,$$

$$\mathbf{x} \cdot \left(\sum_i c_i \mathbf{a}_i \otimes \mathbf{b}_i\right) = \sum_i c_i (\mathbf{x} \cdot \mathbf{a}_i)\mathbf{b}_i.$$

This rule permits dot multiplication of a second-order tensor $\mathbf{A} = a^{ij}\mathbf{e}_i \otimes \mathbf{e}_j$ with a vector $\mathbf{x} = x^i\mathbf{e}_i$ in various bases. The product $\mathbf{A} \cdot \mathbf{x}$ can take several forms,

$$\begin{aligned}\mathbf{A} \cdot \mathbf{x} &= a^{ij}\,\mathbf{e}_i \otimes \mathbf{e}_j \cdot x_k\,\mathbf{e}^k = a^{ij}\,x_k\,(\mathbf{e}_j \cdot \mathbf{e}^k)\,\mathbf{e}_i \\ &= a^{ij}\,x_k\,\delta^k_j\,\mathbf{e}_i = a^{ij}\,x_j\,\mathbf{e}_i \\ &= a_{ij}\,\mathbf{e}^i \otimes \mathbf{e}^j \cdot x^k\,\mathbf{e}_k = a_{ij}\,x^k\,\mathbf{e}^i(\mathbf{e}^j \cdot \mathbf{e}_k) \\ &= a_{ij}\,x^k\,\delta^j_k\,\mathbf{e}^i = a_{ij}\,x^j\,\mathbf{e}^i \\ &= a^{ij}\,\mathbf{e}_i \otimes \mathbf{e}_j \cdot x^k\,\mathbf{e}_k = a^{ij}\,x^k\,\mathbf{e}_i\,(\mathbf{e}_j \cdot \mathbf{e}_k) \\ &= a^{ij}\,x^k\,g_{jk}\,\mathbf{e}_i = a^{i\cdot}_{\cdot k}\,x^k\,\mathbf{e}_i \\ &= a_{ij}\,\mathbf{e}^i \otimes \mathbf{e}^j \cdot x_k\,\mathbf{e}^k = a_{ij}\,x_k\,\mathbf{e}^i(\mathbf{e}^j \cdot \mathbf{e}^k) \\ &= a_{ij}\,x_k\,g^{jk}\,\mathbf{e}^i = a_{i\cdot}^{\cdot k}\,x_k\,\mathbf{e}^i, \end{aligned}$$

and there are analogous expressions for $\mathbf{x} \cdot \mathbf{A}$.

With a canonical basis, these sorts of expressions appear somewhat simpler. Let $\mathbf{B} = b_{ij}\,\mathbf{i}_i \otimes \mathbf{i}_j$ and $\mathbf{y} = y_k\,\mathbf{i}_k$ where $\mathbf{i}_j$ is a canonical basis of $\mathbb{R}^3$. Recalling that for canonical bases the summation convention applies to repeated subscripts, one has

$$\mathbf{B}\cdot\mathbf{y} = b_{ij}\,\mathbf{i}_i\otimes\mathbf{i}_j\cdot y_k\,\mathbf{i}_k = b_{ij}\,y_k\,(\mathbf{i}_j\cdot\mathbf{i}_k)\,\mathbf{i}_i$$
$$= b_{ij}\,y_k\,\delta_{jk}\,\mathbf{i}_i = b_{ij}\,y_j\,\mathbf{i}_i.$$

Note that the components $b_{ij}\,y_j$ of the vector $\mathbf{B}\cdot\mathbf{y}$ are obtained by the rule for multiplying the matrix $[\mathbf{B}] = (b_{ij})$ by the column vector $[\mathbf{y}]^T = (y_1\ y_2\ y_3)^T$.

The operation $\mathbf{A}\cdot\mathbf{x}$ yields a vector which can be represented in any basis. This issue is considered further next.

Representation of a Linear Transformation. Any linear transformation of vectors from $\mathbb{R}^3$ can be represented as a dot product from the left with a uniquely defined second-order tensor. Indeed, a linear transformation f acting in $\mathbb{R}^3$ has the property

$$f(\alpha\mathbf{x}+\beta\mathbf{y}) = \alpha f(\mathbf{x}) + \beta f(\mathbf{y}). \tag{12}$$

Expansion of $\mathbf{x}$ in a basis $\mathbf{e}_i$ produces

$$f(\mathbf{x}) = f(x^k\,\mathbf{e}_k) = f(\mathbf{e}_k)\,x^k.$$

With $\mathbf{f}_k = f(\mathbf{e}_k)$ and $x^k = \mathbf{e}^k\cdot\mathbf{x}$, this becomes $f(\mathbf{x}) = \mathbf{f}_k(\mathbf{e}^k\cdot\mathbf{x})$ so that

$$f(\mathbf{x}) = (\mathbf{f}_k\otimes\mathbf{e}^k)\cdot\mathbf{x}.$$

Hence the required tensor is

$$\mathbf{F} = \mathbf{f}_k\otimes\mathbf{e}^k \tag{13}$$

and the indicated representation is

$$f(\mathbf{x}) = \mathbf{F}\cdot\mathbf{x} \text{ for any } \mathbf{x}\in\mathbb{R}^3. \tag{14}$$

This fact extends to $\mathbb{R}^n$.

The Unit or Metric Tensor

In linear algebra there is a unit matrix I with ones along its main diagonal and zeros elsewhere. When I acts on a vector $\mathbf{x}$, the result is just $\mathbf{x}$:

$$I[\mathbf{x}]^T = [\mathbf{x}]^T.$$

Among the tensors there is also the unit tensor $\mathbf{E}$ such that for every $\mathbf{x}$

$$\mathbf{E}\cdot\mathbf{x} = \mathbf{x} = \mathbf{x}\cdot\mathbf{E}. \tag{15}$$

Guided by the matrix situation one quickly posits that

$$\mathbf{E} = \mathbf{e}_k\otimes\mathbf{e}^k \tag{16}$$

and finds that indeed

$$\mathbf{E}\cdot\mathbf{x} = (\mathbf{e}_k\otimes\mathbf{e}^k)\cdot x^i\,\mathbf{e}_i = x^i\,\mathbf{e}_k(\mathbf{e}^k\cdot\mathbf{e}_i)$$
$$= x^i\,\mathbf{e}_k\,\delta_i^k = x^i\,\mathbf{e}_i = \mathbf{x},$$
$$\mathbf{x}\cdot\mathbf{E} = x_i\,\mathbf{e}^i\cdot(\mathbf{e}_k\otimes\mathbf{e}^k) = x_i\,(\mathbf{e}^i\cdot\mathbf{e}_k)\mathbf{e}^k$$
$$= x_i\,\delta_k^i\,\mathbf{e}^k = x_k\,\mathbf{e}^k = \mathbf{x}.$$

As these relations hold in mixed components, they will hold for any component representations of $\mathbf{E}$ and $\mathbf{x}$. By (16) and a little index manipulation,

$$\mathbf{E} = \mathbf{e}_k\otimes\mathbf{e}^k = g_{ki}\mathbf{e}^i\otimes\mathbf{e}^k = g^{ki}\mathbf{e}_k\otimes\mathbf{e}_i = \mathbf{e}^i\otimes\mathbf{e}_i. \tag{17}$$

So the contravariant and covariant components of $\mathbf{E}$ are the metric coefficients; for this reason $\mathbf{E}$ is also called the *metric tensor*.

The representative matrix of $\mathbf{E}$ in mixed components is $[\mathbf{E}] = I$, the unit matrix; this is true for any initial basis $\mathbf{e}_i$.

Dot Product of Tensors

Next consider the dot product of tensors $\mathbf{A} = a^{ij}\,\mathbf{e}_i\otimes\mathbf{e}_j$ and $\mathbf{B} = b^{ij}\,\mathbf{e}_i\otimes\mathbf{e}_j$:

$$\mathbf{A}\cdot\mathbf{B} = a^{ij}\,\mathbf{e}_i\otimes\mathbf{e}_j\cdot b^{km}\,\mathbf{e}_k\otimes\mathbf{e}_m$$
$$= a^{ij}\,b^{km}\,(\mathbf{e}_j\cdot\mathbf{e}_k)\,\mathbf{e}_i\otimes\mathbf{e}_m$$
$$= a^{ij}\,b^{km}\,g_{jk}\,\mathbf{e}_i\otimes\mathbf{e}_m.$$

Note that one dot multiplies the vectors nearest the dot. (Also note the renaming of indices in the second factor.) Other forms of the dot product are obtained similarly:

$$\mathbf{A}\cdot\mathbf{B} = a_{ij}\,b_{km}\,g^{jk}\,\mathbf{e}^i\otimes\mathbf{e}^m$$
$$= a_{ij}\,b^{jm}\,\mathbf{e}^i\otimes\mathbf{e}_m = a_i^{\cdot j}\,b_{j\cdot}^{\cdot k}\,\mathbf{e}^i\otimes\mathbf{e}_k,$$

and so on. For a canonical basis where $\mathbf{C} = c_{ij}\,\mathbf{i}_i \otimes \mathbf{i}_j$ and $\mathbf{D} = d_{ij}\,\mathbf{i}_i \otimes \mathbf{i}_j$, the result

$$\begin{aligned}\mathbf{C}\cdot\mathbf{D} &= (c_{ij}\,\mathbf{i}_i \otimes \mathbf{i}_j)\cdot(d_{km}\,\mathbf{i}_k \otimes \mathbf{i}_m)\\ &= c_{ij}\,d_{km}\,\delta_{jk}\,\mathbf{i}_i \otimes \mathbf{i}_m = c_{ij}\,d_{jm}\,\mathbf{i}_i \otimes \mathbf{i}_m\end{aligned}$$

yields components obtainable by multiplying the representative matrices [**C**] and [**D**]: (i.e., by computing the matrix $(c_{ij}\,d_{jm})$). It is straightforward to show that any composition of two linear mappings in $\mathbb{R}^3$ can be uniquely represented by the dot product of the two corresponding tensors.

One easily verifies that for any second-order tensor **A**,

$$\mathbf{A}\cdot\mathbf{E} = \mathbf{E}\cdot\mathbf{A} = \mathbf{A}. \tag{18}$$

So **E** is the unit mapping among the second-order tensors as well.

Finally, powers of a tensor **A** can be defined in the expected manner:

$$\mathbf{A}^2 = \mathbf{A}\cdot\mathbf{A}, \qquad \mathbf{A}^3 = \mathbf{A}\cdot\mathbf{A}\cdot\mathbf{A}, \qquad \text{etc.}$$

In practice, tensorial relationships are often studied in the context of canonical bases. But it is crucial to note that if such a relationship can be written in component-free form using the dot product, then it holds in *any* basis. This observation is often used when treating tensorial relationships among physical quantities.

It is worth stressing that linear mappings are not the only objects representable through second-order tensors. The latter are also used to describe mechanical deformations, stresses, and so forth.

Double Dot Product. Given two dyads $\mathbf{a}\otimes\mathbf{b}$ and $\mathbf{c}\otimes\mathbf{d}$, the operation defined by

$$(\mathbf{a}\otimes\mathbf{b}) \cdot\cdot\, (\mathbf{c}\otimes\mathbf{d}) = (\mathbf{b}\cdot\mathbf{c})(\mathbf{a}\cdot\mathbf{d}) \tag{19}$$

is called *double dot multiplication*. It extends in straightforward fashion to more general second-order tensors **A** and **B**, e.g.,

$$\begin{aligned}\mathbf{A} \cdot\cdot\, \mathbf{B} &= a^{ij}\,\mathbf{e}_i \otimes \mathbf{e}_j \cdot\cdot\, b^{km}\,\mathbf{e}_k \otimes \mathbf{e}_m\\ &= a^{ij}\,b^{km}\,(\mathbf{e}_j\cdot\mathbf{e}_k)(\mathbf{e}_i\cdot\mathbf{e}_m)\\ &= a^{ij}\,b^{km}\,g_{jk}\,g_{im}.\end{aligned}$$

Trace of a Second-Order Tensor

The trace of a dyad $\mathbf{a}\otimes\mathbf{b}$ is computed by changing the tensor product operation to the dot product operation:

$$\operatorname{tr}(\mathbf{a}\otimes\mathbf{b}) = \mathbf{a}\cdot\mathbf{b}. \tag{20}$$

This idea extends directly to the case of a general second-order tensor:

$$\operatorname{tr}\mathbf{A} = \operatorname{tr}(a^{ij}\,\mathbf{e}_i \otimes \mathbf{e}_j) = a^{ij}\,\mathbf{e}_i\cdot\mathbf{e}_j = a^{ij}\,g_{ij}.$$

The trace of **A** is one of the principal invariants of **A**; it does not depend on the choice of basis. Direct calculation also reveals that

$$\operatorname{tr}\mathbf{A} = \mathbf{E} \cdot\cdot\, \mathbf{A}. \tag{21}$$

The simplest component form for the trace occurs in mixed components where

$$\operatorname{tr}\mathbf{A} = a_{j\cdot}^{\ \cdot j} = a_{\cdot i}^{i\cdot}\,. \tag{22}$$

Another principal invariant of **A** is the determinant covered next.

Determinant of a Second-Order Tensor

This quantity also takes its simplest form when **A** is in mixed components:

$$\det\mathbf{A} = |a_{i\cdot}^{\ \cdot j}| \tag{23}$$

where $|a_{i\cdot}^{\ \cdot j}|$ is the determinant of the representative matrix for the mixed basis. The value of the determinant does not depend on the basis. It can also be expressed in the forms

$$\det\mathbf{A} = |a_{\cdot j}^{i\cdot}| = g|a^{ij}| = g^{-1}|a_{ij}|$$

where $|\cdot|$ again denotes the determinant of a matrix and g is the determinant of the matrix of metric coefficients (g_{ij}).

The following properties of determinants known from linear algebra also hold for tensor determinants:

$$\begin{aligned}\det\mathbf{A} &= \det\mathbf{A}^T,\\ \det(\mathbf{A}\cdot\mathbf{B}) &= \det\mathbf{A}\,\det\mathbf{B},\\ \det\mathbf{E} &= 1.\end{aligned}$$

The tensor transpose operation appearing in the first property is discussed below.

A tensor having nonzero determinant is said to be *nonsingular*. Such a tensor $\mathbf{A}$ has an inverse tensor $\mathbf{A}^{-1}$ such that

$$\mathbf{A}\cdot\mathbf{A}^{-1}=\mathbf{A}^{-1}\cdot\mathbf{A}=\mathbf{E}.$$

In this case, for each given vector $\mathbf{y}\in\mathbb{R}^3$, the equation $\mathbf{A}\cdot\mathbf{x}=\mathbf{y}$ has a unique solution $\mathbf{x}=\mathbf{A}^{-1}\mathbf{y}$.

Tensor Transposition

Let $\mathbf{A}=a^{ij}\mathbf{e}_i\otimes\mathbf{e}_j$. Its *transpose* $\mathbf{A}^T$ is the second-order tensor

$$\mathbf{A}^T=(a^{ij}\mathbf{e}_i\otimes\mathbf{e}_j)^T=a^{ji}\,\mathbf{e}_i\otimes\mathbf{e}_j.$$

In other representations,

$$\mathbf{A}^T=a_{ji}\,\mathbf{e}^i\otimes\mathbf{e}^j=a_{j\cdot}^{\ \cdot i}\,\mathbf{e}_i\otimes\mathbf{e}^j=a^{j\cdot}_{\ \cdot i}\,\mathbf{e}^i\otimes\mathbf{e}_j.$$

It is straightforward to verify

$$(\mathbf{A}^T)^T=\mathbf{A},$$

the equality familiar for matrices in linear algebra.

Symmetric and Antisymmetric Parts of a Second-Order Tensor. Clearly

$$\mathbf{A}=\tfrac{1}{2}(\mathbf{A}+\mathbf{A}^T)+\tfrac{1}{2}(\mathbf{A}-\mathbf{A}^T),\qquad(24)$$

and furthermore

$$(\mathbf{A}+\mathbf{A}^T)^T=\mathbf{A}^T+(\mathbf{A}^T)^T=\mathbf{A}+\mathbf{A}^T,$$

$$(\mathbf{A}-\mathbf{A}^T)^T=\mathbf{A}^T-(\mathbf{A}^T)^T=-(\mathbf{A}-\mathbf{A}^T).$$

A tensor $\mathbf{A}$ for which $\mathbf{A}=\mathbf{A}^T$ is said to be *symmetric*. A tensor $\mathbf{B}$ for which $\mathbf{B}=-\mathbf{B}^T$ is *antisymmetric*. The equations immediately above show that any second-order tensor $\mathbf{A}$ can be resolved into a sum of a symmetric tensor $\frac{1}{2}(\mathbf{A}+\mathbf{A}^T)$ and an antisymmetric tensor $\frac{1}{2}(\mathbf{A}-\mathbf{A}^T)$. This decomposition is used to construct the tensor of small deformations.

Because the components of a symmetric tensor $\mathbf{A}$ satisfy $a^{ij}=a^{ji}$, only the six components a^{11}, a^{12}, a^{13}, a^{22}, a^{23}, and a^{33} can be specified independently. An antisymmetric tensor whose components satisfy $b^{ij}=-b^{ji}$ can have only three independent components b^{12}, b^{13}, and b^{23}; the diagonal components b^{11}, b^{22}, and b^{33} all vanish.

For a symmetric tensor $\mathbf{A}$ and an antisymmetric tensor $\mathbf{B}$, the following are easily verified:

$$\mathbf{A}\cdot\cdot\mathbf{B}=\mathbf{0},\qquad\mathbf{A}\cdot\mathbf{x}=\mathbf{x}\cdot\mathbf{A},\qquad\mathbf{B}\cdot\mathbf{x}=-\mathbf{x}\cdot\mathbf{B}.$$

Conjugate Vector

Let $\mathbf{B}$ be an antisymmetric second-order tensor. In a canonical basis $\mathbf{i}_j\otimes\mathbf{i}_k$, it is represented as

$$\begin{aligned}\mathbf{B}=&b_{12}\,\mathbf{i}_1\otimes\mathbf{i}_2+b_{13}\,\mathbf{i}_1\otimes\mathbf{i}_3+b_{23}\,\mathbf{i}_2\otimes\mathbf{i}_3\\&-b_{12}\,\mathbf{i}_2\otimes\mathbf{i}_1-b_{13}\,\mathbf{i}_3\otimes\mathbf{i}_1-b_{23}\,\mathbf{i}_3\otimes\mathbf{i}_2.\end{aligned}$$

With

$$\boldsymbol{\omega}=-b_{23}\,\mathbf{i}_1+b_{13}\,\mathbf{i}_2-b_{12}\,\mathbf{i}_3$$

one may easily check that for arbitrary $\mathbf{x}$ the two relations

$$\mathbf{B}\cdot\mathbf{x}=\boldsymbol{\omega}\times\mathbf{x},\qquad\mathbf{x}\cdot\mathbf{B}=\mathbf{x}\times\boldsymbol{\omega},$$

hold. But these are in component-free form so they hold in any frame. The vector $\boldsymbol{\omega}$ is said to be *conjugate* to the tensor $\mathbf{B}$.

Scalar Product of Second-Order Tensors

As the second-order tensors constitute a nine-dimensional linear space, one can define a scalar product operation $\mathbf{A}\odot\mathbf{B}$ for any $\mathbf{A}$ and $\mathbf{B}$:

$$\mathbf{A}\odot\mathbf{B}=\mathbf{A}\cdot\cdot\mathbf{B}^T.\qquad(25)$$

For dyads this takes the form

$$(\mathbf{a}\otimes\mathbf{b})\odot(\mathbf{c}\otimes\mathbf{d})=(\mathbf{a}\otimes\mathbf{b})\cdot\cdot(\mathbf{d}\otimes\mathbf{c})=(\mathbf{b}\cdot\mathbf{d})(\mathbf{a}\cdot\mathbf{c}).$$

Verification of the inner product axioms is straightforward. In component form the scalar product appears variously as

$$\mathbf{A} \odot \mathbf{B} = a_{ij}\, b^{ij} = a^{ij}\, b_{ij} = a^{i\cdot}_{\cdot j}\, b^{\cdot j}_{i\cdot} = a^{\cdot j}_{i\cdot}\, b^{i\cdot}_{\cdot j}.$$

It induces a norm in the usual manner:

$$\|\mathbf{A}\| = \sqrt{\mathbf{A} \odot \mathbf{A}} = \sqrt{a_{ij}\, a^{ij}} = \sqrt{a^{i\cdot}_{\cdot j}\, a^{\cdot j}_{i\cdot}}. \quad (26)$$

Orthogonal Tensors

Some tensors act on vectors in such a way that magnitudes are preserved; i.e., a second-order tensor $\mathbf{Q}$ may have the property that for each $\mathbf{a} \in \mathbb{R}^3$,

$$|\mathbf{Q} \cdot \mathbf{a}| = |\mathbf{a}|. \quad (27)$$

Such a tensor is said to be *orthogonal* and will also preserve dot products in the sense that

$$(\mathbf{Q} \cdot \mathbf{a}) \cdot (\mathbf{Q} \cdot \mathbf{b}) = \mathbf{a} \cdot \mathbf{b}. \quad (28)$$

Indeed, (27) applied to the difference $\mathbf{b} - \mathbf{a}$ gives

$$|\mathbf{Q} \cdot (\mathbf{b} - \mathbf{a})|^2 = |\mathbf{b} - \mathbf{a}|^2.$$

Now $|\mathbf{x}|^2 = \mathbf{x} \cdot \mathbf{x}$, so

$$[\mathbf{Q} \cdot (\mathbf{b} - \mathbf{a})] \cdot [\mathbf{Q} \cdot (\mathbf{b} - \mathbf{a})] = (\mathbf{b} - \mathbf{a}) \cdot (\mathbf{b} - \mathbf{a})$$

and simple manipulations yield

$$|\mathbf{Q}\cdot\mathbf{b}|^2 - 2(\mathbf{Q}\cdot\mathbf{a})\cdot(\mathbf{Q}\cdot\mathbf{b}) + |\mathbf{Q}\cdot\mathbf{a}|^2 = |\mathbf{b}|^2 - 2\mathbf{a}\cdot\mathbf{b} + |\mathbf{a}|^2.$$

But $|\mathbf{Q} \cdot \mathbf{b}|^2 = |\mathbf{b}|^2$ and $|\mathbf{Q} \cdot \mathbf{a}|^2 = |\mathbf{a}|^2$, so (28) holds for any $\mathbf{a}, \mathbf{b} \in \mathbb{R}^3$.

The inverse of an orthogonal tensor $\mathbf{Q}$ is its transpose $\mathbf{Q}^T$:

$$\mathbf{Q}^T \cdot \mathbf{Q} = \mathbf{E}, \quad \text{i.e.,} \quad \mathbf{Q}^T = \mathbf{Q}^{-1}. \quad (29)$$

The proof is straightforward. Any $\mathbf{a}, \mathbf{b}$ satisfy (28), which can be rewritten as

$$(\mathbf{a} \cdot \mathbf{Q}^T) \cdot (\mathbf{Q} \cdot \mathbf{b}) = \mathbf{a} \cdot \mathbf{E} \cdot \mathbf{b}$$

or

$$\mathbf{a} \cdot (\mathbf{Q}^T \cdot \mathbf{Q} - \mathbf{E}) \cdot \mathbf{b} = 0.$$

It is easy to see that if $\mathbf{a} \cdot \mathbf{A} \cdot \mathbf{b} = 0$ for any $\mathbf{a}$ and $\mathbf{b}$, then $\mathbf{A} = \mathbf{0}$. Indeed, let $\mathbf{A} = a^{ij}\mathbf{e}_i \otimes \mathbf{e}_j$. The choices $\mathbf{a} = \mathbf{e}^k$ and $\mathbf{b} = \mathbf{e}^m$ yield $a^{km} = 0$. Hence $\mathbf{Q}^T \cdot \mathbf{Q} - \mathbf{E} = \mathbf{0}$, which is (29).

If $\mathbf{Q}$ is orthogonal, then $\det \mathbf{Q} = \pm 1$ because

$$\begin{aligned}(\det \mathbf{Q})^2 &= \det \mathbf{Q}^T \ \det \mathbf{Q} \\ &= \det(\mathbf{Q}^T \cdot \mathbf{Q}) = \det \mathbf{E} = 1.\end{aligned}$$

If $\det \mathbf{Q} = +1$, then $\mathbf{Q}$ is called a *proper* orthogonal tensor; otherwise it is an *improper* orthogonal tensor. Proper orthogonal tensors correspond to rotations of solid bodies in $\mathbb{R}^3$.

Eigenproblem for a Second-Order Tensor

It has been noted that a linear operator acting in $\mathbb{R}^3$ can be represented by a second-order tensor. In linear algebra, the eigenvalue problem for a linear operator is a central topic. Fortunately the results of that study can be transferred directly to the algebra of tensors. One calls a pair $(\lambda, \mathbf{x} \neq \mathbf{0})$ an eigenpair of a tensor $\mathbf{A}$ if

$$\mathbf{A} \cdot \mathbf{x} = \lambda \mathbf{x}, \quad (30)$$

where λ is an eigenvalue and $\mathbf{x}$ an eigenvector. This equation also can be written as $(\mathbf{A} - \lambda\mathbf{E}) \cdot \mathbf{x} = \mathbf{0}$; by expressing it in matrix form, one can use the results of linear algebra to conclude that a nontrivial solution $\mathbf{x}$ exists only if

$$\det(\mathbf{A} - \lambda\mathbf{E}) = 0.$$

This is the *characteristic equation* for $\mathbf{A}$. Although the above presents no difficulty, another approach proves instructive. In component form, (30) reads

$$a^{ij}\, \mathbf{e}_i \otimes \mathbf{e}_j \cdot x^k\, \mathbf{e}_k = \lambda x^m\, \delta^n_m\, \mathbf{e}_n$$

where the relation $\mathbf{e}_m = \delta^n_m\, \mathbf{e}_n$ has been used. It follows that

$$a^{ij}\, g_{jk}\, x^k\, \mathbf{e}_i = \lambda x^m\, \delta^n_m\, \mathbf{e}_n.$$

Because the $\mathbf{e}_k$ constitute a basis, the equality holds if and only if the coefficients of the same $\mathbf{e}_k$ match, and this leads to three equations in the three unknowns x^k:

$$(a^{i\cdot}_{\cdot k} - \lambda\delta^i_k)x^k = 0 \qquad (i = 1, 2, 3).$$

The necessary and sufficient condition for $\mathbf{x}$ to be nontrivial is that the determinant of the matrix $(a^i_{\cdot k} - \lambda\delta^i_k)$ vanishes. This is the characteristic (cubic) equation for $\mathbf{A}$, which has the form

$$-\lambda^3 + I_1(\mathbf{A})\lambda^2 - I_2(\mathbf{A})\lambda + I_3(\mathbf{A}) = 0. \quad (31)$$

The three quantities $I_k(\mathbf{A})$ are the *principal invariants* of $\mathbf{A}$; they are independent of the choice of basis. Two were encountered above – namely, the trace and determinant of $\mathbf{A}$:

$$I_1(\mathbf{A}) = \operatorname{tr}\mathbf{A},$$
$$I_2(\mathbf{A}) = \tfrac{1}{2}(\operatorname{tr}^2\mathbf{A} - \operatorname{tr}\mathbf{A}^2),$$
$$I_3(\mathbf{A}) = \det\mathbf{A}.$$

Solution of the characteristic equation yields three eigenvalues λ. They may be distinct or repeated and real or complex and are also invariant quantities for $\mathbf{A}$. Rather than studying all the cases that can occur here, the present article will focus on a case important in mechanics.

Eigenproblem for a Second-Order Symmetric Tensor. The first crucial fact is

(1) *All the eigenvalues of a symmetric tensor* $\mathbf{A}$ *are real.*

Indeed, permitting λ to be complex (so that the eigenvector $\mathbf{x}$ in (30) can be complex as well), one may dot multiply both sides of (30) with the complex conjugate $\overline{\mathbf{x}}$ of $\mathbf{x}$:

$$(\mathbf{A}\cdot\mathbf{x})\cdot\overline{\mathbf{x}} = \lambda\mathbf{x}\cdot\overline{\mathbf{x}}.$$

Here $\mathbf{x}\cdot\overline{\mathbf{x}} > 0$ and attention can be turned to the left-hand side. By the symmetry property and real-valued nature of $\mathbf{A}$,

$$(\mathbf{A}\cdot\mathbf{x})\cdot\overline{\mathbf{x}} = \overline{\mathbf{x}\cdot\overline{(\mathbf{A}\cdot\mathbf{x})}} = \overline{(\mathbf{A}\cdot\mathbf{x})\cdot\overline{\mathbf{x}}}.$$

Hence $(\mathbf{A}\cdot\mathbf{x})\cdot\overline{\mathbf{x}}$ is real and so is λ.

(2) *Eigenvectors* $\mathbf{x}_1, \mathbf{x}_2$ *corresponding to distinct eigenvalues* λ_1, λ_2 $(\lambda_1 \neq \lambda_2)$ *are orthogonal.*

By hypothesis,

$$\mathbf{A}\cdot\mathbf{x}_1 = \lambda_1\mathbf{x}_1, \qquad \mathbf{A}\cdot\mathbf{x}_2 = \lambda_2\mathbf{x}_2.$$

Dot multiplying the first equation by $\mathbf{x}_2$ and the second by $\mathbf{x}_1$ from the left, one obtains

$$\mathbf{x}_2\cdot\mathbf{A}\cdot\mathbf{x}_1 = \lambda_1\mathbf{x}_2\cdot\mathbf{x}_1, \qquad \mathbf{x}_1\cdot\mathbf{A}\cdot\mathbf{x}_2 = \lambda_2\mathbf{x}_1\cdot\mathbf{x}_2.$$

By symmetry of $\mathbf{A}$, the left-hand sides of the two equalities are equal and

$$\lambda_1\mathbf{x}_2\cdot\mathbf{x}_1 = \lambda_2\mathbf{x}_1\cdot\mathbf{x}_2.$$

This is possible only if

$$\mathbf{x}_1\cdot\mathbf{x}_2 = 0.$$

Moreover, it is seen that

$$\mathbf{x}_1\cdot\mathbf{A}\cdot\mathbf{x}_2 = 0\,;$$

this and similar relations in the problems of linear elasticity are known as *generalized orthogonality* relations.

(3) *There exists a set of three eigenvectors of* $\mathbf{A}$ *which is orthonormal and hence a basis of* $\mathbb{R}^3$.

If all three λ_k are unequal, one has three eigenvectors $\mathbf{x}_k$ that are mutually orthogonal. Multiplication of $\mathbf{x}_k$ by any nonzero number again produces an eigenvector. So an orthonormal set of eigenvectors can be obtained by scaling the $\mathbf{x}_k$ to unit magnitude. However, it may turn out that an eigenvalue is repeated. If $\lambda_1 = \lambda_2 \neq \lambda_3$, say, then for the eigenvectors $\mathbf{x}_1$ and $\mathbf{x}_2$, one may select any two perpendicular vectors from a two-dimensional subspace of $\mathbb{R}^3$ situated orthogonal to the eigenvector $\mathbf{x}_3$. The resulting eigenvector triplet can be scaled to produce an orthonormal basis. If all three eigenvalues are equal, any nonzero vector of $\mathbb{R}^3$ is an eigenvector; in this case an arbitrary canonical basis of $\mathbb{R}^3$ can be used.

Spectral Representation of a Symmetric Second-Order Tensor. Let $\mathbf{x}_k$ be an orthonormal basis of eigenvectors of $\mathbf{A}$ as constructed above. Its reciprocal basis is composed of the same vectors $\mathbf{x}_k$. Let $\mathbf{A}$ be represented in terms of this basis:

$$\mathbf{A} = a_{ij}\,\mathbf{x}_i \otimes \mathbf{x}_j \qquad \text{(summation understood)}.$$

Now

$$a_{ij} = \mathbf{x}_i \cdot \mathbf{A} \cdot \mathbf{x}_j.$$

Since $\mathbf{A} \cdot \mathbf{x}_j = \lambda_j\,\mathbf{x}_j$ (here and below there is *no* summation over j) one gets

$$a_{ij} = \mathbf{x}_i \cdot (\lambda_j\,\mathbf{x}_j) = \lambda_j\,\delta_{ij},$$

so the a_{ij} are nonzero only on the main diagonal of the matrix. The expansion

$$\mathbf{A} = \lambda_1\,\mathbf{x}_1 \otimes \mathbf{x}_1 + \lambda_2\,\mathbf{x}_2 \otimes \mathbf{x}_2 + \lambda_3\,\mathbf{x}_3 \otimes \mathbf{x}_3 \quad (32)$$

is called a *spectral* or *orthogonal representation* of $\mathbf{A}$. The process of obtaining it is known as *diagonalization*, and the $\mathbf{x}_k$ are the *principal axes* of $\mathbf{A}$. (Note that the latter are nonunique; even when the λ_k are all distinct, the $\mathbf{e}_k$ are defined only up to a sign.) When $\lambda_1 = \lambda_2 = \lambda_3 = \lambda$, the tensor $\mathbf{A}$ is a *ball tensor* proportional to $\mathbf{E}$ such that $\mathbf{A} = \lambda\mathbf{E}$.

Using (32) one easily sees that

$$\begin{aligned}\mathbf{A}^2 &= (\lambda_1\mathbf{x}_1 \otimes \mathbf{x}_1 + \lambda_2\mathbf{x}_2 \otimes \mathbf{x}_2 + \lambda_3\mathbf{x}_3 \otimes \mathbf{x}_3)\\ &\quad \cdot (\lambda_1\mathbf{x}_1 \otimes \mathbf{x}_1 + \lambda_2\mathbf{x}_2 \otimes \mathbf{x}_2 + \lambda_3\mathbf{x}_3 \otimes \mathbf{x}_3)\\ &= \lambda_1^2\,\mathbf{x}_1 \otimes \mathbf{x}_1 + \lambda_2^2\,\mathbf{x}_2 \otimes \mathbf{x}_2 + \lambda_3^2\,\mathbf{x}_3 \otimes \mathbf{x}_3.\end{aligned}$$

Similarly, for any integer m

$$\mathbf{A}^m = {\lambda_1}^m\,\mathbf{x}_1 \otimes \mathbf{x}_1 + {\lambda_2}^m\,\mathbf{x}_2 \otimes \mathbf{x}_2 + {\lambda_3}^m\,\mathbf{x}_3 \otimes \mathbf{x}_3. \quad (33)$$

In the case of a positive symmetric tensor $\mathbf{A}$ (i.e., when $\lambda_k \geq 0$), a positive square root of $\mathbf{A}$ can be introduced:

$$\mathbf{A}^{1/2} = \lambda_1^{1/2}\,\mathbf{x}_1 \otimes \mathbf{x}_1 + \lambda_2^{1/2}\,\mathbf{x}_2 \otimes \mathbf{x}_2 + \lambda_3^{1/2}\,\mathbf{x}_3 \otimes \mathbf{x}_3. \quad (34)$$

There are other square roots of such a tensor $\mathbf{A}$ that are not positive.

A symmetric second-order tensor $\mathbf{A}$ is called *positive definite* if all $\lambda_k > 0$. In this case $\mathbf{A}$ is nonsingular.

Positivity of a symmetric second-order tensor $\mathbf{A}$ can also be expressed in terms of the quadratic form with respect to $\mathbf{x}$:

$$\mathbf{x} \cdot \mathbf{A} \cdot \mathbf{x} \geq 0.$$

A positive tensor $\mathbf{A}$ is positive definite if $\mathbf{x} \cdot \mathbf{A} \cdot \mathbf{x} = 0$ implies $\mathbf{x} = \mathbf{0}$. Equivalence of this with the earlier definition is easily established. For a positive definite symmetric tensor $\mathbf{A}$, its positive square root $\mathbf{A}^{1/2}$ is also positive definite.

Cayley–Hamilton Theorem. The Cayley–Hamilton theorem states that a second-order tensor $\mathbf{A}$ satisfies its characteristic equation (31).

Included here will be a simplified proof holding when $\mathbf{A}$ is symmetric. (The more general result follows from the corresponding theorem for a linear operator, covered in any textbook on linear algebra.) Denote the characteristic polynomial by

$$P(\lambda) = -\lambda^3 + I_1(\mathbf{A})\lambda^2 - I_2(\mathbf{A})\lambda + I_3(\mathbf{A}).$$

Then represent $\mathbf{A}$ in the spectral form (32) and apply $P(\lambda)$ to both sides:

$$\begin{aligned}P(\mathbf{A}) = {} & P(\lambda_1)\,\mathbf{x}_1 \otimes \mathbf{x}_1 + P(\lambda_2)\,\mathbf{x}_2 \otimes \mathbf{x}_2\\ & + P(\lambda_3)\,\mathbf{x}_3 \otimes \mathbf{x}_3.\end{aligned}$$

But the λ_k are the roots of $P(\lambda)$, and it follows that

$$-\mathbf{A}^3 + I_1(\mathbf{A})\mathbf{A}^2 - I_2(\mathbf{A})\mathbf{A} + I_3(\mathbf{A})\mathbf{E} = \mathbf{0} \quad (35)$$

as needed.

The Cayley–Hamilton theorem permits $\mathbf{A}^3$ to be expressed as a second-degree polynomial in $\mathbf{A}$:

$$\mathbf{A}^3 = I_1(\mathbf{A})\mathbf{A}^2 - I_2(\mathbf{A})\mathbf{A} + I_3(\mathbf{A})\mathbf{E}.$$

Using this and multiplying (35) by $\mathbf{A}$, similar formulas for $\mathbf{A}^4$, $\mathbf{A}^5$, and so on can be obtained. Moreover, if $\mathbf{A}$ is nonsingular ($\det \mathbf{A} \neq 0$), one finds $\mathbf{A}^{-1}$ by multiplying (35) by $\mathbf{A}^{-1}$:

$$\mathbf{A}^{-1} = \frac{1}{I_3(\mathbf{A})}[\mathbf{A}^2 - I_1(\mathbf{A})\mathbf{A} + I_2(\mathbf{A})\mathbf{E}].$$

It is similarly possible to express any negative integer power of $\mathbf{A}$ as a second-degree polynomial in $\mathbf{A}$. The same holds for any finite polynomial in $\mathbf{A}$ and $\mathbf{A}^{-1}$ (if $\det \mathbf{A} \neq 0$): it can be represented as a second-degree polynomial in $\mathbf{A}$.

Polar Decomposition of a Nonsingular Tensor. It is important in mechanics that any nonsingular second-order tensor $\mathbf{A}$ can be written as a dot product of an orthogonal tensor $\mathbf{Q}$ and a positive definite symmetric second-order tensor $\mathbf{S}$:

$$\mathbf{A} = \mathbf{S} \cdot \mathbf{Q}. \tag{36}$$

This is known as the *left polar decomposition* of $\mathbf{A}$. Also available is the *right polar decomposition*

$$\mathbf{A} = \mathbf{Q} \cdot \mathbf{R} \tag{37}$$

where $\mathbf{Q}$ is the same as in (36) and $\mathbf{R}$ is a positive definite symmetric tensor.

The decomposition (36) follows from the spectral representation (32). Its construction starts by establishing properties of the tensor $\mathbf{A} \cdot \mathbf{A}^T$; this turns out to be symmetric because

$$(\mathbf{A} \cdot \mathbf{A}^T)^T = (\mathbf{A}^T)^T \cdot \mathbf{A}^T = \mathbf{A} \cdot \mathbf{A}^T,$$

and also positive definite. Next one shows that all of its eigenvalues λ are positive. Indeed one can dot multiply both sides of the eigen-equation $(\mathbf{A} \cdot \mathbf{A}^T) \cdot \mathbf{x} = \lambda \mathbf{x}$ with $\mathbf{x}$ from the left:

$$\mathbf{x} \cdot (\mathbf{A} \cdot \mathbf{A}^T) \cdot \mathbf{x} = \lambda \mathbf{x} \cdot \mathbf{x}.$$

As $\mathbf{x} \cdot \mathbf{x} > 0$ (strictly positive since $\mathbf{x}$ is an eigenvector), attention can be turned to the left-hand side:

$$(\mathbf{x} \cdot \mathbf{A}) \cdot (\mathbf{A}^T \cdot \mathbf{x}) = (\mathbf{x} \cdot \mathbf{A}) \cdot (\mathbf{x} \cdot \mathbf{A}) = |\mathbf{x} \cdot \mathbf{A}|^2 \geq 0.$$

But $\mathbf{x} \cdot \mathbf{A}$ cannot be zero for $\mathbf{A}$ nonsingular. Therefore $\lambda > 0$.

The symmetric, positive definite tensor $\mathbf{A} \cdot \mathbf{A}^T$ has spectral representation

$$\mathbf{A} \cdot \mathbf{A}^T = \sum_{k=1}^{3} \lambda_k \, \mathbf{i}_k \otimes \mathbf{i}_k$$

with $\lambda_k > 0$ and an orthonormal basis $\mathbf{i}_k$ consisting of its eigenvectors. It follows that

$$\mathbf{S} = (\mathbf{A} \cdot \mathbf{A}^T)^{1/2} = \sum_{k=1}^{3} \lambda_k^{1/2} \, \mathbf{i}_k \otimes \mathbf{i}_k$$

is symmetric and positive definite, and this is the tensor $\mathbf{S}$ needed in (36). It remains only to show that

$$\mathbf{Q} = \mathbf{S}^{-1} \cdot \mathbf{A}$$

is orthogonal. One can start by noting that $\mathbf{S}^{-1}$ exists; it can be constructed explicitly as

$$\mathbf{S}^{-1} = \sum_{k=1}^{3} \frac{1}{\sqrt{\lambda_k}} \, \mathbf{i}_k \otimes \mathbf{i}_k$$

and the result verified by multiplication with $\mathbf{S}$. Orthogonality of $\mathbf{Q}$ is established as

$$\begin{aligned}
\mathbf{Q} \cdot \mathbf{Q}^T &= (\mathbf{S}^{-1} \cdot \mathbf{A}) \cdot (\mathbf{S}^{-1} \cdot \mathbf{A})^T \\
&= (\mathbf{S}^{-1} \cdot \mathbf{A}) \cdot [\mathbf{A}^T \cdot (\mathbf{S}^{-1})^T] \\
&= \mathbf{S}^{-1} \cdot (\mathbf{A} \cdot \mathbf{A}^T) \cdot (\mathbf{S}^T)^{-1} \\
&= \mathbf{S}^{-1} \cdot \mathbf{S}^2 \cdot \mathbf{S}^{-1} \\
&= \mathbf{E}.
\end{aligned}$$

It is easy to see that tensor $\mathbf{R}$ from (37) is $\mathbf{R} = \mathbf{Q}^T \cdot \mathbf{S} \cdot \mathbf{Q}$, which is symmetric and positive definite.

Ball Tensor and Deviator Representation. A ball tensor has all three eigenvalues λ equal. It takes the form $\lambda \mathbf{E}$. Corresponding to any second-order tensor $\mathbf{A}$, there is a ball tensor $\frac{1}{3} I_1(\mathbf{A})\mathbf{E}$, often regarded as a sort of "average value" of $\mathbf{A}$. The difference $\mathbf{A} - \frac{1}{3} I_1(\mathbf{A})\mathbf{E}$, showing how $\mathbf{A}$

deviates from its "average ball tensor," is called the *deviator* and is denoted dev $\mathbf{A}$:

$$\mathbf{A} = \tfrac{1}{3}(\operatorname{tr}\mathbf{A})\mathbf{E} + \operatorname{dev}\mathbf{A}. \tag{38}$$

It should be recalled that $I_1(\mathbf{A}) = \operatorname{tr}\mathbf{A} = \lambda_1 + \lambda_2 + \lambda_3$. Whereas $\mathbf{A}$ has eigenvalues $\lambda_1, \lambda_2, \lambda_3$, the tensor-deviator dev $\mathbf{A}$ has eigenvalues $\mu_i = \lambda_i - \frac{1}{3}\operatorname{tr}\mathbf{A}$.

Cross Product of Vectors and Tensors

The cross product for tensors is introduced similarly to the dot product. There are left and right cross products of a vector by a tensor. The rule is that one cross multiplies the vector with the nearest vectors in the dyad representation of the tensor, replacing this dyad vector by the cross product:

$$\begin{aligned}\mathbf{x}\times\mathbf{A} &= x^k\,\mathbf{e}_k \times [a^{ij}\,\mathbf{e}_i\otimes\mathbf{e}_j]\\ &= x^k\,a^{ij}\,[(\mathbf{e}_k\times\mathbf{e}_i)\otimes\mathbf{e}_j],\\ \mathbf{A}\times\mathbf{x} &= [a^{ij}\,\mathbf{e}_i\otimes\mathbf{e}_j]\times x^k\,\mathbf{e}_k\\ &= x^k\,a^{ij}\,[\mathbf{e}_i\otimes(\mathbf{e}_j\times\mathbf{e}_k)].\end{aligned}$$

The metric tensor $\mathbf{E}$ has the special property

$$\mathbf{x}\times\mathbf{E} = \mathbf{E}\times\mathbf{x}.$$

An important application of the cross product is the representation of a proper orthogonal tensor $\mathbf{Q}$. If $\mathbf{Q}$ is realized as the rotation through an angle α about an axis $\mathbf{e}$, then

$$\mathbf{Q} = \mathbf{E}\cos\alpha + (1-\cos\alpha)\mathbf{e}\otimes\mathbf{e} - \mathbf{e}\times\mathbf{E}\sin\alpha.$$

A Few Words About Higher-Order Tensors; Isotropic Tensors

Just as with dyads, one can introduce triads of vectors

$$\mathbf{a}\otimes\mathbf{b}\otimes\mathbf{c},$$

tetrads of vectors

$$\mathbf{a}\otimes\mathbf{b}\otimes\mathbf{c}\otimes\mathbf{c},$$

and so forth. Such products should have the property of linearity with respect to each vector entering in this structure, but not the property of commutativity. Using linear combinations of such entities with equal quantities of vectors, linear spaces of higher-order tensors are generated. A basis of such a space is expressed through the basis of the underlying space of vectors (here $\mathbb{R}^3$). Third-order tensors have the form

$$a^{ijk}\,\mathbf{e}_i\otimes\mathbf{e}_j\otimes\mathbf{e}_k,$$

fourth-order tensors have the form

$$a^{ijkm}\,\mathbf{e}_i\otimes\mathbf{e}_j\otimes\mathbf{e}_k\otimes\mathbf{e}_m,$$

etc. Of course, any basis vector of a polyad such as $\mathbf{e}_i\otimes\mathbf{e}_j\otimes\mathbf{e}_k$ can be transformed to its reciprocal basis vector, resulting in such forms as $\mathbf{e}^i\otimes\mathbf{e}^j\otimes\mathbf{e}^k$ or $\mathbf{e}_i\otimes\mathbf{e}_j\otimes\mathbf{e}^k$. But this must be accompanied by complementary changes in the components (which in this case fill a three-dimensional array) sufficient to ensure that the tensor itself remains an objective entity.

For higher-order tensors, as with second-order tensors, one can introduce dot and cross products, applying them to the near-standing vectors in the decompositions of the tensors. In the case of the dot product, the resulting tensor has order two less than the sum of the orders of the tensors participating in the product:

$$\begin{aligned}\mathbf{A}\cdot\mathbf{B} &= (a^{ijk}\,\mathbf{e}_i\otimes\mathbf{e}_j\otimes\mathbf{e}_k)\cdot(b^{mn}\,\mathbf{e}_m\otimes\mathbf{e}_n)\\ &= a^{ijk}\,b^{mn}(\mathbf{e}_k\cdot\mathbf{e}_m)\,\mathbf{e}_i\otimes\mathbf{e}_j\otimes\mathbf{e}_n.\end{aligned}$$

For the cross product, the result is of order one less than the sum of the orders of the factors:

$$\begin{aligned}\mathbf{A}\times\mathbf{B} &= (a^{ijk}\,\mathbf{e}_i\otimes\mathbf{e}_j\otimes\mathbf{e}_k)\times(b^{mn}\,\mathbf{e}_m\otimes\mathbf{e}_n)\\ &= a^{ijk}\,b^{mn}\,\mathbf{e}_i\otimes\mathbf{e}_j\otimes(\mathbf{e}_k\times\mathbf{e}_m)\otimes\mathbf{e}_n.\end{aligned}$$

Because the cross product of vectors is an axial vector, the cross product of polar tensors is a pseudotensor. An important example is the pseudotensor $-\mathbf{E}\times\mathbf{E}$ known as the *Levi–Civita tensor*. With components consisting of the Levi–Civita symbols ϵ_{ijk}, it is expressed as

$$-\mathbf{E}\times\mathbf{E} = \epsilon_{ijk}\,\mathbf{e}^i\otimes\mathbf{e}^j\otimes\mathbf{e}^k.$$

Isotropic Tensors. A tensor is *isotropic* if its individual components do not change when the basis is rotated. The rotation is specified by an arbitrary orthogonal tensor $\mathbf{Q}$; so if $\mathbf{e}_k$ is a given basis, the rotated basis is $\tilde{\mathbf{e}}_k = \mathbf{Q} \cdot \mathbf{e}_k$.

The zero-order tensors (scalars) are all isotropic. The only first-order isotropic tensor is the zero vector. Let $\mathbf{A}$ be a second-order tensor represented in the initial and rotated frames as

$$\mathbf{A} = a^{ij}\, \mathbf{e}_i \otimes \mathbf{e}_j = \tilde{a}^{ij}\, \tilde{\mathbf{e}}_i \otimes \tilde{\mathbf{e}}_j .$$

If $\mathbf{A}$ is isotropic, then $a^{ij} = \tilde{a}^{ij}$ and

$$\begin{aligned} \mathbf{A} &= \tilde{a}^{ij}\, \tilde{\mathbf{e}}_i \otimes \tilde{\mathbf{e}}_j = a^{ij}\, (\mathbf{Q} \cdot \mathbf{e}_i) \otimes (\mathbf{Q} \cdot \mathbf{e}_j) \\ &= \mathbf{Q} \cdot (a^{ij}\, \mathbf{e}_i \otimes \mathbf{e}_j) \cdot \mathbf{Q}^T . \end{aligned}$$

Therefore $\mathbf{A}$ is isotropic if and only if

$$\mathbf{A} = \mathbf{Q} \cdot \mathbf{A} \cdot \mathbf{Q}^T$$

for any orthogonal tensor $\mathbf{Q}$. It can be shown that a second-order tensor $\mathbf{A}$ is isotropic if and only if it is a ball tensor.

Isotropic tensors of higher order also exist. An important isotropic tensor of fourth order is the tensor of elastic moduli in linear elasticity. All of its components can be presented through two elastic constants, of which the most popular in engineering are the Lamé coefficients and the pair consisting of Young's modulus and Poisson's ratio.

Equation Recap

This section lists selected equations from the present article. It is hardly a comprehensive catalog of such results; more can be found in, e.g., Zhilin (2001), Lurie (2005, 2012), Simmonds (1997), Zubov and Karyakin (2006), Danielson (2003), Dmitrienko (2002), Filho (2016), Itskov (2015), and Lebedev et al. (2010).

Notation Lowercase Greek letters (α, β) denote scalars. Lowercase bold Arabic letters ($\mathbf{a}$, $\mathbf{b}$, $\mathbf{c}$) denote vectors. Uppercase bold Arabic letters ($\mathbf{A}$, $\mathbf{B}$, $\mathbf{C}$) denote second-order tensors.

$$\mathbf{ab} = \mathbf{a} \otimes \mathbf{b}$$

$$(\alpha + \beta)\mathbf{a} \otimes \mathbf{b} = \alpha \mathbf{a} \otimes \mathbf{b} + \beta \mathbf{a} \otimes \mathbf{b} \qquad (\mathbf{a} + \mathbf{b}) \otimes \mathbf{c} = \mathbf{a} \otimes \mathbf{c} + \mathbf{b} \otimes \mathbf{c}$$

$$0\mathbf{a} \otimes \mathbf{b} = \mathbf{0} \otimes \mathbf{b} = \mathbf{a} \otimes \mathbf{0} = \mathbf{0} \otimes \mathbf{0} \qquad \mathbf{a} \otimes (\mathbf{b} + \mathbf{c}) = \mathbf{a} \otimes \mathbf{b} + \mathbf{a} \otimes \mathbf{c}$$

$$\alpha \mathbf{a} \otimes \mathbf{b} + \beta \mathbf{c} \otimes \mathbf{d} = \beta \mathbf{c} \otimes \mathbf{d} + \alpha \mathbf{a} \otimes \mathbf{b} \qquad \alpha(\mathbf{a} \otimes \mathbf{b} + \mathbf{c} \otimes \mathbf{d}) = \alpha \mathbf{a} \otimes \mathbf{b} + \alpha \mathbf{c} \otimes \mathbf{d}$$

$$(\alpha + \beta)(\mathbf{a} \otimes \mathbf{b} + \mathbf{c} \otimes \mathbf{d}) = \alpha(\mathbf{a} \otimes \mathbf{b} + \mathbf{c} \otimes \mathbf{d}) + \beta(\mathbf{a} \otimes \mathbf{b} + \mathbf{c} \otimes \mathbf{d})$$

$$\mathbf{a} \otimes \mathbf{b} = a^i\, b^j\, \mathbf{e}_i \otimes \mathbf{e}_j = a_i\, b_j\, \mathbf{e}^i \otimes \mathbf{e}^j = a^i\, b_j\, \mathbf{e}_i \otimes \mathbf{e}^j = a_i\, b^j\, \mathbf{e}^i \otimes \mathbf{e}_j$$

$$\mathbf{A} = a^{ij}\, \mathbf{e}_i \otimes \mathbf{e}_j = a_{ij}\, \mathbf{e}^i \otimes \mathbf{e}^j = a^{i\cdot}_{\cdot j}\, \mathbf{e}_i \otimes \mathbf{e}^j = a_{i\cdot}^{\cdot j}\, \mathbf{e}^i \otimes \mathbf{e}_j$$

$$a_{k\cdot}^{\cdot j} = a^{ij}\, g_{ik}, \qquad a_{km} = a^{ij}\, g_{ik}\, g_{jm}, \qquad a^{i\cdot}_{\cdot m} = a^{ij}\, g_{jm}$$

$$(\mathbf{a} \otimes \mathbf{b}) \cdot \mathbf{x} = \mathbf{a}(\mathbf{b} \cdot \mathbf{x})$$

$$\mathbf{x} \cdot (\mathbf{a} \otimes \mathbf{b}) = (\mathbf{x} \cdot \mathbf{a})\mathbf{b}$$

$$\mathbf{A} \cdot \mathbf{x} = a^{ij}\, x_j\, \mathbf{e}_i = a_{ij}\, x^j\, \mathbf{e}^i = a^{i\cdot}_{\cdot j}\, x^j\, \mathbf{e}_i = a_{i\cdot}^{\cdot j}\, x_j\, \mathbf{e}^i$$

$$\mathbf{x} \cdot \mathbf{A} = x_i\, a^{ij}\, \mathbf{e}_j = x^i\, a_{ij}\, \mathbf{e}^j = x_i\, a^{i\cdot}_{\cdot j}\, \mathbf{e}^j = x^i\, a_{i\cdot}^{\cdot j}\, \mathbf{e}_j$$

$$f(\alpha\mathbf{x}+\beta\mathbf{y}) = \alpha f(\mathbf{x}) + \beta f(\mathbf{y}) \implies \begin{cases} f(\mathbf{x}) = \mathbf{F}\cdot\mathbf{x} \text{ for any } \mathbf{x}\in\mathbb{R}^3 \\ \mathbf{F} = f(\mathbf{e}_k)\otimes\mathbf{e}^k \end{cases}$$

$$\mathbf{E}\cdot\mathbf{x} = \mathbf{x} = \mathbf{x}\cdot\mathbf{E} \qquad \mathbf{A}\cdot\mathbf{E} = \mathbf{E}\cdot\mathbf{A} = \mathbf{A}$$

$$\mathbf{E} = \mathbf{e}_k\otimes\mathbf{e}^k = g_{ki}\,\mathbf{e}^i\otimes\mathbf{e}^k = g^{ki}\,\mathbf{e}_k\otimes\mathbf{e}_i = \mathbf{e}^i\otimes\mathbf{e}_i$$

$$\mathbf{A}\cdot\mathbf{B} = a^{ij}\,b^{km}\,g_{jk}\,\mathbf{e}_i\otimes\mathbf{e}_m = a_{ij}\,b_{km}\,g^{jk}\,\mathbf{e}^i\otimes\mathbf{e}^m = a_{ij}\,b^{jm}\,\mathbf{e}^i\otimes\mathbf{e}_m = a_i^{\cdot j}\,b_j^{\cdot k}\,\mathbf{e}^i\otimes\mathbf{e}_k$$

$$\mathbf{A}^2 = \mathbf{A}\cdot\mathbf{A}, \qquad \mathbf{A}^3 = \mathbf{A}\cdot\mathbf{A}\cdot\mathbf{A}, \quad \ldots$$

$$(\mathbf{a}\otimes\mathbf{b})\cdot\cdot(\mathbf{c}\otimes\mathbf{d}) = (\mathbf{b}\cdot\mathbf{c})(\mathbf{a}\cdot\mathbf{d})$$

$$\operatorname{tr}(\mathbf{a}\otimes\mathbf{b}) = \mathbf{a}\cdot\mathbf{b}$$

$$\operatorname{tr}\mathbf{A} = a^{ij}g_{ij} = a_j^{\cdot j} = a_{\cdot i}^{i\cdot} = \mathbf{E}\cdot\cdot\mathbf{A}$$

$$\det\mathbf{A} = |a_i^{\cdot j}| = |a_{\cdot j}^{i\cdot}| = g|a^{ij}| = g^{-1}|a_{ij}|$$

$$\det\mathbf{A} = \det\mathbf{A}^T \qquad \det(\mathbf{A}\cdot\mathbf{B}) = \det\mathbf{A}\,\det\mathbf{B} \qquad \det\mathbf{E} = 1$$

$$\det\mathbf{A}\neq 0 \implies \mathbf{A}\cdot\mathbf{A}^{-1} = \mathbf{A}^{-1}\cdot\mathbf{A} = \mathbf{E}$$

$$\mathbf{A}^T = a^{ji}\,\mathbf{e}_i\otimes\mathbf{e}_j = a_{ji}\,\mathbf{e}^i\otimes\mathbf{e}^j = a_j^{\cdot i}\,\mathbf{e}_i\otimes\mathbf{e}^j = a_{\cdot i}^{j\cdot}\,\mathbf{e}^i\otimes\mathbf{e}_j$$

$$(\mathbf{A}^T)^T = \mathbf{A}$$

$$\mathbf{A} = \tfrac{1}{2}(\mathbf{A}+\mathbf{A}^T) + \tfrac{1}{2}(\mathbf{A}-\mathbf{A}^T)$$

$$\mathbf{B}^T = -\mathbf{B} \implies \begin{cases} \mathbf{B}\cdot\mathbf{x} = \boldsymbol{\omega}\times\mathbf{x} \text{ and } \mathbf{x}\cdot\mathbf{B} = \mathbf{x}\times\boldsymbol{\omega} \\ \boldsymbol{\omega} = -b_{23}\,\mathbf{i}_1 + b_{13}\,\mathbf{i}_2 - b_{12}\,\mathbf{i}_3 \end{cases}$$

$$(\mathbf{a}\otimes\mathbf{b})\odot(\mathbf{c}\otimes\mathbf{d}) = (\mathbf{b}\cdot\mathbf{d})(\mathbf{a}\cdot\mathbf{c})$$

$$\mathbf{A}\odot\mathbf{B} = \mathbf{A}\cdot\cdot\mathbf{B}^T = a_{ij}\,b^{ij} = a^{ij}\,b_{ij} = a_{\cdot j}^{i\cdot}\,b_{i\cdot}^{\cdot j} = a_{i\cdot}^{\cdot j}\,b_{\cdot j}^{i\cdot}$$

$$\|\mathbf{A}\| = \sqrt{\mathbf{A}\odot\mathbf{A}} = \sqrt{a_{ij}\,a^{ij}} = \sqrt{a_{\cdot j}^{i\cdot}\,a_{i\cdot}^{\cdot j}}$$

$$|\mathbf{Q}\cdot\mathbf{a}| = |\mathbf{a}| \implies \begin{cases} (\mathbf{Q}\cdot\mathbf{a})\cdot(\mathbf{Q}\cdot\mathbf{b}) = \mathbf{a}\cdot\mathbf{b} \\ \mathbf{Q}^T = \mathbf{Q}^{-1} \\ \det\mathbf{Q} = \pm 1 \end{cases}$$

$$\mathbf{A}\cdot\mathbf{x} = \lambda\mathbf{x} \qquad (\mathbf{x}\neq\mathbf{0})$$

$$-\lambda^3 + I_1(\mathbf{A})\lambda^2 - I_2(\mathbf{A})\lambda + I_3(\mathbf{A}) = 0$$

$$I_1(\mathbf{A}) = \operatorname{tr}\mathbf{A} \qquad I_2(\mathbf{A}) = \tfrac{1}{2}(\operatorname{tr}^2\mathbf{A} - \operatorname{tr}\mathbf{A}^2) \qquad I_3 = \det\mathbf{A}$$

$$\mathbf{A} = \mathbf{A}^T \implies \mathbf{A} = \lambda_1\,\mathbf{x}_1\otimes\mathbf{x}_1 + \lambda_2\,\mathbf{x}_2\otimes\mathbf{x}_2 + \lambda_3\,\mathbf{x}_3\otimes\mathbf{x}_3$$

$$-\mathbf{A}^3 + I_1(\mathbf{A})\mathbf{A}^2 - I_2(\mathbf{A})\mathbf{A} + I_3(\mathbf{A})\mathbf{E} = \mathbf{0}$$

$$\mathbf{A}^{-1} = \frac{1}{I_3(\mathbf{A})}[\mathbf{A}^2 - I_1(\mathbf{A})\mathbf{A} + I_2(\mathbf{A})\mathbf{E}]$$

$$\mathbf{A} = \tfrac{1}{3}(\operatorname{tr}\mathbf{A})\mathbf{E} + \operatorname{dev}\mathbf{A}$$

$$\mathbf{x} \times \mathbf{A} = x^k a^{ij} [(\mathbf{e}_k \times \mathbf{e}_i) \otimes \mathbf{e}_j]$$
$$\mathbf{A} \times \mathbf{x} = x^k a^{ij} [\mathbf{e}_i \otimes (\mathbf{e}_j \times \mathbf{e}_k)]$$
$$\mathbf{x} \times \mathbf{E} = \mathbf{E} \times \mathbf{x}$$

$$\underbrace{a^{ijk}\, \mathbf{e}_i \otimes \mathbf{e}_j \otimes \mathbf{e}_k}_{\text{order } 3} \cdot \underbrace{b^{mn}\, \mathbf{e}_m \otimes \mathbf{e}_n}_{\text{order } 2} = \underbrace{a^{ijk}\, b^{mn} (\mathbf{e}_k \cdot \mathbf{e}_m)\, \mathbf{e}_i \otimes \mathbf{e}_j \otimes \mathbf{e}_n}_{\text{order } (3+2)-2=3}$$

$$\underbrace{a^{ijk}\, \mathbf{e}_i \otimes \mathbf{e}_j \otimes \mathbf{e}_k}_{\text{order } 3} \times \underbrace{b^{mn}\, \mathbf{e}_m \otimes \mathbf{e}_n}_{\text{order } 2} = \underbrace{a^{ijk}\, b^{mn}\, \mathbf{e}_i \otimes \mathbf{e}_j \otimes (\mathbf{e}_k \times \mathbf{e}_m) \otimes \mathbf{e}_n}_{\text{order } (3+2)-1=4}$$

Cross-References

- Derivatives of Vectors and Tensors
- Integration Formulas for Vectors and Tensors
- Korn's Inequality
- Vectors

References

Danielson D (2003) Vectors and tensors in engineering and physics. Westview Press, Boulder

Dmitrienko Y (2002) Tensor analysis and nonlinear tensor functions. Springer, New York

Filho E (2016) Tensor calculus for engineers and physicists. Springer, New York

Itskov M (2015) Tensor algebra and tensor analysis for engineers: with applications to continuum mechanics. Springer, New York

Lebedev L, Cloud M, Eremeyev V (2010) Tensor analysis with applications in mechanics. World Scientific, Singapore

Lurie A (2005) Theory of elasticity. Springer, New York

Lurie A (2012) Non-linear theory of elasticity. North Holland, Amsterdam

Simmonds J (1997) A brief on tensor analysis. Springer, New York

Zhilin P (2001) Vectors and second-rank tensors in three-dimensional space. Nestor, St. Petersburg (in Russian)

Zubov L, Karyakin M (2006) Tensor calculus: basic theory. University Books, Moscow (in Russian)

Terminal Ballistics

- Penetration Mechanics of Rigid Projectiles in Metallic Targets

Textiles

- Impact of Textile Structures

Theoretical Damage Evolution Modeling

- Phenomenological Model of Orthotropic Damage in Polymer Matrix Composites

Theory of Discontinuities

- Dynamic Equations, Verification of Hyperbolicity via the Theory of Discontinuities

Theory of Materials

- Coleman-Noll Procedure for Classical and Generalized Continuum Theories

Theory of Microforces

- Coleman-Noll Procedure for Classical and Generalized Continuum Theories

Theory of Porous Media

- Coupled Problems in Biological Systems

Theory of structures

- Axiomatic/Asymptotic Method and Best Theory Diagram for Composite Plates and Shells
- Classical and Advanced Modeling of Rotating Composite Blades and Rotors

Thermal Conduction and Thermal Radiation by Means of Generalized Continuum

- Thermal Effects by Means of Two-Component Cosserat Continuum

Thermal Effects by Means of Two-Component Cosserat Continuum

Elena A. Ivanova
Department of Theoretical Mechanics, Peter the Great Saint Petersburg Polytechnic University, Saint Petersburg, Russia
Institute for Problems in Mechanical Engineering of Russian Academy of Sciences, Saint Petersburg, Russia

Synonyms

Thermal conduction and thermal radiation by means of generalized continuum; Thermal phenomena by means of continuum with microstructure; Thermal processes by means of micropolar continuum; Thermodynamic processes by means of continuum with rotational degrees of freedom

Definition

A model of thermal effects in a conventional material is based on an idea to introduce two-component Cosserat continuum and to interpret characteristics of motion and interactions associated with the rotational degrees of freedom as mechanical analogies of thermodynamic quantities. The material under consideration has no microstructure, inclusions, etc. Motion associated with the rotational degrees of freedom has no relation to the real motion of the material particles. This model is not similar to the models used in kinetic theories, and it is not based on statistical methods. This model is constructed within the framework of continuum mechanics and by using the methods of continuum mechanics.

Introduction

A mechanical model, which can be a basis for description of thermal processes within the framework of continuum mechanics and by using the methods of continuum mechanics, is developed since 2010. It is discussed in a number of publications (see Ivanova 2010, 2011, 2012, 2013, 2017). This model is based on an idea to introduce a continuum with an internal structure and additional degrees of freedom and to interpret characteristics of motion and interactions associated with the internal structure as mechanical analogies of temperature and other thermodynamic quantities. It is important to note that a physical object under consideration is a conventional material without microstructure, inclusions, etc. This material has elastic and thermodynamic properties. The internal structure and internal rotational degrees of freedom inherent in the model are used for simulating thermal processes in the material. Motion associated with the internal degrees of freedom has no relation to the real motion of the material particles. Characteristics of motion associated with the internal rotational degrees of freedom, as well as characteristics of interactions associated with the internal rotational degrees of freedom, should be considered as analogies of thermodynamic quantities.

There are the kinetic theories that include rotational degrees of freedom (see, e.g., Warner and Harold 1972; Giesekus 1985; Bird et al. 1987) as well as the kinetic theories that take into

account internal degrees of freedom (see, e.g., Jehring 1984). The model of thermal processes under discussion is not similar to these models. It is based on quite different ideas and approaches without using statistical methods and concepts of kinetic theories.

The idea of mathematical description of various physical phenomena in microcosm by using models based on a continuum with rotational degrees of freedom was repeatedly asserted by Pavel Andreevich Zhilin (1942–2005), and this idea was realized by him as applied to the description of electromagnetic and quantum mechanical phenomena (see Zhilin 2001, 2003, 2006a,b, 2012, 2015). The model considered in the present paper is a realization of Zhilin's ideas as applied to the description of thermal phenomena.

Different Views on the Nature of Heat

Starting from antiquity, there exist different viewpoints on the nature of heat (see Rosenberger 1887; Whittaker 1910; Gliozzi 1965; Müller 2007). According to one point of view, heat is a state of a body. For example, Roger Bacon (1214–1292) and Johannes Kepler (1571–1630) adhered to this opinion. In accordance with another point of view, heat is a substance. Galileo Galilei (1564–1642) formulated the hypothesis of existence of the imponderable fluid accounting for heat. Afterward, this imponderable fluid was called the caloric fluid. Antoine Laurent de Lavoisier (1743–1794), Pierre Simon de Laplace (1749–1827), and Jean Baptiste Joseph Fourier (1768–1830) were adherents of the caloric fluid theory. The success and popularity of the caloric fluid in the seventeenth to eighteenth centuries was caused by the fact that predictions of the theory were verified by the experiments carried out at that time. The caloric fluid theory was recognized to be erroneous only in the nineteenth century when, due to the works by Julius Robert Mayer (1814–1878), James Prescott Joule (1818–1889), Hermann Helmholtz (1821–1894), and William Thomson, Lord Kelvin (1824–1907), the principle of equivalence of heat and energy became firmly established and the heat conservation law, which had dominated earlier, was completely replaced by the energy balance equation (the first law of thermodynamics). Robert Boyle (1627–1691) assumed heat to be associated with the molecular motion. In fact, his assumption was the start of the kinetic theory, which was further developed by Rudolf Clausius (1822–1888), James Clerk Maxwell (1831–1879), Ludwig Boltzmann (1844–1906), and Josiah Willard Gibbs (1839–1903). Besides the caloric fluid theory and the kinetic theory of gas, a number of different mechanical models of thermal processes were suggested by outstanding scientists of past centuries, namely, Leonhard Euler (1707–1783), Mikhail V. Lomonosov (1711–1765), Benjamin Thompson (1753–1814), Humphry Davy (1778–1829), Thomas Young (1773–1829), and Augustin Louis Cauchy (1789–1857). Nevertheless, the interpretation of temperature as the average kinetic energy of the chaotic motion of atoms and molecules has been generally accepted up to now. The question whether this interpretation is a reflection of some physical reality can be clarified by Maxwell's remark toward the kinetic theory (see Maxwell 1860, p. 378):

> . . . If the properties of such a system of bodies are found to correspond to those of gases, an important physical analogy will be established, which may lead to more accurate knowledge of the properties of matter. If experiments on gases are inconsistent with the hypothesis of these propositions, then our theory, though consistent with itself, is proved to be incapable of explaining the phenomena of gases. In either case it is necessary to follow out the consequences of the hypothesis.

It is important to note that temperature cannot be measured directly. In order to measure temperature, we have to measure a physical quantity, a change of which is a sign of the change in temperature. Then, we have to calculate the value of temperature taking into account the fixed points of temperature scale and using a formula that relates the change in chosen physical quantity and the change in temperature. Thus, there is no reason to believe that measuring temperature we measure the average kinetic energy of the chaotic motion of atoms and molecules. Thus,

the interpretation of temperature adopted in the kinetic theory is rather a mathematical model than a physical reality. That is why any alternative model of thermal processes, the mathematical description of which is reduced to the known equations, is of interest from a theoretical point of view.

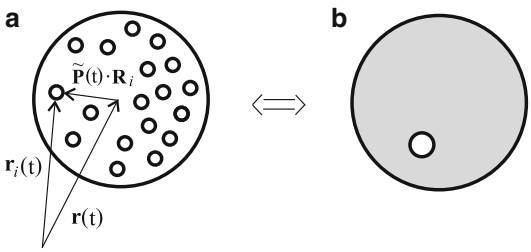

Fig. 1 A quasi-rigid body and its approximate model (the one-rotor gyrostat), which are equivalent in a first approximation

The Physical Meaning of the Model

According to the concepts of modern physics, atoms have a very complex internal structure. For example, they can be in different energy states and possess the ability to radiate and absorb the energy quanta and elementary particles. These facts should be taken into account when the properties of a single atom or a molecule consisting of several atoms are studied. When modeling a medium which consists of millions of atoms, many properties of atoms can be ignored or taken into account integrally, and it should be done so. For example, when modeling crystal lattices, very simple models of atoms are used, namely, atoms are assumed to be mass points or infinitesimal rigid bodies. For modeling a medium with a combination of various physical properties (mechanical, thermal, electric, and magnetic), more complicated models of atoms should be used. These are the models considering atoms as complex particles with internal structure and internal degrees of freedom. There are two different types of particles with an internal structure: particles with internal translational degrees of freedom (deformable particles) and particles with internal rotational degrees of freedom (multi-spin particles). Continua consisting of particles of the first type are called micromorphic continua. Continua consisting of particles of the second type are called micropolar continua. In principle, both deformable particles and multi-spin ones can be used to model atoms, and, consequently, both the micromorphic and micropolar continua can be used to model a medium with some nonmechanical properties.

In the model under consideration, atoms are assumed to be multi-spin particles like a quasi-rigid body (see Fig. 1a). The quasi-rigid body is a rigid body in the sense that the distances between any two points of this particle are kept unchanged under arbitrary motions of the quasi-rigid body. However, unlike the standard rigid body, the quasi-rigid body contains several rotors inside. Each rotor can rotate independently, and the rotation of rotors does not change the inertia tensor of the quasi-rigid body. In fact, the quasi-rigid body is a multi-rotor gyrostat that consists of a carrier body and a number of rotors rotating independently relative to the carrier body. For the first time, the multi-spin particles were introduced in Zhilin (2001, 2003, 2006a,b, 2012, 2015). The idea to consider the multi-spin particles (the multi-rotor gyrostats) as models of atoms was also stated in the cited works.

When modeling atoms by the multi-rotor gyrostats, the motion of carrier bodies characterizes the motion of atoms as rigid bodies. It is the motion of atoms that causes mechanical strains and mechanical stresses in the material medium. The rotors simulate elementary particles constituting the atoms. Pursuant to this model, the motion of rotors simulates the change in the internal state of atoms, and the internal state of atoms determines all the physical processes occurring in the material medium, namely, electrical, magnetic, and thermal. The multi-rotor gyrostat is rather complicated model with a large number of parameters. Therefore, for modeling a heat-conducting elastic medium, a simpler model of atom, namely, a one-rotor gyrostat (see Fig. 1b) is used instead of the multi-rotor gyrostat. It is important to note that the one-rotor gyrostat retains key features of

the multi-rotor gyrostat since the expressions for the kinetic energy, the linear momentum, and the angular momentum of the one-rotor gyrostat coincide with those of the multi-rotor gyrostat in a first approximation. In a continuum theory, the physical characteristics averaged over a representative volume are used. The dynamic properties of a representative volume of the continuous medium have no qualitative difference from the dynamic properties of particles in the representative volume.

The Basic Ideas of the Approach

The one-rotor gyrostat continuum is considered. The one-rotor gyrostat is a particle that consists of the carrier body and the rotor (see Fig. 2). The rotor can rotate independently of the carrier body rotation, but it cannot execute translatory motion relative to the carrier body. Thus, the one-rotor gyrostat has nine degrees of freedom, three translational ones, and six rotational ones. Free space between the gyrostats is filled up by the ether. The ether is shown in Fig. 2 as the body-points in the space between the gyrostats.

The main ideas of the description of thermoelastic processes by means of the mechanical model with internal rotational degrees of freedom consist in the following:

- The one-rotor gyrostat continuum is used for modeling solids, liquids, and gases. This continuum is considered to be elastic. The interaction of carrier bodies of gyrostats is attributed to the mechanical processes. The interaction of rotors of gyrostats models thermal processes. The interaction of the carrier bodies and the rotors provides the interplay of mechanical and thermal processes.
- The gyrostats (which model material particles) are considered to be embedded into some medium occupying the whole infinite space. This medium represents the physical vacuum, the field, the ether, or something like that.
- It is assumed that all gyrostats interact with the ether by means of elastic moments associated with the rotational degrees of freedom. Due to the fact that the ether fills the whole infinite space and interacts with all gyrostats, it plays a double role in the model.
- On the one hand, it is assumed that all interactions of gyrostats with each other are performed by the instrumentality of the ether. To be exact, the carrier bodies of different gyrostats interact through the agency of the ether, and the rotors belonging to different gyrostats interact also via the ether. From a mathematical point of view, this means that the constitutive equations for all quantities characterizing the stress state of the one-rotor gyrostat continuum depend not only on the properties of the carrier bodies and the rotors of the gyrostats but also on the elastic properties and the stress–strain state of the ether filling the space between the gyrostats.
- On the other hand, it is assumed that the ether provides a dissipation of gyrostats energy. Since the gyrostats interact with the ether, their motion causes appearance of waves in the ether. As a result, certain part of the gyrostats energy is spent on formation of the

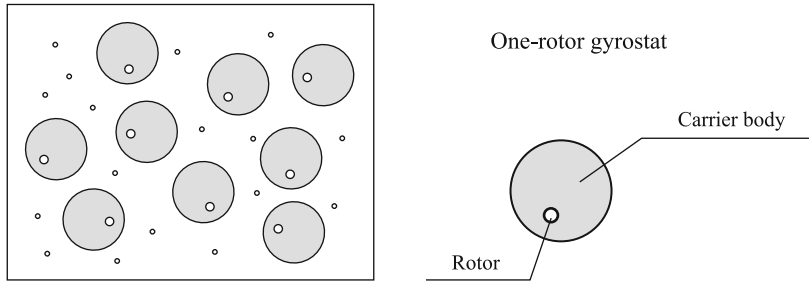

Fig. 2 An elementary volume of the continuum of one-rotor gyrostats together with the continuum of body-points in the space between the gyrostats (on the left-hand side) and the one-rotor gyrostat (on the right-hand side)

waves. Since the ether is considered to be infinite, waves carrying away the gyrostats energy do not come back. The result is the dissipation of the gyrostats energy into the ether.

- The dissipation of the gyrostats energy into the ether becomes apparent in the material medium in the form of the heat conduction and the internal damping. The heat conduction mechanism is supposed to be provided only by the moment interactions between the rotors and the ether. The internal damping mechanism can be provided in different ways, both due to the kinematic connection between the rotors and the carrier bodies and thanks to the interaction of the carrier bodies with the ether.

A Model of the Ether

Initially, a two-component medium that consists of the one-rotor gyrostat continuum simulating the conventional substance and the body-point continuum simulating the ether is considered. This two-component medium is assumed to be conservative. The following assumptions are made with respect to the ether:

- The ether particles are much smaller than elementary particles of the conventional substance. The structure of the ether particles coincides with the structure of the rotors that belong to the gyrostats.
- The ether is assumed to be a medium that is less dense than the conventional substance. The ether particles fill the space between elementary particles of the conventional substance, and the elementary particles interact with each other via the ether particles.
- The interactions of ether particles with each other and the interactions of ether particles with the elementary particles of the conventional substance are based only on the rotational degrees of freedom and the principle of moment interactions. There are no interactions between these particles by means of forces. Thus, from a continuum mechanics point of view, the model of ether is the special case of the Cosserat continuum.
- The ether is an infinite medium, i.e., it occupies the whole space. The ether is assumed to be an elastic medium. However, due to its infinite extent, the ether carries away the energy of rotational motion of material particles located in it. When the particles interact with the ether, their motion disturbs the ether and causes appearance of waves in it. Since the ether is infinite, the waves cannot be reflected from the boundaries, and hence, they cannot come back. Thus, the part of the material particles' energy, which is spent on formation of the waves in the ether, is irretrievably lost.

The Interaction of the Ether with Material Particles

Interacting with the material particles via the rotational degrees of freedom, the boundless ether creates a moment of viscous damping acting on the material particles. A structure of the moment of viscous damping is chosen in accordance with the results obtained by solving two model problems (see Ivanova 2011, 2012). The model considered in Ivanova (2011) consists of the semi-infinite inertial elastic rod (a one-dimensional model of the ether) that is connected with the rotor by means of the inertialess spring working in torsion (rotation about the axis of the rod) see Fig. 3, on the left-hand side). The rotation of the rotor disturbs the elastic rod and causes the torsion waves in it. If the rod had a limited size, the waves would be reflected from the boundary and come back. In this case, the system would be conservative. The dissipation of the rotor energy occurs only due to the infinite length of the rod and the absence of sources at infinity. As shown in Ivanova (2011), after eliminating the variables that characterize the rod motion, the problem is reduced to the set of equations describing the rotor motion. In the set of equations, there is the equation that contains the moment of viscous damping characterizing

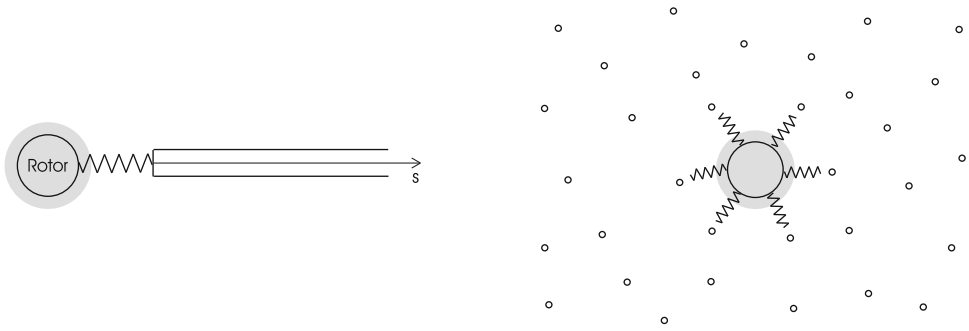

Fig. 3 Two models of interaction between the rotors and the ether: the 1D model on the left-hand side and the 3D model on the right-hand side

the energy radiation in the ambient medium. It is proved that the moment of viscous damping is proportional to the angular momentum of the rotor, and the coefficient of damping depends on the parameters of the rod and the torsional stiffness of the spring connecting the rotor and the rod. The spherically symmetric three-dimensional model is considered in Ivanova (2012). It consists of the spherical source (the spherical surface each point of which is the rotor) and the infinite inertial elastic continuum modeling the ether (see Fig. 3, on the right-hand side). All rotors of the spherical source are connected with the continuum by means of the inertialess springs working in torsion (rotation about a radius of the spherical source). As shown in Ivanova (2012), after eliminating the variables characterizing the ether motion, the problem is reduced to the set of equations that contain the dissipative term proportional to the angular momentum. The coefficient of viscous damping has the same dependence on the model parameters as in the one-dimensional case discussed above.

It is important to note that, in essence, the model problems considered above demonstrate the description of a heat wave radiation. The heat transfer by radiation can be represented in different ways. On the one hand, it is generally accepted that only electromagnetic waves propagate and it is precisely these waves that cause heating of matter when interacting with it. On the other hand, one can assume that waves of different nature, namely, heat waves, propagate together with electromagnetic waves. The model problems considered above are the realization of the latter viewpoint. A similar approach is developed in Ivanova et al. (2007) where it is suggested an original method of description of the rotational molecular spectra lying in the infrared range and associated with the thermal radiation. This method is based on the continuum mechanics model with the rotational degrees of freedom.

The One-Rotor Gyrostat Continuum

Further, only the continuum of one-rotor gyrostats is considered. In this case, the ether plays the role of an external factor with respect to the continuum under study. The influence of the ether on the one-rotor gyrostats is modeled by the moment of viscous damping the structure of which is chosen in accordance with the results obtained by solving the model problems considered above. Thus, by eliminating the ether, a nonconservative model of the one-rotor gyrostat continuum is obtained.

Below the following notations are used: $\mathbf{r}$ is a position vector of some point in space; ρ_* is the mass density at the reference configuration; $\mathbf{I} = I\mathbf{E}$ and $\mathbf{J} = J\mathbf{E}$ are the mass densities of inertia tensors of the carrier bodies and the rotors, respectively, where $\mathbf{E}$ is the unit tensor; $\mathbf{u}(\mathbf{r}, t)$ is the displacement vector; $\mathbf{v}(\mathbf{r}, t)$ is the velocity vector; $\boldsymbol{\varphi}(\mathbf{r}, t)$ and $\tilde{\boldsymbol{\omega}}(\mathbf{r}, t)$ are the rotation vector and the angular velocity vector of the carrier bodies; and $\boldsymbol{\theta}(\mathbf{r}, t)$ and $\boldsymbol{\omega}(\mathbf{r}, t)$ are the rotation vector and the angular velocity vector of the

rotors. The linear theory is considered. Therefore, the kinematic relations have the form

$$\mathbf{v} = \frac{d\mathbf{u}}{dt}, \qquad \tilde{\boldsymbol{\omega}} = \frac{d\boldsymbol{\varphi}}{dt}, \qquad \boldsymbol{\omega} = \frac{d\boldsymbol{\theta}}{dt}. \tag{1}$$

The balance equations of the linear momentum for the gyrostats and of the angular momentum for the carrier bodies of gyrostats are

$$\nabla \cdot \boldsymbol{\tau} + \rho_* \mathbf{f} = \rho_* \frac{d\mathbf{v}}{dt},$$
$$\nabla \cdot \boldsymbol{\mu} + \boldsymbol{\tau}_\times + \rho_* \mathbf{m} = \rho_* I \frac{d\tilde{\boldsymbol{\omega}}}{dt}. \tag{2}$$

Here ∇ is the gradient operator; $\boldsymbol{\tau}$ is the stress tensor; $\boldsymbol{\mu}$ is the moment stress tensor modeling the interaction of the carrier bodies of gyrostats; $\mathbf{f}$ is the mass density of external forces; and $\mathbf{m}$ is the mass density of external moments acting on the carrier bodies of gyrostats. The balance equation of the angular momentum for the rotors of gyrostats has the form

$$\nabla \cdot \mathbf{T} + \rho_* \mathbf{L} = \rho_* J \frac{d\boldsymbol{\omega}}{dt}, \tag{3}$$

where $\mathbf{T}$ is the moment stress tensor modeling the interaction of the rotors of gyrostats and $\mathbf{L}$ is the mass density of external moments acting on the rotors.

In view of Eqs. (2) and (3), the energy balance equation is written as

$$\frac{d(\rho_* U)}{dt} = \boldsymbol{\tau}^T \cdot\cdot \frac{d\boldsymbol{\varepsilon}}{dt} + \boldsymbol{\mu}^T \cdot\cdot \frac{d\boldsymbol{\kappa}}{dt} + \mathbf{T}^T \cdot\cdot \frac{d\boldsymbol{\vartheta}}{dt}, \tag{4}$$

where U is the internal energy density per unit mass and the double scalar product is defined as $\mathbf{ab} \cdot\cdot \mathbf{cd} = (\mathbf{b} \cdot \mathbf{c})(\mathbf{a} \cdot \mathbf{d})$. The strain tensors $\boldsymbol{\varepsilon}$, $\boldsymbol{\kappa}$, and $\boldsymbol{\vartheta}$ are determined by the formulas

$$\boldsymbol{\varepsilon} = \nabla \mathbf{u} + \mathbf{E} \times \boldsymbol{\varphi}, \qquad \boldsymbol{\kappa} = \nabla \boldsymbol{\varphi}, \qquad \boldsymbol{\vartheta} = \nabla \boldsymbol{\theta}. \tag{5}$$

The Main Hypotheses

Further a special case of the theory of one-rotor gyrostat continuum based on two hypotheses is considered.

Hypothesis 1. Vector $\mathbf{L}$ is a sum of the moment $\mathbf{L}_h$ characterizing external actions of all sorts and the moment of linear viscous damping

$$\mathbf{L}_f = -\beta J \boldsymbol{\omega}, \tag{6}$$

where β is the coefficient of damping. The moment $\mathbf{L}_f$ models the influence of the ether (the body-points positioned in the space between the gyrostats) that causes the dissipation of the rotors energy. The moment $\mathbf{L}_h$ models the influence of external ponderable bodies that is passed by means of the ether. It can model actions of various physical nature, e.g., heat supply, electromagnetic excitation, or some kind of radiation. The main difference between the moment $\mathbf{L}_h$ and the moment $\mathbf{L}_f$ is the fact that the moment $\mathbf{L}_h$ occurs only when there are some ponderable bodies, whereas the moment $\mathbf{L}_f$ occurs regardless of the presence or absence of other bodies. The structure of moment (6) is chosen in accordance with the results obtained by solving the model problems considered above.

Hypothesis 2. The moment stress tensor $\mathbf{T}$ characterizing the interactions between the rotors is the spherical part of tensor

$$\mathbf{T} = T\,\mathbf{E}. \tag{7}$$

Assumption (7) is based on the following interpretations. The interaction of the carrier bodies of gyrostats is attributed to the mechanical processes. The interaction of the rotors of gyrostats models thermal processes, and the interaction of the carrier bodies and the rotors provides the interplay of mechanical and thermal processes. The moment interaction between the rotors is considered to be analogy of temperature. Since temperature is a scalar, the moment stress tensor $\mathbf{T}$ must be characterized by one scalar quantity. Hence, it must be the spherical part of tensor (see Eq. (7)).

Thermodynamic Analogies

In view of Eq. (7), the energy balance equation (4) is reduced to the form

$$\frac{d(\rho_* U)}{dt} = \boldsymbol{\tau}^T \cdot\cdot \frac{d\boldsymbol{\varepsilon}}{dt} + \boldsymbol{\mu}^T \cdot\cdot \frac{d\boldsymbol{\kappa}}{dt} + T\,\frac{d\vartheta}{dt}, \qquad \vartheta = \operatorname{tr}\boldsymbol{\vartheta}. \tag{8}$$

If Eq. (8) is considered to be the energy balance equation for the classical medium, then the last term on the right-hand side of this equation should be interpreted as the thermodynamic one. Since the quantity T has the sense of temperature analogy, the quantity ϑ acquires the meaning of volume density of entropy analogy. The units of measurement of the temperature analogy and the entropy analogy that are introduced within the framework of the considered model are different from the standard units of measurement of temperature and entropy. Indeed, the unit of measurement of T is N/m, whereas the unit of measurement of temperature is kelvin; the unit of measurement of ϑ is 1/m, whereas the unit of measurement of volume density of entropy is $\mathrm{J/(m^3\,K)}$. This obstacle can be overcome by introducing a normalization factor a and changing the variables:

$$T = aT_a, \quad \vartheta = \frac{1}{a}\,\vartheta_a, \quad \boldsymbol{\theta} = \frac{1}{a}\,\boldsymbol{\theta}_a, \quad \boldsymbol{\omega} = \frac{1}{a}\,\boldsymbol{\omega}_a, \quad \mathbf{L}_h = a\mathbf{L}_h^a, \quad J = a^2 J_a. \tag{9}$$

Here T_a is the temperature that can be measured by a thermometer. Its unit of measurement is kelvin. Correspondingly, ϑ_a is the volume density of entropy. Its unit of measurement is $\mathrm{J/(m^3\,K)}$. In the case of the linear theory, the normalization factor a can be eliminated from all equations.

A Model of Heat-Conductive Elastic Material

Now the model of continuum satisfying the hypotheses stated above is considered. In view of the hypotheses, the balance equation of the angular momentum for rotors takes the form

$$\nabla T_a - \rho_* \beta J_a \boldsymbol{\omega}_a + \rho_* \mathbf{L}_h^a = \rho_* J_a \frac{d\boldsymbol{\omega}_a}{dt}. \tag{10}$$

In view of Eqs. (1), (5), (8), and (9), from Eq. (10), it follows one of the forms of the heat conduction equation, namely,

$$\Delta T_a - \rho_* \beta J_a \frac{d\vartheta_a}{dt} - \rho_* J_a \frac{d^2\vartheta_a}{dt^2} = -\rho_* \nabla \cdot \mathbf{L}_h^a, \tag{11}$$

where the term $\rho_* \nabla \cdot \mathbf{L}_h^a$ plays the role of a heat supply. The heat conduction Eq. (11) can be reduced to the conventional form. In order to do this, it is necessary to express ϑ_a in terms of temperature and strain tensors by using the constitutive equations that are given below.

According to the energy balance equation (8), the internal energy density is a function of the strain tensors $\boldsymbol{\varepsilon}$, $\boldsymbol{\kappa}$ and the scalar strain measure ϑ (or the volume density of entropy ϑ_a that is the same thing). In the linear theory, the internal energy density $\rho_* U$ is assumed to be a quadratic form of the quantities listed above. In this case, the constitutive equations are written as

$$\begin{aligned} \boldsymbol{\tau}^T &= \boldsymbol{\tau}_0^T + {}^4\mathbf{C}_1 \cdot\cdot \boldsymbol{\varepsilon} + {}^4\mathbf{C}_2 \cdot\cdot \boldsymbol{\kappa} \\ &\quad + \mathbf{C}_4\,(\vartheta_a - \vartheta_a^*), \boldsymbol{\mu}^T = \boldsymbol{\mu}_0^T + \boldsymbol{\varepsilon} \cdot\cdot {}^4\mathbf{C}_2 \\ &\quad + {}^4\mathbf{C}_3 \cdot\cdot \boldsymbol{\kappa} + \mathbf{C}_5\,(\vartheta_a - \vartheta_a^*), \\ T_a &= T_a^* + \boldsymbol{\varepsilon} \cdot\cdot \mathbf{C}_4 + \boldsymbol{\kappa} \cdot\cdot \mathbf{C}_5 + C_6\,(\vartheta_a - \vartheta_a^*). \end{aligned} \tag{12}$$

Here $\boldsymbol{\tau}_0$ and $\boldsymbol{\mu}_0$ are the initial stresses; T_a^* is the value of absolute temperature at which the thermodynamic parameters are determined; ϑ_a^* is the corresponding value of volume density of entropy; ${}^4\mathbf{C}_1$, ${}^4\mathbf{C}_2$, and ${}^4\mathbf{C}_3$ are the fourth-rank stiffness tensors; $\mathbf{C}_4$ and $\mathbf{C}_5$ are the second-rank tensors characterizing the interplay of mechanical and thermodynamic processes; and C_6 is the scalar quantity characterizing the specific heat.

In view of the foregoing analogies between the mechanical and thermodynamic quantities, the set of Eqs. (1), (2), (5), (9), (11), and (12) can be considered as the mathematical description of a conventional material which possesses elastic and thermodynamic properties.

An Isotropic Chiral Medium

The model of continuum discussed above contains both polar and axial material tensors. The fourth-rank tensors ${}^4\mathbf{C}_1$ and ${}^4\mathbf{C}_3$ and the second-rank tensor $\mathbf{C}_5$ are polar. The fourth-rank tensor ${}^4\mathbf{C}_2$ and the second-rank tensor $\mathbf{C}_4$ are axial. In the case of an isotropic chiral medium, polar and axial tensors have the same structure. To be exact, the fourth-rank tensors and the second-rank ones have the form

$$
\begin{aligned}
{}^4\mathbf{C}_1 &= C_1\mathbf{E}\mathbf{E} + C_2\sum_{i=1}^{3}\mathbf{e}_i\mathbf{E}\,\mathbf{e}_i \\
&\quad + C_3\sum_{i=1}^{3}\sum_{j=1}^{3}\mathbf{e}_i\mathbf{e}_j\mathbf{e}_i\mathbf{e}_j, \\
\mathbf{C}_4 &= C_4\mathbf{E}, \qquad (13)
\end{aligned}
$$

where $\mathbf{e}_1$, $\mathbf{e}_2$, and $\mathbf{e}_3$ are the mutually orthogonal unit vectors. In the case of an isotropic non-chiral medium, the polar tensors ${}^4\mathbf{C}_1$, ${}^4\mathbf{C}_3$, and $\mathbf{C}_5$ have the form (13), and the axial tensors ${}^4\mathbf{C}_2$ and $\mathbf{C}_4$ are equal to zero. At the same time, it is known that tensor $\mathbf{C}_4$ characterizing the thermal expansion is not equal to zero. That is why, the isotropic media that are chiral with respect to the microstructure are considered in the presented theory.

The question is, what sorts of engineering materials can be qualified as chiral media? It is obvious, it depends on what properties of a material and what processes in the material are that we want to study. If we want to study only the mechanical properties and processes, then almost all materials can be qualified as non-chiral media. The only exceptions are materials consisting of sufficiently large particles that do not have a mirror symmetry, such as materials consisting of large polymer molecules having a helical structure or materials containing the DNA molecules. If we want to model a conventional material taking into account not only its mechanical properties but in addition some other its physical properties, then a representative volume of the continuum must reflect the properties of the material at the microlevel, i.e., the properties of the material that are conditioned by the state of its atoms. Atoms consist of elementary particles with spin. The presence of spin eliminates the mirror symmetry. That is why, in order to model a conventional material taking into account not only its mechanical properties but in addition some other its physical properties, we should consider this material as a chiral medium. Certainly, the foregoing assertion concerns only the method of modeling that is based on using the Cosserat continuum with the microstructure.

The Hyperbolic Thermoelasticity and the Classical One

It is known that when describing mechanical processes in three-dimensional media, the moment interactions and the rotation inertia can be neglected. In accordance with this fact, it is assumed that $\boldsymbol{\mu} = \mathbf{0}$, $\mathbf{m} = \mathbf{0}$, $I = 0$, and hence, $\boldsymbol{\tau} = \boldsymbol{\tau}^T$. For the medium that is chiral with respect to the microstructure, in view of Eq. (13), the constitutive equations (12) take the form

$$
\begin{aligned}
\boldsymbol{\tau} &= \boldsymbol{\tau}_0 + C_1\varepsilon\mathbf{E} + (C_2 + C_3)\boldsymbol{\varepsilon}^s \\
&\quad + C_4\,(\vartheta_a - \vartheta_a^*)\mathbf{E}, \quad \varepsilon = \operatorname{tr}\boldsymbol{\varepsilon}^s, \\
T_a &= T_a^* + C_4\varepsilon + C_6\,(\vartheta_a - \vartheta_a^*), \\
\boldsymbol{\varepsilon}^s &= \frac{1}{2}\left(\nabla\mathbf{u} + \nabla\mathbf{u}^T\right). \qquad (14)
\end{aligned}
$$

The parameters of the model are chosen as follows:

$$
\begin{aligned}
C_1 &= K_{ad} - \frac{2}{3}G, \quad C_2 + C_3 = G, \\
C_4 &= -\frac{\alpha K_{iz}T_a^*}{\rho_* c_v}, \quad C_6 = \frac{T_a^*}{\rho_* c_v}, \\
\beta J_a &= \frac{T_a^*}{\rho_*\lambda}. \qquad (15)
\end{aligned}
$$

where K_{iz} and $K_{ad} = K_{iz} + \alpha^2 K_{iz}^2 T_a^*/(\rho_* c_v)$ are the isothermal and adiabatic modules of compression, G is the shear modulus, α is the volume coefficient of thermal expansion, c_v is the

T

specific heat at constant volume, and λ is the heat conduction coefficient. It is easy to see that the inverse coefficient of heat conduction is directly proportional to the dynamic coefficient of damping $\rho_* \beta J_a$, the inverse specific heat is directly proportional to the angular stiffness C_6 characterizing the moment interaction between the rotors, and the volume coefficient of thermal expansion is directly proportional to the stiffness C_4 characterizing the dependence of the stress tensor on the angular strains and the dependence of the moment stress tensor on the linear strains.

In view of Eq. (15), the set of Eqs. (2), (11), and (14) can be reduced to the form

$$\begin{gathered}
\nabla \cdot \boldsymbol{\tau} + \rho_* \mathbf{f} = \rho_* \frac{d^2 \mathbf{u}}{dt^2}, \\
\boldsymbol{\tau} = \boldsymbol{\tau}_0 + \left(K_{iz} - \frac{2}{3} G \right) \varepsilon \mathbf{E} + 2G \, \boldsymbol{\varepsilon}^s - \alpha K_{iz} (T_a - T_a^*) \, \mathbf{E}, \\
\Delta T_a - \frac{\rho_* c_v}{\lambda} \left(\frac{dT_a}{dt} + \frac{1}{\beta} \frac{d^2 T_a}{dt^2} \right) = \frac{\alpha K_{iz} T_a^*}{\lambda} \left(\frac{d\varepsilon}{dt} + \frac{1}{\beta} \frac{d^2 \varepsilon}{dt^2} \right) - \rho_* \nabla \cdot \mathbf{L}_h^a.
\end{gathered} \tag{16}$$

The parameter β^{-1} is usually called the heat flux relaxation time. If the parameter β^{-1} becomes zero on conditions that the product βJ_a remains finite, then the set of Eqs. (16) is equivalent to the classical statement of coupled problem of thermoelasticity (see, e.g., Nowacki 1976). If the parameter β^{-1} is not equal to zero, then Eq. (16) is the statement of problem of the hyperbolic type thermoelasticity (see Lord and Shulman 1967).

Nonlinear Models of Heat Transfer: State of the Art

Nonlinear thermal processes are actively studied and discussed in the modern literature. Without claiming to be an exhaustive literature review, we indicate the main research areas in the field of nonlinear thermal conductivity and denote a place of the presented theory among the other models.

Many papers covering only mathematical questions are regularly published for several decades. Various aspects of constructing analytical, semi-analytic, and numerical solutions of the nonlinear heat conduction equations are discussed in such papers see, e.g., Campo (1982), Jordan et al. (1987), Polyanin et al. (2000), Ebadian and Darania (2008), and Habibi et al. (2015). Such works usually deal with the simplest nonlinear heat conduction equations. The nonlinearity of these equations consists in the fact that the material constants of the linear equations are replaced by some functions of temperature (more often by polynomials). Among the mathematical works, it is worth mentioning the papers where the authors consider laser heat sources (see, e.g., Fong et al. 2010), as this type of thermal influences is most often found in the modern literature. Another large group of publications consists of applied works, which are devoted to modeling nonlinear thermal processes in technical devices (see, e.g., Grudinin et al. 2011; Chaibi et al. 2012; Huang et al. 2012; Markides et al. 2013). In such works, the mutual influence of thermal processes and processes of other physical nature (optical, electrical, magnetic) is usually taken into account. Other distinctive features of applied works are the use of numerical methods, the use of parameters of specific technical devices in calculations, and the comparison of modeling results with the experimental data. The models of nonlinear thermal processes in the widest scale range, from geophysical processes (see, e.g., Mottaghy and Rath 2006), up to biological processes at the molecular level (see, e.g., LeMesurier 2008), are presented in the modern literature. There are a large number of papers devoted to studying nonlinear effects associated with thermal radiation (see, e.g., Khandekar et al.

2015; Ananth et al. 2015). There exist a variety of mathematical models used to describe various thermal processes. Some of them are based on classical concepts, and others are based on quantum-mechanical concepts. However, purely empirical relations, which are not based on any models, play an important role in the majority of nonlinear theories.

The main feature of the linear theory presented in this paper and its nonlinear analogue presented in Ivanova (2017) is that these theories provide the description of two fundamentally different processes of heat transfer (heat conduction and thermal radiation) within the framework of one model. Another feature of the present approach is the fact that it is based on the mechanical model different from those used in statistical physics and quantum mechanics.

Cross-References

- Cosserat Media
- Dispersion Relations for the Coupled Hyperbolic Thermoelasticity
- Thermoelastic Waves in a Medium with Heat-flux Relaxation
- Zhilin, Pavel Andreevich

References

Ananth P, Dinesh A, Sugunamma V, Sandeep N (2015) Effect of nonlinear thermal radiation on stagnation flow of a Casson fluid towards a stretching sheet. Ind Eng Lett 5(8):70–79

Bird RB, Armstrong RC, Hassager O (1987) Dynamics of polymeric liquids. Fluid mechanics, vol 1. Wiley, New York

Campo A (1982) Estimate of the transient conduction of heat in materials with linear thermal properties based on the solution for constant properties. Heat Mass Transf 17(1):1–9

Chaibi M, Fernández T, Mimouni A, Rodriguez-Tellez T, Tazón A, Mediavilla A (2012) Nonlinear modeling of trapping and thermal effects on GaAs and GaN MESFET/HEMT devices. Progr Electromagn Res 124:163–186

Ebadian A, Darania P (2008) Study of exact solutions of nonlinear heat equations. Comput Appl Math 27(2):107–121

Fong E, Lam TT, Davis SE (2010) Nonlinear heat conduction in isotropic and orthotropic materials with laser heat source. J Thermophys Heat Transf 24(1):104–111

Giesekus H (1985) Constitutive equations for polymer fluids based on the concept of configuration-dependent molecular mobility: a generalized mean-configuration model. J Non-Newton 17:349–372

Gliozzi M (1965) Storia della fisica. Storia delle scienze, vol 2. UTET, Torino

Grudinin I, Lee H, Chen T, Vahala K (2011) Compensation of thermal nonlinearity effect in optical resonators. Opt Express 19(8):7365–7372

Habibi M, Oloumi M, Hosseinkhani H, Magidi S (2015) Numerical investigation into the highly nonlinear heat transfer equation with bremsstrahlung emission in the inertial confinement fusion plasmas. Contrib Plasma Phys 55(9):677–684

Huang C, Fan J, Zhu L (2012) Dynamic nonlinear thermal optical effects in coupled ring resonators. AIP Adv 2(032131):1–8

Ivanova EA (2010) Derivation of theory of thermoviscoelasticity by means of two-component medium. Acta Mech 215:261–286

Ivanova EA (2011) On one model of generalized continuum and its thermodynamical interpretation. In: Altenbach H, Maugin G, Erofeev V (eds) Mechanics of generalized continua. Springer, Berlin, pp 151–174

Ivanova EA (2012) Derivation of theory of thermoviscoelasticity by means of two-component Cosserat continuum. Tech Mech 32:273–286

Ivanova EA (2013) Description of mechanism of thermal conduction and internal damping by means of two component Cosserat continuum. Acta Mech 225:757–795

Ivanova EA (2017) Description of nonlinear thermal effects by means of two-component Cosserat continuum. Acta Mech 228:2299–234

Ivanova EA, Krivtsov AM, Zhilin PA (2007) Description of rotational molecular spectra by means of an approach based on rational mechanics. Z Angew Math Mech 87(2):139–149

Jehring L (1984) Kinetic theory of a gas with internal degrees of freedom. J Appl Math Mech 64(12):529–536

Jordan A, Khaldi S, Benmouna M, Borucki A (1987) Study of non-linear heat transfer problems. Revue de Physique Appliquee 22(1):101–105

Khandekar C, Pick A, Johnson SG, Rodriguez AW (2015) Radiative heat transfer in nonlinear Kerr media. Phys Rev B 91(115406):1–9

LeMesurier B (2008) Modeling thermal effects on nonlinear wave motion in biopolymers by a stochastic discrete nonlinear Schrödinger equation with phase damping. Contin Dyn Syst Ser S 1(2):317–327

Lord H, Shulman Y (1967) A generalized dynamical theory of thermoelasticity. J Mech Phys Solids 15:299–309

Markides CN, Osuolale A, Solanki R, Stan GBV (2013) Nonlinear heat transfer processes in a two-phase thermofluidic oscillator. Appl Energy 104:958–977

Maxwell JC (1860) Illustrations of the dynamical theory of gases. W. D. NIVEN, M.A., F.R.S.(ed) In: The scientific papers of James Clerk Maxwell, vol 1. Dover Publications, New York
Mottaghy D, Rath V (2006) Latent heat effects in subsurface heat transport modeling and their impact on palaeotemperature reconstructions. Geophys J Int 164:236–245
Müller I (2007) A history of thermodynamics: the doctrine of energy and entropy. Springer, Berlin
Nowacki W (1976) Dynamic problems of thermoelasticity. Noordhoof International, Leyden
Polyanin AD, Zhurov AI, Vyaz'min AV (2000) Exact solutions of nonlinear heat- and mass-transfer equations. Theor Found Chem Eng 34(5):403–415
Rosenberger F (1887) Die geschichte der physik. Dritter teil. Geschichte der physik in den letzten hundert jahren. Fr. Vieweg und Sohn, Braunschweig
Warner J, Harold R (1972) Kinetic theory and rheology of dilute suspensions of finitely extendible dumbbells. Ind Eng Chem Fund 11(3):379–387
Whittaker E (1910) A history of the theories of aether and electricity. The classical theories. Thomas Nelson and Sons Ltd, London
Zhilin PA (2001, in Russian) Theoretical mechanics. Polytechnic University Publishing House, St. Petersburg
Zhilin PA (2003, in Russian) Theoretical mechanics. Fundamental laws of mechanics. Polytechnic University Publishing House, St. Petersburg
Zhilin PA (2006a, in Russian) Advanced problems in mechanics, vol 1. IPME RAS, St. Petersburg
Zhilin PA (2006b) Advanced problems in mechanics, vol 2. IPME RAS, St. Petersburg
Zhilin PA (2012, in Russian) Rational continuum mechanics. Polytechnic University Publishing House, St. Petersburg
Zhilin PA (2015, in Russian) Rigid body dynamics. Polytechnic University Publishing House, St. Petersburg

Thermal Phenomena by Means of Continuum with Microstructure

▸ Thermal Effects by Means of Two-Component Cosserat Continuum

Thermal Processes by Means of Micropolar Continuum

▸ Thermal Effects by Means of Two-Component Cosserat Continuum

Thermal Stress and Low-Cycle Fatigue

▸ Creep Fatigue

Thermal Stresses

▸ Fractional Calculus in Thermoelasticity
▸ Macromechanics of Laminates

Thermal Waves

▸ Nonlocal Transport Equations for Small Systems and Fast Processes

Thermodynamic Processes by Means of Continuum with Rotational Degrees of Freedom

▸ Thermal Effects by Means of Two-Component Cosserat Continuum

Thermoelastic Diffusion

▸ Thermoelastic Diffusion Theory for Piezoelectric Materials

Thermoelastic Diffusion Theory for Piezoelectric Materials

Moncef Aouadi
UR Systèmes dynamiques et applications, Ecole Nationale d'Ingénieurs de Bizerte, Université de Carthage, Menzel Abderrahman, Tunisia

Synonyms

Green-Naghdi theory; Piezoelectric; Thermoelastic diffusion

Definition

Piezoelectricity is the ability of some materials to generate an electric charge in response to applied mechanical stress.

Cross effects of heat and mass diffusion exchange with the environment arising from and inside nuclear reactors influence their design and operations. Thermoelastic diffusion material is an elastic deformable solid allowing for changes in temperature and mass diffusion. Diffusion can be defined as the random walk of an ensemble of particles from regions of high concentration to regions of lower concentration. Thermodiffusion in an elastic solid is due to coupling of the fields of temperature, mass diffusion, and that of strain.

Green and Naghdi theory of types I, II, and III are three thermomechanical theories of deformable continua. The type I coincides with the classical heat conduction based on Fourier's law. The type II and III models are based on entropy balance law rather than the usual entropy inequality and formulated by the thermal displacement. The type II and III models overcome the unnatural property of type I model (based on Fourier's law) of infinite propagation speed and imply finite wave propagation.

Overview

Since the discovery of the piezoelectric effect by the Curie brothers (Curie and Curie 1880), considerable research activity has been focused on understanding the origins of the piezoelectric effect and in developing materials with desirable piezoelectric characteristics for applications as sensors and actuators. The theory of thermo-piezoelectricity was first proposed by Mindlin (1961, 1979). The physical laws for the thermo-piezoelectric materials have been explored by Nowacki (1978, 1979). It is well-known that heat conduction based on the classical Fourier's law allows the phenomena of "infinite diffusion velocity." This is not well accepted from a physical point of view. Nonclassical thermal laws came into existence during the last decades to eliminate these shortcomings. One of these theories may be mentioned that of Green and Naghdi (1991, 1993, 1995).

However, the effects of the elastic, electric, thermal, and diffusion fields together have never been studied simultaneously. By combining all these fields, three nonlinear and linear models are derived here in the frame of Green-Naghdi models of types I, II, and III (Green and Naghdi 1991, 1993, 1995). The general equations of motion and constitutive equations are derived for a general anisotropic piezoelectric thermoelastic diffusion material. The type I model coincides with the classical one, where heat and diffusion waves propagate with infinite velocity. In type II model, the heat and diffusion waves allowed to propagate with finite velocity but without dissipating energy. The type III model permits propagation of both thermal and diffusion waves at finite speeds with dissipating energy.

Nonlinear Theory

A continuous body is considered that at time τ_0 occupies a bounded region Ω of the Euclidean three-dimensional space with smooth boundary $\partial\Omega$. The configuration Ω is taken as reference configuration and refers the motion of the continuum to the reference configuration. Fixed system of rectangular cartesian axes, X_i denotes the coordinates of a point in the reference configuration and with x_i the coordinates of the same point at time t, where $x_i = \chi_i(X_1, X_2, X_3, t)$ is continuously differentiable.

As in theories of single materials, in mixture theory, each constituent can be assigned a reference configuration and a motion $\mathbf{x} = \chi_a(\mathbf{X}_a, t)$, where χ_a is the deformation function for the ath constituent, $\mathbf{X}_a$ is the position of a particle of the ath constituent in its reference configuration, and $\mathbf{x}$ is the spatial position occupied at the time t by the particle labeled $\mathbf{X}_a$. The velocity of $\mathbf{X}_a$ at time t is defined by $\mathbf{x}'_a = \partial\chi_a(\mathbf{X}_a, t)/\partial t$, where the prime denotes the material derivative following the motion of the ath constituent.

According to the mixture theory (Bowen 1976), an immobile parent and N mobile constituents occupy a volume B with surface ∂B. Denote $\mathbf{x}_p(\mathbf{X}, t)$ and $\mathbf{x}_m(\mathbf{X}, t)$ as the locations of the constituent where the subscript p refers to the immobile parent part with density $\tilde{\rho}_p(\mathbf{X}, t)$ and m refers to the mobile constituents with density $\tilde{\rho}_m(\mathbf{X}, t)$. Thus the mixture density, relative velocity of the constituents, and the mixture mean velocity are

$$\tilde{\rho} = \tilde{\rho}_p + \sum_{m=1}^{N} \tilde{\rho}_m, \quad \mathbf{x}'_p = 0, \mathbf{x}'_m = \frac{\partial \mathbf{x}_m}{\partial t}(\mathbf{X}_m, t), \quad \dot{\mathbf{x}} = \frac{1}{\tilde{\rho}} \sum_{m=1}^{N} \tilde{\rho}_m \mathbf{x}'_m, \tag{1}$$

where

$$\tilde{\rho} d\tilde{v} = \rho dv, \quad \tilde{\rho}_p d\tilde{v} = \rho_p dv, \quad \tilde{\rho}_m d\tilde{v} = \rho_m dv. \tag{2}$$

Here the quantities with " ˜ " are used for the current configuration. The quantities without " ˜ " are used for reference configuration.

In the material description, the balance of mass for each constituent and the balance of mass for the mixture (as a whole) may be expressed, in the current configuration, as

$$\frac{\partial}{\partial t} \int_{\tilde{B}} \tilde{\rho}_m d\tilde{v} = - \int_{\partial \tilde{B}} \tilde{\mathbf{n}} \cdot (\mathbf{x}'_m - \dot{\mathbf{x}}) \tilde{\rho}_m d\tilde{a}, \quad \frac{\partial}{\partial t} \int_{\tilde{B}} \tilde{\rho}_p d\tilde{v} = \int_{\partial \tilde{B}} \tilde{\mathbf{n}} \cdot \dot{\mathbf{x}} \, \tilde{\rho}_p \, d\tilde{a}, \tag{3}$$

where we have neglected the rate of mass supplied to the mth constituent per unit volume caused by chemical reactions. The balance equation for $\tilde{\rho}$ follows from Eqs. (1) and (3). It has the form

$$\frac{\partial}{\partial t} \int_{\tilde{B}} \tilde{\rho} d\tilde{v} = 0. \tag{4}$$

Introducing the reference mass densities by means of relations (2) and taking into account the known relation between the unit normal $\tilde{\mathbf{n}}$ to the boundary $\partial \tilde{B}$ in the current configuration and the unit normal $\mathbf{n}$ to the boundary ∂B in the reference configuration, namely,

$$\tilde{\mathbf{n}} d\tilde{a} = \mathbf{n} \cdot \operatorname{grad} \mathbf{x} \, \frac{\rho}{\tilde{\rho}} da$$

we can write Eqs. (3) and (4) in the reference configuration as

$$\frac{\partial}{\partial t} \int_{B} \rho_m dv = - \int_{\partial B} \mathbf{n} \cdot \operatorname{grad} \mathbf{x} \cdot (\mathbf{x}'_m - \dot{\mathbf{x}}) \rho_m da, \quad \frac{\partial}{\partial t} \int_{B} \rho_p dv = \int_{\partial B} \mathbf{n} \cdot \operatorname{grad} \mathbf{x} \cdot \dot{\mathbf{x}} \, \rho_p \, da,$$

$$\frac{\partial}{\partial t} \int_{B} \rho dv = 0.$$

Using the divergence theorem, we obtain

$$\dot{\rho}_m + \operatorname{div}(\rho_m \operatorname{grad} \mathbf{x} \cdot (\mathbf{x}'_m - \dot{\mathbf{x}})) = 0, \quad \dot{\rho}_p - \operatorname{div}(\rho_p \operatorname{grad} \mathbf{x} \cdot \dot{\mathbf{x}}) = 0, \quad \dot{\rho} = 0, \tag{5}$$

where

$$\dot{\rho}_m = \frac{\partial \rho_m}{\partial t}(\mathbf{X}, t),$$
$$\dot{\rho}_p = \frac{\partial \rho_p}{\partial t}(\mathbf{X}, t),$$
$$\dot{\rho} = \frac{\partial \rho}{\partial t}(\mathbf{X}, t).$$

If ρ does not depend of space coordinates, Eq. $(5)_1$ can be rewritten as

$$\dot{C}_m = -\text{div}(C_m \text{grad}\,\mathbf{x} \cdot V_m), \tag{6}$$

where C_m is the mass concentration of the mobile constituents defined as $C_m = \rho_m/\rho$ and $V_m = \mathbf{x}'_m - \dot{\mathbf{x}}$. If we define the constituent mass flux by $\eta_m = C_m \text{grad}\,\mathbf{x} \cdot V_m$, then the balance of mass for each constituent requires that (balance law)

$$\dot{C}_m = -\text{div}\,\eta_m \quad \text{or} \quad \dot{C} = -\eta_{k,k}. \tag{7}$$

Moreover, following the arguments of Green and Naghdi (1991, 1993, 1995), for every subregion B of Ω and every time t, the balance equations for the energy and the entropy are

$$\int_B \rho(\dot{x}_i \ddot{x}_i + \dot{e})dv = \int_B \rho(f_i \dot{x}_i + sT)dv + \int_B E_i \dot{D}_i dv + \int_{\partial B} (t_i \dot{x}_i - q)da,$$
$$\int_B \rho \dot{S} dv = \int_B \rho(s + \xi)dv - \int_{\partial B} \Phi da. \tag{8}$$

Here e, f_i, s, S, and ξ are the internal energy, the body force, the external rate of supply of entropy, the entropy, and the internal rate of production of entropy, respectively, per unit mass. T is the absolute temperature, D_i the electric displacement field, E_i the electric intensity, t_i is the stress vector, and q and Φ are the internal flux of heat and entropy, respectively, per unit mass measured per unit area of the surface ∂B.

By using the invariance property under superposed rigid translations, from Eq. (8), it follows the momentum balance equation

$$\int_B \rho \ddot{x}_i dv = \int_B \rho f_i dv + \int_{\partial B} t_i da \tag{9}$$

and the angular momentum balance equation

$$\hat{T}_{ik} = \hat{T}_{ki}$$

where $\hat{T}_{ik}$ is the second Piola-Kirchhoff stress tensor, whereas the first Piola-Kirchhoff stress tensor satisfies the relation $x_{i,j} T_{jk} = x_{k,j} T_{ji}$. The first and second Piola-Kirchhoff stress tensors are related as $\hat{T}_{ik} = x_{i,j} T_{jk}$. Moreover, under suitable hypotheses of regularity, the classical technique of the Cauchy tetrahedron applied to Eqs. $(7)_2$, (8) and (9) yields

$$\Phi = \Phi_k n_k,$$
$$t_i = T_{ik} n_k,$$
$$q = q_k n_k,$$
$$\eta = \eta_k n_k, \tag{10}$$

where Φ_k are the components of the entropy flux vector, q_k are the components of the heat flux vector, η_k are the components of the flux of mass diffusion, and n_i are the components of the unit outward normal to ∂B. The electric field that develops in piezoelectrics can assumed to be quasi-static because the velocity of the elastic waves is much smaller than the velocity of electromagnetic waves. Therefore, the magnetic field M, due to the elastic waves is negligible. This fact implies that rot $E = \frac{\partial M}{\partial t} \approx 0$; hence the

Maxwell's equations for the quasi-static electric fields become

$$D_{j,j} = \varphi, \qquad E_k = -\phi_{,k}, \tag{11}$$

where E_i are the components of the electric field, D_i are the components of the electric displacement, φ is the density of free charge, and ϕ is the electric potential. Thanks to the arbitrariness of B, we obtain the following local form for the balance equations:

$$\begin{aligned} &\rho\ddot{x}_i = T_{ki,k} + \rho f_i, \quad \rho\dot{S} = \rho(s+\xi) - \Phi_{k,k}, \quad \dot{C} = -\eta_{k,k}, \\ &\rho\dot{e} = T_{ki}\dot{x}_{i,k} + E_i\dot{D}_i + \rho sT - q_{k,k}, \quad D_{k,k} = \varphi, \quad E_k = -\phi_{,k}. \end{aligned} \tag{12}$$

We consider the following specific Helmholtz free energy per unit mass

$$\Psi = e - TS - \frac{1}{\rho}E_i D_i. \tag{13}$$

According to Lebon et al. (2006), we assume the following relation

$$T\Phi_k = q_k - P\eta_k, \tag{14}$$

where P is the chemical potential. Combining (12), (13) and (14), we obtain

$$\begin{aligned} \rho(\dot{\Psi} + \dot{T}S) = {} & T_{ki}\dot{x}_{i,k} - \rho\xi T - \Phi_k T_{,k} \\ & - \eta_k P_{,k} + P\dot{C} - \dot{E}_k D_k. \end{aligned} \tag{15}$$

In the following, we distinguish the three types of the Green-Naghdi theory.

(1) *Type I – classical theory*

In the classical context of heat conduction based on Fourier's law, we assume $\xi = 0$ and the following entropy production inequality

$$\rho\dot{S} + \left(\frac{q_i}{T}\right)_{,i} - \left(\frac{P\eta_i}{T}\right)_{,i} - \rho s \geq 0. \tag{16}$$

Inserting $(12)_{2,3}$, (14), and (15) into (16), we obtain the Clausius-Duhem inequality

$$-\rho(\dot{\Psi} + \dot{T}S) + T_{ki}\dot{x}_{i,k} - \frac{1}{T}q_k T_{,k} - \eta_k P_{,k} + P\dot{C} + \frac{1}{T}P\eta_k T_{,k} - \dot{E}_k D_k \geq 0. \tag{17}$$

From (17), one can conclude that the response functions Ψ, T_{kj}, S, P, D_k are assumed to depend on the set of the independent variables $\mathscr{A}_0 = (x_{i,k}, T, C, E_k)$ and function Ψ must satisfy

$$x_{i,j}\frac{\partial\Psi}{\partial x_{k,j}} = x_{k,j}\frac{\partial\Psi}{\partial x_{i,j}}.$$

Thus, the constitutive equations are taken in the form $\mathscr{F} = \widehat{\mathscr{F}}(\mathscr{A}_0)$ and the response functions are assumed of C^1-class. The chain rule gives

$$\dot{\Psi} = \frac{\partial\Psi}{\partial x_{j,k}}\dot{x}_{j,k} + \frac{\partial\Psi}{\partial T}\dot{T} + \frac{\partial\Psi}{\partial C}\dot{C} + \frac{\partial\Psi}{\partial E_k}\dot{E}_k. \tag{18}$$

The comparison of Eqs. (17) and (18) yields

$$\begin{aligned} &-\rho\left(\frac{\partial\Psi}{\partial T} + S\right)\dot{T} - \left(\rho\frac{\partial\Psi}{\partial x_{j,k}} - T_{kj}\right)\dot{x}_{j,k} - \left(\rho\frac{\partial\Psi}{\partial C} - P\right)\dot{C} - \left(\rho\frac{\partial\Psi}{\partial E_k} + D_k\right)\dot{E}_k \\ &\quad - \frac{1}{T}q_k T_{,k} - \eta_k P_{,k} + \frac{1}{T}P\eta_k T_{,k} \geq 0. \end{aligned} \tag{19}$$

From this inequality, we deduce the following constitutive equations:

$$S = -\frac{\partial \Psi}{\partial T}, \quad T_{kj} = \rho \frac{\partial \Psi}{\partial x_{j,k}},$$

$$P = \rho \frac{\partial \Psi}{\partial C}, \quad D_k = -\rho \frac{\partial \Psi}{\partial E_k},$$

$$-\frac{1}{T} q_k T_{,k} - \eta_k P_{,k} + \frac{1}{T} P \eta_k T_{,k} \geq 0. \quad (20)$$

(2) *Type II – dissipationless theory*

Green and Naghdi (1991, 1993, 1995) introduced the thermal displacement α whose derivative coincides with the absolute temperature, i.e., $\dot{\alpha} = T$. This scalar, on the macroscopic scale, is regarded as representing some "mean" thermal displacement magnitude on the molecular scale. In a similar way, we introduce a scalar function β related to the chemical potential by the equation $\dot{\beta} = P$.

The response functions Ψ, T_{kj}, S, P, Φ_k, η_k, D_k, ξ are assumed to depend on the set of the independent variables $\mathscr{A}_1 = (x_{i,k}, T, C, \alpha_{,k}, \beta_{,k}, E_k)$. Thus, the constitutive equations are taken in the form $\mathscr{F} = \widehat{\mathscr{F}}(\mathscr{A}_1)$ and the response functions are assumed of C^1-class. Using the chain rule

$$\dot{\Psi} = \frac{\partial \widehat{\Psi}}{\partial x_{j,k}} \dot{x}_{j,k} + \frac{\partial \widehat{\Psi}}{\partial T} \dot{T} + \frac{\partial \widehat{\Psi}}{\partial C} \dot{C} + \frac{\partial \widehat{\Psi}}{\partial \alpha_{,k}} \dot{\alpha}_{,k} + \frac{\partial \widehat{\Psi}}{\partial \beta_{,k}} \dot{\beta}_{,k} + \frac{\partial \widehat{\Psi}}{\partial E_k} \dot{E}_k, \quad (21)$$

the comparison of Eqs. (15) and (21) yields

$$\left(\rho \frac{\partial \widehat{\Psi}}{\partial T} + \rho S\right) \dot{T} + \left(\rho \frac{\partial \widehat{\Psi}}{\partial x_{j,k}} - T_{kj}\right) \dot{x}_{j,k} + \left(\rho \frac{\partial \widehat{\Psi}}{\partial \alpha_{,k}} + \Phi_k\right) \dot{\alpha}_{,k} + \left(\rho \frac{\partial \widehat{\Psi}}{\partial \beta_{,k}} + \eta_k\right) \dot{\beta}_{,k}$$

$$+ \left(\rho \frac{\partial \widehat{\Psi}}{\partial C} - P\right) \dot{C} + \left(\rho \frac{\partial \widehat{\Psi}}{\partial E_k} + D_k\right) \dot{E}_k + \rho T \xi = 0. \quad (22)$$

The compatibility of the constitutive equations with the energy equation gives

$$\Psi = \widehat{\Psi}(\mathscr{A}_1), \quad S = -\frac{\partial \widehat{\Psi}(\mathscr{A}_1)}{\partial T}, \quad T_{kj} = \rho \frac{\partial \widehat{\Psi}(\mathscr{A}_1)}{\partial x_{j,k}}, \quad \Phi_k = -\rho \frac{\partial \widehat{\Psi}(\mathscr{A}_1)}{\partial \alpha_{,k}}$$

$$\eta_k = -\rho \frac{\partial \widehat{\Psi}(\mathscr{A}_1)}{\partial \beta_{,k}}, \quad P = \rho \frac{\partial \widehat{\Psi}(\mathscr{A}_1)}{\partial C}, \quad D_k = -\rho \frac{\partial \widehat{\Psi}(\mathscr{A}_1)}{\partial E_k}, \quad \xi = 0. \quad (23)$$

T

Equation $\xi = 0$ means that conduction occurs without internal entropy production. For this, type II model is called without energy dissipation.

(3) *Type III – dissipation theory*

For type III, we add the dependency on the temperature gradient $\dot{\alpha}_{,k}$ and on the chemical potential gradient $\dot{\beta}_{,k}$. Hence, the previous response functions (of type II) are assumed to depend on the set of the independent variables:

$$\begin{aligned}\mathscr{A}_2 &= (x_{i,k}, T, C, \alpha_{,k}, \beta_{,k}, \dot{\alpha}_{,k}, \dot{\beta}_{,k}, E_k)\\ &= (x_{i,k}, T, C, \alpha_{,k}, \beta_{,k}, T_{,k}, P_{,k}, E_k).\end{aligned}$$

In this case, using the chain rule

$$\dot{\Psi} = \frac{\partial \widehat{\Psi}}{\partial x_{j,k}}\dot{x}_{j,k} + \frac{\partial \widehat{\Psi}}{\partial T}\dot{T} + \frac{\partial \widehat{\Psi}}{\partial C}\dot{C} + \frac{\partial \widehat{\Psi}}{\partial \alpha_{,k}}T_{,k} + \frac{\partial \widehat{\Psi}}{\partial \beta_{,k}}P_{,k} + \frac{\partial \widehat{\Psi}}{\partial T_{,k}}\dot{T}_{,k} + \frac{\partial \widehat{\Psi}}{\partial P_{,k}}\dot{P}_{,k} + \frac{\partial \widehat{\Psi}}{\partial E_k}\dot{E}_k, \tag{24}$$

the comparison of Eqs. (15) and (24) yields

$$\frac{\partial \widehat{\Psi}}{\partial T_{,k}} = 0\,, \quad \frac{\partial \widehat{\Psi}}{\partial P_{,k}} = 0,$$

that is $\Psi = \widehat{\Psi}(x_{i,k}, T, C, \alpha_{,k}, \beta_{,k}, E_k) = \widehat{\Psi}(\mathscr{A}_1)$, and

$$S = -\frac{\partial \widehat{\Psi}(\mathscr{A}_1)}{\partial T}, \quad T_{kj} = \rho\frac{\partial \widehat{\Psi}}{\partial x_{j,k}}(\mathscr{A}_1), \quad P = \rho\frac{\partial \widehat{\Psi}}{\partial C}(\mathscr{A}_1), \quad D_k = -\rho\frac{\partial \widehat{\Psi}}{\partial E_k}(\mathscr{A}_1) \tag{25}$$

$$\left(\rho\frac{\partial \widehat{\Psi}}{\partial \alpha_{,k}} + \Phi_k\right)T_{,k} + \left(\rho\frac{\partial \widehat{\Psi}}{\partial \beta_{,k}} + \eta_k\right)P_{,k} + \rho T\xi = 0. \tag{26}$$

It is clear that the type III model relies on an entropy balance law, given by (26), rather than an entropy inequality. Equation (26) is imposed to ensure that conduction occurs with internal entropy production, $\xi \neq 0$. For this, type III model is called with energy dissipation.

Linear Theory

The deformations and the changes of temperature, concentration, and electric potential are assumed to be very small with respect to the reference configuration

$$\begin{aligned}x_i - X_i &= u_i = \varepsilon u_i',\\ T - T_0 &= \theta = \varepsilon\theta',\\ C - C_0 &= \gamma = \varepsilon\gamma',\\ \phi - \phi_0 &= \psi = \varepsilon\psi',\end{aligned}$$

where T_0, C_0, and ϕ_0 are, respectively, the (constant) absolute temperature, concentration, and electric potential in the reference configuration, ε is a constant small enough for squares and higher powers to be neglected, and u_i', θ', γ', and ψ' are independent on ε. The linearized version of the balance equations $(12)_{1,3,5,6}$, (14) and the strain tensor are, respectively,

$$\rho\ddot{u}_i = T_{ij,j} + \rho f_i\,, \quad \dot{\gamma} = -\eta_{i,i}\,, \quad D_{i,i} = \varphi\,, \quad E_k = -\psi_{,k}\,, \quad T_0\Phi_k = q_k\,, \quad e_{ik} = \frac{1}{2}(u_{i,k} + u_{k,i}). \tag{27}$$

(1) *Green-Naghdi theory of type I*

We consider a free energy Ψ in the quadratic approximation

$$\begin{aligned}\rho\Psi_0 = &-\frac{\rho c_E}{2T_0}\theta^2 + \frac{1}{2}\nu\gamma^2 + \frac{1}{2}A_{ijkl}e_{ij}e_{kl}\\ &-\frac{1}{2}\chi_{ij}E_iE_j + a_{ij}e_{ij}\theta + b_{ij}e_{ij}\gamma - \varpi\theta\gamma\\ &+ H_{ijk}e_{ij}E_k - a_iE_i\theta - b_iE_i\gamma, \end{aligned} \tag{28}$$

where c_E is the specific heat at constant strain, A_{ijkl} is the tensor of elastic constants, χ_{ij} is the tensor of electric constants, and a_{ij} and b_{ij} are the tensors of thermal and diffusion expansions, respectively. The constants ϖ and ν are measures of thermodiffusion and diffusive effects, respectively. Using (28), the relations (20) yield

$$\begin{aligned} T_{ij} &= A_{ijkl}e_{kl} + H_{ijk}E_k + a_{ij}\theta + b_{ij}\gamma, & \rho S &= -a_{ij}e_{ij} + a_iE_i + \tfrac{\rho c_E}{T_0}\theta + \varpi\gamma,\\ P &= b_{ij}e_{ij} - b_iE_i - \varpi\theta + \nu\gamma, & D_k &= -H_{kij}e_{ij} + \chi_{kj}E_j + a_k\theta + b_k\gamma. \end{aligned} \tag{29}$$

Replacing $(29)_3$ into the other equations, we obtain

$$\begin{aligned} T_{ij} &= \alpha_{ijkl}e_{kl} + M_{ijk}E_k + \gamma_{ij}\theta + \beta_{ij}P,\\ \rho S &= -\gamma_{ij}e_{ij} + c_iE_i + c\theta + \kappa P,\\ \gamma &= -\beta_{ij}e_{ij} + d_iE_i + \kappa\theta + mP,\\ D_k &= -M_{kij}e_{ij} + \zeta_{kj}E_j + c_k\theta + d_kP, \end{aligned} \tag{30}$$

where P is considered in (30) as a state variable instead of γ and

$$\begin{aligned} &\alpha_{ijkl} = A_{ijkl} - \frac{1}{\nu}b_{ij}b_{kl}, \quad \gamma_{ij} = a_{ij} + \frac{\varpi}{\nu}b_{ij}, \quad \beta_{ij} = \frac{1}{\nu}b_{ij}, \quad c = \frac{\rho_0 c_E}{T_0} + \frac{\varpi^2}{\nu}, \quad \kappa = \frac{\varpi}{\nu},\\ &m = \frac{1}{\nu}, \quad d_i = \frac{b_i}{\nu}, \quad M_{ijk} = H_{ijk} + b_{ij}\frac{b_k}{\nu}, \quad c_i = a_i + \frac{\varpi}{\nu}b_i, \quad \zeta_{kj} = \chi_{kj} + \frac{1}{\nu}b_kb_j, \end{aligned} \tag{31}$$

satisfying the following symmetry relations

$$\alpha_{ijkl} = \alpha_{klij}, \quad M_{ijkl} = M_{klij}, \quad \zeta_{ij} = \zeta_{ji}, \quad \gamma_{ij} = \gamma_{ji}, \quad \beta_{ij} = \beta_{ji}. \tag{32}$$

In the following, we assume that $cm - \kappa^2 > 0$. This condition implies that $c\theta^2 + 2\kappa\theta P + mP^2 > 0$, which is needed to stabilize the following evolutive equations. In the context of the linear theory, the inequality (20) becomes

T

$$-\frac{1}{T}q_k\theta_{,k} - \eta_k P_{,k} \geq 0, \tag{33}$$

which leads to the linear approximations for q_i (Fourier's law) and η_i (Fick's law), respectively,

$$q_i = -k_{ij}\theta_{,j}, \qquad \eta_i = -h_{ij}P_{,j}, \tag{34}$$

where k_{ij} and h_{ij} are the tensors of thermal and diffusion conductivity, respectively. The combining of $(12)_2$ (with $\xi = 0$) and $(27)_5$ gives the linear entropy equation

$$\rho\dot{S} = -\frac{1}{T_0}q_{i,i} + \rho s. \tag{35}$$

By inserting $(30)_1$ into $(27)_1$, $(30)_2$ into (35) combined with $(34)_1$, $(30)_3$ into $(27)_2$ combined with $(34)_2$, we obtain the (classical) evolutive equations (for thermoelastic diffusion piezoelectric materials) of type I

$$\begin{aligned}
\rho\ddot{u}_i &= (\alpha_{ijkl}e_{kl} - M_{ijk}\psi_{,k} + \gamma_{ij}\theta + \beta_{ij}P)_{,j} + \rho f_i,\\
c\dot{\theta} + \kappa\dot{P} &= \gamma_{ij}\dot{e}_{ij} + c_i\dot{\psi}_{,i} + \tfrac{1}{T_0}(k_{ij}\theta_{,j})_{,i} + \rho s,\\
m\dot{P} + \kappa\dot{\theta} &= \beta_{ij}\dot{e}_{ij} + d_i\dot{\psi}_{,i} + (h_{ij}P_{,j})_{,i},\\
\varphi &= \left(-M_{kij}e_{ij} - \zeta_{kj}\psi_{,j} + c_k\theta + d_kP\right)_{,k}.
\end{aligned} \tag{36}$$

(2) *Green-Naghdi theory of type II*

The set of the independent variables for the Green-Naghdi model of type II (without energy dissipation) becomes $\widetilde{\mathscr{A}}_2 = (e_{ik}, \theta, \gamma, \tau_{,k}, \wp_{,k}, E_k)$, where

$$\tau = \int_{t_0}^{t}\theta ds, \quad \wp = \int_{t_0}^{t} P ds.$$

The free energy Ψ can be expanded in a power series of the independent variables

$$\begin{aligned}
\rho\Psi = \rho\Psi_0 &+ \frac{1}{2}K_{ij}\tau_{,i}\tau_{,j} + \frac{1}{2}L_{ij}\wp_{,i}\wp_{,j} + c_{ij}\tau_{,i}\wp_{,j} + A_{ijk}e_{ij}\tau_{,k} + B_{ijk}e_{ij}\wp_{,k}\\
&+ f_k\tau_{,k}\theta + g_k\wp_{,k}\theta + p_k\tau_{,k}\gamma + r_k\wp_{,k}\gamma + \sigma_{jk}E_k\tau_{,j} + \upsilon_{jk}E_k\wp_{,j},
\end{aligned} \tag{37}$$

where Ψ_0 is given by (28) and K_{ij} and L_{ij} are tensors of thermal and diffusion conductivity, respectively. The tensor c_{ij} is the measure of thermodiffusion gradient displacement. From (23) and (37), we obtain the following linear constitutive equations:

$$\begin{aligned}
T_{ij} &= A_{ijkl}e_{kl} + H_{ijk}E_k + a_{ij}\theta + b_{ij}\gamma + A_{ijk}\tau_{,k} + B_{ijk}\wp_{,k},\\
\rho S &= -a_{ij}e_{ij} + a_iE_i + \tfrac{\rho c_E}{T_0}\theta + \varpi\gamma - f_k\tau_{,k} - g_k\wp_{,k},\\
P &= b_{ij}e_{ij} - b_iE_i - \varpi\theta + \nu\gamma + p_k\tau_{,k} + r_k\wp_{,k},\\
q_k &= T_0\Phi_k = -T_0(A_{ijk}e_{ij} + \sigma_{jk}E_j + f_k\theta + p_k\gamma + K_{kj}\tau_{,j} + c_{kj}\wp_{,j}),\\
\eta_i &= -B_{ijk}e_{kj} - \upsilon_{ik}E_k - g_i\theta - r_i\gamma - c_{ij}\tau_{,j} - L_{ij}\wp_{,j},\\
D_k &= -H_{ijk}e_{ij} + \chi_{kj}E_j + a_k\theta + b_k\gamma - \sigma_{jk}\tau_{,j} - \upsilon_{jk}\wp_{,j},\\
\xi &= 0.
\end{aligned} \tag{38}$$

Substituting $(38)_3$ into the other equations, we obtain the following constitutive equations where P is a state variable instead of γ:

$$\begin{aligned}
T_{ij} &= \alpha_{ijkl}e_{kl} + M_{ijk}E_k + \gamma_{ij}\theta + \beta_{ij}P + \chi_{ijk}\tau_{,k} + \omega_{ijk}\wp_{,k},\\
\rho S &= -\gamma_{ij}e_{ij} + c_i E_i + c\theta + \kappa P - u_k\tau_{,k} - v_k\wp_{,k}\\
\gamma &= -\beta_{ij}e_{ij} + d_i E_i + \kappa\theta + mP - w_k\tau_{,k} - z_k\wp_{,k},\\
q_k &= T_0\Phi_k = -T_0(\chi_{ijk}e_{ij} + \pi_{jk}E_k + u_k\theta + w_k P + \tilde{k}_{kj}\tau_{,j} + d_{kj}\wp_{,j}),\\
\eta_i &= -\omega_{ijk}e_{kj} - \varsigma_{ik}E_k - v_i\theta - z_i P - d_{ij}\tau_{,j} - \tilde{h}_{ij}\wp_{,j},\\
D_k &= -M_{kij}e_{ij} + \zeta_{kj}E_j + c_k\theta + d_k P - \pi_{jk}\tau_{,j} - \varsigma_{jk}\wp_{,j},\\
\xi &= 0,
\end{aligned} \tag{39}$$

where

$$\begin{aligned}
&\chi_{ijk} = A_{ijk} - \frac{1}{\nu}b_{ij}p_k, \quad \omega_{ijk} = B_{ijk} - \frac{1}{\nu}b_{ij}r_k, \quad u_k = f_k + \frac{\varpi}{\nu}p_k, \quad v_k = g_k + \frac{\varpi}{\nu}r_k,\\
&w_k = \frac{1}{\nu}p_k, \quad z_k = \frac{1}{\nu}r_k, \quad \pi_{jk} = \sigma_{jk} + \frac{1}{\nu}b_k p_j, \quad \varsigma_{jk} = \upsilon_{jk} + \frac{1}{\nu}b_k r_j\\
&\tilde{k}_{ij} = K_{ij} + \frac{1}{\nu}p_i p_j, \quad d_{ij} = c_{ij} + \frac{1}{\nu}p_i r_j, \quad \tilde{h}_{ij} = L_{ij} + \frac{1}{\nu}r_i r_j
\end{aligned} \tag{40}$$

satisfying the following symmetry relations

$$\chi_{ijkl} = \chi_{klij}, \quad \omega_{ij} = \omega_{ji}, \quad \pi_{ij} = \pi_{ji}, \quad \varsigma_{ij} = \varsigma_{ji}, \quad d_{ij} = d_{ji}, \quad \tilde{k}_{ij} = \tilde{k}_{ji}, \quad \tilde{h}_{ij} = \tilde{h}_{ji}. \tag{41}$$

The other coefficients in (39) are defined by (31) and (32). By substituting (39) into (27) and $(12)_2$ (with $\xi = 0$), we obtain the following evolutive equations of type II:

$$\begin{aligned}
\rho\ddot{u}_i &= (\alpha_{ijkl}e_{kl} - M_{ijk}\psi_{,k} + \gamma_{ij}\theta + \beta_{ij}P + \chi_{ijk}\tau_{,k} + \omega_{ijk}\wp_{,k})_{,j} + \rho f_i,\\
c\ddot{\tau} + \kappa\ddot{\wp} &= \gamma_{ij}\dot{e}_{ij} + c_i\dot{\psi}_{,i} + (\chi_{ijk}e_{ij} - \pi_{jk}\psi_{,j} + u_k\theta + w_k P + \tilde{k}_{kj}\tau_{,j} + d_{kj}\wp_{,j})_{,k}\\
&\quad + u_k\dot{\tau}_{,k} + v_k\dot{\wp}_{,k} + \rho s,\\
m\ddot{\wp} + \kappa\ddot{\tau} &= \beta_{ij}\dot{e}_{ij} + d_i\dot{\psi}_{,i} + (\omega_{ijk}e_{kj} - \varsigma_{ik}\psi_{,k} + v_i\theta + z_i P + d_{ij}\tau_{,j} + \tilde{h}_{ij}\wp_{,j})_{,i}\\
&\quad + w_k\dot{\tau}_{,k} + z_k\dot{\wp}_{,k},\\
\varphi &= (-M_{kij}e_{ij} - \zeta_{kj}\psi_{,j} + c_k\theta + d_k P - \pi_{jk}\tau_{,j} - \varsigma_{jk}\wp_{,j})_{,k}.
\end{aligned} \tag{42}$$

(3) *Green-Naghdi theory of type III*

The set of the independent variables for the Green-Naghdi model of type III (with energy dissipation) becomes

$$\widetilde{\mathscr{A}}_2 = (e_{ik}, \theta, \gamma, \tau_{,k}, \wp_{,k}, \theta_{,k}, P_{,k}).$$

According to (25), Ψ is given by (37) and the constitutive equations T_{ij}, S, γ, and D_k are equal to $(39)_{1,2,3,6}$, respectively, while the condition (26) leads to

$$\left(\rho\frac{\partial\widehat{\Psi}}{\partial\tau_{,k}}+\widehat{\Phi}_k\right)\theta_{,k}+\left(\rho\frac{\partial\widehat{\Psi}}{\partial\wp_{,k}}+\widehat{\eta}_k\right)P_{,k}+\rho T_0\hat{\xi}=0. \tag{43}$$

In the context of linear theory, the condition (43) is satisfied if we choose

$$\begin{aligned}
q_k &= T_0\Phi_k=-T_0\left(\chi_{ijk}e_{ij}+\pi_{jk}E_k+u_k\theta+w_kP+\tilde{k}_{kj}\tau_{,j}+d_{kj}\wp_{,j}+\tilde{K}_{kj}\theta_{,j}+\tilde{c}_{kj}P_{,j}\right),\\
\eta_i &= -\left(\omega_{ijk}e_{kj}+\varsigma_{ik}E_k+v_i\theta+z_iP+d_{ij}\tau_{,j}+\tilde{h}_{ij}\wp_{,j}+\tilde{H}_{ij}P_{,j}+\tilde{c}_{ij}\theta_{,j}\right),\\
\rho\xi &= \tilde{H}_{ij}P_{,i}P_{,j}+\tilde{K}_{ij}\theta_{,i}\theta_{,j}+2\tilde{c}_{ij}P_{,j}\theta_{,i}
\end{aligned} \tag{44}$$

where $\tilde{H}_{ij}$, $\tilde{K}_{ij}$, and $\tilde{c}_{ij}$ are characteristic tensors of type III model satisfying

$$\tilde{K}_{ij}=\tilde{K}_{ji},\quad \tilde{H}_{ij}=\tilde{H}_{ji}\quad \tilde{c}_{ij}=\tilde{c}_{ji}.$$

Using the chemical potential as a state variable instead of the concentration, we obtain the following evolutive equations of type III:

$$\begin{aligned}
\rho\ddot{u}_i &= (\alpha_{ijkl}e_{kl}-M_{ijk}\psi_{,k}+\gamma_{ij}\theta+\beta_{ij}P+\chi_{ijk}\tau_{,k}+\omega_{ijk}\wp_{,k})_{,j}+\rho f_i,\\
c\ddot{\tau}+\kappa\ddot{\wp} &= \gamma_{ij}\dot{e}_{ij}+c_i\dot{\psi}_{,i}+(\chi_{ijk}e_{ij}-\pi_{jk}\psi_{,j}+u_k\theta+w_kP+\tilde{k}_{kj}\tau_{,j}+d_{kj}\wp_{,j})_{,k}\\
&\quad+(\tilde{K}_{kj}\theta_{,j}+\tilde{c}_{kj}P_{,j})_{,k}+u_k\dot{\tau}_{,k}+v_k\dot{\wp}_{,k}+\rho s,\\
m\ddot{\wp}+\kappa\ddot{\tau} &= \beta_{ij}\dot{e}_{ij}+d_i\dot{\psi}_{,i}+(\omega_{ijk}e_{kj}-\varsigma_{ik}\psi_{,k}+v_i\theta+z_iP+d_{ij}\tau_{,j}+\tilde{h}_{ij}\wp_{,j})_{,i}\\
&\quad+(\tilde{H}_{ij}P_{,j}+\tilde{c}_{ij}\theta_{,j})_{,i}+w_k\dot{\tau}_{,k}+z_k\dot{\wp}_{,k},\\
\varphi &= (-M_{kij}e_{ij}-\zeta_{kj}\psi_{,j}+c_k\theta+d_kP-\pi_{jk}\tau_{,j}-\varsigma_{jk}\wp_{,j})_{,k}.
\end{aligned} \tag{45}$$

Remark that the evolutive equations (42) of type II (without energy dissipation) can be deduced from the evolutive equations (45) of type III (with energy dissipation) by taking $\tilde{K}_{ij}=\tilde{H}_{ij}=\tilde{c}_{ij}=0$.

To the field of equations of type I, II, and III we add boundary and initial conditions. Summarizing, the following initial boundary value problems are to be solved:

(1) *Type I problem*: Find $(u_i,\dot{u}_i,\theta,P)$ solution to (36) subject to the initial conditions

$$u_i(\cdot,0)=u_i^0,\quad \dot{u}_i(\cdot,0)=v_i^0,\quad \theta(\cdot,0)=\theta^0,\quad P(\cdot,0)=P^0,\ \text{ in } \Omega,$$

and the boundary conditions

$$T_{ji}n_j=\tilde{f}_i \text{ on } \partial\Omega_\sigma\times\mathscr{I},\ \ q_in_i=\tilde{q} \text{ on } \partial\Omega_q\times\mathscr{I},\ \ \eta_in_i=\tilde{\eta} \text{ on } \partial\Omega_\eta\times\mathscr{I},\ \ D_in_i=\tilde{D} \text{ on } \partial\Omega_D\times\mathscr{I}, \tag{46}$$

$$u_i=\tilde{u_i} \text{ on } \partial\Omega_u\times\mathscr{I},\ \ \theta=\tilde{\theta} \text{ on } \partial\Omega_\theta\times\mathscr{I},\ \ P=\tilde{P} \text{ on } \partial\Omega_P\times\mathscr{I},\ \ \phi=\tilde{\phi} \text{ on } \partial\Omega_\phi\times\mathscr{I},$$

where $\mathscr{I} = (0, \infty)$, $\tilde{u_i}$, $\tilde{\theta}$, $\tilde{P}$, and $\tilde{\phi}$ are prescribed functions, u_i^0, v_i^0, θ^0, and P^0 are given, and

$$\partial\Omega = \partial\Omega_u \cup \partial\Omega_\sigma = \partial\Omega_\theta \cup \partial\Omega_q = \partial\Omega_P \cup \partial\Omega_\eta = \partial\Omega_\phi \cup \partial\Omega_D,$$

$$\partial\Omega_u \cap \partial\Omega_\sigma = \partial\Omega_\theta \cap \partial\Omega_q = \partial\Omega_P \cap \partial\Omega_\eta = \partial\Omega_\phi \cap \partial\Omega_D = \emptyset.$$

(2) *Type II problem*: Find $(u_i, \dot{u}_i, \tau, \theta, \wp, P)$ solution to (42) subject to the initial conditions

$$\begin{aligned} &u_i(\cdot, 0) = u_i^0, \quad \dot{u}_i(\cdot, 0) = v_i^0, \quad \tau(\cdot, 0) = \tau^0, \\ &\theta(\cdot, 0) = \theta^0, \quad \wp(\cdot, 0) = \wp^0, \quad P(\cdot, 0) = P^0 \text{ in } \Omega, \end{aligned} \tag{47}$$

and the boundary conditions (46) and

$$u_i = \tilde{u_i} \text{ on } \partial\Omega_u \times \mathscr{I}, \quad \tau = \tilde{\tau} \text{ on } \partial\Omega_\tau \times \mathscr{I}, \quad \wp = \tilde{\wp} \text{ on } \partial\Omega_\wp \times \mathscr{I}, \quad \phi = \tilde{\phi} \text{ on } \partial\Omega_\phi \times \mathscr{I} \tag{48}$$

where $\tilde{u_i}$, $\tilde{\tau}$, $\tilde{\wp}$, $\tilde{\phi}$, $\tilde{f_i}$, $\tilde{q}$, $\tilde{\eta}$, and $\tilde{D}$ are prescribed functions, u_i^0, v_i^0, τ^0, θ^0, $\wp^0$, and P^0 are given, and

$$\partial\Omega = \partial\Omega_u \cup \partial\Omega_\sigma = \partial\Omega_\tau \cup \partial\Omega_q = \partial\Omega_\wp \cup \partial\Omega_\eta = \partial\Omega_\phi \cup \partial\Omega_D,$$

$$\partial\Omega_u \cap \partial\Omega_\sigma = \partial\Omega_\tau \cap \partial\Omega_q = \partial\Omega_\wp \cap \partial\Omega_\eta = \partial\Omega_\phi \cap \partial\Omega_D = \emptyset.$$

(3) *Type III problem*: Find $(u_i, \dot{u}_i, \tau, \theta, \wp, P)$ solution to (45) subject to the initial conditions (47) and the boundary conditions (46) and (48).

Conclusion

Nonlinear as well as linear theories are derived for thermoelastic diffusion piezoelectric materials within Green-Naghdi theory of type I (Fourier's law), II, and III. It is shown that there exists coupling between piezoelectricity, temperature, and chemical potential. Only models of types II and III permit propagation of thermal and diffusion waves at finite speeds. Keeping in view the increasing interest of heat and mass exchange with the environment in piezoelectric elastic materials, the three derived models will be of great importance in many engineering applications as well as the mathematical study of their qualitative properties.

References

Bowen RN (1976) Theory of mixture. In: Eringen AC (ed) Continuum physics, vol III. Academic, New York
Curie J, Curie P (1880) Développement, par pression, de l'électricité polaire dans les cristaux hémièdres à faces inclinées. C R Acad Sci 91:294–295
Green AE, Naghdi PM (1991) A re-examination of the basic postulates of thermomechanics. Proc R Soc Lond A 432:171–194
Green AE, Naghdi PM (1993) On thermoelasticity without energy dissipation. J Elast 31:189–208
Green AE, Naghdi PM (1995) A unified procedure for construction of theories of deformable media, Classical continuum physics, Generalized continua, Mixtures of interacting continua. Proc R Soc Lond A 448:335–356, 357–377, 379–388
Lebon G, Desaive T, Dauby P (2006) A unified extended thermodynamics descrition of diffusion, thermo-diffusion, suspension and porous media. Trans ASME 73:16–20
Mindlin RD (1961) On the equations of motion of piezoelectric crystals, problems of continuum. In: Muskelishvili NI (ed) Mechanics, 70th Birthday Volume. SIAM, Philadelphia, pp 282–290
Mindlin RD (1979) Equation of high frequency of thermopiezoelectric, crystals plates, interactions in elastic solids. Springer, Wein
Nowacki W (1978) Some general theorems of thermopiezoelectricity. J Therm Stresses 1:171–182
Nowacki W (1979) Foundation of linear piezoelectricity. In: Parkus H (ed) Interactions in elastic solids. Springer, Wein

Thermoelastic Waves

Martin Ostoja-Starzewski
Department of Mechanical Science and Engineering, Institute for Condensed Matter Theory, and Beckman Institute, University of Illinois at Urbana-Champaign, Urbana, IL, USA

Synonyms

Hyperbolic theories; Maxwell-Cattaneo; Relaxation times; Thermoelasticity; Waves

Definition

Thermoelastic waves are disturbances involving thermal and elastic fields, typically stemming from the coupling of constitutive equations at the local continuum level. Depending on basic postulates and physical applications, there exist various types of such waves.

Introduction

Thermoelastic waves can be viewed as an extension of elastic waves of isothermal elastodynamics accounting for the interactions between thermal and mechanical fields in the interior of a body due to an external thermomechanical load. From a mathematics' perspective, they can also be defined as solutions to initial-boundary value problems of a hyperbolic thermoelastodynamics (HT). Various theories of HT have been proposed in the literature since the late 1960s, followed by a milestone book of Nowacki (1975), the first fundamental monograph on dynamic thermoelasticity. Both the linear and nonlinear thermoelastic waves have been discussed since then by publishing the original papers and monographs devoted to the subject. In the following, five theories of thermoelastic waves are discussed:

(i) Thermoelasticity proposed in 1967 by Lord and Shulman (L-S Theory)
(ii) Temperature-Rate Dependent Thermoelasticity introduced in 1972 by Green and Lindsay (G-L Theory)
(iii) Low-Temperature Thermoelasticity proposed in 1996 by Hetnarski and Ignaczak (H-I Theory)
(iv) Thermoelasticity Without Energy Dissipation formulated in 1993 by Green and Naghdi (G-N Theory)
(v) Dual-Phase-Lag Thermoelasticity proposed in 1998 by Chandrasekharaiah and Tzou (C-T Theory)

Thermoelastic Waves Propagating in the L-S Model

The hyperbolic L-S model is described by the field equations, in which, by a comparison to the governing equations of classic hyperbolic-parabolic thermoelasticity, the Fourier law of heat conduction is replaced by the Maxwell-Cattaneo equation involving a single relaxation time (Ignaczak and Ostoja-Starzewski 2010, section 1.2). Accordingly, a thermoelastic wave is defined as an ordered array of functions [**u**, **E**, **S**, θ, η, **q**], in which **u, E, S,** θ, η and **q** denote the displacement, strain, Cauchy stress, temperature, entropy, and heat flux fields, respectively, that comply with the governing equations of the L-S theory. These fields are defined on a Cartesian product $B \times [0, \infty)$ where B is a domain occupied by the model and $[0, \infty)$ is the time interval. By eliminating four functions from the six that define a thermoelastic wave, one can obtain the field equations of L-S theory in terms of various mechanical and thermal variables, such as $(\mathbf{u}, \theta)$, $(\mathbf{u}, \mathbf{q})$, $(\mathbf{S}, \theta)$, and $(\mathbf{S}, \mathbf{q})$. Thus, a pair of thermomechanical variables (,) formed from the variables that define a thermoelastic wave corresponds to the wave if the remaining variables of the wave can be restored from the pair. For example, a pair (**u**, θ) that satisfies the displacement-temperature equations of the L-S theory, subject to suitable initial and boundary conditions, is a pair corresponding to a thermoelastic wave because it generates the fields **E**, **S**, η, and **q** in such a way that the ordered array of functions [**u**, **E**, **S**, θ, η, **q**] represents a thermoelastic wave corresponding to an external thermomechanical load applied to the body B over the time interval $[0, \infty)$.

An initial-boundary value problem for a pair (**u**, θ) in which the initial conditions are imposed on $\mathbf{u}, \dot{\mathbf{u}}, \theta$ and $\dot{\theta}$, and the mixed thermomechanical boundary conditions are postulated, is called a mixed displacement-temperature problem (MDTP) of the L-S theory. For an inhomogeneous anisotropic thermoelastic body of that theory, the physical properties of a wave are represented by the set of constitutive variables $\{\theta_0, t_0; \rho, c_E; \mathbf{K}, \mathbf{M}; \mathbf{C}\}$ in which θ_0 and t_0 are a fixed uniform reference temperature and a constant relaxation time, respectively; $\rho = \rho(x)$ and $c_E = c_E(x)$ are the mass density and the specific heat for zero strain (scalar) fields, respectively; $\mathbf{K} = \mathbf{K}(x)$ and $\mathbf{M} = \mathbf{M}(x)$ are the conductivity and the stress-temperature (second-order) tensor fields, respectively; and $\mathbf{C} = \mathbf{C}(x)$ is the elasticity (fourth-order) tensor field; while the external thermomechanical load in the MDTP of L-S theory is represented by an ordered array of functions $\left[\mathbf{b}, r; \mathbf{u_0}, \dot{\mathbf{u}}_\mathbf{0}; \vartheta_0, \dot{\vartheta}_0; \mathbf{u}', \mathbf{s}'; \theta', q'\right]$ in which $\mathbf{b} = \mathbf{b}(x, t)$ and $r = r(x, t)$ are the body force and heat supply fields, respectively; $(\mathbf{u_0}, \vartheta_0)$ and $\left(\dot{\mathbf{u}}_\mathbf{0}, \dot{\vartheta}\right)$ are the initial values of $(\mathbf{u}, \vartheta)$ and $\left(\dot{\mathbf{u}}, \dot{\vartheta}\right)$, respectively; and $\mathbf{u}'$, $\mathbf{s}'$, θ, and q' denote the boundary displacement, traction, temperature, and normal heat flux fields, respectively.

Clearly, the MDTP of L-S theory is an extension of the mixed displacement problem of the classical hyperbolic isothermal elastodynamics (Hetnarski and Ignaczak 2011, p. 232), and a number of theorems of L-S theory that generalize those of classic elastodynamics have been obtained in the literature. In particular, the domain of influence theorem of L-S theory that generalizes that of classical elastodynamics (Gurtin 1972, p. 257) holds true:

Theorem 1 (Domain of influence theorem for the mixed displacement-temperature problem of L-S theory). Let $(\mathbf{u}, \theta)$ be a solution to the MDTP of L-S theory. Let *B(t)* denote a support of the thermomechanical load for a fixed time t, i.e., the set of points of $\overline{B}$ on which the load does not vanish over the time interval $[0, t]$. Let c be a constant of the velocity dimension that satisfies the inequality

$$c \geq \mathbf{max}\,(c_1, c_2), \tag{1}$$

where

$$c_1 = \sup_{B,|\mathbf{m}|=1} \left[|\mathbf{M}^*| + \left(|\mathbf{A}| + |\mathbf{M}^*|^2 \right)^{1/2} \right]$$
$$c_2 = \sup_{B} \left[|\mathbf{M}^*| + \left(t_0^{-1} |\mathbf{K}^*| + |\mathbf{M}^*|^2 \right)^{1/2} \right] \tag{2}$$

Here, $\mathbf{A} = \mathbf{A}(x, \mathbf{m})$ is the (second-order) "acoustic tensor in the propagation direction $\mathbf{m}$" which is defined for any unit vector $\mathbf{m}$ and for arbitrary vector $\mathbf{a}$ by the relation

$$\mathbf{A}\,(x, \mathbf{m})\ \mathbf{a} = \rho^{-1}\,(x)\ \mathbf{C}\ [\mathbf{a} \otimes \mathbf{m}]\ \mathbf{m} \tag{3}$$

while

$$\mathbf{M}^*(x) = \frac{1}{2}\left[\frac{\theta_0}{\rho(x)\ c_E(x)} \right]^{1/2} \mathbf{M}(x) \tag{4}$$

and

$$\mathbf{K}^*(x) = c_E^{-1}(x)\ \mathbf{K}(x) \tag{5}$$

Let $B^*(t)$ be the set

$$B^*(t) = \left\{ x \in \overline{B} : B(t) \cap \overline{\Sigma\,(x, \mathrm{ct})} \neq \varnothing \right\} \tag{6}$$

where $\Sigma(x, \mathrm{ct})$ is an open ball of the radius ct and center at x. Then

$$\mathbf{u} = \mathbf{0}, \quad \theta = 0 \quad \text{on} \quad \left\{ \overline{B} - B^*(t) \right\} \times [0, t] \tag{7}$$

Proof of Theorem 1, in which $B^*(t)$ is the domain of influence of the data at time t, is given in Ignaczak et al. (1986).

Theorem 1 implies that for a finite time t and for a bounded set $B(t)$, the thermoelastic disturbance generated by a pair (**u,** θ) vanishes outside of a bounded set $B^*(t)$ the diameter of which depends on the load support, the bounds on the thermomechanical constitutive fields, and the relaxation time t_0. This theorem also shows that the thermoelastic disturbance propagates as a wave from the domain $B(t)$ with a finite speed equal to or less than the speed c; in particular, a thermoelastic disturbance produced by an external thermomechanical load of a bounded support cannot invade an unbounded body in a finite time.

An analysis of the velocities c_1 and c_2 indicates that c_1 is finite and $c_2 \to \infty$ as $t_0 \to 0 + 0$; hence, $c \to \infty$ as $t_0 \to 0 + 0$. Therefore, if the relaxation time goes to zero, the disturbance gains an infinite speed, as should be expected, since in this limiting case, the mixed displacement-temperature problem of L-S theory reduces to a mixed displacement-temperature problem of classical hyperbolic-parabolic thermoelasticity. An analysis of the velocities c_1 and c_2 also shows that for a weakly acoustic and heat-conductive L-S model, the maximum speed of a thermoelastic wave is given by the simple formula

$$c_0 = 2\sup_{\overline{B}} \left(\left| \mathbf{M}^* \right| \right) \tag{8}$$

Notably, for the finite values of $|\mathbf{A}|$, $|\mathbf{M}^*|$, and $|\mathbf{K}^*|$, the velocities $c_1$and c_2, respectively, represent upper bounds on the velocities of quasi-elastic and of quasi-thermal waves propagating in the body, since for $|\mathbf{M}^*| = 0$ the velocities c_1 and c_2 reduce to a maximum speed of an elastic wave (Gurtin 1972, p. 257) and a maximum speed of a heat wave (Ignaczak and Ostoja-Starzewski 2010, p. 82), respectively.

The speed formulas (2) and (8) could be used to determine the physical properties of a thermoelastic material in a lab experiment in which both a quasi-elastic wave and a quasi-thermal wave are observed.

Finally, note that the other results on thermoelastic waves of L-S theory that should prove useful for both mechanical engineers and applied mathematicians may be found in Ignaczak and Ostoja-Starzewski (2010).

Thermoelastic Waves Propagating in the G-L Model

The G-L model is characterized by a system of PDEs in which, in comparison to the relations of hyperbolic-parabolic thermoelasticity, the

constitutive relations for the stress tensor and the entropy are generalized by introducing two different relaxation times into consideration. A displacement-temperature wave propagating in the G-L model complies with the system of field equations for a pair $(\mathbf{u}, \theta)$ subject to the initial and boundary conditions similar to those of L-S theory. The domain of influence theorem for a mixed displacement-temperature problem of the G-L theory that is similar to Theorem 1 holds true:

Theorem 2 (Domain of influence theorem for MDTP of G-L theory). Let $(\mathbf{u}, \theta)$ be a solution to MDTP of G-L theory. Let *B(t)* denote a support of the thermomechanical load for the problem. Let c be a constant of the velocity dimension that satisfies the inequality

$$c \geq \mathbf{max}\ \left(c_1', c_2'\right) \tag{9}$$

in which

$$\begin{aligned} c_1' &= \sup_{B,|\mathbf{m}|=1} \left[\left|\mathbf{M}^*\right| + \left(|\mathbf{A}| + \left|\mathbf{M}^*\right|^2 \right)^{1/2} \right] \\ c_2' &= \sup_{B} \left[(t_1/t_0) \left|\mathbf{M}^*\right| + \left(t_0^{-1} \left|\mathbf{K}^*\right| \right.\right. \\ &\quad \left.\left. + (t_1/t_0)^2 \left|\mathbf{M}^*\right|^2 \right)^{1/2} \right] \end{aligned} \tag{10}$$

Here, t_0 and t_1 are the relaxation times that satisfy the inequalities $t_1 \geq t_0 > 0$; and the tensor fields $\mathbf{A}$, $\mathbf{M}^*$, and $\mathbf{K}^*$ are given by Eqs. (3), (4), and (5), respectively. Let $B^*(t)$ be the set defined by (6) in which c satisfies the inequality (9). Then

$$\mathbf{u} = \mathbf{0}, \quad \theta = 0 \quad \text{on } \left\{ \overline{B} - B^*(t) \right\} \times [0, t] \tag{11}$$

Proof of Theorem 2 is given in Carbonaro and Ignaczak (1987).

A physical interpretation of Theorem 2 is similar to that of Theorem 1. Moreover, the definition of c implies that the velocities c_1' and c_2' correspond, respectively, to the maximum speed of a quasi-elastic and a quasi-thermal wave propagating in the G-L model; and for $|\mathbf{M}^*| = 0$ they reduce to the maximum speed of a pure elastic and a pure thermal wave, respectively.

Also, for a weakly acoustic and heat-conductive L-G model, the maximum speed of a thermoelastic wave is determined by the simple formula

$$c_0' = 2\ (t_1/t_0) \sup_{\overline{B}} \left(\left|\mathbf{M}^*\right| \right) \tag{12}$$

In addition, since $t_1 \geq t_0 > 0$,

$$\left(c_1', c_2'\right) = (c_1, c_2) \ \text{ and } c_0' = c_0 \tag{13}$$

if $t_1 = t_0 > 0$ and t_0 of the G-L model is identified with t_0 of the L-S model.

For a spherically symmetric Cauchy problem of the G-L theory, a thermoelastic wave (u, θ), corresponding to an instantaneous heat source concentrated at the origin of spherical coordinates (r, ϑ, γ) $[0 \leq r \leq \infty,\ 0 \leq \vartheta \leq \pi,\ 0 \leq \gamma < 2\pi]$, takes the form

$$(u, \theta) = \left(u^{(1)}, \theta^{(1)}\right) + \left(u^{(2)}, \theta^{(2)}\right) \tag{14}$$

where $(u^{(1)}, \vartheta^{(1)})$ and $(u^{(2)}, \vartheta^{(2)})$ are the outgoing spherical quasi-elastic and quasi-thermal waves propagating with the velocities $c^{(1)}$ and $c^{(2)}$, respectively. The associated domain of influence is to be identified with a ball $\Sigma(0, ct)$ where $c = \mathbf{max}\ (c^{(1)}, c^{(2)})$ (Ignaczak and Ostoja-Starzewski 2010, section 7.4).

An attempt to verify the G-L theory in a lab experiment has been made in Suh and Burger (1998a, b), where laser-induced waves propagating in a plate are compared with those of the L-G theory. Since, in general, the G-L theory has not been verified successfully by a laboratory experiment, to discuss numerically the solutions to particular initial-boundary value problems of G-L theory, a virtual set of physical constants is used, which reduces to that of classical theories such as the elastodynamics and heat wave theory when $t_1/t_0 \to 1$ and $t_0 > 0$.

Thermoelastic Waves Propagating in the H-I Model

The H-I model proposed by Hetnarski and Ignaczak in 1990s has been introduced in an attempt to describe low-temperature soliton-like thermoelastic waves (Ignaczak 1990; Hetnarski and Ignaczak 1996, 1997). The model is characterized by a system of nonlinear field equations in which, in comparison to the system of classical hyperbolic-parabolic linear thermoelasticity, both the free energy and the heat flux vector depend not only on the absolute temperature and the strain tensor but also on "elastic" heat flow that satisfies a nonlinear evolution equation and enters a modified Fourier law and a modified free energy formula, respectively, through linear and quadratic terms.

For a one-dimensional case in which the body is homogeneous, isotropic, and of infinite extent ($|x| \leq \infty$), a thermoelastic wave can be described by a pair of functions (u, Φ) satisfying the nonlinear dimensionless field equations

$$\begin{aligned} &\left(\Phi_{tt} - \Phi_{xxt} + \omega\, \Phi_{xt}^2\right) \mathbf{exp}\,(-\omega\, \Phi_t) - \omega\, \Phi_x \Phi_{xt} \\ &- \Phi_{xx} - \omega^{-1} u_{xt} \mathbf{exp}\,(-\omega\, \Phi_t) = 0 \\ &\omega^{-1}\left(u_{xx} - \zeta^2 u_{tt}\right) + \in \Phi_{xt} \mathbf{exp}\,(-\omega\, \Phi_t) = 0 \\ &\text{for} \quad |x| \leq \infty, \quad t \geq 0 \end{aligned} \tag{15}$$

In Eq. (15) the usual index notation for partial derivatives is introduced; while $\omega\Phi$ and u denote an elastic heat flow potential and a displacement in the x-direction, respectively; moreover, ω, ϵ, and ζ stand for a low-temperature parameter ($\omega << 1$), a thermoelastic coupling constant, and an inertia coefficient, respectively.

The absolute temperature $T = T(x, t)$, the total heat flux $q = q(x, t)$, and the stress $\Sigma = \Sigma(x, t)$ in the x-direction are given in terms of (u, Φ) by

$$T\,(x, t) = \mathbf{exp}\,(-\omega\, \Phi_t) \tag{16}$$

$$q\,(x, t) = \omega\, \Phi_x + \omega\, \Phi_{xt} \mathbf{exp}\,(-\omega\, \Phi_t) \tag{17}$$

$$\Sigma\,(x, t) = u_x - \in [\mathbf{exp}\,(-\omega\, \Phi_t) - 1] \tag{18}$$

Equations $(15)_1$ and $(15)_2$ represent, respectively, the balance of energy and the equation of motion of the one-dimensional H-I model. The exponential form of $T = T(x, t)$ in (16) is selected in such a way that the one-dimensional nonlinear evolution equation of the model is satisfied. Equation (17) represents a modified Fourier law in which $\omega\Phi_x$ is the elastic heat flow and the second term on RHS of (17) stands for a heat flux of classic type. Finally, (18) represents a one-dimensional stress-strain-temperature relation.

Note that Eq. (15) forms a highly nonlinear coupled system of PDEs involving a small parameter ω, so an asymptotic analysis may be used to obtain approximate solutions to these equations. The case $\omega = 0$ corresponds to a thermodynamical equilibrium at which $T = 1$, $q = 0$, $u = 0$, and $\Sigma = 0$. Also, when $u = 0$ and $\epsilon = 0$, Eqs. (15), (16), (17), and (18) reduce to those of a low-temperature nonlinear rigid heat conductor.

A class of closed-form solutions to Eq. (15) may be obtained by looking for a pair (u, Φ) in the form

$$u{=}u(s), \quad \Phi{=}\Phi(s); \quad s{=}x{-}vt, \quad |x| \leq \infty, \quad t{\geq}0 \tag{19}$$

where v is a positive constant. Such a pair then represents a plane progressive wave propagating with the velocity v in the x-direction.

A soliton-like thermoelastic wave of H-I theory is defined as a triplet $[T(s), q(s), \Sigma(s)]$ generated by a pair $[u(s), \Phi(s)]$ that satisfies Eq. (15) for $|s| \leq \infty$ subject to the boundary conditions

$$\begin{aligned} &T(-\infty){=}T(+\infty) = 1; \quad q(-\infty){=}q(+\infty){=}0; \\ &\Sigma\,(-\infty) = \Sigma\,(+\infty) = 0 \end{aligned} \tag{20}$$

The following two-part theorem holds true:

Theorem 3 (i) If $\widehat{\zeta} = \zeta\ \omega^{-1/2} \geq 1$ and $\in > 0$, then there are two soliton-like thermoelastic waves $(T, q, \Sigma)_1$ and $(T, q, \Sigma)_2$ propagating with the velocities v_1 and v_2, respectively, in the x-direction, where

$$v_1 = \omega^{-1/2}\widehat{\zeta}^{-1/2}\left\{\frac{1+\epsilon+\widehat{\zeta}}{2\widehat{\zeta}} - \left[\left(\frac{1+\epsilon+\widehat{\zeta}}{2\widehat{\zeta}}\right)^2 - 1\right]^{1/2}\right\}^{1/2}$$
$$v_2 = \omega^{-1/2}\widehat{\zeta}^{-1/2}\left\{\frac{1+\epsilon+\widehat{\zeta}}{2\widehat{\zeta}} + \left[\left(\frac{1+\epsilon+\widehat{\zeta}}{2\widehat{\zeta}}\right)^2 - 1\right]^{1/2}\right\}^{1/2} \tag{21}$$

(ii) If ω and ζ are both independent of each other and relatively small, there are two fast-moving soliton-like thermoelastic waves, each revealing a fountain effect in a neighborhood of the moving front and each close to the thermodynamical equilibrium far from the front; two self-equilibrated forces parallel to the direction of motion and applied to the wall in a neighborhood of the moving front secure the thermodynamical equilibrium of the wave.

Proof of Theorem 3 is given in Hetnarski and Ignaczak (1996).

An alternative form of the one-dimensional governing equations of the H-I theory is the matrix PDE (Ignaczak and Domanski 2017)

$$\frac{\partial}{\partial t}\mathbf{u} + \mathbf{A}(\mathbf{u})\frac{\partial}{\partial x}\mathbf{u} + \mathbf{B}\frac{\partial^2}{\partial x^2}\mathbf{u} = \mathbf{0} \tag{22}$$

for an unknown vector field

$$\mathbf{u} = [T, b, u_t, u_x]; \quad \mathbf{u} = \mathbf{u}(x,t), \quad |x| \le \infty, \quad t \ge 0 \tag{23}$$

where $b = b(x,t)$ is the elastic heat flow in the x-direction; while $\mathbf{A}(\mathbf{u})$ and $\mathbf{B}$ are the 4×4 matrices defined by

$$\mathbf{A}(\mathbf{u}) = \begin{bmatrix} -b/T & 1 & T & 0 \\ 1/T & 0 & 0 & 0 \\ \epsilon/\zeta & 0 & 0 & -1/\zeta^2 \\ 0 & 0 & -1 & 0 \end{bmatrix} \tag{24}$$

and

$$\mathbf{B} = \begin{bmatrix} -1 & 0 & 0 & 0 \\ 0 & 0 & 0 & 0 \\ 0 & 0 & 0 & 0 \\ 0 & 0 & 0 & 0 \end{bmatrix} \tag{25}$$

Clearly, the matrix $\mathbf{A}(\mathbf{u})$ becomes singular in the neighborhood of absolute zero temperature.

The matrix PDE (22) can be used to find an asymptotic solution to the associated Cauchy problem with a weakly perturbed initial condition:

Find $\mathbf{u}^\varepsilon = \mathbf{u}^\varepsilon(x,t)$ that satisfies the field equation

$$\frac{\partial}{\partial t}\mathbf{u}^\varepsilon + \mathbf{A}\left(\mathbf{u}^\varepsilon\right)\frac{\partial}{\partial x}\mathbf{u}^\varepsilon + \mathbf{B}\frac{\partial^2}{\partial x^2}\mathbf{u}^\varepsilon = \mathbf{0} \quad \text{for} \quad |x| < \infty, \quad t > 0 \tag{26}$$

subject to the initial condition

$$\mathbf{u}^\varepsilon(x,0) = \mathbf{u_0} + \varepsilon\,\mathbf{u}^*(\varepsilon\,x) + \mathbf{0}\left(\varepsilon^2\right) \quad \text{for} \quad |x| < \infty \tag{27}$$

where ε is a small positive number, $\mathbf{u_0} = [T_0, 0, 0, 0]^T$ with $T_0 > 0$, and $\mathbf{u}^* = \mathbf{u}^*(y)$ is a prescribed function for $|y| < \infty$.

With regard to the problem (26) and (27), the following theorem holds true.

Theorem 4 An asymptotic solution to the Cauchy problem, described by Eqs. (26) and (27), which represents a nonlinear low-temperature and small-strain thermoelastic wave propagating along the x-axis, takes the form

$$\mathbf{u}^\varepsilon(x,t) = \mathbf{u_0} + \varepsilon\sum_{i=1}^{4} a_i(\eta_i)\,\mathbf{r_i}(\mathbf{u_0}) + \mathbf{0}\left(\varepsilon^2\right) \quad \text{for} \quad |x| \le \infty, \quad t \ge 0 \tag{28}$$

where $a_i = a_i(\eta_i)$ for $|\eta_i| \le \infty$ is a solution to the nonlinear transport equation

$$\frac{d}{d\eta_i}\left[H_i a_i^2(\eta_i) + \frac{d}{d\eta_i}a_i(\eta_i)\right] = 0, \quad \eta_i = \varepsilon(x - \lambda_i t) \tag{29}$$

Here, $\mathbf{r_i}(\mathbf{u_0})$ stands for the unit right eigenvector of the matrix $\mathbf{A}(\mathbf{u}_0)$ corresponding to the

real-valued eigenvalue $\lambda_i = \lambda_i(\mathbf{u_0})$, η_i is a slow variable of the function $a_i = a_i(\eta_i)$, and H_i is defined by

$$H_i = -\frac{1}{2}\left[\left(r_{i3} - \frac{r_{i2}}{T_0}\right) - \frac{r_{i1}}{T_0^2}\frac{l_{i2}}{l_{i1}}\right] \tag{30}$$

where $r_{ik}(l_{ik})$ denotes the kth component of the unit right (left) eigenvector $\mathbf{r_i}(\mathbf{l_i})$ of the matrix $\mathbf{A}(\mathbf{u}_0)$ for $i, k = 1, 2, 3, 4$.

Proof of Theorem 4 is given in Ignaczak and Domanski (2017).

It is also shown in Ignaczak and Domanski (2017) that, for a particular Cauchy problem described by Eqs. (26) and (27) in which the initial data are generated by a closed-form solution to the transport Eqs. (29), the principal part of the asymptotic solution (28) is a sum of four traveling thermoelastic waves admitting blow-up amplitudes.

Thermoelastic Waves Propagating in the G-N Model

The G-N model, proposed by Green and Naghdi (1993), is described by a system of PDE in which, in comparison to classic thermoelasticity system, the Fourier law of heat conduction is replaced by a heat flux rate-temperature gradient relation. As a result, a thermoelastic wave propagating in G-N model and corresponding to the displacement-temperature initial-boundary value problem is characterized in terms of a pair $(\mathbf{u}, \theta)$ that satisfies the displacement-temperature field equations in which the energy equation does not contain the temperature rate $\dot{\theta}$. As a result, a solution $(\mathbf{u}, \theta)$ to the problem represents an undamped thermoelastic wave, and this motivates the name of G-N theory as thermoelasticity without energy dissipation (TWED). For the L-S model the displacement-temperature energy equation does contain $\dot{\theta}$; similarly, $\dot{\theta}$ is included in the displacement-temperature energy equation of the G-L theory. This is a reason why the L-S and G-L models represent materials transmitting damped thermoelastic waves. The existence of damped thermoelastic waves in the L-S and G-L theories has been revealed in a number of papers devoted to theoretical (Achenbach 1968; Ignaczak 1978) and applied aspects (Ignaczak 1989; Hetnarski and Ignaczak 1993, 1994) of these theories.

A Saint-Venant's principle associated with an initial-boundary value problem of the G-N theory is presented in Nappa (1998). A uniqueness theorem for a natural stress-entropy flux initial-boundary value problem of G-N theory is proved in Chandrasekharaiah (1996a), while the continuous dependence of a solution to the displacement-temperature initial-boundary value problem on the thermomechanical load in G-N theory is established in Iesan (1998). The undamped character of one-dimensional thermoelastic waves propagating in the G-N model is discussed in Chandrasekharaiah (1996b).

Thermoelastic Waves Propagating in the C-T Model

The C-D model, proposed by Chandrasekharaiah and Tzou in 1998 (Tzou 1995; Chandrasekharaiah 1998), is an extension of the classical hyperbolic-parabolic thermoelastic model in which the Fourier law is replaced by an approximation to a modified Fourier law with two different time translations: a phase lag of the heat flux τ_q and a phase lag of the temperature gradient τ_θ. A Taylor series approximation of the modified Fourier law together with the remaining field equations leads to a complete system of equations describing a dual-phase-lag thermoelastic model. The model transmits thermoelastic disturbances in a wave-like manner if the approximation is linear with respect to τ_q and τ_θ and $0 \leq \tau_\theta < \tau_q$. In this case, the linear approximation of the modified Fourier law together with the energy balance equation for a rigid heat conductor leads to Jeffreys-type hyperbolic heat conduction equations (Joseph and Preziosi 1989, 1990; Tamma and Zhou 1998).

For a C-T model based on the Taylor series approximation of the modified Fourier law

which is quadratic in τ_q and linear in τ_θ, a displacement-temperature initial-boundary value problem involving the third order time derivatives of an unknown solution can be formulated. Such a problem is then a natural extension of the displacement-temperature problem of the L-S theory. Similarly to the case of the L-S and G-L models, no combined experimental data are available that might be used to determine τ_q and τ_θ as well as the remaining thermomechanical properties of the C-T model. Finally, note that the principle of Saint-Venant's type in terms of a pair (**S**, **q**) for the dual-phase-lag thermoelastic model has not been obtained up to date.

Closure

The five models described by the L-S, G-L, H-I, G-N, and C-T theories have been a stepping stone for a number of researchers in the field of wave propagation problems in solids from the beginning of the twenty-first century up to this day. For example, a unified presentation of the L-S, G-L, and G-N theories is proposed in Bagri and Eslami (2007a, b); while a phase-lag Green-Naghdi thermoelasticity is published in Karamany and Ezzat (2016). A thermoelasticity with a memory-dependent derivative that includes as particular cases the L-S, G-L, and C-T theories is presented in Ezzat et al. (2016); and a spatial behavior of solutions to the three-phase-lag heat conduction equation is discussed in Quintanilla (2009). Also, a scale-dependent homogenization is applied to the G-L theory where conductivity and stiffness are wide-sense stationary ergodic random fields in Ostoja-Starzewski et al. (2015). The L-S and G-L have also provided a basis for an extension of thermoelasticity with finite wave speeds to account for viscous effects in solids (Ostoja-Starzewski 2014) and fluids (Ostoja-Starzewski and Khayat 2017). Less attention has been paid to the H-I model for which a method of weakly nonlinear asymptotics to solve the one-dimensional Cauchy problem with a weakly perturbed, the initial condition, is presented in this survey (Ignaczak and Domanski 2017).

The results presented in this survey extend those of Hetnarski and Ignaczak (2000) and also make use of the entries from the *Encyclopedia of Thermal Stresses* (Ignaczak 2014; Ignaczak and Hetnarski 2014).

This brief review ends with a note that many effects of coupled generalized thermoelastic vis-à-vis classical responses have been examined in a number of problems involving interaction of one or two half-spaces: rigid die sliding on a deformable body, surface or interface wave propagation, and dynamic thermoelastic fracture, e.g., Brock (2005, 2006, 2008).

Acknowledgment Expert comments of J. Ignaczak helped improve this chapter. This work has partially been supported by the NSF under grant CMMI-1462749.

References

Achenbach JD (1968) The influence of heat conduction on propagating stress jumps. J Mech Phys Solids 16: 273–282

Bagri A, Eslami MR (2007a) A unified generalized thermoelastic formulation; applications to thick functionally graded cylinders. J Thermal Stress 30:911–930

Bagri A, Eslami MR (2007b) A unified generalized thermoelasticity: solution for cylinders and spheres. Int J Mech Sci 49:1325–1335

Brock LM (2005) Thermal relaxation effects in rapid sliding contact with friction. Acta Mech 176:185–196

Brock LM (2006) Debonding of a thermoelastic material from a rigid substrate at any constant speed: thermal relaxation effects. Acta Mech 184:185–196

Brock LM (2008) Stoneley signals in perfectly bonded dissimilar thermoelastic half-spaces with and without thermal relaxation. J Mech Mater Struct 2(9): 1723–1742

Carbonaro B, Ignaczak J (1987) Some theorems in temperature-rate dependent thermoelasticity for unbounded domains. J Thermal Stress 10:193–220

Chandrasekharaiah DS (1996a) A uniqueness theorem in the theory of thermoelasticity without energy dissipation. J Thermal Stress 19:267–272

Chandrasekharaiah DS (1996b) One-dimensional wave propagation in the linear theory of thermoelasticity without energy dissipation. J Thermal Stress 19: 695–710

Chandrasekharaiah DS (1998) Hyperbolic thermoelasticity: a review of recent literature. Appl Mech Rev 51:705–729

Ezzat MA, El-Karamany AS, El-Bary AA (2016) Modeling of memory-dependent derivative in generalized thermoelasticity. Eur Phys J Plus 131(372):1–12

Green AE, Naghdi PM (1993) Thermoelasticity without energy dissipation. J Elast 31:189–208
Gurtin ME (1972) The linear theory of elasticity. In: Encyclopedia of physics, mechanics of solids II, VIa/2, Springer-Verlag, Berlin
Hetnarski RB, Ignaczak J (1993) Generalized thermoelasticity: closed-form solutions. J Thermal Stress 16: 473–498
Hetnarski RB, Ignaczak J (1994) Generalized thermoelasticity: response of semi-space to a short laser pulse. J Thermal Stress 17:377–396
Hetnarski RB, Ignaczak J (1996) Soliton-like waves in a low-temperature nonlinear thermoelastic solid. Int J Eng Sci 34:1767–1787
Hetnarski RB, Ignaczak J (1997) On soliton-like thermoelastic waves. Appl Anal 65:183–204
Hetnarski RB, Ignaczak J (2000) Nonclassical dynamical thermoelasticity. Int J Solids Struct 37:215–224
Hetnarski RB, Ignaczak J (2011) The mathematical theory of elasticity, 2nd edn. CRC Press/Taylor and Francis Group, Boca Raton
Iesan D (1998) On the theory of thermoelasticity without energy dissipation. J Thermal Stress 21:295–307
Ignaczak J (1978) Decomposition theorem for thermoelasticity with finite wave speeds. J Thermal Stress 1:41–52
Ignaczak J (1989) Generalized thermoelasticity and its applications. In: Hetnarski RB (ed) Thermal stresses III. Elsevier, New York, pp 279–354
Ignaczak J (1990) Soliton-like solutions in a nonlinear dynamic coupled thermoelasticity. J Thermal Stress 13:73–98
Ignaczak J (2014) Domain of influence theorems in generalized thermoelasticity, encyclopedia of thermal stresses, vol 2. Springer, Dordrecht, pp 996–1003
Ignaczak J, Domanski W (2017) An asymptotic approach to one-dimensional model of nonlinear thermoelasticity at low temperatures and small strains. J Thermal Stress 40:1030–1039
Ignaczak J, Hetnarski RB (2014) Generalized thermoelasticity: mathematical formulation, encyclopedia of thermal stresses, vol 4. Springer, Dordrecht, pp 1974–1986
Ignaczak J, Ostoja-Starzewski M (2010) Thermoelasticity with finite wave speeds. Oxford University Press, Oxford
Ignaczak J, Carbonaro B, Russo R (1986) Domain of influence theorem in thermoelasticity with one relaxation time. J Thermal Stress 9:79–91
Joseph DD, Preziosi L (1989) Heat waves. Rev Mod Phys 62:41–73
Joseph DD, Preziosi L (1990) Addendum to the paper: heat waves. Rev Mod Phys 62:375–391
Karamany AS, Ezzat MA (2016) On the phase-lag Green-Naghdi thermoelasticity theories. Appl Math Model 40:5643–5659
Nappa L (1998) Spatial decay estimates for the evolution equations of linear thermoelasticity without energy dissipation. J Thermal Stress 21:581–592
Nowacki W (1975) Dynamic problems of thermoelasticity. In: Francis PH, Hetnarski RB (eds) Noordhoff Int. Publ. Leyden & PWN-Polish Scientific Publishers, Warsaw
Ostoja-Starzewski M (2014) Viscothermoelasticity with finite wave speeds: thermomechanical laws. Acta Mech 225(4–5):1277–1285
Ostoja-Starzewski M, Khayat RE (2018) Oldroyd fluids with hyperbolic heat conduction. Mech Res Comm 93:108–113
Ostoja-Starzewski M, Costa L, Ranganathan SI (2015) Scale-dependent homogenization of random hyperbolic thermoelastic solids. J Elast 118:243–250
Quintanilla R (2009) Spatial behavior of solutions of the three-phase-lag heat equation. Appl Math Comput 213:153–162
Suh CS, Burger CP (1998a) Thermoelastic modeling of laser-induced stress-waves in plates. J Thermal Stress 21:829–847
Suh CS, Burger CP (1998b) Effects of thermomechanical coupling and relaxation times on wave spectrum in dynamic theory of generalized thermoelasticity. J Appl Mech 65:605–613
Tamma KK, Zhou X (1998) Macroscale and microscale thermal transport and thermomechanical interactions: some noteworthy perspectives. J Thermal Stress 21:405–449
Tzou DY (1995) A unified approach for heat conduction from macro to micro-scales. J Heat Transf 117:8–16

Thermoelastic Waves in a Medium with Heat-Flux Relaxation

Mikhail B. Babenkov[1,2] and Evgeniy Yu. Vitokhin[2]
[1]Institute for Problems in Mechanical Engineering RAS, Saint Petersburg, Russia
[2]Peter the Great Saint-Petersburg Polytechnic University, Saint Petersburg, Russia

Synonyms

Lord-Shulman thermoelasticity; Propagation of thermal elastic waves in a medium with heat-flux relaxation constant

Definition

Thermoelastic waves are the solutions of the equations of coupled thermoelasticity. In the case

of hyperbolic thermoelasticity, the solution is the sum of two traveling waves. The first terms are called quasithermal components, and the second terms are quasielastic components. These components of thermoelastic waves propagate in the medium with different velocities, dispersion, and attenuation rate.

Introduction

Propagation of thermoelastic waves may be useful for determining the thermomechanical characteristics of micro- and nanoscale objects, such as thin plates and rods, which are used in micro- and nanoelectromechanical devices (MEMS and NEMS). Temperature substantially affects the thermomechanical properties of layered nanomaterials, since the thinner the layer, the more it is sensitive to temperature effects (Haque and Saif 2005). A number of experimental (Poletkin et al. 2012) and theoretical papers (Wang et al. 2011) are dedicated to the thermoelastic wave propagation processes in nanometer-sized films. Some numerical studies of the hyperbolic thermoelasticity problems were done in Yu et al. (2006), Melnik (2001), and Youssef (2005). An extensive review on the hyperbolic thermoelasticity is given in Igna and Ostoja-Starzewski (2010) and Chandrasekharaiah (1998).

The second half of the century brought a surge of interest in the hyperbolic theory of thermal conductivity. The topic was thoroughly researched, and the numerous studies devoted to the theory were published (Chandrasekharaiah 1998; Jou et al. 1996; Wang 1965; Engelbrecht and Maugin 1996; Tzou 1997). Over recent decades, the problems of coupled hyperbolic thermoelasticity have drawn a certain attention (see, e.g., Igna and Ostoja-Starzewski 2010; Ivanova 2010, 2011, 2012, 2014). The following article illustrates how the boundary conditions influence the contribution of the wave terms of the hyperbolic heat conduction equation to the overall solution of a coupled thermoelasticity problem.

The Equations of the Hyperbolic Thermal Conductivity and Thermoelasticity

One of the most well-known approaches describing the wave nature of the heat propagation processes in an elastic medium was proposed by Lord and Shulman (1967). This approach is based on the generalized Fourier law, taking into account the relaxation time of the heat flux τ:

$$\tau \dot{\boldsymbol{h}} + \boldsymbol{h} = -\lambda \nabla T, \tag{1}$$

where $\boldsymbol{h}$ is the heat flux, λ is the coefficient of thermal conductivity, ∇ is the Hamiltonian operator, and T is the temperature. The heat equation using generalized Fourier's law (1) can be derived as follows. The energy balance equation for the undeformable medium has the form

$$\rho \dot{U} = -\nabla \cdot \boldsymbol{h} + \rho q, \tag{2}$$

where ρ is the density, U is the mass density of the internal energy, and q is the mass density of the internal heat sources. Since the medium is undeformable, $\rho = \text{const}$.

If the temperature deviation from its initial value T^* is small, the mass density of the internal energy can be represented as follows:

$$U = c_v \tilde{T}, \qquad \tilde{T} = T - T^*, \tag{3}$$

where c_v is the specific heat at a constant volume.

After introducing (3) into (2) and applying generalized Fourier's law (1) to eliminate the heat fluxes, the Maxwell-Cattaneo equation is obtained:

$$\lambda \Delta \tilde{T} - \rho c_v \left(\dot{\tilde{T}} + \tau \ddot{\tilde{T}} \right) = -\rho \left(q + \tau \dot{q} \right) \tag{4}$$

A deformable medium taking into account the thermal effects is considered.

The continuum dynamics equation in the local form is as follows:

$$\nabla \cdot \boldsymbol{\sigma} + \rho \boldsymbol{f} = \rho \ddot{\boldsymbol{u}}, \tag{5}$$

where $\boldsymbol{\sigma}$ is the stress tensor, $\boldsymbol{f}$ is the body forces vector, and $\boldsymbol{u}$ is the displacement vector.

The relation between the stress, strain, and temperature, known as the Duhamel-Neumann law, can be written as follows:

$$\boldsymbol{\sigma} = \left(K - \frac{2}{3}G\right)\varepsilon \boldsymbol{E} + 2G\boldsymbol{e} - \alpha K \tilde{T}\boldsymbol{E}, \quad (6)$$

where K the isothermal bulk modulus, G is the shear modulus, $\boldsymbol{e}$ is the strain tensor ($\varepsilon = \operatorname{tr}\boldsymbol{e}$), $\boldsymbol{E}$ is the unit tensor, and α is the volumetric coefficient of thermal expansion.

Introducing (6) to equation of motion (5) without taking into account bulk forces:

$$\left(K - \frac{2}{3}G\right)\nabla\varepsilon + 2G\nabla\cdot\boldsymbol{e} - \alpha K\nabla\tilde{T} = \rho\ddot{\boldsymbol{u}}. \quad (7)$$

Calculating the divergence of (7), one obtains an equation describing three-dimensional deformation of a thermoelastic medium:

$$\left(K + \frac{4}{3}G\right)\Delta\varepsilon - \alpha K\Delta\tilde{T} = \rho\ddot{\varepsilon} \quad (8)$$

Calculating the curl of (5), one obtains an equation for the shear waves. The temperature terms are absent from this equation. However, the temperature change may affect the shear strain, because the shear and bulk strain are coupled by boundary conditions. Hereinafter, such boundary conditions are considered under which shear and bulk strain are independent.

In order to obtain the analytical solution, it's convenient to operate the equation of motion in terms of stress. To do that, one can calculate the trace of (6) and express the strain tensor in terms of the stress and temperature. The equations of coupled hyperbolic thermoelasticity for bulk deformations can be written:

$$\begin{gathered}\left(K + \frac{4}{3}G\right)\Delta\sigma - \alpha K\rho\ddot{\tilde{T}} - \rho\ddot{\sigma} = 0 \\ \lambda\Delta\tilde{T} - \left(\frac{\alpha^2K^2T^*}{K + \frac{4}{3}G} + \rho c_v\right)\left(\dot{\tilde{T}} + \tau\ddot{\tilde{T}}\right) - \frac{\alpha K T^*}{K + \frac{4}{3}G}(\dot{\sigma} + \tau\ddot{\sigma}) = -\rho\,(q + \tau\dot{q}),\end{gathered} \quad (9)$$

where $\sigma = 1/3\operatorname{tr}\boldsymbol{\sigma}$.

If the heat-flux relaxation time τ in (9) tends to zero, then the solution of this system will tend to the solution of the classical problem of the thermoelasticity of the parabolic type.

Thermoelastic Waves in a Layer with Internal Heat Sources

Problem Statement

An infinite layer, which is exposed to the laser radiation, is considered (Vitokhin and Babenkov 2016a,b). If the layer is irradiated uniformly over the entire surface, waves will propagate only along the x axis. The interaction of a laser and a medium is modeled by the Beer-Lambert law (Fig. 1):

$$J(x) = J_0 e^{-\gamma x},$$

where J_0 is the laser intensity and γ is the attenuation coefficient of the medium. Eventually, the value of J_0 depends not only on the

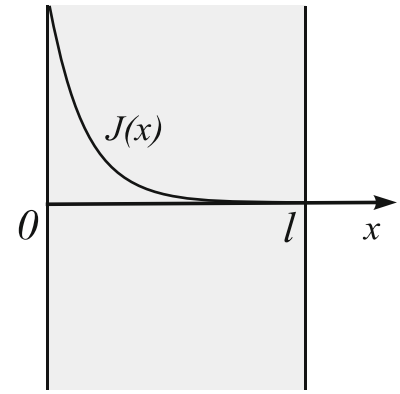

Fig. 1 The hyperbolic thermoelasticity problem for an infinite layer under the influence of a laser impulse

properties of the laser but also on the properties of a surface. A part of the incident radiation reflects from the surface; with this in mind, the value of J_0 is considered to have the sense of the laser radiation intensity absorbed by the material. The dependence of the laser intensity on time is quite difficult and, therefore, J_0 is assumed to be an average characteristic. Generally, there are two characteristics of the short laser impulse found in the literature: exposure duration δ_0 and energy E_0 absorbed per unit area. Thus, the laser intensity is considered to be a function of the form

$$\tilde{J}(x,t) = \begin{cases} J_0 e^{-\gamma x}, & 0 \le t \le \delta_0; \\ 0, & t > \delta_0. \end{cases}$$

And

$$E(x) \equiv \int_0^\infty \tilde{J}(x,t)dt = J_0\delta_0 e^{-\gamma x}$$
$$\Rightarrow \quad E_0 \equiv E(0) = J_0\delta_0.$$

The Dirac delta function $\delta(t-0)$ is usually adopted to model the time dependence of the laser intensity, because such an approximation allows to obtain an exact analytical solution. The scale factor is selected so that full energy E_0 absorbed per unit area during the time of exposure would be consistent with the experimental data. It is readily seen that function $J(x,t)$ satisfying the above conditions has the form

$$\hat{J}(x,t) = E_0 e^{-\gamma x}\delta(t-0). \tag{10}$$

Subsequently,

$$E(x) \equiv \int_0^\infty \hat{J}(x,t)dt = E_0 e^{-\gamma x}.$$

Hereinafter, formula (10) will be used for the laser intensity. The relation between heat supply rate per unit volume $\rho q(x,t)$ and the laser intensity is determined by the energy balance equation:

$$\hat{J}(x,t) - \rho q(x,t)dx - \hat{J}(x+dx,t) = 0.$$

Expanding function $\hat{J}(x+dx,t)$ in the Taylor series and taking into account (10):

$$E_0 e^{-\gamma x}\delta(t-0) - \rho q(x,t)dx - E_0 e^{-\gamma x}$$
$$\delta(t-0)(1-\gamma dx) = 0.$$

From the last equation, it follows that

$$q(x,t) = \frac{E_0\gamma}{\rho}e^{-\gamma x}\delta(t-0), \qquad E_0 = J_0\delta_0. \tag{11}$$

At the initial moment of time the layer is unperturbed, the thermal and mechanical loads are absent:

$$\dot{u}\big|_{t=0} = 0; \quad u\big|_{t=0} = 0; \tag{12}$$

$$\dot{\tilde{T}}\big|_{t=0} = 0; \quad \tilde{T}\big|_{t=0} = 0; \tag{13}$$

If the problem is formulated in terms of the stresses, then the initial conditions must be formulated for the stress instead of the strain:

$$\dot{\sigma}\big|_{t=0} = 0; \quad \sigma\big|_{t=0} = 0; \tag{14}$$

A Constant Temperature Kept at the Unconstrained Boundaries of the Layer

The boundary conditions have the form

$$\sigma\big|_{x=0} = 0; \quad \sigma\big|_{x=l} = 0;$$
$$\tilde{T}\big|_{x=0} = 0; \quad \tilde{T}\big|_{x=l} = 0; \tag{15}$$

Solution is shown in Fig. 2; the curves are plotted for the moments of time τ, 3τ, and 5τ. The left curves are plotted for $\gamma > \gamma_0$; the right curves are plotted for $\gamma < \gamma_0$, where $\gamma_0 = \sqrt{\rho c_v/(4\lambda\tau)}$. Jumps and discontinuities arise in the presented solutions because of the Dirac delta function is adopted to approximate a time dependence of the laser intensity while impacting the specimen and, as well, the form of the non-Fourier source term containing the first time derivative of the Dirac delta function.

A cooling region can be observed under the boundary conditions of the first kind if $\gamma > \gamma_0$ (Babenkov and Ivanova 2014) due to the amplitude of the wave reflected from the irradiated border with the opposite sign is sufficient to alter the sign of the original wave in the vicinity of the irradiated surface.

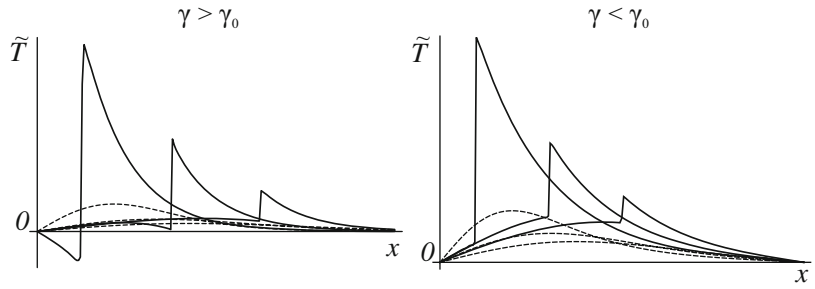

Fig. 2 The analytical solution of the heat conduction problem. The temperature at the boundaries is kept constant. Solid lines show the solution of the hyperbolic heat conduction problem; dashed lines show the solution of the classical heat conduction problem

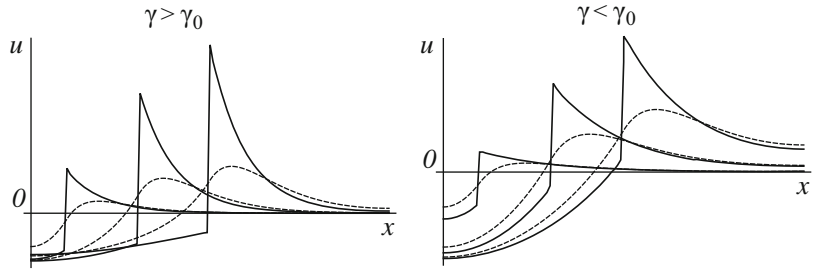

Fig. 3 The analytical solution of the semi-coupled thermoelasticity problem. The temperature at the unconstrained boundaries is kept constant. The solid lines show the solution of the hyperbolic thermoelasticity problem; the dashed lines show the solution of the classical thermoelasticity problem

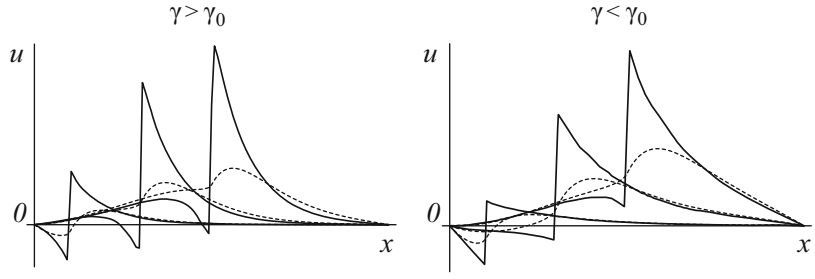

Fig. 4 The analytical solution of the semi-coupled thermoelasticity problem with the constrained borders kept at a constant temperature. Solid lines represent curves of the hyperbolic thermoelasticity; dotted lines represent classical curves

Curves in Fig. 3 and Fig. 4 show solution for the layer exposed to the short laser pulse (11).

The curves are obtained for the case if the velocities of thermal and acoustic waves are equal. The solution is plotted at the following times: τ, 3τ, and 5τ. The left curves are plotted for $\gamma > \gamma_0$; the right curves are plotted for $\gamma < \gamma_0$. With the growth of the absorption constant γ, the difference between the displacements in classical and hyperbolic thermoelasticity problems increases.

The graph in Fig. 3 illustrates the hyperbolic thermoelasticity problem solution. It has two salient points, while the graph plotted using the classical thermoelasticity is smooth. Under these boundary conditions, the most noticeable

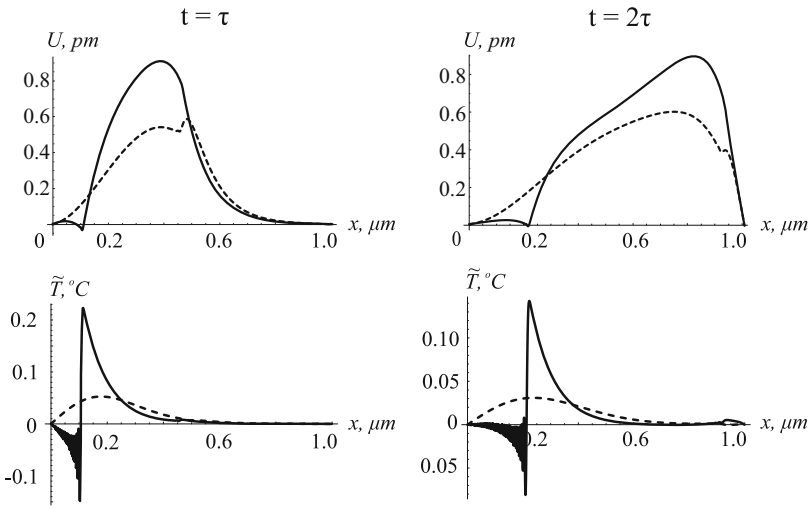

Fig. 5 The numerical solution of the coupled thermoelasticity problem with the constrained borders kept at a constant temperature. The solid lines represent curves of the hyperbolic thermoelasticity; the dotted lines represent classical curves

difference between the hyperbolic and classical uncoupled thermoelasticities is achieved. The velocities of the quasiacoustic and quasithermal fronts in a coupled problem are not equal to the sound and heat velocities in an uncoupled problem due to the influence of the coupling effects on the dispersion law (Babenkov 2013).

A Constant Temperature Kept at the Constrained Boundaries of the Layer

The boundary conditions have the form

$$u\big|_{x=0} = 0; \quad u\big|_{x=l} = 0;$$
$$\tilde{T}\big|_{x=0} = 0; \quad \tilde{T}\big|_{x=l} = 0; \qquad (16)$$

Figure 5 shows the numerical solution of the coupled thermoelasticity problem. The copper layer is exposed to a short laser pulse (11). At the initial moment time, the layer was in the unperturbed state. Curves on the left are built at $t = \tau = 0.1$ ns, graphics right at $t = 2\tau$. In the hyperbolic thermoelasticity at the front of the quasithermal wave, the minimum displacement values are observed; the maximum displacements are observed at the quasiacoustic front. In the classical thermoelasticity, the displacement values on quasiacoustic and quasithermal fronts are lower than in the hyperbolic thermoelasticity. The maximum difference between the displacements in the classical and hyperbolic thermoelasticity is observed at the quasiacoustic front.

The Insulated and Constrained Boundaries of the Layer

The boundary conditions have the form

$$u\big|_{x=0} = 0; \quad u\big|_{x=l} = 0;$$
$$h\big|_{x=0} = 0; \quad h\big|_{x=l} = 0; \qquad (17)$$

Solution at the moments of time τ, 2τ, and 5τ is presented in Fig. 6. The curves on the left are plotted for $\gamma > \gamma_0$; the curves on the right are plotted for $\gamma < \gamma_0$. If $\gamma > \gamma_0$, the temperature maximum is located at the wave front, coinciding with the salient point (the observation time is of the order of τ). If $\gamma < \gamma_0$, then the temperature maximum is located at the irradiated boundary ($x = 0$).

Figure 7 illustrates solution at the following times: τ, 2τ, and 5τ. The curves are obtained for the case if the velocities of thermal and acoustic waves are equal. The curves on the left are plotted for $\gamma > \gamma_0$; the curves on the right are plotted for $\gamma < \gamma_0$.

Starting from a certain moment of time, if $\gamma < \gamma_0$, one can observe a displacements

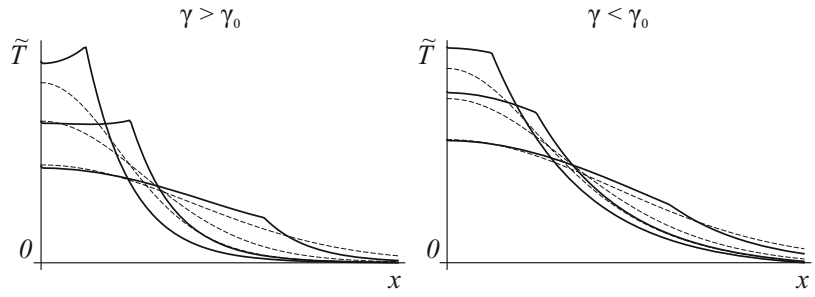

Fig. 6 The analytical solution of the thermal conductivity problem with the thermally insulated boundaries. Solid lines represent curves for the hyperbolic thermal conductivity; the dotted lines represent curves for the Fourier thermal conductivity

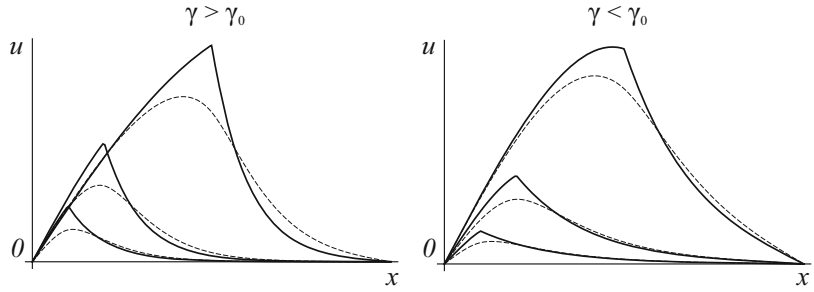

Fig. 7 The analytical solution of the semi-coupled thermoelasticity problem with the thermally insulated and constrained boundaries. Solid lines represent curves of the hyperbolic thermal conductivity; dotted lines represent curves for the Fourier thermal conductivity

extremum located to the left of the wavefront. In the semi-coupled thermoelasticity problem, if $\gamma > \gamma_0$, the displacement extremum is always located on the wave front.

The numerical solution of the coupled thermoelasticity problem for the copper layer is shown in Fig. 8. The curves on the left are built at $t = \tau = 0.1$ ns; the curves on the right are built at $t = 2\tau$. The most noticeable difference between the displacements of the classical and hyperbolic thermoelasticities is achieved at the quasithermal front.

The curves in Figs. 6 and 8 show that over the time the temperature of the irradiated border in the hyperbolic problem of thermoelasticity can be either larger or smaller than in the classical one. However, the temperature difference is small in these cases. Also, the displacement obtained via the hyperbolic and classical thermoelasticity does not have qualitative differences, and the observed quantitative differences are neglectable.

The Insulated and Unconstrained Boundaries of the Layer

The boundary conditions have the form

$$\sigma\big|_{x=0} = 0; \quad \sigma\big|_{x=l} = 0;$$
$$h\big|_{x=0} = 0; \quad h\big|_{x=l} = 0; \tag{18}$$

Figure 9 illustrates solution at the following times: τ, 2τ, and 5τ. The curves are obtained for the case if the velocities of thermal and acoustic waves are equal. The curves on the left are plotted for $\gamma > \gamma_0$; the curves on the right are plotted for $\gamma < \gamma_0$.

Figure 9 shows that the difference between the displacements calculated via the classical

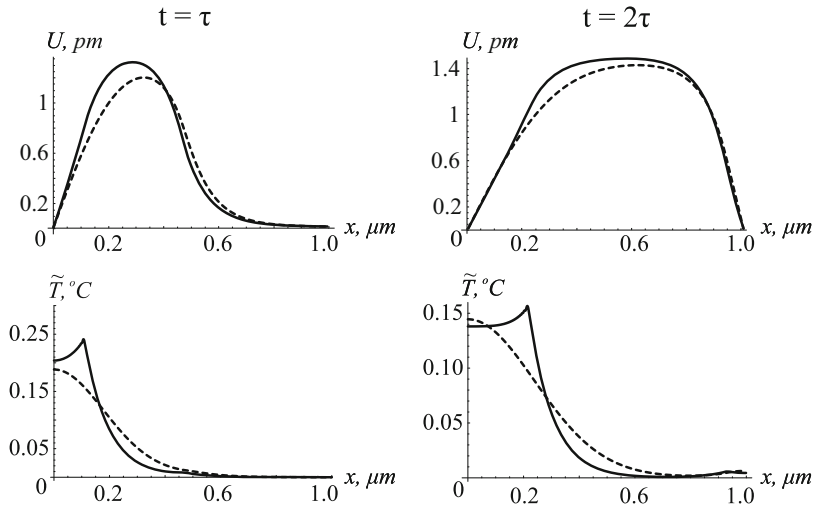

Fig. 8 The numerical solution of the semi-coupled thermoelasticity problem with the thermally insulated and constrained boundaries. Solid lines represent curves of the hyperbolic thermal conductivity; dotted lines represent curves for the Fourier thermal conductivity

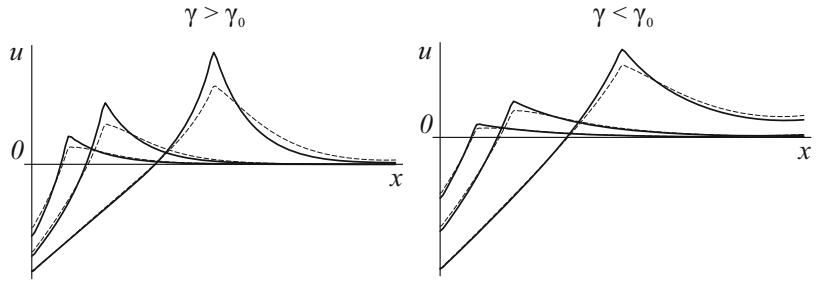

Fig. 9 The analytical solution of the semi-coupled thermoelasticity problem with the thermally insulated and unconstrained boundaries. Solid lines represent curves of the hyperbolic thermal conductivity; dotted lines represent curves for the Fourier thermal conductivity

and hyperbolic theories increases with attenuation coefficient γ. The temperature extremums in Fig. 6 do not qualitatively affect the displacements shown in Fig. 9.

Numerical solution for the copper layer is shown in Fig. 10. The curves on the left are plotted for $t = \tau = 0.1$ ns; the curves on the right are plotted for $t = 2\tau$ ns. As in the previous case, the most noticeable difference between the displacements calculated via classical and hyperbolic theories is achieved at the quasithermal front. As seen from a comparison of Figs. 8 and 10, the mechanical boundary conditions have little effect on the temperature distribution in the layer, due to the smallness of the thermal expansion coefficient.

As can be seen in Fig. 9, the difference between the classical and hyperbolic solutions under the chosen boundary conditions is less noticeable, than in the previously considered cases.

The numerical solution of the coupled problem and the analytical solution of the semi-coupled problem demonstrate negative displacements extremum, which disappears over a short period of time. This means that at the initial time period, the points of the layer are moving toward the radiation source. The same

T

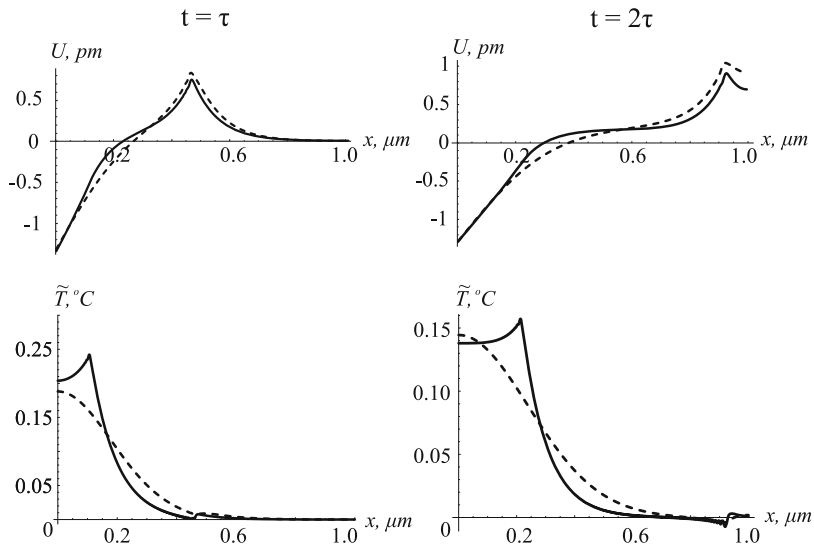

Fig. 10 The numerical solution of the coupled thermoelasticity problem with the thermally insulated and unconstrained boundaries. Solid lines represent curves for the hyperbolic thermal conductivity; dotted lines represent curves for the Fourier thermal conductivity

effect is observed in the solution of the classical problem.

The displacements peak values in the semi-coupled hyperbolic thermoelasticity (Fig. 9, solid lines) are greater than in the classical thermoelasticity problem (Fig. 9, dashed lines). On the contrary, the displacements peak values in the coupled hyperbolic thermoelasticity (Fig. 10) are less than in classical one. Such effect is observed because the solution presented in Fig. 9 is obtained if quasithermal and quasielastic wave components propagate with an equal speed. The resulting thermoelastic wave is formed of these components by adding up its amplitudes. However, in the coupled statement, the component's velocities cannot be equal. In this case, the numerical solution reflects the actual behavior of the material better.

The Stress Distribution

If the boundaries are unconstrained, a jump is observed at the acoustic front (Fig. 11a, d). The compression zone is observed before the front, and the extension zone is observed after the front. If the boundaries are constrained, one can observe a salient point at the acoustic front and a compression zone in its neighborhood (Fig. 11b, c).

Conclusion

In linear problems, increasing the heating pulse amplitude can achieve arbitrarily high temperatures in the solution. In order to use the linear theory, it is necessary that the deviation of the temperature from its reference value does not exceed appr. 10 °C (Nowacki 1975), so the material parameters could be treated as constants. On the other hand, the minimum temperature deviation that can be captured by the modern experimental equipment is near 0.3 °C (Magunov 2002). At times not exceeding the heat-flux relaxation time $t \approx \tau$ or $t < \tau$ ($\tau > 10^{-12}$ s, the theoretical estimates are made for metals), the difference in the temperature peaks obtained within each of the theories is large enough that the results of measurements can determine which theory models the thermoelastic wave propagation process more accurately.

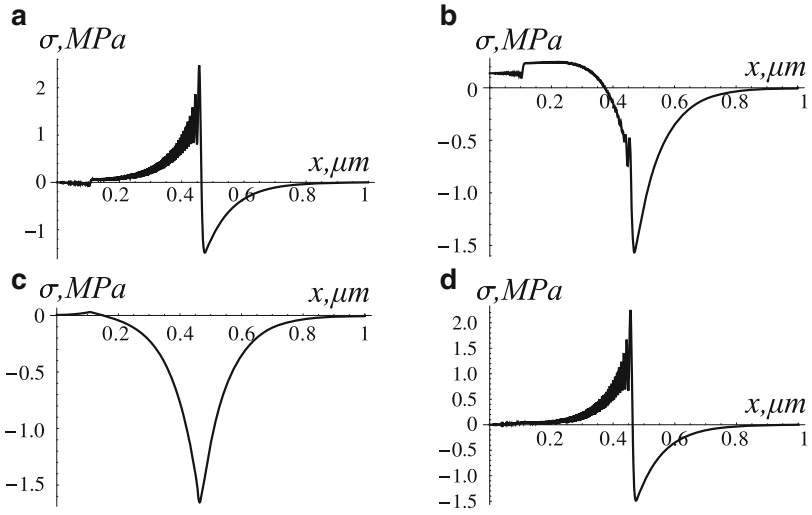

Fig. 11 Numerically evaluated displacements in the layer subjected to the laser pulse under the various boundary conditions at $t = \tau = 0{,}1$ ns. Unconstrained boundaries of the layer are kept at a constant temperature (**a**); the boundaries of the layer are constrained and kept at a constant temperature (**b**); the boundaries of the layer are constrained and insulated (**c**); the boundaries of the layer are thermally insulated and unconstrained (**d**)

If the time resolution of the measurement equipment is less than the heat-flux relaxation constant τ, then the effects of hyperbolic thermoelasticity are supposed to be observed experimentally.

Cross-References

- Computational Methods for Coupled Problems
- Continuum Mechanics with Spontaneous Violations of the Second Law of Thermodynamics
- Nonlocal Transport Equations for Small Systems and Fast Processes
- System of Symmetric Hyperbolic Equations, Extended Thermodynamics of Gases
- Thermal Effects by Means of Two-Component Cosserat Continuum

References

Babenkov MB (2013) Propagation of harmonic perturbations in a thermoelastic medium with heat relaxation. J Appl Mech Tech Phys 54(2):277–286

Babenkov MB, Ivanova EA (2014) Analysis of the wave propagation processes in heat transfer problems of the hyperbolic type. Contin Mech Thermodyn 26(4): 483–502

Chandrasekharaiah DS (1998) Hyperbolic thermoelasticity: a review of recent literature. Appl Mech Rev 51(12):705–729

Engelbrecht J, Maugin GA (1996) Deformation waves in thermoelastic media and the concept of internal variables. Arch Appl Mech 66(3):200–207

Haque MA, Saif MTA (2005) Thermo-mechanical properties of nano-scale freestanding aluminum films. Thin Solid Films 484(1):364–368

Ignaczak J, Ostoja-Starzewski M (2010) Thermoelasticity with finite wave speeds. Oxford University Press, Oxford

Ivanova EA (2010) Derivation of theory of thermoviscoelasticity by means of two-component medium. Acta Mech 215(1):261–286

Ivanova EA (2011) On one model of generalised continuum and its thermodynamical interpretation. In: Altenbach H, Maugin GA, Erofeev V (eda) Mechanics of generalized Continua. Springer, Berlin, pp 151–174

Ivanova EA (2012) Derivation of theory of thermoviscoelasticity by means of two-component Cosserat continuum. Tech Mech 32(2–5):273–286

Ivanova EA (2014) Description of mechanism of thermal conduction and internal damping by means of two component Cosserat continuum. Acta Mech 225(3): 757–795

Jou D, Casas-Vazquez J, Lebon G (1996) Extended irreversible thermodynamics. Springer, Berlin/Heidelberg

Lord HW, Shulman YA (1967) generalized dynamical theory of thermoelasticity. J Mech Phys Solids 15(5):299–309
Magunov AN (2002) Laser thermometry of solids: state of the art and problems. Meas Tech 45(2): 173–181
Melnik RV (2001) Discrete models of coupled dynamic thermoelasticity for stress-temperature formulations. Appl Math Comput 122(1):107–132
Nowacki W (1975) Dynamic problems of thermoelasticity. Springer Science & Business Media, Springer, Netherlands
Poletkin KV, Gurzadyan GG, Shang J, Kulish V (2012) Ultrafast heat transfer on nanoscale in thin gold films. Appl Phys B 107(1):137–143
Tzou DY (1997) Macro-to-microscale heat transfer. The lagging behaviour. Taylor and Francis, New York
Vitokhin EYu, Babenkov MB (2016a) Numerical and analytical studies of the propagation of thermoelastic waves in a medium taking into account heat flow relaxation. J Appl Mech Tech Phys 57(3): 537–549
Vitokhin EYu, Babenkov MB (2016b) Influence of boundary conditions on the solution of a hyperbolic thermoelasticity problem. Contin Mech Thermodyn 29(2): 457–475
Wang CC (1965) The principle of fading memory. Arch Ration Mech Anal 18(5):343–366
Wang H-D, Wei-Gang Ma, Xing Z, Wei W, Guo Z-Y (2011) Theoretical and experimental study on the heat transport in metallic nanofilms heated by ultrashort pulsed laser. Int J Heat Mass Transf 54(4): 967–974
Youssef HM (2005) State-space approach on generalized thermoelasticity for an infinite material with a spherical cavity and variable thermal conductivity subjected to ramp-type heating. Can Appl Math Q 13:4
Yu N, Imatan S, Inoue T (2006) Hyperbolic thermoelastic analysis due to pulsed heat input by numerical simulation. JSME Int J Ser A Solid Mech Mater Eng 49(2):180–187

Thermoelasticity

▸ Thermoelastic Waves

Thermoelasticity: From Particle Dynamics to Continuum Mechanics

▸ Discrete and Continuum Thermomechanics

Thermomechanical Processing of Steels and Alloys: Multilevel Modeling

Peter Trusov, Alexey Shveykin, Nikita Kondratev, and Elena Makarevich
Mathematical Modelling of Systems and Processes, Perm National Research Polytechnic University, Perm, Russia

Synonyms

Crystal plasticity; Thermomechanical treatment of polycrystals

Definition

Technological processes of thermomechanical treatment consist of heating, cooling, and inelastic deformation operations which are applied one by one or in some combinations. The main goal of the thermomechanical processing is putting the material structure to a state which insures that the products gain certain required operational physical and mechanical properties. The multilevel models of materials are effective in simulating and improving the processes of thermomechanical treatment. These models make it possible to explicitly describe a changing structure of materials at different scale levels.

Introduction

Physical and mechanical properties of polycrystalline materials are determined by their internal structure at different scale levels. Thermomechanical processing which includes heating, cooling, and inelastic deformation is operated successively or in a combined way; it is oriented on the material structure changing (grain form and size, defect structures, phase composition) aiming to improve the operational physical and mechanical properties.

The majority of the processes which lead to the material structure changing take place during thermomechanical processing. Some of them are caused by the temperature change, such as recovery, polygonization, and recrystallization; other processes are caused by inelastic deformation (depending on temperature), such as the intragranular sliding of dislocations, rotation of the crystallite lattice, grain boundary sliding, crystallite fragmentation, etc.

To describe some particular processes of thermomechanical treatment (with strictly stipulated processing conditions and for a certain initial state of materials), it is possible to use the empirical methods or theoretical methods based on the macrophenomenological theory of thermo-elasto-plasticity. However, if it is necessary to create models which describe processes in a wide range of impacts, it is impossible to use the latter ones. The reason is that there is a great variety of scenarios describing material structure changing, thus a great variety of parameters at the macroscale level which are determined by this structure. So, to determine the rational regimes of thermomechanical processing, it is necessary to develop the constitutive models which include an explicit description of the structure evolution at meso- and microscale levels of polycrystalline materials.

When it comes to creating models able to describe the structure evolution of polycrystalline materials, the approach based on the explicit introduction of special parameters (internal variables) into the structure of constitutive relations is becoming generally recognized. These parameters describe the state and evolution of meso- and microstructures; and evolutional (kinetic) equations are formulated for them (McDowell 2005; Guo et al. 2005; Zhao and Sheng 2006; Trusov et al. 2010; Saï 2011; Maugin 2015, etc.). Within the framework of this approach, the hypothesis is accepted which states that the reaction of the material at each time-moment is determined by the values of the tensor's thermomechanical characteristics of the material, the finite set of internal variables, the parameters of thermomechanical impacts, and their time derivatives by the required order at the moment of time under study. It is necessary to note that in this case the history of the impacts is not forgotten and its "carriers" are the internal variables which are added into the structure of the model. In recent decades the multilevel models which are based on crystal plasticity (elastoviscoplasticity) are widely used to implement this approach (Ghoniem et al. 2003; McDowell 2008, 2010; Roters et al. 2010; Trusov and Shveykin 2013a,b, etc.). Soon the development of functional materials will become one of the major prospects of material processing, such as creating new materials with certain characteristics that are optimal for a specific industrial problem (or function). Thus, it is possible to use the multilevel models of materials to achieve these goals.

Multilevel Constitutive Models of Materials

Within the multilevel approach, each material point (representative volume) at a scale level 1 is associated with an inhomogeneous region at a lower scale level 2 (Fig. 1) and so on for the subsequent scale levels. Thus, only two levels (e.g., macro- and mesolevels) can be introduced to describe the approach and its algorithms. The scale level 1 will be the upper one, and the scale level 2 will be the lower one.

Parameters of the evolving structure, current physical and mechanical properties, damage, and inelastic strains are determined at the lower scale level by an explicit description of the physical mechanisms of inelastic deformation under the effects that are determined at the upper scale level (from the solution of the boundary value problem at the macrolevel). The changed values of the evolving internal parameters are considered when clarifying the material response at the upper scale level.

In modeling researchers determine the number of levels based on the considered process analysis, the required detailing, and known or supposed deformation mechanisms. For example, in simulating the inelastic deformation of polycrystalline metals, the hierarchy of the scale levels is determined as macrolevel-mesolevel (the

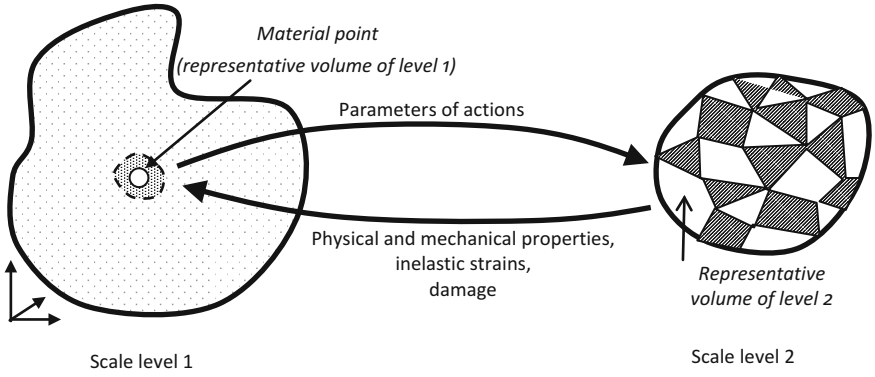

Fig. 1 The scheme of the scale level interaction

level of a crystallite (grain, subgrain, fragment))-microlevel (dislocation structure).

The type of the relations connecting the parameters from different scale levels (the choice of the loading parameters at the upper scale level to be used in the model of the lower scale level and, contrariwise, the way of determining the explicit internal variables of the upper scale level using the model of the lower scale level) is one of the key classification features of the multilevel models. According to this feature, three main groups of models can be specified, such as statistical, self-consistent, and direct ones.

Statistical models (Asaro and Needleman 1985; Bronkhorst et al. 1992; van Houtte 2009; Dancette et al. 2010; Trusov et al. 2013, etc.) are based on considering mesolevel elements (individual grains or aggregates of grains, subgrains) being relatively independent from each other. The aggregation of the mesolevel elements with the macrolevel element (the representative macrovolume) is carried out by some characteristics and some kinematic or static hypotheses accepted a priori (usually the Taylor hypothesis about deformation homogeneity is accepted (Taylor 1938); such models are usually called the Taylor-type models). As for other characteristics, the statistical averaging is performed.

In the self-consistent models (Wagner et al. 1991; Habraken 2004; M'Guil et al. 2009; Beyerlein et al. 2011, etc.) at the mesolevel, one describes the behavior of single mesolevel elements in the surrounding matrix with the effective characteristics of the material which are determined iteratively according to the properties of the mesolevel elements using a particular averaging procedure for the latter ones.

As for direct models (Cailletaud et al. 2003; Anand 2004; Roters 2011; Ardeljan et al. 2014, etc.), the physical models are used as constitutive ones for each grain (subgrain, fragment) being a part of the investigated material volume. In the majority of papers, the finite element method is used to implement the direct models. This model is even more resource-intensive than the self-consistent one.

The key part of multilevel models is a set of relations for the mesolevel individual crystallites (the well-known term called "crystal plasticity" is caused by this fact). One of the most popular definitions of the mesolevel constitutive model says that it is a combination of the constitutive equations given below (Bronkhorst et al. 1992; Kalidindi et al. 1992; Anand 2004; Horstemeyer et al. 2005; Khadyko et al. 2016, etc.) which describe the main mechanisms at the level of crystallites, i.e., intragranular dislocation sliding and rotation of crystallite lattices.

The classical multiplicative decomposition of the deformation gradient $\mathbf{f}$ is used (Kröner 1960; Lee 1969):

$$\mathbf{f} \equiv \overset{\mathrm{o}}{\nabla} \mathbf{x}^{\mathrm{T}} = \mathbf{f}^{\mathrm{e}} \cdot \mathbf{f}^{\mathrm{p}}. \tag{1}$$

In (1) $\overset{\mathrm{o}}{\nabla}$ is the Hamilton operator determined in the reference configuration, $\mathbf{x}$ is the radius vector of the material particle, and $\mathbf{f}^{\mathrm{e}}$ and $\mathbf{f}^{\mathrm{p}}$ are the elastic and plastic constituents of the deformation gradient.

The plastic constituent $\mathbf{f}^{\mathrm{p}}$ of the deformation gradient $\mathbf{f}$ is determined from the following equation:

$$\dot{\mathbf{f}}^{\mathrm{p}} \cdot \mathbf{f}^{\mathrm{p}-1} = \sum_{k=1}^{\mathrm{K}} \dot{\gamma}^{(k)} \overset{\mathrm{o}}{\mathbf{b}}{}^{(k)} \overset{\mathrm{o}}{\mathbf{n}}{}^{(k)}, \qquad (2)$$

where $\overset{\mathrm{o}}{\mathbf{b}}{}^{(k)}$ and $\overset{\mathrm{o}}{\mathbf{n}}{}^{(k)}$ are the unit vectors of the sliding direction and normals to the slip plane of the edge dislocations (in the reference configuration), $\dot{\gamma}^{(k)}$ is the shear rate of the k-th slip system, ($\gamma^{(k)}$ is the accumulated shear in the k-th slip system), and K is the number of slip systems for the type of crystallites being considered. The slip planes and Burgers' vector orientation, along which the translational motion (slip) of the edge dislocations is carried out, are known in the crystallites. These are the most densely packed planes and directions. For example, in the FCC metals, the sliding of the edge dislocations is carried out in the planes of the {111}-system along the direction <110>. It is assumed that in the two-level models, the motion of the dislocations which are homogeneously distributed in the volume is uniform. It makes it possible to consider shears along the slip systems instead of separate dislocations' motion. One of the prospects in studying multilevel models is to introduce the microscale level with the defect structure consideration into the model structure, i.e., to formulate equations for the change of dislocation density and other defects (Beyerlein and Tome 2008; Austin and McDowell 2011; Barton et al. 2011, etc.).

To determine the shear rate $\dot{\gamma}^{(k)}$ in the slip systems, the viscoplastic equation (probably, it was first proposed in the following works (Asaro 1983; Asaro and Needleman 1985)) is used in many models (Ghoniem et al. 2003; McDowell 2008, 2010; Roters et al. 2010; Trusov and Shveykin 2013a,b, etc.):

$$\dot{\gamma}^{(k)} = \dot{\gamma}_0 \left(\tau^{(k)}/\tau_{\mathrm{c}}^{(k)}\right)^{\mathrm{m}} \mathrm{H}\left(\tau^{(k)} - \tau_{\mathrm{c}}^{(k)}\right), \qquad (3)$$

where $\tau^{(k)}$ and $\tau_{\mathrm{c}}^{(k)}$ are the shear and critical shear stresses in the k-th slip system, $\dot{\gamma}_0$ is the shear rate along the slip system at the moment when the shear stress reaches the critical value, m is the rate sensitivity of the material, and H(·) is the Heaviside function. The shear stress in the k-th slip system is determined according to the relation $\tau^{(k)} = (J\,\mathbf{f}^{\mathrm{eT}} \cdot \boldsymbol{\sigma} \cdot \mathbf{f}^{\mathrm{e}-\mathrm{T}}) : (\overset{0}{\mathbf{n}}{}^{(k)} \overset{0}{\mathbf{b}}{}^{(k)})$, where $\boldsymbol{\sigma}$ is the Cauchy stress tensor and $J = \det \mathbf{f}$. In a general case, the critical shear stresses $\tau_{\mathrm{c}}^{(k)}$ are the functions of shear along the slip systems accumulated by a current instant of time and the history of their changes. The equations which describe their changes are of major importance in the constitutive models, and the corresponding relations for the evolution $\tau_{\mathrm{c}}^{(k)}$ have been proposed in many studies (Holmedal et al. 2008; Gérard et al. 2013; Khadyko et al. 2016, etc.). The alternative ones are the elastic-plastic models (Lin 1957; Weng 1980; Tokuda and Kratochvil 1984; Anand and Kothari 1996; McGinty and McDowell 2006, etc.) where it is required that the shear stresses should be equal to the critical ones for all the active slip systems.

In order to determine stresses, many works use relations in a "classical" unloaded configuration gained from the actual one by the affine transformation $\mathbf{f}^{\mathrm{e}-1}$:

$$\mathbf{k} = \overline{\boldsymbol{\pi}}_0 : \mathbf{c}^{\mathrm{e}} \qquad (4)$$

where $\mathbf{k} = J\,\mathbf{f}^{\mathrm{e}-1} \cdot \boldsymbol{\sigma} \cdot \mathbf{f}^{\mathrm{e}-\mathrm{T}}$ is the second Piola-Kirchhoff stress tensor, $\mathbf{c}^{e} = 1/2\left(\mathbf{f}^{\mathrm{eT}} \cdot \mathbf{f}^{\mathrm{e}} - \mathbf{I}\right)$ is the elastic Cauchy-Green strain tensor, and $\overline{\boldsymbol{\pi}}_0$ is the fourth-rank elasticity tensor defined in an unloaded configuration.

Within this popular statement, the rotations of the crystallite lattice are supposed to be determined by the orthogonal part of $\mathbf{R}^{\mathrm{e}}$ from the polar decomposition $\mathbf{f}^{\mathrm{e}}$. An alternative way is the Taylor full-constrained model (van Houtte et al. 2005) which is largely used in rigid-plastic and elastic-plastic models. If the elastic strains are small, the mentioned models give similar results (Horstemeyer et al. 2005). This fact is confirmed

by the similar simulation results of the texture formation, when these models are used in the studies of different authors.

Thus, to determine stress Eqs. (1), (2), (3), and (4) are used. They are supplemented by the equations used to describe the change of the critical stress of shears along the slip systems $\tau_c^{(k)}$, as well as for the crystallite lattice rotation. This formulation is proposed for the case of large displacement gradients. In fact, it is unacceptable to describe the majority of thermomechanical treatment processes for metals and alloys by using the hypothesis about the small displacement gradients, as in this case large displacement gradients are found experimentally, so the geometrically nonlinear formulation is necessary for the corresponding boundary value problems.

The equilibrium (momentum) equations and force boundary conditions become nonlinear, when the problem is formulated in terms of the reference configuration (in case of using the second Piola-Kirchhoff stress tensor). Apart from it, it is difficult to utilize the contact boundary conditions. In view of this fact, it is preferable to formulate the boundary value problem in terms of the current (or unloaded) configuration using the rate form for this purpose which is convenient for numerical simulation. In this case it is possible to find a stepwise solution entailing the reconfiguration of the computational domain (including contact surfaces). The system of the constitutive relations in terms of the current configuration can be written as follows:

$$\boldsymbol{\kappa}^{\mathrm{cr}} = d\boldsymbol{\kappa}/dt + \boldsymbol{\kappa}\cdot\overline{\boldsymbol{\omega}} - \overline{\boldsymbol{\omega}}\cdot\boldsymbol{\kappa} = \overline{\boldsymbol{\pi}} : \left(l - \bar{\boldsymbol{\omega}} - \sum_{k=1}^{K} \dot{\gamma}^{(k)}\mathbf{b}^{(k)}\mathbf{n}^{(k)}\right), \tag{5}$$

$$\dot{\gamma}^{(k)} = \dot{\gamma}_0 \left(\tau^{(k)}/\tau_c^{(k)}\right)^{\mathrm{m}} \mathrm{H}(\tau^{(k)} - \tau_c^{(k)}), \quad \mathrm{k} = 1, \ldots, \mathrm{K}, \tag{6}$$

$$\tau^{(k)} = \boldsymbol{\kappa} : \mathbf{b}^{(k)}\mathbf{n}^{(k)}, \ \mathrm{k} = 1, \ldots, \mathrm{K}, \tag{7}$$

$$\dot{\tau}_c^{(k)} = \left\langle equation\ to\ determine\ \dot{\tau}_c^{(k)} \right\rangle, \ \mathrm{k} = 1, \ldots, \mathrm{K}, \tag{8}$$

$$\overline{\boldsymbol{\omega}} = \left\langle equation\ to\ determine\ \overline{\boldsymbol{\omega}} \right\rangle. \tag{9}$$

In the simultaneous Eqs. (5), (6), (7), (8), and (9) $\boldsymbol{\kappa} = \overset{\mathrm{o}}{\rho}/\hat{\rho}\,\boldsymbol{\sigma}$ is the weighted Kirchhoff stress tensor, $\overline{\boldsymbol{\omega}}$ is the spin of the moving coordinate system which is connected to the lattice, $\overline{\boldsymbol{\pi}}$ is the tensor of elastic properties (its components are constant in the basis of the moving coordinate system), $\mathbf{l}$ is the velocity gradient, $\mathbf{b}^{(k)}$ and $\mathbf{n}^{(k)}$ are the unit vectors of the sliding direction and normals to the slip plane of the edge dislocations (in the reference configuration), and "cr" index designates the corotational derivative. The same equation (8) is used to determine the critical shear stress rate $\dot{\tau}_c^{(k)}$. The critical shear stresses satisfied the additivity property for various mechanisms of hardening and softening (see comment after formula (3); variant of equation (8) can be found in Trusov et al. 2012, 2013). Equation (9) is used to determine the lattice spin $\overline{\boldsymbol{\omega}}$; it can be found in Trusov et al. (2016). As for the lattice spin, it defines the moving coordinate system rotation rate. The moving coordinate system should be connected with the symmetric elements of the material. In Mandel (1973) the author states that it is necessary to determine the corotational derivative for a crystallite related to the crystallographic direction and plane. In this case, for an observer these tensors will change as indifferent ones in a fixed laboratory coordinate system; and it results in satisfying the material indifference principle in contrast to the case when the linear constitutive relation is formulated in the current configuration by accepting that the material property tensor is constant, i.e., the necessity of complying with this principle

implies that the tensor of properties can only be isotropic (Truesdell 1977). The improvement of the models which describe crystallite lattice rotations by accounting for the occurrence of the force (momentum) factors due to the defects interaction (Trusov et al. 2012) is considered as a prospect in developing the models based on the crystal plasticity approach.

When elastic strains are small (which is characteristic for metals and alloys), it can be shown that the formulation in (5), (6), (7), (8), and (9) is similar to the one that is described above for the case of using similar rotation models (Shveykin and Trusov 2016). As mentioned before the equation system (5), (6), (7), (8), and (9) in the statistical models is used for the number of crystallites; the response at the macrolevel (for the integration point in solving the boundary value problem) is determined by averaging. In the direct models, the equation system (5), (6), (7), (8), and (9) is used for each integration point.

The mesolevel equations that are given here as an example can be used to describe only the "simplest" processes of inelastic deformation. It is necessary to take into account the temperature and all important physical processes (including phase transformations) in the model structure during the simulation of most thermomechanical treatment processes.

Main Physical Mechanisms Occurring in the Processes of Thermomechanical Treatment

The main "carriers" of the inelastic deformation mechanisms in mono- and polycrystals are the linear defects of the crystal lattice, i.e., dislocations (Hirth and Lothe 1968). Scientists used these defects to argue against the assumption which referred to the beginning of the twentieth century concerning the shift of the atomic planes of an ideal crystal with respect to each other (Taylor 1934; Orowan 1934; Polanyi 1934). There is no need for a simultaneous failure of all the bonds between the neighboring atoms along the shear plane in inelastic deformation; the local failure and reconstruction of such bonds in the neighborhood of the dislocation line by the relay mechanism are enough. There are two main types of dislocations, such as edge and screw ones. The mixed type of dislocations having the form of the dislocation loops dominates in real crystals (Hirth and Lothe 1968). Burgers' vector is the main characteristic of a dislocation which is determined by the difference between a closed circle in the defect-free crystal and a closed circle including the dislocation line (Burgers' contour). Dislocations possessed with such Burgers' vector can be complete, and magnitude of this vector equals to the atomic spacing in the closest-packed direction. Motions of these dislocations lead to the identity transition of the crystal lattice, otherwise the dislocations are called incomplete or partial. Stacking fault energy is the main characteristic of a crystal material which describes the dislocation ability to be decomposed onto split dislocations (two partial dislocations and a stacking fault between them). Numerically, the stacking fault energy is equal to the repulsive force of the partial dislocations (per unit length) or the surface tension force of the stacking fault. The dislocation splitting and/or branching is determined by Frank's energetic criterion (Frank 1949) and the condition that the sum Burgers' vector of the reacting dislocations should be equal to the sum Burgers' vector of the formed dislocations (Hirth and Lothe 1968). The occurrence of partial dislocations initiates the twinning dislocations and implements the appropriate twinning mechanism (Cottrell and Bilby 1951), while their interaction leads to the formation of the dislocation barriers (Hirth 1961). In the process of inelastic deformation, the dislocations interact with defects of different types, and it provides strengthening. The increased temperatures cause the formation of jogs and kinks at the dislocation line, the activation of the diffusion processes by contributing to metals' softening.

The other important mechanism of inelastic deformation is twinning which does not prevail in metals with a big amount of slip systems (cubic lattice crystals). Twinning takes place in metals in which dislocation sliding along some slip systems is limited (hexagonal close-packed crystals). But it is experimentally confirmed that

the deformation by twinning is also found in metals with a cubic crystal lattice at low homological temperatures in materials with the low stacking fault energy and under increased rates of deformation (Honeycombe 1984). The appearing twins initiate a significant change in the material response, since they form effective barriers for the motion of the edge dislocations. Thus, in simulation of elastic-plastic deformation processes, it is necessary to take into consideration not only the motion of the edge dislocations but also the twinning as the mechanism of inelastic deformation and hardening. In crystal plasticity the representation of deformation by a combination of shears is usually used to describe twinning. The magnitude of a shear is fixed for each type of a crystal lattice. In this case, the shear strains are determined by the volume fraction of twins. The directions and planes of shear depend on the temperature of deformation (Hirth and Lothe 1968). It is known from the experiments that the propensity of a material to twinning rises when the temperature starts to decrease. Together with the temperature impacts, the strain rate has a significant influence on the twinning process. In deformation with rates that are lower than a critical value, twinning is not found in the samples (Hirth and Lothe 1968).

Inelastic deformation leads to the creation of defects at different scale levels. The temperature rise in inelastic deformation activates a number of processes which result in a significant change of the defect structure. Among them the "recovery" process has the lowest temperatures. As a result of the temperature rise during the "recovery," there comes the decrease of the defects' concentration appearing during inelastic deformation. The activation energy of such transformations has the minimum value. As a result, certain processes are in progress at the stage of "recovery," such as the point defect annihilation (vacancies and interstitial atoms) and the clustering of interstitial atoms (extrinsic stacking fault) and point defects (intrinsic stacking fault) and the flux of point defects to dislocations, dislocation structures, boundaries of grains/phase/twins, and external surfaces which decreases the concentration of point defects.

A further increase of the heat treatment temperature activates the "polygonization" process with the motion and redistribution of the dislocations that lead to their partial annihilation, as well as to the formation of the small-angle boundaries. The term of "polygonization," as noted in the works of Cahn (Cahn 1949, 1950), was proposed by E. Orowan; the works (Orowan 1954; Beck 1954, etc.) are also dedicated to studying polygonization.

At increased temperatures the dislocations of opposite signs start to annihilate; the rest of the dislocations are attracted or repulsed by their elastic fields. Finally, the dislocations form the "walls" which separate the crystal into the blocks that are disoriented relatively to each other by small angles. To arrange the edge dislocations into the walls, besides conservative movement (dislocation glide), some edge dislocations should go over into the neighboring planes by the diffusion way (dislocation climb). In case of the multiple glide, the formation of low-angle boundaries due only to gliding and climbing is impossible. The motion of screw dislocations is added to the process. As a result, the cellular structure and the volume dislocation tangles ("cell walls") are formed. The driving force of such a process is the interaction of the elastic fields of dislocations which leads to the formation of the boundaries encircling the cells. During further heating these boundaries become thinner and transform into flat low-angle sub-boundaries, while the cells transform into subgrains. At the same time, some dislocations from the cell volume are involved into the formed sub-boundaries influenced by the elastic forces.

Recrystallization is the next stage of the structure changing for deformable metals and alloys under higher temperatures. Recrystallization is a process of a complete or partial replacement of some grains of a certain phase which contain various structural imperfections by other grains of the same phase which possess more ideal structure (Lakhtin and Leontieva 1980). The process is effected by the process of generation, or both by generation and motion, or only by motion of high-angle boundaries (Friedel et al. 1964; Lakhtin and Leontieva 1980; Honeycombe 1984;

Gorelik et al. 2005). As a result of heating, when a certain temperature level (temperature threshold of recrystallization) reaches a given preliminary intensity of the plastic strain, the nucleations of new grains start to form and grow at the areas where the lattice distortion is higher (the boundaries of the deformed grains, twin boundaries, intersections of slip planes, shear bands, and other defects). The lattice of new grains is almost undistorted, it has a much smaller density of the defects, and, as a rule, it is separated from the other part of the matrix by the high-angle boundaries. The growth of "new" grains is predominantly carried out by the diffusion way (the atoms of "old" deformed grains are attached to the nucleation). The process of recrystallization is more energetically advantageous than the process of "recovery," as it is accompanied by the free energy decrease. There is a certain classification of recrystallization based on the type of applied loads in scientific literature (Gorelik et al. 2005). The preliminary plastic strain and further temperature impacts without active deformation loadings initiate a so-called static recrystallization. In the process of hot plastic deformation (a simultaneous influence of external loadings and temperature), the dynamic recrystallization takes place. Postdynamic recrystallization occurs after hot deformation and, in case of the absence of deformation loading, by a rapid growth of the recrystallization centers prepared during deformation. When the primary recrystallization is finished in the process of further heating, the collective recrystallization can take place, i.e., the growth of some recrystallized grains due to others. This occurs as a result of the migration of high-angle boundaries, when the grains with convex boundaries "are eaten" by the grains with concave boundaries (Lakhtin and Leontieva 1980). The reason for such recrystallization is the decrease of the grain boundary (surface) energy, as the boundary length decreases in the process of grains' growth; and larger grains start to appear. The result of heating after primary recrystallization can be different, i.e., some grains have the crystallographic orientation which is favorable for further growth, the concentration of defects (the value of the volume density of internal energy) which is smaller than other grains have, and a higher mobility of the grain boundaries due to the inhomogeneous distribution of the solute. In view of the foregoing, the majority of the fine-grained crystals and a small number of coarse-grained ones are formed. Such process is called the secondary recrystallization.

The solid-state phase transformations which take place in the material as a result of the thermomechanical impact and entail the change of the material crystal structure play an important role in the processes of thermomechanical treatment of steels and alloys (Kurdumov et al. 1977; Kashchenko et al. 1996; Kouznetsova and Geers 2008; Bhadeshia and Honeycombe 2017). If a material can exist in different crystal modifications, then its most stable phase is that corresponding to the lower level of free energy under fixed conditions. Herewith the crystal lattice type resulting from phase transformation depends on complex interaction of atoms and electrons. The use of the thermodynamics theory allows connecting the stability of one or another crystal modification with the connecting forces, amplitude, and frequency of atom fluctuations which are naturally determined by the structure and state of the atoms. The solid-state phase transformations comply with the common laws of crystallization related to the occurrence and growth of new phase nucleuses. Solid-state phase transformations are effected in the solid anisotropic medium; therefore, during transformation the atoms (belonging to different modifications) on the contiguous facets of the initial and new phases take their positions according to the principle of the structural and dimensional conformity, i.e., a nucleus of a new phase in the solid anisotropic medium should be oriented in such a way that it contacts the initial ("old") phase by its crystal planes which have most similar structural sizes (Dankov 1943; Konobeevsky 1943; Kurdumov et al. 1977; Bhadeshia and Honeycombe 2017). Solid-state phase transformations take place in such a way that a stable nucleus is formed in the conditions which correspond to the thermodynamic stability of the new phase due to the fluctuations of energy, configuration, or density (concentration); the nucleus is characterized

with a different arrangement of atoms determining a new crystal lattice. According to the principle of the structural and dimensional conformity, the order of atoms' arrangement is changing by their regular displacement in the lattice of the initial phase; under this displacement the energy of a given volume of the transformed material reaches its minimum (Entin 1960). This mechanism of a new phase formation during transformation at the solid anisotropic medium creates the situation when the crystals of a new modification become regularly oriented toward the initial crystals. In the solid-state phase transformation, the grain structure of the material starts to change, and it is connected to the formation of new phase grains which differ from the grains of the initial phase in their shape and sizes. Such microstructure change in solid-state phase transformations is used in a number of technological processes related to the thermomechanical treatment of alloys (annealing of the second kind, hardening, etc.).

All the available solid-state phase transitions which result from the cooling of austenite (perlitic, bainitic, and martensitic ones (Kurdumov et al. 1977; Bhadeshia and Honeycombe 2017)) are found in steels. Austenite is an interstitial solid solution of carbon in $\gamma - Fe$ (face-centered cubic lattice). Martensite is a supersaturated solid solution of the substitution in $\alpha - Fe$ (body-centered cubic (tetragonal) lattice) appearing as a result of $\gamma - \alpha$ transformation in case of a lack of carbon diffusion. Perlite is an eutectoid mixture of ferrite ($\alpha - Fe$) and cementite (or special carbides). A bainitic structure can consist of ferrite, carbides, and residual austenite. Thus, depending on the conditions of the process, a transformation can be fulfilled either by the normal (diffusive) mechanism (if the interphase boundary is non-coherent) or by the martensitic (diffusionless) mechanism (if the interphase boundary is coherent). An important feature of the diffusion phase transformations is the formation of a new phase that is accompanied by the redistribution of the alloying elements and carbon and requires the diffusive redistribution of atoms for long distances. Various phase transformations under thermomechanical impacts and their kinetics depend on the composition of the steel and parameters of the thermomechanical influence such as temperature, heating conditions, duration of exposure, cooling rate, mechanical loading, etc.

The description of the phase transformation process is based on using the thermodynamic approach. The determination of the thermodynamic driving forces of phase transformations is based on the dissipation inequality. Different thermodynamic potentials such as internal energy, Helmholtz free energy, Gibbs free energy, and entropy can be used wherein. The choice of the thermodynamic potential depends on the distinctive features of the problem under consideration. The phase transformation criteria are formulated in terms of the thermodynamic driving force when the phase transformation is there, if the thermodynamic force reaches some critical value, which is the parameter of the material. The kinetic equations are formulated for the fractions of all the coexisting phases in the structure of the material which describe the phase fraction changing (velocity of changing) depending on the parameters of the process.

About the Multilevel Models of Steels and Alloys Aiming to Describe Thermomechanical Processing

The multilevel approach with internal variables is quite promising for the simulation of the recrystallization processes (Raabe and Becker 2000). As a rule, the crystal plasticity-based models that are integrated into the software realization of the finite element method are used herewith (Bate 1999; Roters et al. 2010; Takaki and Tomita 2010). In this case the position of a boundary for the recrystallized grains is determined by the Monte Carlo method, the cellular automation, or the phase field method. Two stages can be distinguished in the recrystallization simulation, i.e., the simulation of new grains' nucleation and of the motion of the boundaries of the recrystallized grains. In order to simulate the nucleation stage of grains, the statistical methods are actively

utilized which use the physical analysis of the preferable positions of new grain generations. The additional internal variable is introduced into the structure of the constitutive model during the simulation of the motion of new high-angle boundaries. The most important of them is the driving force which acts on the boundary of a new grain, the boundary normal growth rate, and the boundary mobility. For many polycrystalline materials, especially for the chemically clear ones, the boundary motion rate is determined as a multiplication of the driving force and mobility value (Rollett et al. 2004). The mobility parameter is a function of temperature; and it is characterized by the Arrhenius-type equation. For many polycrystalline materials, the main driving force for the normal boundary motion is the difference of the stored energy (in inelastic deformation) between two neighboring grains. The driving force also depends on the intergranular energy, the atomic structure of the boundary, the misorientation between the neighboring grains, the location of the boundary, the curvature of the boundary, triple junctions, and the density of vacancies in the neighboring grains. Disperse particles, the presence of other phases, micropores, and the impurity atoms initiate the deceleration of the boundary migration.

It is one of the priority objectives to consider phase transformations which occur in materials during the simulation of the thermomechanical treatment of steels and alloys. A correct description of how materials change their structure (including those which are caused by the phase transformations occurring in the material, when it is under treatment) using the multilevel constitutive modeling provides an effective instrument aiming to develop new methods of creating materials with a given set of properties, as well as optimizing the already available materials and technologies of their treatment. It is quite resource-intensive to have an experimental study of this issue, especially in case of the complex thermomechanical loading; therefore, it is important for solid mechanics to develop the constitutive models which will describe the state and evolution of the material structure taking into account solid phase transformations occurring in the material (Bhadeshia and Honeycombe 2017).

Traditionally, there are two main approaches to the modeling of the solid phase transformations. The first approach is based on an explicit consideration of interphase boundaries with regard to the conditions at the boundary of the phases in the deformed material and the kinetics of a new phase development. The second approach is connected with the elaboration of models based on the introduction of the additional state parameters which characterize particular features of the material structure "on average" (e.g., the concentration of a new phase) and the formulation of the constitutive equations for these parameters.

An explicit introduction of interphase boundaries into consideration (Grinfeld et al. 1990; Yeremeyev et al. 2007, etc.) allows to describe the phase transformations from the point of view of solid mechanics using many ideas of the classical theory of phase transformations by J. Gibbs. The material microstructure changing in the process of the phase transformation generates the intrinsic strains of the transformation and leads to the elasticity modules' changing. In this case, the boundary of the phases in the elastic material is considered as a surface where the strain field is discontinuous, while the stress field is continuous. The occurrence of an equilibrium-discontinuous strain field in the elastic body requires the availability of the areas in the strain field where Hadamard's inequality is broken, which is a necessary condition of the stability under small strains. In this case, to ensure the balance at the boundary of the phases, certain conditions are set, such as the preservation of the material continuity, force continuity, and the condition which is the analog of the chemical potentials' equality in Gibbs' theory. So, there comes the limitation in determining the phase boundary form and appropriate strains at the boundary. This entails the concept of the phase transition zone which boundary determines the ultimate surface of transformation in the strain field.

It is quite often that the phase field method is applied to simulate both the diffusion phase transformations and the diffusionless (marten-

sitic) transformations at the mesolevel (when the simulation is fulfilled for the volume consisting of several grains) (Cahn and Hilliard 1958; Chen and Khachaturyan 1991; Wang et al. 1993; Karma and Olabi 2001; Steinbach and Apel 2006; Yamanaka et al. 2010; Bellon 2012; Choudhury 2017, etc.). This approach assumes the availability of a "fuzzy" "diffusion" boundary between the phases in contrast to the classical methods that use the concept of a "sharp boundary." In the approach of the "diffusion boundary," the form and mutual arrangement of the regions of single phases are described by an aggregate of the parameters determining their volume fractions φ_i. The value of the parameter can change from 0 to 1; $\varphi_i = 0$ corresponds to the region without i phase, and $\varphi_i = 1$ means that the region is a single-phased one. So, the microstructure (except for grain boundaries, defects, etc.) can be described by a set of single-phase domains separated by the boundaries, where more than one value of φ_i differs from zero. So, in the approach of the "diffusional boundary," the form changing (and hence, the position of the boundary) in time is determined implicitly by changing the phase fractions. The change of the phase fractions in time is described by the kinetic equation which is received in the framework of the thermodynamics of irreversible processes, i.e., the linear connection between the phase fractions' changing rate and the derivative of the thermodynamic potential with respect to this parameter is used. The phase transformations which occur in isothermal conditions are investigated more often. And in this case, the free energy is used as a thermodynamic potential. But there are works aiming to study the non-isothermal processes, when the entropy is chosen as a thermodynamic potential (Loginova et al. 2001). Free energy is usually determined as a sum of chemical, elastic, and "gradient" parts. In case of describing the diffusion phase transformations (besides the kinetic equation for the phase fractions), the equations of diffusion are solved to determine the change of concentrations for the alloying elements and carbon. In this case the chemical energy of the system depends on the concentration of the alloying elements and carbon.

The macrophenomenological approach that is based on using the kinetic equations to describe the new phase fraction, nascent as a result of a solid phase transformation at the level of the sample (Avrami 1940; Koistinen and Marburger 1959), is rather widespread in describing the thermomechanical processing of steel constructions. Within the framework of this approach in determining the volume fraction of martensite, the phenomenological exponential relation by Koistinen and Marburger is often used:

$$\xi = \xi_A^0 \left(1 - e^{-k(M_S - \theta)}\right), \tag{10}$$

where ξ_A^0 is a volume fraction of austenite at the initial moment, k is the material parameter, M_S is the temperature of the martensite transformation beginning, and θ is temperature. For the volume fraction of the phase (formed by the diffusion mechanism), the Johnson-Mehl-Avrami-Kolmogorov equation is usually used:

$$\xi = \xi^{\max} \left(1 - e^{-bt^n}\right), \tag{11}$$

where $\xi^{\max}$ is a limit fraction of a new phase and b and n are the material parameters. In this case all the material parameters are determined upon the diagram of the isothermal transformation for the modeled steel. The described macrophenomenological relations (10) and (11) determining the phase fractions are formulated based on the hypothesis that the nucleuses of the new phase are supposed to be randomly allocated in the area; the growth rate is supposed to be independent from the degree of transformation, and the growth goes with an equal rate in either direction. There is a great number of works which offer different modifications of kinetic equations (10) and (11). As a rule, these modifications are based on adding the functional dependences of the material parameters from the parameters of the external impact such as temperature and applied loading.

Unlike the traditional macrophenomenological approaches to the simulation of phase transformations which have been described in short earlier, the use of the multilevel approach allows to describe the mechanisms connected with the

phase transformations at that scale level, where they take place in the real material. Multilevel modeling allows supplementing the structure of the model with the relations describing different processes affecting each other, such as inelastic deformation at the level of crystallites, changing the phase composition of the material, and, consequently, changing its properties in the process of the thermomechanical impact, changing the temperature conditions, etc. To describe the solid phase transformations, the additional internal variables are entered into the structure of the multilevel constitutive model (1), (2), (3), (4), (5), (6), (7), (8), and (9) which have been provided earlier. These internal variables characterize the material structure changing at various scale levels in the process of phase transformation, for example, the fractions of all the phases coexisting in the material in the fixed conditions of the process under consideration. The evolutional equations which are based on the physical concept about the modeled process are formulated for the internal variables of the model.

As a rule, in simulation of the phase transformations at the mesolevel, when the modeled area is a single grain or an aggregate of grains, one uses the models which are based on crystal plasticity with the introduction of some additional parameters considering the phase transformations occurring in the material (Olson and Cohen 1975; Cherkaoui et al. 1998; Iwamoto 2004; Turteltaub and Suiker 2006; Kouznetsova and Geers 2008; Tjahjanto et al. 2008; Lee et al. 2010; Fischlschweiger et al. 2012; Yadegari et al. 2012, etc.). In case of modeling the thermomechanical processing using this approach, the phase composition for the material representative volume of some scale level is determined depending on the influencing external conditions. As a result of phase transformations, the material volume under consideration can be partially or completely turned into a new phase. Each phase is characterized by a certain complex of the homogenous properties and known microstructure. Particularly, the phases can differ in their composition and the type of the material crystallite lattice (or the parameters of the crystallite lattice).

As a rule, the extended multiplicative decomposition of the deformation gradient is used in such models which includes (besides the elastic and the plastic constituents) the part characterizing the configuration change due to the phase transformation. Therefore, relation (1) is transformed into the following one:

$$\mathbf{f} = \mathbf{f}^{\mathrm{e}} \cdot \mathbf{f}^{\mathrm{p}} \cdot \mathbf{f}^{\mathrm{tr}}, \tag{12}$$

where $\mathbf{f}^{\mathrm{tr}}$ is the transformation part of the deformation gradient. To determine the transformation constituent of the deformation gradient, we use all the available information and the physically based hypothesis about the new nascent phase of the material. For example, in the simulation of the martensite transformation, the transformation part of the deformation gradient can be determined upon the Bain deformation for each variant of the martensite.

As a rule, the description of a phase transformation in the structure of a multilevel model is based on using the thermodynamic approach. Wherein, each phase can be described as an area having a specific thermodynamic potential in the equilibrium state which is different from the potentials of other phases. Within the framework of the representative volume of the material, the phase transformations are executed under the influence of the thermodynamic driving forces. The thermodynamic driving force of the transformation can be determined based on the approaches of the classical thermodynamics of the irreversible processes (de Groot 1951; Christian 2002; Kondepudi and Prigogine 2015; Winterbone and Turan 2015). As a rule, the common structure of the thermodynamic driving forces of phase transformations can be determined based on the dissipation inequality. Depending on the features of the solved problem, different thermodynamic potentials can be used therein (internal energy, Helmholtz free energy, Gibbs free energy, entropy). More often the criteria of phase transformations are also formulated in terms of the thermodynamic force, i.e., the phase transformation is there, if the value of the thermodynamic driving force reaches the critical level which is the material parameter.

The kinetic equations are formulated for the fractions of all the coexisting phases in the structure of the material representative volume at the scale level. These equations describe the change of the phase fraction (velocity of changing) depending on the process parameters.

So, the evolutional equations for the phase fractions are added to the system of Eqs. (5), (6), (7), (8), and (9):

$$\dot{\xi}^{(j)} = \left\langle \textit{equation to determine } \dot{\xi}^{(j)} \right\rangle,\ j=1,\ldots,M, \tag{13}$$

where $\xi^{(j)}$ is the j-phase fraction formed as a result of the phase transformation and M is a common quantity of the phases which can be formed as a result of the phase transformation. As a rule, the rate of changing for the phase fraction j is a function depending on the temperature and thermodynamic driving force of the transformation of the initial phase to the phase j.

Inelastic strains of the representative volume element at a scale level in Eq. (5) for the case of the phase transformation can be determined by averaging the inelastic strains of the separate phases weighted with their fractions. To describe the non-isothermal processes, the dependence from the temperature is also added to the structure of the relations (5), (6), (7), (8), and (9). Besides, the additional constituent characterizing the transformational strains connected to the phase transformation in the material is added to the right part of the relation (5). Thus, to describe the processes of the material thermomechanical treatment, the system of Eqs. (5), (6), (7), (8), and (9) for the element of a scale level can be reorganized in the following way, for example:

$$\begin{aligned}
&\boldsymbol{\kappa}^{\mathrm{cr}} = d\boldsymbol{\kappa}/dt + \boldsymbol{\kappa}\cdot\overline{\boldsymbol{\omega}} - \overline{\boldsymbol{\omega}}\cdot\boldsymbol{\kappa} = \overline{\boldsymbol{\pi}} : \left(l - \overline{\boldsymbol{\omega}} - \sum_{i=1}^{N} \xi^{(i)} \sum_{k=1}^{K} \dot{\gamma}^{(k)} \mathbf{b}^{(k)} \mathbf{n}^{(k)} - \mathbf{l}^{\mathrm{th}} - \mathbf{l}^{\mathrm{tr}} \right), \\
&\dot{\gamma}^{(k)} = \dot{\gamma}_0 \left(\tau^{(k)} / \tau_{\mathrm{c}}^{(k)} \right)^{\mathrm{m}} \mathrm{H}\left(\tau^{(k)} - \tau_{\mathrm{c}}^{(k)} \right),\ \mathrm{k} = 1,\ldots,\mathrm{K}, \\
&\tau^{(k)} = \boldsymbol{\kappa} : \mathbf{n}^{(k)} \mathbf{b}^{(k)},\ \mathrm{k} = 1,\ldots,\mathrm{K}, \\
&\dot{\tau}_{\mathrm{c}}^{(k)} = \left\langle \textit{equation to determine } \dot{\tau}_{\mathrm{c}}^{(k)} \right\rangle,\ \mathrm{k} = 1,\ldots,\mathrm{K}, \\
&\overline{\boldsymbol{\omega}} = \left\langle \textit{equation to determine } \overline{\boldsymbol{\omega}} \right\rangle, \\
&\dot{\xi}^{(j)} = \left\langle \textit{equation to determine } \dot{\xi}^{(j)} \right\rangle,\ j = 1,\ldots,M,
\end{aligned} \tag{14}$$

where $\mathbf{l}^{\mathrm{th}}$ is the thermal component of the velocity gradient which can be found as $\mathbf{l}^{\mathrm{th}} = \boldsymbol{\alpha}\dot{\theta}$ (where $\boldsymbol{\alpha}$ is the thermal expansion tensor determined for the multiphase material volume by weighing the thermal expansion tensors of the separate phases with fractions of these phases, respectively); $\mathbf{l}^{\mathrm{tr}}$ is the transformation component of the velocity gradient which appears due to the phase transformation in the considered material volume which can be determined from the relation $\mathbf{l}^{\mathrm{tr}} = \sum_{j=1}^{M} \dot{\xi}^{(j)} \mathbf{f}_j^*$, where $\mathbf{f}_j^*$ is the transformation velocity gradient describing the transformation of the initial phase to the phase j and determined by the type of the current phase transformation. The tensor of elastic properties $\overline{\boldsymbol{\pi}}$ of the multiphase representative volume is determined similarly by the rule of mixture. Of course, the structure of the constitutive model relations at the mesolevel (14) can also be expanded by taking into consideration other mechanisms of inelastic deformation.

So, the authors have shortly characterized the multilevel constitutive models and described certain approaches to their application in order to specify the processes of thermomechanical treatment.

Cross-References

- Discrete and Continuum Thermomechanics
- Finite Element Methods
- Size Effect in Nanomaterials
- Truesdell's and Zhilin's Approaches: Derivation of Constitutive Equations

References

Anand L (2004) Single-crystal elasto-viscoplasticity: application to texture evolution in polycrystalline metals at large strains. Comput Methods Appl Mech Eng 193:5359–5383

Anand L, Kothari MA (1996) A computational procedure for rate–independent crystal plasticity. J Mech Phys Solids 44(4):525–558

Ardeljan M, Beyerlein IJ, Knezevic M (2014) A dislocation density based crystal plasticity finite element model: application to a two-phase polycrystalline HCP/BCC composites. J Mech Phys Solids 66:16–31

Asaro RJ (1983) Micromechanics of crystals and polycrystals. Adv Appl Mech 23:1–115

Asaro RJ, Needleman A (1985) Texture development and strain hardening in rate dependent polycrystals. Acta Metall 33(6):923–953

Austin R, McDowell D (2011) A dislocation-based constitutive model for viscoplastic deformation of FCC metals at very high strain rates. Int J Plast 27:1–24

Avrami M (1940) Kinetics of phase change. II: transformation–time relations for random distribution of nuclei. J Chem Phys 8:212

Barton NR, Bernier JV, Becker R et al (2011) A multiscale strength model for extreme loading conditions. J Appl Phys 109(7):073501

Bate P (1999) Modelling deformation microstructure with the crystal plasticity finite–element method. Philos Trans R Soc Lond A Math Phys Eng Sci 357(1756):1589–1601

Beck PA (1954) Annealing of cold worked metals. Adv Phys 3(11):245–324

Bellon P (2012) Phase field methods. Compr Nucl Mater 1:411–432

Beyerlein IJ, Tome CN (2008) A dislocation-based constitutive law for pure Zr including temperature effects. Int J Plast 24:867–895

Beyerlein IJ, McCabe RJ, Tome CN (2011) Effect of microstructure on the nucleation of deformation twins in polycrystalline high-purity magnesium: a multiscale modeling study. J Mech Phys Solids 59:988–1003

Bhadeshia H, Honeycombe R (2017) Steels: microstructure and properties, 4th edn. Elsevier, Amsterdam

Bronkhorst CA, Kalidindi SR, Anand L (1992) Polycrystalline plasticity and the evolution of crystallographic texture in FCC metals. Philos Trans R Soc Lond A Math Phys Eng Sci 341(1662):443–477

Cahn RW (1949) Recrystallization of single crystals after plastic bending. J Inst Met 76(2):121–143

Cahn RW (1950) A new theory of recrystallization nuclei. Proc Phys Soc Sect A 63(4):323

Cahn JW, Hilliard JE (1958) Free energy of a nonuniform systems. I. Interfacial free energy. J Chem Phys 28:258–266

Cailletaud G, Diard O, Feyel F, Forest S (2003) Computational crystal plasticity: from single crystal to homogenized polycrystal. Tech Mech 23(2–4):130–145

Chen L-Q, Khachaturyan A (1991) Computer simulation of structural transformations during precipitation of an ordered intermetallic phase. Acta Mater 39:2533–2551

Cherkaoui M, Berveiller M, Sabar H (1998) Micromechanical modeling of martensitic transformation induced plasticity (trip) in austenitic single crystals. Int J Plast 14(7):597–626

Choudhury A (2017) Phase-field modeling as a method relevant for modeling phase transformation during interdiffusion. In: Aloke P, Divinski S (eds) Handbook of solid state diffusion. Volume 1, Diffusion fundamentals and techniques. Elsevier, Amsterdam, pp 363–389

Christian JW (2002) The theory of transformations in metals and alloys, 3rd edn. Elsevier, Amsterdam

Cottrell AH, Bilby BA (1951) LX. A mechanism for the growth of deformation twins in crystals. Lond Edinb Dubl Phil Mag J Sci 42(329):573–581

Dancette S, Delannay L, Jodlowski T, Giovanola J (2010) Multisite model prediction of texture induced anisotropy in brass. Int J Mater Form 3(1):251–254

Dankov PD (1943) The mechanism of phase transformation from the point of view of the principle of orientational and dimensional correspondence. Izv Sector Phys Chem Anal USSR Acad Sci 16(1):82–95 (in Russian)

de Groot SR (1951) Thermodynamics of irreversible processes. North-Holland Publishing Company, Amsterdam

Entin RI (1960) The transformation of austenite into steel. Metallurgy, Moscow (in Russian)

Fischlschweiger M, Cailletaud G, Antretter T (2012) A mean-field model for transformation induced plasticity including backstress effects for non-proportional loadings. Int J Plast 37:53–71

Frank FC (1949) Discussion on paper by NF Mott: mechanical properties of metals. Physica 15:131–133

Friedel J, Smoluchowski R, Kurti N (1964) Dislocations. Pergamon Press Ltd., Elsevier

Gérard C, Cailletaud G, Bacroix B (2013) Modeling of latent hardening produced by complex loading paths in FCC alloys. Int J Plast 42:194–212

Ghoniem NM, Busso EP, Kioussis N, Huang H (2003) Multiscale modelling of nanomechanics and micromechanics: an overview. Philos Mag 83(31–34):3475–3528

Gorelik SS, Dobatkin SV, Kaputkina LM (2005) Recrystallization of metals and alloys. MISIS, Moscow (in Russian)

Grinfeld MA (1990) Metody mekhaniki sploshnykh sred v teorii fazovykh prevrashcheniy [Methods of continuum mechanics in the theory of phase transitions]. Nauka, Moscow (in Russian)

Guo YB, Wen Q, Horstemeyer MF (2005) An internal state variable plasticity-based approach to determine dynamic loading history effects on material property in manufacturing processes. Int J Mech Sci 47:1423–1441

Habraken AM (2004) Modelling the plastic anisotropy of metals. Arch Comput Meth Eng 11(1):3–96

Hirth JP (1961) On dislocation interactions in the FCC lattice. J Appl Phys 32(4):700–706

Hirth JP, Lothe J (1968) Theory of dislocations. McGraw-Hill, New York

Holmedal B, Van Houtte P, An Y (2008) A crystal plasticity model for strain-path changes in metals. Int J Plast 24:1360–1379

Honeycombe RWK (1984) Plastic deformation of metals. Edward Arnold, London

Horstemeyer MF, Potirniche GP, Marin EB (2005) Crystal plasticity. In: Yip S (ed) Handbook of materials modeling. Springer, Dordrecht, pp 1133–1149

Iwamoto T (2004) Multiscale computational simulation of deformation behavior of TRIP steel with growth of martensitic particles in unit cell by asymptotic homogenization method. Int J Plast 20:841–869

Kalidindi SR, Bronkhorst CA, Anand L (1992) Crystallographic texture evolution in bulk deformation processing of FCC metals. J Mech Phys Solids 40(3):537–569

Karma A, Olabi A-G (2001) Phase field methods. In: Buschow KHJ et al (eds) Encyclopedia of materials: science and technology, 2nd edn. Elsevier, Amsterdam, pp 6873–6886

Kashchenko MP, Letuchev VV, Yablonskaya TN, Teplyakova LA (1996) A model of the formation of macroshear bands and strain-induced martensite with (HHL) boundaries. Phys Met Metallogr 82(4):329–336

Khadyko M, Dumoulin S, Cailletaud G, Hopperstad OS (2016) Latent hardening and plastic anisotropy evolution in AA6060 aluminium alloy. Int J Plast 76: 51–74

Koistinen DP, Marburger RE (1959) A general equation prescribing the extent of the austenite-martensite transformation in pure ironcarbon alloys and plain carbon steels. Acta Metall 7:59–60

Kondepudi D, Prigogine I (2015) Modern thermodynamics: from heat engines to dissipative structures. Wiley, Chichester

Konobeevsky ST (1943) To the theory of phase transformations. J Exper Theor Phys 13(6):185–214 (in Russian)

Kouznetsova VG, Geers MGD (2008) A multi-scale model of martensitic transformation plasticity. Mech Mater 40:641–657

Kröner E (1960) Allgemeine kontinuumstheorie der versetzungen und eigenspannungen. Arch Ration Mech Anal 4:273–334

Kurdumov GV, Utievskiy LM, Entin RI (1977) The transformations in iron and steel. Nauka, Moscow (in Russian)

Lakhtin Yu M, Leontieva VP (1980) Materials science. Mechanical Engineering, Moscow (in Russian)

Lee EH (1969) Elastic plastic deformation at finite strain. ASME J Appl Mech 36:1–6

Lee M-G, Kim S-J, Han HN (2010) Crystal plasticity finite element modeling of mechanically induced martensitic transformation (MIMT) in metastable austenite. Int J Plast 26:688–710

Lin TH (1957) Analysis of elastic and plastic strains of a face – centered cubic crystal. J Mech Phys Solids 5(1):143–149

Loginova I, Amberg G, Agren J (2001) Phase-field simulations of nonisothermaly binary alloy solidification. Acta Mater 49:573–581

Mandel J (1973) Equations constitutives et directeurs dans les milieux plastiques et viscoplastiquest. Int J Solids Struct 9:725–740

Maugin GA (2015) The saga of internal variables of state in continuum thermo-mechanics (1893–2013). Mech Res Commun 69:79–86

McDowell DL (2005) Internal state variable theory. In: Yip S (ed) Handbook of materials modeling. Springer, Dordrecht, pp 1151–1169

McDowell DL (2008) Viscoplasticity of heterogeneous metallic materials. Mater Sci Eng R 62:67–123

McDowell DL (2010) A perspective on trends in multiscale plasticity. Int J Plast 26:1280–1309

McGinty RD, McDowell DL (2006) A semi–implicit integration scheme for rate independent finite crystal plasticity. Int J Plast 22:996–1025

M'Guil S, Ahzi S, Youssef H, Baniassadi M, Gracio JJ (2009) A comparison of viscoplastic intermediate approaches for deformation texture evolution in face-centered cubic polycrystals. Acta Mater 57:2496–2508

Olson GB, Cohen M (1975) Kinetics of strain-induced martensitic nucleation. Metall Trans A 6A:791–795

Orowan E (1934) Zur kristallplastizität. I. Zeitschrift für Physik A Hadrons and Nuclei 89(9):605–613

Orowan E (1954) Dislocations in metals. American Institute of Metals, New York

Polanyi M (1934) Über eine Art Gitterstörung, die einen kristall plastisch machen könnte. Zeitschrift für Physik A Hadrons and Nuclei 89(9):660–664

Raabe D, Becker RC (2000) Coupling of a crystal plasticity finite-element model with a probabilistic cellular automaton for simulating primary static recrystallization in aluminium. Model Simul Mater Sci Eng 8(4):445–462

Rollett A, Humphreys FJ, Rohrer GS, Hatherly M (2004) Recrystallization and related annealing phenomena. Elsevier, Oxford

Roters F (2011) Advanced material models for the crystal plasticity finite element method: development of a general CPFEM framework. RWTH Aachen, Aachen

Roters F, Eisenlohr P, Hantcherli L, Tjahjanto DD, Bieler TR, Raabe D (2010) Overview of constitutive laws, kinematics, homogenization and multiscale

methods in crystal plasticity finite-element modeling: theory, experiments, applications. Acta Mater 58: 1152–1211
Saï K (2011) Multi-mechanism models: present state and future trends. Int J Plast 27:250–281
Shveykin AI, Trusov PV (2016) The comparison of geometrically nonlinear elastoviscoplastic constitutive relations formulated in terms of current configuration and formulated in terms of the stress free configuration. Phys Mesomech 19(5):48–57 (in Russian)
Steinbach I, Apel M (2006) Multi-phase field model for solid state transformation with elastic strain. Phys D 217:153–160
Takaki T, Tomita Y (2010) Static recrystallization simulations starting from predicted deformation microstructure by coupling multi-phase-field method and finite element method based on crystal plasticity. Int J Mech Sci 52(2):320–328
Taylor GI (1934) The mechanism of plastic deformation of crystals. Part I. Theoretical. Proc R Soc Lond Ser A Containing Pap Math Phys Character 145(855): 362–387
Taylor GI (1938) Plastic strain in metals. J Inst Metals 62:307–324
Tjahjanto DD, Turteltaub S, Suiker ASJ (2008) Crystallographically based model for transformation-induced plasticity in multiphase carbon steels. Contin Mech Thermodyn 19:399–422
Tokuda M, Kratochvil J (1984) Prediction of subsequent yield surface by a simple mechanical model of polycrystal. Arch Mech 36(5–6):661–672
Truesdell C (1977) A first course in rational continuum mechanics. Academic, New York
Trusov PV, Shveykin AI (2013a) Multilevel crystal plasticity models of single- and polycrystals. Statistical models. Phys Mesomech 16(1):23–33
Trusov PV, Shveykin AI (2013b) Multilevel crystal plasticity models of single- and polycrystals. Direct models. Phys Mesomech 16(2):99–124
Trusov PV, Ashikhmin VN, Volegov PS, Shveykin AI (2010) Constitutive relations and their application to the description of microstructure evolution. Phys Mesomech 13(1–2):38–46
Trusov PV, Shveykin AI, Nechaeva ES, Volegov PS (2012) Multilevel models of inelastic deformation of materials and their application for description of internal structure evolution. Phys Mesomech 15(3–4): 155–175
Trusov PV, Volegov PS, Shveykin AI (2013) Multilevel model of inelastic deformation of FCC polycrystalline with description of structure evolution. Comput Mater Sci 79:429–441
Trusov PV, Shveykin AI, Yanz A Yu (2016) About motion decomposition, frame independent derivatives and constitutive relations from the view point of a multilevel modeling. Phys Mesomech 19(2):47–65 (in Russian)
Turteltaub S, Suiker ASJ (2006) A multiscale thermomechanical model for cubic to tetragonal martensitic phase transformations. Int J Solids Struct 43:4509–4545
van Houtte P (2009) Crystal plasticity based modelling of deformation textures. In: Haldar A, Suwas S, Bhattacharjee D (eds) Microstructure and texture in steels. Springer-Verlag, London, pp 209–224
van Houtte P, Li S, Seefeldt M, Delannay L (2005) Deformation texture prediction: from the Taylor model to the advanced Lamel model. Int J Plast 21:589–624
Wagner F, Canova G, Van Houtte P, Molinari A (1991) Comparison of simulated and experimental deformation textures for BCC metals. Textures Microstruct 14–18: 1135–1140
Wang Y, Chen L-Q, Khachaturyan AG (1993) Kinetics of straininduced morphological transformation in cubic alloys with a miscibility gap. Acta Metall Mater 41(1): 279–296
Weng GJ (1980) Dislocation theories of work hardening and yield surfaces of single crystals. Acta Mech 37 (3–4):217–230
Winterbone D, Turan A (2015) Advanced thermodynamics for engineers, 2nd edn. Butterworth-Heinemann Elsevier Ltd, Oxford, United Kingdom
Yadegari S, Turteltaub S, Suiker ASJ (2012) Coupled thermomechanical analysis of transformation-induced plasticity in multiphase steels. Mech Mater 53:1–14
Yamanaka A, Takaki T, Tomita Y (2010) Elastoplastic phase-field simulation of martensitic transformation with plastic deformation in polycrystal. Int J Mech Sci 52:245–250
Yeremeyev VA, Freidin AB, Sharipova LL (2007) The stability of the equilibrium of two-phase elastic solids. J Appl Math Mech 71:61–84
Zhao J, Sheng D (2006) Strain gradient plasticity by internal-variable approach with normality structure. Int J Solids Struct 43:5836–5850

Thermomechanical Treatment of Polycrystals

▸ Thermomechanical Processing of Steels and Alloys: Multilevel Modeling

Thermomechanics

▸ Continuum Mechanics with Spontaneous Violations of the Second Law of Thermodynamics

Thick Plate

▸ Classical Plate Problems
▸ Direct Derivation of Plate Theories

Thick Shells

▸ Elastic Shells, Linear Shear-Deformable Theory

Thin Bodies Embedded in Fractional Derivative Viscoelastic Medium, Dynamic Response

Yury A. Rossikhin and Marina V. Shitikova
Research Center on Dynamics of Solids and Structures, Voronezh State Technical University, Voronezh, Russia
Research Center for Wave Dynamics of Solids and Structures, Voronezh State Technical University, Voronezh, Russia

Synonyms

Dynamic response; Fractional derivative viscoelastic medium; Thin plates and shells

Definition

Damped vibrations of such elastic thin bodies as plates and circular cylindrical shells embedded into a viscoelastic medium, the rheological features of which are described by fractional derivatives, are considered in this entry.

Backgrounds

Interest in fractional calculus has quickened profoundly in the past few decades, resulting in a large body of articles devoted to this challenge, which is clearly emphasized in a set of review papers published in the field (Rossikhin and Shitikova 1997a, 2010; Gaul 1999; Shimizu and Zhang 1999). The most recent state-of-the-art article Rossikhin and Shitikova (2010) is devoted to the analysis of new trends and recent results carried out during the last decade in the field of fractional calculus application to mechanics of materials and dynamic problems of structural mechanics, while the historical survey about two parallel ways in the progress of fractional calculus in mechanics of solids can be found in Rossikhin (2010).

It has been shown in Rossikhin and Shitikova (2010) that during the last decade fractional calculus entered the mainstream of engineering analysis and has been widely applied to structural dynamics problems both in discrete and continuous equations. However, the majority of papers are mainly concerned with investigation of vibrations of one-degree-of-freedom systems.

In this entry, it will be shown how the utilization of the Rayleigh hypothesis together with the modal analysis in dynamic problems of the systems with an infinite number of degrees of freedom, such as thin plates and shells, could be useful in reducing to the dynamic response of a finite or infinite set of uncoupled linear oscillators, the theory of which is well developed.

Damped Vibrations of N-Degree-of-Freedom Mechanical Systems

It is known (Clough and Penzien 1975) that during the analysis of linear damped vibrations of N-degree-of-freedom mechanical systems, their equations of motion could be reduced to a finite set of uncoupled equations in the generalized coordinates, each of which describes damped vibrations of a mechanical oscillator. The equation of motion of such systems in the vector form could be written as

$$m\ddot{\mathbf{V}} + c\dot{\mathbf{V}} + k\mathbf{V} = \mathbf{P}(t), \tag{1}$$

where $\mathbf{V}$ is the displacement vector, an overdot denotes the derivative with respect to the time t, m is the matrix of lumped masses with the elements m_n, k is the stiffness matrix with the elements k_n, c is the damping matrix with the elements c_n, and $\mathbf{P}(t)$ is the force vector.

Yury A. Rossikhin: deceased.

Suppose that

$$c = a_0 m + a_1 k, \tag{2}$$

where a_0 and a_1 are certain coefficients, and represent the solution of Eq. (1) and the force $P(t)$ in terms of the expansions in eigenvectors φ_i $(i = 1, \ldots, N)$ of the given problem, i.e.,

$$\begin{aligned} V &= \varphi_1 Y_1 + \varphi_2 Y_2 + \ldots + \varphi_N Y_N \ , \\ P(t) &= \varphi_1 P_1 + \varphi_2 P_2 + \ldots + \varphi_N P_N \ , \end{aligned} \tag{3}$$

then substituting (3) in (1) with account for the orthogonality conditions of the eigenvectors

$$\begin{aligned} &\varphi_m^{\mathrm{T}} m \varphi_n = \varphi_m^{\mathrm{T}} k \varphi_n = \varphi_m^{\mathrm{T}} c \varphi_n = 0 \quad (m \neq n), \\ &\varphi_m^{\mathrm{T}} m \varphi_n = M_n \ , \quad \varphi_m^{\mathrm{T}} k \varphi_n = \omega_n^2 M_n \ , \\ &\varphi_m^{\mathrm{T}} c \varphi_n = \tau_n \omega_n^2 M_n \quad (m = n), \end{aligned} \tag{4}$$

and then applying the Laplace transformation yield

$$\left(p^2 + \omega_n^2 \tau_n p + \omega_n^2\right) \bar{Y}_n = \bar{F}_n \quad (i = 1, \ldots, N), \tag{5}$$

where p is the Laplace transform parameter, $\bar{F}_n = \bar{P}_n M_n^{-1}$, and an overbar denotes the Laplace transform; a_0 and a_1 are the coefficients of proportionality; Y_i and P_i $(i = 1, \ldots, N)$ are the generalized displacements and forces, respectively; an upper index T denotes the transposed vector; ω_n is the $n-$th frequency of natural vibrations; and τ_n is the retardation time for the $n-$th mode.

Each equation from (5) describes the damped vibrations of a mechanical oscillator, damping features of which are described by the classical Kelvin-Voigt model.

If the Kelvin-Voigt model involves fractional derivative, then Eq. (5) is written as (Rossikhin and Shitikova 1997a,b)

$$\left(p^2 + \omega_n^2 \tau_n^{\gamma} p + \omega_n^2\right) \bar{Y}_n = \bar{F}_n \quad (i = 1, \ldots, N), \tag{6}$$

where γ $(0 < \gamma \leq 1)$ is the order of the fractional derivative (fractional parameter).

Reference to Eqs. (5) and (6) shows that viscosity of the mechanical system has the modal character, which is verified by experimental data Abdel-Ghaffar and Scanlan (1985).

From Eq. (6) it follows

$$\bar{Y}_n = \frac{\bar{F}_n}{\bar{f}_n} \quad (i = 1, \ldots, N), \tag{7}$$

$$\bar{f}_n = p^2 + æ_n^2 p + \omega_n^2, \tag{8}$$

where $æ_n^2 = \omega_n^2 \tau_n^{\gamma}$.

In order to convert from the Laplace domain to the time domain via the Mellin-Fourier inversion formula

$$Y_n(t) = \frac{1}{2\pi i} \int_{c-i\infty}^{c+i\infty} \bar{Y}_n(p) \mathrm{e}^{pt} \mathrm{d}p \ , \tag{9}$$

it is needed to find all particular points of the function $\bar{Y}_n(p)$. This function possesses the branch points $p = 0$ and $p = -\infty$ and has the simple poles at the same magnitudes of p, which are the roots of the characteristic equation

$$\bar{f}_n = 0 \ . \tag{10}$$

Since for the multivalued functions possessing branch points the inversion formula is valid only for the first sheet of the Riemann surface, then for calculating the integral in (9) the closed contour of integration with a cut along the real negative axes should be used (Rossikhin and Shitikova 1997a,b). Applying Jordan's lemma and the main theorem of the residue theory, integral (9) can be written in the form

$$Y_n(t) = Y_n^{\mathrm{drift}}(t) + Y_n^{\mathrm{vibr}}(t), \tag{11}$$

$$Y_n^{\mathrm{drift}}(t) = \frac{1}{2\pi i} \int_0^{\infty} \left[\bar{Y}_n(se^{-i\pi}) - \bar{Y}_n(se^{i\pi})\right] e^{-st} \mathrm{d}s, \tag{12}$$

$$Y_n^{\mathrm{vibr}}(t) = \sum_k \mathrm{res}\left[\bar{Y}_n(p_k) e^{p_k t}\right], \tag{13}$$

T

where the summation is carried out along all isolated singular points (poles) $p = p_k$.

The first term (12) of (11) describes the drift of the equilibrium position of the $n-$th oscillator and is governed by the relaxation-retardation processes occurring in the mechanical system, while the second term (13) describes its damped vibrations around the drifting position of equilibrium and is determined by the inertia forces and dissipative forces.

For utilizing (11), (12), and (13) to construct the final expression for $Y_n(t)$, it is needed to investigate the root $p_n = -r_n e^{\pm i\psi} = \alpha_n \pm i\Omega_n$ locus of the characteristic equation (10), where α_n and Ω_n are the damping coefficient and the vibration frequency of the $n-$th oscillator. This procedure is described in detail in Rossikhin and Shitikova (1997a,b), as well as in entry ▸ Linear and Nonlinear Vibrations: Fractional Oscillators in *Encyclopedia of Continuum Mechanics*.

Knowing the roots of the characteristic equation, it is possible to construct the Green function $G_n(t)$ based on (11), (12), and (13) if put $\bar{F}_n = 1$ in (7) (Rossikhin and Shitikova 2010)

$$G_n(t) = A_{0n}(t) + A_n e^{-\alpha_n t}\sin(\Omega_n t - \varphi_n), \tag{14}$$

$$A_n = 2\left[4r_n^2 + \gamma^2 æ_n^2 r_n^{2(\gamma-1)} + 4\gamma æ_n r_n^{\gamma}\cos(2-\gamma)\psi\right]^{-1/2}, \tag{15}$$

$$\tan\varphi_n = -\frac{2r_n\cos\psi + \gamma æ_n r_n^{\gamma-1}\cos(1-\gamma)\psi}{2r_n\sin\psi - \gamma æ_n r_n^{\gamma-1}\sin(1-\gamma)\psi}, \tag{16}$$

$$A_{0n}(t) = \int_0^\infty r^{-1}B_n(\tau)\exp(-t/\tau)\mathrm{d}\tau, \tag{17}$$

and

$$B_n(\tau) = \frac{\sin\pi\gamma}{\pi}\frac{\tau(1+\tau^2\omega_n^2)^{-1}}{(1+\tau^2\omega_n^2)æ_n^{-1}\tau_n^{\gamma-2} + (1+\tau^2\omega_n^2)^{-1}æ_n\tau_n^{2-\gamma} + 2\cos\pi\gamma} \tag{18}$$

is the function of distribution of the retardation times corresponding to the $n-$th oscillator.

Knowing the Green function, $Y_n(t)$ is found as

$$Y_n(t) = \int_0^t G_n(t-t')F_n(t')\mathrm{d}t'. \tag{19}$$

Below it will be shown how an infinite set of uncoupled equations in the generalized displacements could be found for thin plates and cylindrical shells, i.e., for systems with infinite degrees of freedom.

Free Vibrations of an Elastic Plate in a Viscous Medium

Dynamic response of an elastic rectangular plate vibrating in a viscous medium, damping features of which are modeled by fractional derivatives, could be analyzed using the equations describing in-plane and transverse vibrations of such a plate written in the dimensionless form as (Rossikhin and Shitikova 2006)

$$\frac{\partial^2 u_1}{\partial x^2} + \frac{1-\nu}{2}\beta_1^2\frac{\partial^2 u_1}{\partial y^2} + \frac{1+\nu}{2}\beta_1\frac{\partial^2 u_2}{\partial x\partial y} = \ddot{u}_1 + \mu D^{\gamma}u_1 - q_1 \tag{20}$$

$$\beta_1^2\frac{\partial^2 u_2}{\partial y^2} + \frac{1-\nu}{2}\frac{\partial^2 u_2}{\partial x^2} + \frac{1+\nu}{2}\beta_1\frac{\partial^2 u_1}{\partial x\partial y} = \ddot{u}_2 + \mu D^{\gamma}u_2 - q_2 \tag{21}$$

$$\frac{\beta_2^2}{12}\left(\frac{\partial^4 u_3}{\partial x^4} + 2\beta_1^2\frac{\partial^4 u_3}{\partial x^2\partial y^2} + \beta_1^4\frac{\partial^4 u_3}{\partial y^4}\right) = -\ddot{u}_3 - \mu D^{\gamma}u_3 + q_3, \tag{22}$$

where $u_1(x, y, t)$, $u_2(x, y, t)$, and $u_3(x, y, t)$ are displacements of the points of the plate's median surface in three mutually orthogonal directions x, y, z, two of which, x and y, lie in the plate surface, and the third one, z, is out of the plate plane; q_1, q_2, and q_3 are the intensities of the

given external loads applied in the $x-$, $y-$, and $z-$directions, respectively; ν is the Poisson's ratio; μ is the damping coefficient; $\beta_1 = a/b$ and $\beta_2 = h/a$ are the parameters depending on the plate's dimensions; a and b are the plate's dimensions along the $x-$ and $y-$axes, respectively; h is the plate thickness; and the fractional derivative is defined as (Rossikhin and Shitikova 1997a)

$$D^{\gamma} Z = \frac{\mathrm{d}}{\mathrm{d}t} \int_0^t \frac{Z(\tau)\mathrm{d}\tau}{\Gamma(1-\gamma)(t-\tau)^{\gamma}}.$$

From reference to Eqs. (20), (21), and (22) it follows that in-plane and out-of-plane vibrations of such a plate are uncoupled, while the in-plane motions are described by a set of two linear coupled Eqs. (20) and (21). That is why the behavior of each mode of the coupled equations was modeled in Rossikhin and Shitikova (2006) by the behavior of a two-mass oscillator (Rossikhin and Shitikova 2001); in so doing the oscillators corresponding to different modes are separated from each other.

Below another approach resulting in decoupling of the equations for the in-plane vibrations and utilizing equations of one-mass oscillators is proposed following (Rossikhin and Shitikova 2012).

Thus, assume for simplicity that Eqs. (20), (21), and (22) are subjected to the boundary conditions of the Navier type. Then the displacements and the external loads can be represented in the form

$$u_i(x, y, t) = \sum_{m=1}^{\infty} \sum_{n=1}^{\infty} x_{i\,mn}(t)\eta_{i\,mn}(x, y), \quad (i = 1, 2, 3) \tag{23}$$

$$q_i(x, y, t) = \sum_{m=1}^{\infty} \sum_{n=1}^{\infty} y_{i\,mn}(t)\eta_{i\,mn}(x, y), \quad (i = 1, 2, 3), \tag{24}$$

where m and n are integers; $x_{i\,mn}$ and $y_{i\,mn}$ are the generalized displacements and forces, respectively; and $\eta_{i\,mn}(x, y)$ are the eigenfunctions of the given problem:

$$\begin{aligned} \eta_{1\,mn}(x, y) &= \cos \pi m x \sin \pi n y, \\ \eta_{2\,mn}(x, y) &= \sin \pi m x \cos \pi n y, \\ \eta_{3\,mn}(x, y) &= \sin \pi m x \sin \pi n y \end{aligned} \tag{25}$$

at $0 \le x \le 1$ and $0 \le y \le 1$.

Substituting (23) and (24) in Eqs. (20), (21), and (22), using the conditions of orthogonality of the eigenfunctions (25) on the segments $0 \le x, y \le 1$, and applying the Laplace transform to the resulting set of equations yield

$$p^2 \bar{x}_{\alpha\,mn} + S^{mn}_{\alpha\beta} \bar{x}_{\beta\,mn} + p^{\gamma} \mu^{mn}_{\alpha\beta} \bar{x}_{\beta\,mn} = \bar{y}_{\alpha\,mn}, \tag{26}$$

$$(p^2 + \mu_{mn} p^{\gamma} + P_{mn}) \bar{x}_{3\,mn} = \bar{y}_{3\,mn}, \tag{27}$$

where Greek letters take on the magnitudes of 1 and 2, the summation is carried out over two repeated indices, the elements of the matrix $S^{mn}_{\alpha\beta}$ and P_{mn} are defined as follows:

$$S^{mn}_{11} = \pi^2 \left(m^2 + \frac{1-\nu}{2} \beta_1^2 n^2 \right),$$

$$S^{mn}_{12} = S^{mn}_{21} = \pi^2 \frac{1+\nu}{2} \beta_1 mn,$$

$$S^{mn}_{22} = \pi^2 \left(\frac{1-\nu}{2} m^2 + \beta_1^2 n^2 \right),$$

$$P_{mn} = \pi^4 \frac{\beta_2^2}{12} \left(m^2 + \beta_1^2 n^2 \right)^2,$$

and the modal viscosity μ_{mn} is assumed to satisfy the Rayleigh hypothesis, i.e., $\mu_{mn} = æ_{mn} S^{mn}_{\alpha\beta}$ with the value æ taken for convenience as $æ_{mn} = \tau^{\gamma}_{mn}$.

Then Eq. (26) can be rewritten as

$$p^2 \bar{x}_{\alpha\,mn} + S^{mn}_{\alpha\beta} \bar{x}_{\beta\,mn} (1 + p^{\gamma} \tau^{\gamma}_{mn}) = \bar{y}_{\alpha\,mn}. \tag{28}$$

Since the matrix $S^{mn}_{\alpha\beta}$ is symmetric, then it possesses two real eigenvalues

$$p_i^2 = -\omega^2_{i\,mn}, \quad \omega^2_{1\,mn} = \pi^2 (m^2 + \beta_1^2 n^2),$$

$$\omega^2_{1\,mn} = \pi^2 \frac{1-\nu}{2} (m^2 + \beta_1^2 n^2), \tag{29}$$

T

which are in correspondence with two mutually orthogonal eigenvectors:

$$l^{\mathrm{I}}_{mn}\left\{l^{\mathrm{I}}_{1\,mn}=\frac{\pi m}{\omega_{1\,mn}},\quad l^{\mathrm{I}}_{2\,mn}=\frac{\pi\beta_1 n}{\omega_{1\,mn}}\right\}, \tag{30}$$

$$l^{\mathrm{II}}_{mn}\left\{l^{\mathrm{II}}_{1\,mn}=\frac{\pi\beta_1 n}{\omega_{1\,mn}},\quad l^{\mathrm{II}}_{2\,mn}=-\frac{\pi m}{\omega_{1\,mn}}\right\}. \tag{31}$$

Thus, the matrix $S^{mn}_{\alpha\beta}$ and the vectors $\bar{x}_{\alpha\,mn}$ and $\bar{y}_{\alpha\,mn}$ can be expanded in terms of the vectors (30) and (31) as

$$\begin{aligned} S^{mn}_{\alpha\beta} &= \omega^2_{1\,mn} l^{\mathrm{I}}_{\alpha\,mn} l^{\mathrm{I}}_{\beta\,mn} + \omega^2_{2\,mn} l^{\mathrm{II}}_{\alpha\,mn} l^{\mathrm{II}}_{\beta\,mn},\\ \bar{x}_{\alpha\,mn} &= \bar{X}_{1\,mn} l^{\mathrm{I}}_{\alpha\,mn} + \bar{X}_{2\,mn} l^{\mathrm{II}}_{\alpha\,mn},\\ \bar{y}_{\alpha\,mn} &= \bar{Y}_{1\,mn} l^{\mathrm{I}}_{\alpha\,mn} + \bar{Y}_{2\,mn} l^{\mathrm{II}}_{\alpha\,mn}. \end{aligned} \tag{32}$$

Substituting (32) in Eqs. (28) and multiplying the net relationships successively by $l^{\mathrm{I}}_{\alpha\,mn}$ and $l^{\mathrm{II}}_{\alpha\,mn}$, the two following equations could be found

$$\left[p^2+\omega^2_{1\,mn}(1+p^\gamma\tau^\gamma_{mn})\right]\bar{X}_{1\,mn}=\bar{Y}_{1\,mn}, \tag{33}$$

$$\left[p^2+\omega^2_{2\,mn}(1+p^\gamma\tau^\gamma_{mn})\right]\bar{X}_{2\,mn}=\bar{Y}_{2\,mn}. \tag{34}$$

Equation (27) rewritten in the similar form

$$\left[p^2+\Omega^2_{mn}(1+p^\gamma\tau_{1\,mn})\right]\bar{X}_{3\,mn}=\bar{Y}_{3\,mn} \tag{35}$$

should be added to (33) and (34), where $\Omega^2_{mn}=P_{mn}$ is the natural frequency of the out-of-plane vertical vibrations.

Reference to Eqs. (33), (34), and (35) shows that these equations differ from Eq. (6) only by notations of the values entering in these equations, and thus, further procedure for the construction of the solution should be the same as for the Kelvin-Voigt fractional one-mass oscillator (see details in Sec.2, as well as in Rossikhin and Shitikova 1997a,b).

Linear Vibrations of a Circular Cylindrical Shell Being in a Viscous Medium

Now let us consider an elastic circular cylindrical shell of radius R and length l being in a viscous medium. Equations describing vibrations of such a shell in the dimensionless form can be written as (Rossikhin and Shitikova 2010, 2012)

$$\frac{\partial^2 u_1}{\partial x^2}+\frac{1-\nu}{2}\beta_1^2\frac{\partial^2 u_1}{\partial\varphi^2}+\frac{1+\nu}{2}\beta_1\frac{\partial^2 u_2}{\partial x\partial\varphi}-\nu\beta_1\frac{\partial u_3}{\partial x}=\ddot{u}_1+\mu_{11}D^\gamma u_1-q_1, \tag{36}$$

$$\beta_1^2\frac{\partial^2 u_2}{\partial\varphi^2}+\frac{1-\nu}{2}\frac{\partial^2 u_2}{\partial x^2}+\frac{1+\nu}{2}\beta_1\frac{\partial^2 u_1}{\partial x\partial\varphi}-\beta_1^2\frac{\partial u_3}{\partial\varphi}=\ddot{u}_2+\mu_{22}D^\gamma u_2-q_2, \tag{37}$$

$$\frac{\beta_2^2}{12}\left(\frac{\partial^4 u_3}{\partial x^4}+2\beta_1^2\frac{\partial^4 u_3}{\partial x^2\partial\varphi^2}+\beta_1^4\frac{\partial^4 u_3}{\partial\varphi^4}\right)+\beta_1^2 u_3-\nu\beta_1\frac{\partial u_1}{\partial x}-\beta_1^2\frac{\partial u_2}{\partial\varphi}=-\ddot{u}_3-\mu_{33}D^\gamma u_3+q_3, \tag{38}$$

where the $x-$axis is directed along the axis of the cylinder; φ is the polar angle in the plane perpendicular to the $x-$axis; $u_1(x,\varphi,t)$, $u_2(x,\varphi,t)$, and $u_3(x,\varphi,t)$ are the dimensionless displacements of the points of the shell's median surface in three mutually orthogonal directions x,φ,r; r is the polar radius; q_1, q_2, and q_3 are the intensities of the given external loads applied in the $x-$, $\varphi-$, and $r-$directions, respectively; ν is Poisson's ratio; μ_{ii} are the damping coefficients; $\beta_1=l/R$ and $\beta_2=h/l$ are the parameters depending on the shell's dimensions; and h is the shell thickness.

The set of Eqs. (36), (37), and (38) also admits the solution of the Navier type (23) and (24), where the variable y should be substituted by φ.

Substituting then (23) and (24) in (36), (37), and (38), using the conditions of orthogonality of eigenfunctions within the domains of $0\le x\le 1$

and $0 \le \varphi \le 2\pi$, and applying the Laplace transformation to the resulting equations yield

$$\left[p^2\delta_{ij} + \mu_{ij}^{mn} p^{\gamma} + S_{ij}^{mn}\right] \bar{\mathbf{x}}_{j\,mn} = \bar{\mathbf{q}}_{i\,mn}, \quad (39)$$

where Latin indices take on the magnitudes of 1, 2, and 3; the summation is carried out over two repeated indices, $\mu_{ij}^{mn} = \tau^{\gamma} S_{ij}^{mn}$; and the elements of the matrix S_{ij}^{mn} are defined as follows:

$$\begin{aligned}
S_{11}^{mn} &= \pi^2 \left(m^2 + \frac{1-\nu}{2}\,\beta_1^2 n^2\right),\\
S_{12}^{mn} &= S_{21}^{mn} = \pi^2\,\frac{1+\nu}{2}\,\beta_1 mn\,,\\
S_{13}^{mn} &= S_{31}^{mn} = \nu\beta_1 \pi m,\\
S_{23}^{mn} &= S_{32}^{mn} = \beta_1^2 \pi n\,,\\
S_{22}^{mn} &= \pi^2 \left(\frac{1-\nu}{2}\,m^2 + \beta_1^2 n^2\right),\\
S_{33}^{mn} &= \pi^4\,\frac{\beta_2^2}{12}\left(m^2 + \beta_1^2 n^2\right)^2.
\end{aligned}$$

Since the matrix S_{ij}^{mn} is symmetric, then it has three real eigenvalues

$$p_i^2 = -\Omega_{i\,mn}^2, \quad (i = 1, 2, 3) \quad (40)$$

which are in correspondence with three mutually orthogonal eigenvectors

$$\mathbf{L}_{mn}^{\mathrm{I}}\left\{L_{i\,mn}^{\mathrm{I}}\right\}, \quad \mathbf{L}_{mn}^{\mathrm{II}}\left\{L_{i\,mn}^{\mathrm{II}}\right\}, \quad \mathbf{L}_{mn}^{\mathrm{III}}\left\{L_{i\,mn}^{\mathrm{III}}\right\}. \quad (41)$$

Thus, the matrix S_{ij}^{mn} and the vectors $\bar{\mathbf{x}}_{i\,mn}$ and $\bar{\mathbf{q}}_{i\,mn}$ can be expanded in terms of the vectors (41) as

$$\begin{aligned}
S_{ij}^{mn} &= \Omega_{1\,mn}^2 L_{i\,mn}^{\mathrm{I}} L_{j\,mn}^{\mathrm{I}} + \Omega_{2\,mn}^2 L_{i\,mn}^{\mathrm{II}} L_{j\,mn}^{\mathrm{II}}\\
&\quad + \Omega_{3\,mn}^2 L_{i\,mn}^{\mathrm{III}} L_{j\,mn}^{\mathrm{III}}, \quad (42)\\
\bar{x}_{i\,mn} &= \bar{X}_{1\,mn} L_{i\,mn}^{\mathrm{I}} + \bar{X}_{2\,mn} L_{i\,mn}^{\mathrm{II}}\\
&\quad + \bar{X}_{3\,mn} L_{i\,mn}^{\mathrm{III}}, \quad (43)\\
\bar{q}_{i\,mn} &= \bar{Q}_{1\,mn} L_{i\,mn}^{\mathrm{I}} + \bar{Q}_{2\,mn} L_{i\,mn}^{\mathrm{II}}\\
&\quad + \bar{Q}_{3\,mn} L_{i\,mn}^{\mathrm{III}}. \quad (44)
\end{aligned}$$

Substituting (42), (43), and (44) in (39) yields

$$\begin{aligned}
&\left[p^2\delta_{ij} + \left(1 + p^{\gamma}\tau^{\gamma}\right)\left(\Omega_{1\,mn}^2 L_{i\,mn}^{\mathrm{I}} L_{j\,mn}^{\mathrm{I}}\right.\right.\\
&\left.\left. + \Omega_{2\,mn}^2 L_{i\,mn}^{\mathrm{II}} L_{j\,mn}^{\mathrm{II}} + \Omega_{3\,mn}^2 L_{i\,mn}^{\mathrm{III}} L_{j\,mn}^{\mathrm{III}}\right)\right]\\
&\times \left(\bar{X}_{1\,mn} L_{j\,mn}^{\mathrm{I}} + \bar{X}_{2\,mn} L_{j\,mn}^{\mathrm{II}} + \bar{X}_{3\,mn} L_{j\,mn}^{\mathrm{III}}\right)\\
&= \bar{Q}_{1\,mn} L_{i\,mn}^{\mathrm{I}} + \bar{Q}_{2\,mn} L_{i\,mn}^{\mathrm{II}} + \bar{Q}_{3\,mn} L_{i\,mn}^{\mathrm{III}}. \quad (45)
\end{aligned}$$

Multiplying (45) successively by $L_{i\,mn}^{\mathrm{I}}$, $L_{i\,mn}^{\mathrm{II}}$, and $L_{i\,mn}^{\mathrm{III}}$ and considering that

$$\begin{aligned}
L_{i\,mn}^{\mathrm{I}} L_{i\,mn}^{\mathrm{II}} &= L_{i\,mn}^{\mathrm{I}} L_{i\,mn}^{\mathrm{III}} = L_{i\,mn}^{\mathrm{II}} L_{i\,mn}^{\mathrm{III}} = 0,\\
L_{i\,mn}^{\mathrm{I}} L_{i\,mn}^{\mathrm{I}} &= L_{i\,mn}^{\mathrm{II}} L_{i\,mn}^{\mathrm{II}} = L_{i\,mn}^{\mathrm{III}} L_{i\,mn}^{\mathrm{III}} = 1, \quad (46)
\end{aligned}$$

the three following equations could be found

$$\left[p^2 + \Omega_{1\,mn}^2 (1 + p^{\gamma}\tau_{mn}^{\gamma})\right] \bar{X}_{1\,mn} = \bar{Q}_{1\,mn}, \quad (47)$$

$$\left[p^2 + \Omega_{2\,mn}^2 (1 + p^{\gamma}\tau_{mn}^{\gamma})\right] \bar{X}_{2\,mn} = \bar{Q}_{2\,mn}, \quad (48)$$

$$\left[p^2 + \Omega_{3\,mn}^2 (1 + p^{\gamma}\tau_{mn}^{\gamma})\right] \bar{X}_{3\,mn} = \bar{Q}_{3\,mn}. \quad (49)$$

Reference to Eqs. (47), (48), and (49) shows that these equations differ from Eq. (6) only by notations of the values entering in these equations, and thus, further procedure for the construction of the solution should be the same as that for mechanical oscillators.

Conclusion

It has been shown that the introduction of the modal viscosity, i.e., the assumption that each mode of vibrations has its own damping coefficient and its own retardation time, together with the Rayleigh hypothesis allows one to reduce the problem of linear vibrations of such thin elastic bodies as a rectangular plate and a cir-

cular cylindrical shell in a fractional derivative viscoelastic medium to the problem of vibrations of an infinite set of viscoelastic oscillators based on the fractional derivative Kelvin-Voigt model.

The suggested approach for decoupling equations of motion could be generalized for solving dynamic problems of nonlinear weakly damped vibrations of thin bodies (see entry ▸ Linear and Nonlinear Vibrations: Fractional Oscillators).

Cross-References

- ▸ Classical Beams and Plates in a Fractional Derivative Medium, Impact Response
- ▸ Fractional Operator Models of Viscoelasticity
- ▸ Linear and Nonlinear Vibrations: Fractional Oscillators

References

Abdel-Ghaffar AM, Scanlan RH (1985) Ambient vibration studies of Golden Gate Bridge. I: suspended structure. ASCE J Eng Mech 111(4):463–482

Clough RW, Penzien J (1975) Dynamics of structures. McGraw-Hill, New York

Gaul L (1999) The influence of damping on waves and vibrations. Mech Syst Signal Proc 13(1):1–30

Rossikhin YA (2010) Reflections on two parallel ways in the progress of fractional calculus in mechanics of solids. Appl Mech Rev 63(1), Article ID 010701

Rossikhin YA, Shitikova MV (1997a) Application of fractional derivatives to the analysis of damped vibrations of viscoelastic single mass systems. Acta Mech 120(1–4):109–125

Rossikhin YA, Shitikova MV (1997b) Applications of fractional calculus to dynamic problems of linear and nonlinear hereditary mechanics of solids. Appl Mech Rev 50(1):15–67

Rossikhin YA, Shitikova MV (2001) A new method for solving dynamic problems of fractional derivative viscoelasticity. Int J Eng Sci 39:149–176

Rossikhin YA, Shitikova MV (2006) Analysis of damped vibrations of linear viscoelastic plates with damping modeled with fractional derivatives. Signal Proc 86:2703–2711

Rossikhin YA, Shitikova MV (2010) Application of fractional calculus for dynamic problems of solid mechanics: novel trends and recent results. Appl Mech Rev 63(1), Article ID 010801

Rossikhin YA, Shitikova MV (2012) Analysis of damped vibrations of thin bodies embedded into a fractional derivative viscoelastic medium. J Mech Behav Mater 21(5–6):155–159

Shimizu N, Zhang W (1999) Fractional calculus approach to dynamic problems of viscoelastic materials. JSME Int J Ser C 42(4):825–837

Thin Elastic Shells, Lagrangian Geometrically Nonlinear Theory

Wojciech Pietraszkiewicz
Faculty of Civil and Environmental Engineering, Department of Mechanics of Materials and Structures, Gdańnsk University of Technology, Gdańnsk, Poland

Synonyms

Kirchhoff-Love nonlinear shell model; Small-strain thin shell theory

Definition

The Lagrangian nonlinear theory of thin elastic shells is a special case of geometrically nonlinear theory of elasticity. Here the shell thickness is assumed to be much smaller than the smallest radius of curvature of the shell middle surface. As a result, the shell deformation can approximately be described only by stretching and bending of its middle surface. As compared with the classical linear theory of thin elastic shells discussed in another entry in this Encyclopaedia (Pietraszkiewicz 2018b), in this case only strains in the shell space are assumed to be small, while rotations are initially not restricted. Due to nonlinearity of deformation, one can formulate the nonlinear thin shell relations in various descriptions: Eulerian, Lagrangian, mixed,

etc. The most important for applications in shell structures are the Lagrangian shell relations formulated entirely in the undeformed midsurface base. This base is usually the only one known in advance.

Introduction

The quite general Lagrangian thin shell relations were proposed already by Galimov (1951) applying two steps. First, the corresponding simple Eulerian equilibrium equations and boundary conditions were given in the unknown deformed midsurface base. Then appropriate transformation rules were applied to express the vectorial Eulerian quantities in terms of the Lagrangian ones. Unfortunately, under such transformations the fourth scalar (rotational) boundary condition was still referred to the deformed lateral boundary surface. Only much later, it was proved (Makowski and Pietraszkiewicz 1989) that such a transformation of the fourth kinematic boundary condition does not lead, in general, to the fourth Lagrangian displacemental boundary condition, because some differential one-form associated with the virtual rotation parameter referred to the deformed boundary is not integrable in terms of translation surface derivatives. This was the reason why no variational principles could be constructed for such quasi-Lagrangian shell theory even for conservative surface and boundary loadings.

The entirely Lagrangian thin shell relations were worked out by Pietraszkiewicz and Szwabowicz (1981) using a modified tensor of change of curvature. These relations were reworked for the classical tensor of change of curvature (Pietraszkiewicz 1984) together with several consistently simplified versions of shell relations under small strains and restricted rotations as well as two incremental formulations of the relations in the total Lagrangian and updated Lagrangian descriptions.

In this note, the entirely Lagrangian nonlinear theory of thin elastic shells is outlined. It is based on the following three assumptions:

1. The strains in the shell space are small, but rotations of material elements are initially not restricted.
2. The material elements, which are normal to the shell middle surface in the undeformed placement, remain normal to the deformed shell midsurface and do not change their lengths. This assumption allows one to approximately describe the nonlinear shell deformation only by stretching and bending of its middle surface.
3. The state of elastic stress in the shell space is approximately plane. This means that the effects of transverse shear stresses and of normal stresses, acting on surfaces parallel to the middle surface, may be neglected in the elastic strain energy density.

To be concise, the assumptions 2. and 3. are used to derive the approximate equilibrium equations and boundary conditions from the postulated principle of virtual displacements for the shell midsurface. The resulting shell relations are initially formulated for unrestricted surface deformation measures and unrestricted displacements. Then consistently approximated relations under small elastic strains are discussed. Finally, several simplified sets of shell relations under additional consistently restricted rotations of material elements are given.

Geometry and Deformation of the Shell Base Surface

Let $\mathcal{P}$ be the region of three-dimensional Euclidean point space $\mathcal{E}$ occupied by the shell in the undeformed placement. The position vector of any point $\mathrm{P} \in \mathcal{P}$ relative to a reference point $\mathrm{O} \in \mathcal{E}$ can be given by

$$\mathbf{p}\left(\theta^{\alpha}, \xi\right) = \mathrm{p}^{i}\left(\theta^{\alpha}\right)\mathbf{i}_{i} = \boldsymbol{r}\left(\theta^{\alpha}\right) + \xi \boldsymbol{n}\left(\theta^{\alpha}\right), \quad (1)$$

where $\mathbf{i}_i$, $i = 1, 2, 3$, are three orthonormal vectors, θ^{α}, $\alpha = 1, 2$, are the curvilinear surface coordinates, $-h/2 \leq \xi \leq +h/2$ is the distance from the shell midsurface $\mathcal{M}$ defined by the posi-

tion vector $\boldsymbol{r}(\theta^\alpha)$, $\boldsymbol{n}(\theta^\alpha)$ is the unit normal vector orienting $\mathcal{M}$, and h is the shell thickness. In thin shell theory, it is understood that h be constant and small as compared with the smallest radius of curvature R of $\mathcal{M}$ and with linear dimensions of $\mathcal{P}$.

Geometry of the base surface $\mathcal{M}$ is described by the following fields (Pietraszkiewicz 2018a): the natural base vectors $\boldsymbol{a}_\alpha = \partial \boldsymbol{r}/\partial\theta^\alpha \equiv \boldsymbol{r}_{,\alpha}$, the covariant components $a_{\alpha\beta} = \boldsymbol{a}_\alpha \cdot \boldsymbol{a}_\beta$ of the surface metric tensor with determinant $a = \det(a_{\alpha\beta})$, the dual (contravariant) base vectors $\boldsymbol{a}^\beta$ such that $\boldsymbol{a}_\alpha \cdot \boldsymbol{a}^\beta = \delta_\alpha^\beta$, where $\delta_1^1 = \delta_2^2 = 1$, $\delta_2^1 = \delta_1^2 = 0$, the unit normal vector $\boldsymbol{n} = \boldsymbol{a}_1 \times \boldsymbol{a}_2/|\boldsymbol{a}_1 \times \boldsymbol{a}_2|$, and the covariant components $b_{\alpha\beta} = -\boldsymbol{a}_\alpha \cdot \boldsymbol{n}_{,\beta} = -\boldsymbol{n}_{,\alpha} \cdot \boldsymbol{a}_\beta$ of the surface curvature tensor. The contravariant metric components $a^{\alpha\beta} = \boldsymbol{a}^\alpha \cdot \boldsymbol{a}^\beta$ are used to raise indices of surface vectors and tensors, for example, $\boldsymbol{a}^\beta = a^{\beta\alpha}\boldsymbol{a}_\alpha$, $b_\beta^\alpha = a^{\alpha\lambda}b_{\lambda\beta}$ etc., where the summation convention over the repeated indices is used.

The shell base surface in the deformed placement $\overline{\mathcal{M}}$ is described by the position vector $\overline{\boldsymbol{r}}(\theta^\alpha) = \boldsymbol{r}(\theta^\alpha) + \boldsymbol{u}(\theta^\alpha)$, where θ^α are the surface curvilinear convective coordinates and $\boldsymbol{u} = u_\alpha \boldsymbol{a}^\alpha + w\boldsymbol{n}$ is the translation vector field. The geometric quantities describing $\overline{\mathcal{M}}$ are analogous to those describing $\mathcal{M}$, only now they are marked by the overbar: $\overline{\boldsymbol{a}}_\alpha = \overline{\boldsymbol{r}}_{,\alpha}$, $\overline{a}_{\alpha\beta} = \overline{\boldsymbol{a}}_\alpha \cdot \overline{\boldsymbol{a}}_\beta$, $\overline{a} = \det(\overline{a}_{\alpha\beta}) > 0$, $\overline{\boldsymbol{a}}^\beta \cdot \overline{\boldsymbol{a}}_\alpha = \delta_\alpha^\beta$, $\overline{\boldsymbol{n}} = \overline{\boldsymbol{a}}_1 \times \overline{\boldsymbol{a}}_2/|\overline{\boldsymbol{a}}_1 \times \overline{\boldsymbol{a}}_2|$, $\overline{b}_{\alpha\beta} = -\overline{\boldsymbol{n}}_{,\alpha} \cdot \overline{\boldsymbol{a}}_\beta = -\overline{\boldsymbol{a}}_\alpha \cdot \overline{\boldsymbol{n}}_{,\beta}$, $\overline{a}^{\alpha\beta} = \overline{\boldsymbol{a}}^\alpha \cdot \overline{\boldsymbol{a}}^\beta$, etc. The barred quantities can be expressed through analogous unbarred ones and the vector $\boldsymbol{u}$ by the relations (Pietraszkiewicz 1980, 1989)

$$\begin{aligned} \overline{\boldsymbol{a}}_\alpha &= \boldsymbol{a}_\alpha + \boldsymbol{u}_{,\alpha} = l_{\cdot\alpha}^\lambda \boldsymbol{a}_\lambda + \varphi_\alpha \boldsymbol{n}, \\ \overline{\boldsymbol{n}} &= \tfrac{1}{2j}\varepsilon^{\alpha\beta}\overline{\boldsymbol{a}}_\alpha \times \overline{\boldsymbol{a}}_\beta = n^\lambda \boldsymbol{a}_\lambda + n\boldsymbol{n}, \end{aligned} \tag{2}$$

where

$$l_{\alpha\beta} = a_{\alpha\beta} + u_{\alpha|\beta} - b_{\alpha\beta}w, \quad \varphi_\alpha = w_{,\alpha} + b_\alpha^\lambda u_\lambda, \tag{3}$$

$$\begin{aligned} &\varepsilon^{\alpha\beta} = (\boldsymbol{a}^\alpha \times \boldsymbol{a}^\beta) \cdot \boldsymbol{n}, \quad j = \sqrt{\frac{\overline{a}}{a}}, \\ &n_\mu = \tfrac{1}{j}\varepsilon^{\alpha\beta}\varepsilon_{\lambda\mu}\varphi_\alpha l_{\cdot\beta}^\lambda, \quad n = \tfrac{1}{2j}\varepsilon^{\alpha\beta}\varepsilon_{\lambda\mu}l_{\cdot\alpha}^\lambda l_{\cdot\beta}^\mu. \end{aligned} \tag{4}$$

The metric and curvature tensor components of $\overline{\mathcal{M}}$ are given by

$$\overline{a}_{\alpha\beta} = a_{\alpha\beta} + 2\gamma_{\alpha\beta}, \quad \overline{b}_{\alpha\beta} = b_{\alpha\beta} - \kappa_{\alpha\beta}, \tag{5}$$

$$\begin{aligned} \gamma_{\alpha\beta} &= \frac{1}{2}\left(\overline{\boldsymbol{a}}_\alpha \cdot \overline{\boldsymbol{a}}_\beta - a_{\alpha\beta}\right) \\ &= \frac{1}{2}\left(l_{\cdot\alpha}^\lambda l_{\lambda\beta} + \varphi_\alpha\varphi_\beta - a_{\alpha\beta}\right), \\ \kappa_{\alpha\beta} &= \overline{\boldsymbol{a}}_\alpha \cdot \overline{\boldsymbol{n}}_{,\beta} + b_{\alpha\beta} \\ &= l_{\lambda\alpha}\left(n^\lambda\big|_\beta - b_\beta^\lambda n\right) + \varphi_\alpha\left(n_{,\beta} + b_\beta^\lambda n_\lambda\right) \\ &\quad + b_{\alpha\beta}. \end{aligned} \tag{6}$$

Here $\gamma_{\alpha\beta}$ are the Lagrangian components of the surface strains while $\kappa_{\alpha\beta}$ are the Lagrangian components of the surface changes of curvatures (briefly bendings). Both surface deformation measures are symmetric: $\gamma_{\alpha\beta} = \gamma_{\beta\alpha}, \kappa_{\alpha\beta} = \kappa_{\beta\alpha}$. The components $\gamma_{\alpha\beta}$ are quadratic polynomials of u_α, w and their first surface derivatives, while the $\kappa_{\alpha\beta}$ are nonrational functions of u_α, w and their first as well as second surface derivatives. The nonrationality of $\kappa_{\alpha\beta}$ is caused by the invariant j, where

$$j^2 = 1 + 2\gamma_\alpha^\alpha + 2\left(\gamma_\alpha^\alpha\gamma_\beta^\beta - \gamma_\beta^\alpha\gamma_\alpha^\beta\right). \tag{7}$$

The boundary contour $\partial\mathcal{M}$ of $\mathcal{M}$ consists of the finite set of piecewise smooth curves $\boldsymbol{r}(s) = \boldsymbol{r}[\theta^\alpha(s)]$, where s is the arc length along $\partial\mathcal{M}$. In each regular point $M \in \partial\mathcal{M}$ two unit vectors are defined: the tangent $\boldsymbol{\tau} = d\boldsymbol{r}/ds \equiv \boldsymbol{r}' = \boldsymbol{a}_\alpha\tau^\alpha$ and the outward normal $\boldsymbol{\nu} = \boldsymbol{\tau} \times \boldsymbol{n} = \boldsymbol{a}_\alpha\nu^\alpha \equiv \boldsymbol{r}_{,\nu}$, $\nu^\alpha = \varepsilon^{\alpha\beta}\tau_\beta$, where $\boldsymbol{r}_{,\nu}$ means the outward normal derivative of $\boldsymbol{r}$ at $\partial\mathcal{M}$.

The position vector of the deformed boundary contour $\partial\overline{\mathcal{M}}$ is given by $\overline{\boldsymbol{r}}(s) = \boldsymbol{r}(s) + \boldsymbol{u}(s)$, where s is the convective coordinate. The following relations are satisfied along $\partial\overline{\mathcal{M}}$:

$$\begin{aligned} \overline{\boldsymbol{r}}' &= \overline{\boldsymbol{a}}_\alpha\tau^\alpha = \boldsymbol{\tau} + \boldsymbol{u}' = a_\tau\overline{\boldsymbol{\tau}}, \\ \overline{\boldsymbol{r}}_{,\nu} &= \overline{\boldsymbol{a}}_\alpha\nu^\alpha = \boldsymbol{\nu} + \boldsymbol{u}_{,\nu}, \\ \overline{\boldsymbol{n}} &= j^{-1}\overline{\boldsymbol{r}}_{,\nu} \times \overline{\boldsymbol{r}}', \end{aligned} \tag{8}$$

$$a_\tau = |\,\overline{\boldsymbol{r}}'\,| = \sqrt{1 + 2\boldsymbol{u}' \cdot \boldsymbol{\tau} + \boldsymbol{u}' \cdot \boldsymbol{u}'},$$
$$j^2 = |\overline{\boldsymbol{r}}_{,\nu}|^2 |\overline{\boldsymbol{r}}'|^2 - |\overline{\boldsymbol{r}}_{,\nu} \cdot \overline{\boldsymbol{r}}'|^2. \tag{9}$$

All the barred quantities appearing in (2), (5), (6), (8), and (9) are understood to be expressed through components of the translation vector $\boldsymbol{u}$ and its surface derivatives in the undeformed bases $\boldsymbol{a}_\alpha, \boldsymbol{n}$ or $\boldsymbol{\nu}, \boldsymbol{\tau}, \boldsymbol{n}$, respectively.

Lagrangian Equilibrium Conditions

Let the shell be loaded by the surface force $\boldsymbol{f} = f^\alpha \boldsymbol{a}_\alpha + f\boldsymbol{n}$ and the surface couple $\boldsymbol{m} = \overline{\boldsymbol{n}} \times (m^\alpha \overline{\boldsymbol{a}}_\alpha)$ vector fields, both measured per unit area of $\mathcal{M}$, as well as by the boundary force $\boldsymbol{n}^* = n^*_\nu \boldsymbol{\nu} + n^*_\tau \boldsymbol{\tau} + n^* \boldsymbol{n}$ and the boundary couple $\boldsymbol{m}^* = \overline{\boldsymbol{n}} \times \left(m^*_\nu \overline{\boldsymbol{\nu}} + m^*_\tau \overline{\boldsymbol{\tau}}\right)$ vectors, both given per unit length of $\partial\mathcal{M}$. Then for any additional kinematically admissible virtual translation $\delta\boldsymbol{u} = \delta u_\alpha \boldsymbol{a}^\alpha + \delta w \boldsymbol{n}$ the following Lagrangian principle of virtual displacements should be satisfied (Pietraszkiewicz 1984, 1989):

$$\begin{aligned}\iint_{\mathcal{M}} \left(N^{\alpha\beta}\delta\gamma_{\alpha\beta} + M^{\alpha\beta}\delta\kappa_{\alpha\beta}\right) da \\ = \iint_{\mathcal{M}} \left(\boldsymbol{f} \cdot \delta\boldsymbol{u} + \boldsymbol{m} \cdot \delta\boldsymbol{\omega}\right) da \\ + \int_{\partial\mathcal{M}_f} \left(\boldsymbol{n}^* \cdot \delta\boldsymbol{u} + \boldsymbol{m}^* \cdot \delta\boldsymbol{\omega}_\tau\right) ds.\end{aligned} \tag{10}$$

In (10), $N^{\alpha\beta}$ and $M^{\alpha\beta}$ are symmetric components of the internal 2nd Piola-Kirchhoff type surface stress and couple resultant tensors, $\delta\boldsymbol{\omega}$ and $\delta\boldsymbol{\omega}_\tau$ are the virtual rotation vectors on $\mathcal{M}$ and $\partial\mathcal{M}$, respectively, while the virtual surface deformation measures are given by

$$\begin{aligned}\delta\gamma_{\alpha\beta} &= \frac{1}{2}\left(\delta\boldsymbol{u}_{,\alpha} \cdot \overline{\boldsymbol{a}}_\beta + \overline{\boldsymbol{a}}_\alpha \cdot \delta\boldsymbol{u}_{,\beta}\right), \\ \delta\kappa_{\alpha\beta} &= \frac{1}{2}\left(\overline{\boldsymbol{n}}_{,\alpha} \cdot \delta\boldsymbol{u}_{,\beta} + \overline{\boldsymbol{n}}_{,\beta} \cdot \delta\boldsymbol{u}_{,\alpha}\right. \\ &\quad \left. + \overline{\boldsymbol{a}}_\alpha \cdot \delta\overline{\boldsymbol{n}}_{,\beta} + \overline{\boldsymbol{a}}_\beta \cdot \delta\overline{\boldsymbol{n}}_{,\alpha}\right).\end{aligned} \tag{11}$$

Variating the three constraints $\overline{\boldsymbol{n}} \cdot \overline{\boldsymbol{a}}_\alpha = 0$, $\overline{\boldsymbol{n}} \cdot \overline{\boldsymbol{n}} = 1$ satisfied on $\overline{\mathcal{M}}$, one obtains $\delta\overline{\boldsymbol{n}} \cdot \overline{\boldsymbol{a}}_\alpha = -\overline{\boldsymbol{n}} \cdot \delta\boldsymbol{u}_{,\alpha}, \delta\overline{\boldsymbol{n}} \cdot \overline{\boldsymbol{n}} = 0$, so that $\delta\overline{\boldsymbol{n}} = -\overline{\boldsymbol{a}}^\alpha (\overline{\boldsymbol{n}} \cdot \delta\boldsymbol{u}_{,\alpha})$. On the other hand, $\delta\boldsymbol{\omega}$ on $\overline{\mathcal{M}}$ should satisfy $\delta\overline{\boldsymbol{n}} = \delta\boldsymbol{\omega} \times \overline{\boldsymbol{n}}$. As a result, in (10) one has $\boldsymbol{m} \cdot \delta\boldsymbol{\omega} = -m^\alpha \overline{\boldsymbol{n}} \cdot \delta\boldsymbol{u}_{,\alpha}$ on $\mathcal{M}$.

Introducing (11) and the above relation for $\boldsymbol{m} \cdot \delta\boldsymbol{\omega}$ to (10) and applying the surface divergence theorem (Pietraszkiewicz 2018a), one can transform (10) into

$$\begin{aligned}&- \iint_{\mathcal{M}} \left[\left(\boldsymbol{T}^\alpha + m^\alpha \overline{\boldsymbol{n}}\right)\big|_\alpha + \boldsymbol{f}\right] \cdot \delta\boldsymbol{u}\, da \\ &+ \int_{\partial\mathcal{M}_f} \left\{\left[\left(\boldsymbol{T}^\alpha + m^\alpha \overline{\boldsymbol{n}}\right)\nu_\alpha - \boldsymbol{n}^*\right] \cdot \delta\boldsymbol{u}\right. \\ &\left. + \left(M^{\alpha\beta}\nu_\alpha \overline{\boldsymbol{a}}_\beta\right) \cdot \delta\overline{\boldsymbol{n}} - \boldsymbol{m}^* \cdot \delta\boldsymbol{\omega}_\tau\right\} ds \\ &+ \int_{\partial\mathcal{M}_d} \left[\left(\boldsymbol{T}^\alpha + m^\alpha \overline{\boldsymbol{n}}\right)\nu_\alpha \cdot \delta\boldsymbol{u}\right. \\ &\left. + \left(M^{\alpha\beta}\nu_\alpha \overline{\boldsymbol{a}}_\beta\right) \cdot \delta\overline{\boldsymbol{n}}\right] ds = 0,\end{aligned} \tag{12}$$

where

$$\begin{aligned}\boldsymbol{T}^\alpha &= N^{\alpha\beta}\overline{\boldsymbol{a}}_\beta + M^{\alpha\beta}\overline{\boldsymbol{n}}_{,\beta} \\ &\quad + \left[\left(M^{\kappa\rho}\overline{\boldsymbol{a}}_\rho\right)|_\kappa \cdot \overline{\boldsymbol{a}}^\alpha\right]\overline{\boldsymbol{n}},\end{aligned} \tag{13}$$

and $\partial\mathcal{M}_d = \partial\mathcal{M} \backslash \partial\mathcal{M}_f$ is the complementary part of $\partial\mathcal{M}$ along which the displacement boundary conditions are prescribed.

The vector $\overline{\boldsymbol{n}}(s)$ along $\partial\mathcal{M}$ satisfies only two constraints $\overline{\boldsymbol{r}}' \cdot \overline{\boldsymbol{n}} = 0$, $\overline{\boldsymbol{n}} \cdot \overline{\boldsymbol{n}} = 1$. This means that in order to establish the unique position of $\overline{\boldsymbol{\nu}}, \overline{\boldsymbol{\tau}}, \overline{\boldsymbol{n}}$ relative to $\boldsymbol{\nu}, \boldsymbol{\tau}, \boldsymbol{n}$ one has to know not only three components of $\boldsymbol{u}(s)$ (thus also $\boldsymbol{u}'(s)$) but additionally one scalar function $\varphi(s) = \varphi[\boldsymbol{u}_{,\nu}(s), \boldsymbol{u}'(s)]$ describing the rotational deformation between the bases. The meaning of $\varphi(\boldsymbol{u}_{,\nu}, \boldsymbol{u}')$ is not unique and depends on how the rotational deformation is defined.

The structure of the Lagrangian boundary conditions along $\partial\mathcal{M}$ has been discussed by Makowski and Pietraszkiewicz (1989) with the help of integrability conditions of some differential one-forms. It has been found, in particular, that the general relation for $\delta\overline{\boldsymbol{n}}\left(\varphi, \boldsymbol{u}'\right)$ at the boundary contour can be given in the form

$$\delta\overline{\boldsymbol{n}} = \boldsymbol{q}\ \delta\varphi + \boldsymbol{L}\delta\boldsymbol{u}'. \tag{14}$$

Since $\delta\overline{\boldsymbol{n}} = \delta\boldsymbol{\omega}_\tau \times \overline{\boldsymbol{n}}$ along the boundary contour, one obtains $\boldsymbol{m}^* \cdot \delta\boldsymbol{\omega}_\tau = (\boldsymbol{m}^* \times \overline{\boldsymbol{n}}) \cdot \delta\overline{\boldsymbol{n}}$. Introducing this relation together with (14) into the curvilinear integrals of (12), after integration by parts one can transform them into

$$\begin{aligned}
&\int_{\partial\mathcal{M}_f} \left[\left(\boldsymbol{P}+m_\nu\overline{\boldsymbol{n}}-\boldsymbol{P}^*\right)\cdot\delta\boldsymbol{u}+\left(M-M^*\right)\,\delta\varphi\right]\,ds \\
&\quad+\sum_{M_n\in\partial\mathcal{M}_f}\left(\boldsymbol{F}_n-\boldsymbol{F}_n^*\right)\cdot\delta\boldsymbol{u}_n \\
&\quad+\int_{\partial\mathcal{M}_d}\left[\left(\boldsymbol{P}+m_\nu\overline{\boldsymbol{n}}\right)\cdot\delta\boldsymbol{u}\right]\,ds \\
&\quad+\sum_{M_n\in\partial\mathcal{M}_d}\boldsymbol{F}_n\cdot\delta\boldsymbol{u}_n=0,
\end{aligned} \tag{15}$$

where

$$\begin{aligned}
&\boldsymbol{F}=-\boldsymbol{L}^T\left(M^{\alpha\beta}\overline{\boldsymbol{a}}_\beta\nu_\alpha\right),\ \boldsymbol{F}^*=-\boldsymbol{L}^T\left(\boldsymbol{m}^*\times\overline{\boldsymbol{n}}\right), \\
&\boldsymbol{P}=\boldsymbol{T}^\alpha\nu_\alpha+\boldsymbol{F}',\ \boldsymbol{P}^*=\boldsymbol{n}^*+\boldsymbol{F}^{*\prime},\ m_\nu=m^\alpha\nu_\alpha, \\
&M=\boldsymbol{q}\cdot\left(M^{\alpha\beta}\overline{\boldsymbol{a}}_\beta\nu_\alpha\right),\ M^*=\boldsymbol{q}\cdot\left(\boldsymbol{m}^*\times\overline{\boldsymbol{n}}\right), \\
&\boldsymbol{F}_n=\boldsymbol{F}_n\left(s_n+0\right)-\boldsymbol{F}_n\left(s_n-0\right),\ \boldsymbol{u}_n=\boldsymbol{u}\left(s_n\right).
\end{aligned} \tag{16}$$

Kinematically admissible virtual displacements satisfy $\delta\boldsymbol{u}=\boldsymbol{0}$, $\delta\varphi=0$, and $\delta\boldsymbol{u}_n=\boldsymbol{0}$ along $\partial\mathcal{M}_d$, so that the second integral in (15) identically vanishes. This requires the displacement boundary conditions $\boldsymbol{u}-\boldsymbol{u}^*=\boldsymbol{0}$, $\varphi-\varphi^*=0$ along $\partial\mathcal{M}_d$ to be satisfied and $\boldsymbol{u}_n-\boldsymbol{u}_n^*=\boldsymbol{0}$ should be assured at each point of irregularity $M_n\in\partial\mathcal{M}_d$, where the starred symbols mean the prescribed quantities.

Then with $(15)_1$ as the second row of (12), the principle of virtual displacements requires the following local Lagrangian equilibrium conditions to be satisfied:

- The equilibrium equations

$$\left(\boldsymbol{T}^\alpha+m^\alpha\overline{\boldsymbol{n}}\right)\big|_\alpha+\boldsymbol{f}=\boldsymbol{0}\qquad\text{in}\quad\mathcal{M}, \tag{17}$$

- The natural force static boundary conditions

$$\begin{aligned}
&\boldsymbol{P}+m_\nu\overline{\boldsymbol{n}}-\boldsymbol{P}^*=\boldsymbol{0}, \\
&M-M^*=0\qquad\text{along}\quad\partial\mathcal{M}_f,
\end{aligned} \tag{18}$$

- The concentrated forces $\boldsymbol{F}_n-\boldsymbol{F}_n^*$ applied to each point of irregularity $M_n\in\partial\mathcal{M}_f$.

Particularly simple useful expression for φ was proposed in Pietraszkiewicz and Szwabowicz (1981) as

$$\varphi\equiv n_\nu=\overline{\boldsymbol{n}}\cdot\boldsymbol{\nu}=\frac{1}{j}\left(\boldsymbol{u}'\times\boldsymbol{\nu}-\boldsymbol{n}\right)\cdot\boldsymbol{u}_{,\nu} \tag{19}$$

following from (8). Varying the two constraints along $\partial\overline{\mathcal{M}}$, one obtains $-\delta\overline{\boldsymbol{n}}\cdot\overline{\boldsymbol{r}}'=\overline{\boldsymbol{n}}\cdot\delta\boldsymbol{u}'$, $\delta\overline{\boldsymbol{n}}\cdot\overline{\boldsymbol{n}}=0$ from which it follows that $\delta\overline{\boldsymbol{n}}\times\left(\overline{\boldsymbol{r}}'\times\overline{\boldsymbol{n}}\right)=\overline{\boldsymbol{n}}\left(\overline{\boldsymbol{n}}\cdot\delta\boldsymbol{u}'\right)$. The vector product of this formula by $\boldsymbol{\nu}$ from the left side after transformations leads to

$$\begin{aligned}
&\delta\overline{\boldsymbol{n}}=\frac{1}{e_\nu}\left[\left(\overline{\boldsymbol{r}}'\times\overline{\boldsymbol{n}}\right)\delta n_\nu+\left(\boldsymbol{\nu}\times\overline{\boldsymbol{n}}\right)\overline{\boldsymbol{n}}\cdot\delta\boldsymbol{u}'\right], \\
&e_\nu=\boldsymbol{\nu}\cdot\left(\overline{\boldsymbol{r}}'\times\overline{\boldsymbol{n}}\right),
\end{aligned} \tag{20}$$

so that in the formula (14) one has

$$\boldsymbol{q}=\frac{1}{e_\nu}\left(\overline{\boldsymbol{r}}'\times\overline{\boldsymbol{n}}\right),\qquad\boldsymbol{L}=\frac{1}{e_\nu}\left(\boldsymbol{\nu}\times\overline{\boldsymbol{n}}\right)\otimes\overline{\boldsymbol{n}}, \tag{21}$$

where $\otimes$ is the tensor product.

Other particular cases of φ suggested in Makowski and Pietraszkiewicz (1989) are: the function $\vartheta_\nu=a_\tau^{-2}\left(\overline{\boldsymbol{n}}-\boldsymbol{n}\right)\cdot\overline{\boldsymbol{a}}_\nu$ proposed by Novozhilov and Shamina (1975) and the angle ω_τ of total rotation of the boundary element defined in Pietraszkiewicz (1979) by the relation $2\cos\omega_\tau=\overline{\boldsymbol{\nu}}\cdot\boldsymbol{\nu}+\overline{\boldsymbol{\tau}}\cdot\boldsymbol{\tau}+\overline{\boldsymbol{n}}\cdot\boldsymbol{n}-1$. Corresponding formulas for $\boldsymbol{q}$, $\boldsymbol{L}$ and for the boundary conditions were given in Pietraszkiewicz (1989, 1993).

The Lagrangian vector shell relations derived above have their natural scalar representations in terms of translations u_α, w in the known undeformed base $\boldsymbol{a}_\alpha$, $\boldsymbol{n}$ of $\mathcal{M}$, displacements u_ν, u_τ, w, φ in the known undeformed base $\boldsymbol{\nu}$, $\boldsymbol{\tau}$, $\boldsymbol{n}$ along $\partial\mathcal{M}$ and the surface stress resultants and stress couples $N^{\alpha\beta}$, $M^{\alpha\beta}$ (Pietraszkiewicz 1984, 1989). These scalar relations are very complex, because they are still valid for unrestricted surface deformation measures $\gamma_{\alpha\beta}$, $\kappa_{\alpha\beta}$ and unrestricted displacements $\boldsymbol{u}$ on $\mathcal{M}$ and $\boldsymbol{u}$, φ along $\partial\mathcal{M}$.

Small Elastic Strains

When the strains in the shell space are assumed to be small, i.e., $\max(\gamma_{\alpha\beta}, h\kappa_{\alpha\beta}) = \eta \ll 1$, some shell relations derived so far can be consistently simplified. In particular, in $\mathcal{M}$ one has

$$j \simeq 1, \quad \overline{a}^{\alpha\beta} \simeq a^{\alpha\beta} - 2\gamma^{\alpha\beta} \simeq a^{\alpha\beta},$$
$$n_\mu \simeq \varphi_\lambda l^\lambda_{\cdot\mu} - \varphi_\mu l^\lambda_{\cdot\lambda}, \quad n \simeq \frac{1}{2}\left(l^\lambda_{\lambda} l^\mu_{\mu} - l^\lambda_{\cdot\mu} l^\mu_{\cdot\lambda}\right). \tag{22}$$

With (22) the surface bendings defined in $(6)_2$ become the third-degree polynomials in u_α, w as well as their surface first and second derivatives.

Along $\partial\mathcal{M}$ one can simplify some relations into

$$j \simeq 1, \quad \overline{\boldsymbol{n}} \simeq \overline{\boldsymbol{r}}_{,\nu} \times \overline{\boldsymbol{r}}', \quad n_\nu \simeq \left(\boldsymbol{u}' \times \boldsymbol{\nu} - \boldsymbol{n}\right) \cdot \boldsymbol{u}_{,\nu}, \tag{23}$$

so that n_ν becomes the quadratic polynomial in the displacement derivatives.

With (22) the simplified scalar equilibrium equations (17) were explicitly given in Pietraszkiewicz (1989), while with (23) the simplified scalar static boundary conditions were formulated in Pietraszkiewicz (2001).

When the shell is made of an elastic material, the principle (10) requires the existence of the surface strain energy density $\Sigma(\gamma_{\alpha\beta}, \kappa_{\alpha\beta})$, per unit area of $\mathcal{M}$, such that $N^{\alpha\beta} = \partial\Sigma/\partial\gamma_{\alpha\beta}$ and $M^{\alpha\beta} = \partial\Sigma/\partial\kappa_{\alpha\beta}$. The explicit expression for Σ depends on the shell material properties, but also on the undeformed shell geometry: its thickness, curvatures of $\mathcal{M}$, the internal structure across the thickness, etc.

In case of a homogeneous isotropic shell undergoing small elastic strains, already (Love 1927) used $\Sigma(\gamma_{\alpha\beta}, \kappa_{\alpha\beta})$ consisting of the sum of two quadratic functions describing stretching and bending energies of the shell. The error of such approximation was analyzed in several papers. In particular, according to Koiter (1960, 1966, 1980) and John (1965) the consistently approximated strain energy density is given indeed by the sum of two quadratic functions

$$\Sigma = \frac{h}{2} H^{\alpha\beta\lambda\mu}\left(\gamma_{\alpha\beta}\gamma_{\lambda\mu} + \frac{h^2}{12}\kappa_{\alpha\beta}\kappa_{\lambda\mu}\right) + O\left(Eh\eta^2\theta^2\right),$$
$$H^{\alpha\beta\lambda\mu} = \frac{E}{2(1+\nu)}\left(a^{\alpha\lambda}a^{\beta\mu} + a^{\alpha\mu}a^{\beta\lambda} + \frac{2\nu}{1-\nu}a^{\alpha\beta}a^{\lambda\mu}\right). \tag{24}$$

Here E is the Young modulus and ν is the Poisson ratio of the linearly elastic isotropic material, while the small parameter θ is defined by

$$\theta = \max\left(\frac{h}{b}, \frac{h}{l}, \frac{h}{L}, \sqrt{\frac{h}{R}}, \sqrt{\eta}\right), \tag{25}$$

where b is the distance from the lateral shell boundary surface, l is the smallest wave length of geometric patterns of $\mathcal{M}$, L is the smallest wave length of deformation patterns on $\mathcal{M}$, and $O(.)$ means "of the order of". The material tensor $H^{\alpha\beta\lambda\mu}$ corresponds to the plane stress state in the shell in accordance with the assumption 3. indicated in Introduction.

With $(24)_1$, the constitutive equations are defined by

$$N^{\alpha\beta} = \frac{\partial\Sigma}{\partial\gamma_{\alpha\beta}} = \frac{Eh}{1-\nu^2}\left[(1-\nu)\gamma^{\alpha\beta} + \nu a^{\alpha\beta}\gamma^\kappa_\kappa\right] + O\left(Eh\eta\theta^2\right),$$
$$M^{\alpha\beta} = \frac{\partial\Sigma}{\partial\kappa_{\alpha\beta}} = \frac{Eh^3}{12\left(1-\nu^2\right)}\left[(1-\nu)\kappa^{\alpha\beta} + \nu a^{\alpha\beta}\kappa^\kappa_\kappa\right] + O\left(Eh^2\eta\theta^2\right). \tag{26}$$

Summarizing, the boundary value Lagrangian equilibrium problem of thin isotropic shells undergoing small elastic strains can be

formulated in terms of three translations u_α, w of $\mathcal{M}$ as the basic independent field variables. The BVP consists of three scalar equilibrium equations (17) in $\mathcal{M}$, the four natural static (18) and/or four work-conjugate displacement boundary conditions along $\partial\mathcal{M}_f$ or $\partial\mathcal{M}_d$, the concentrated forces $\boldsymbol{F}_n - \boldsymbol{F}_n^*$ applied to each point of irregularity $M_n \in \partial\mathcal{M}_f$, the constitutive equations (26), and the kinematic relations (6) in which the approximate relations (22) and (23) have been used. Unfortunately, these consistently simplified relations are still too complex for engineering applications.

Restricted Rotations

According to the Cauchy theorem, the shell deformation about a point of $\mathcal{M}$ can be exactly decomposed into a rigid-body translation, a pure stretch along principal directions of strain and a rigid-body rotation. Since in the previous section the shell relations have been consistently simplified under small elastic strains, several simpler versions of the displacement shell relations can be constructed by imposing consistent restrictions upon the rotations of the shell material elements (Pietraszkiewicz 1977, 1980, 1984).

A finite rotation may be described by an angle of rotation ω about an axis of rotation fixed in space by a unit vector $\boldsymbol{e}$. In mathematics, the rotation is usually defined by the second-order tensor $\boldsymbol{R}(\omega, \boldsymbol{e})$ such that $\boldsymbol{R}^T = \boldsymbol{R}^{-1}$, $\det \boldsymbol{R} = +1$. Alternatively, for $|\omega| < \pi/2$ the rotation can be uniquely described by some finite rotation vector such as $\boldsymbol{\Omega} = \boldsymbol{e}\sin\omega$ or $\boldsymbol{\theta} = \boldsymbol{e}\,2\tan\omega/2$. The magnitude of the rotation can be classified in terms of the small parameter θ defined in (25) as follows: (a) $\omega \le O(\theta^2)$ – the small rotation, (b) $\omega = O(\theta)$ – the moderate rotation, (c) $\omega = O\left(\theta\sqrt{\theta}\right)$ – the large rotation, and (d) $\omega = O(1)$ – the finite rotation. However, the shell structures are usually quite rigid for in-surface deformation being flexible for out-of-surface deformation. To account this property, one can associate the names "small, moderate, large, finite" rotation with the particular components $\Omega_\alpha = \boldsymbol{\Omega} \cdot \boldsymbol{a}_\alpha$ and $\Omega = \boldsymbol{\Omega} \cdot \boldsymbol{n}$ of $\boldsymbol{\Omega}$.

In the geometrically nonlinear theory of thin shells $\boldsymbol{\Omega}$ is expressed through translations of $\mathcal{M}$ by the consistent reduction of the exact formula (Pietraszkiewicz 1977, f. (3.7.17) or 1984, f. (2.3.11)):

$$\boldsymbol{\Omega} \simeq \varepsilon^{\beta\alpha}\left[\varphi_\alpha\left(1+\frac{1}{2}\theta_\kappa^\kappa\right) - \frac{1}{2}\varphi^\lambda\left(\theta_{\lambda\alpha} - \omega_{\lambda\alpha}\right)\right]\boldsymbol{a}_\beta + \phi\boldsymbol{n}, \tag{27}$$

$$\begin{aligned} &\theta_{\alpha\beta} = \tfrac{1}{2}\left(u_{\alpha|\beta} + u_{\beta|\alpha}\right) - b_{\alpha\beta}w, \\ &\omega_{\alpha\beta} = \tfrac{1}{2}\left(u_{\beta|\alpha} - u_{\alpha|\beta}\right), \\ &\phi = \tfrac{1}{2}\varepsilon^{\alpha\beta}u_{\beta|\alpha}, \quad \boldsymbol{\phi} = \varepsilon^{\beta\alpha}\varphi_\alpha + \phi\boldsymbol{n}. \end{aligned} \tag{28}$$

Here $\theta_{\alpha\beta}$ are components of the linearized strains while φ_α, ϕ describe the linearized rotation vector $\boldsymbol{\phi}$.

For any restriction imposed on $\boldsymbol{\Omega}$ the estimates for φ_α, ϕ follow from (27) and those for $\theta_{\alpha\beta}$ follow from solving $(6)_1$ with $\gamma_{\alpha\beta} = O(\eta)$. Then the consistently simplified expressions for $\gamma_{\alpha\beta}$ and $\kappa_{\alpha\beta}$ can be established taking account of accuracy of Σ in $(24)_1$. In such estimation procedure covariant surface derivatives are estimated dividing their maximal value by the large parameter

$$\lambda = \frac{h}{\theta} = \min\left(b, l, L, \sqrt{hR}, \frac{1}{\sqrt{\eta}}\right). \tag{29}$$

Within *small rotations* $\varphi_\alpha = O(\theta^2)$, $\omega_{\alpha\beta} = O(\theta^2)$, $\theta_{\alpha\beta} = O(\theta^2)$, and the shell deformation measures are consistently approximated by $\gamma_{\alpha\beta} = \theta_{\alpha\beta} + O(\eta\theta^2)$, $\kappa_{\alpha\beta} = -1/2(\varphi_{\alpha|\beta} + \varphi_{\beta|\alpha}) + O(\eta\theta/\lambda)$. These characterize the linear bending theory of thin elastic shells treated in many books and papers, see for example Koiter (1961).

Within *moderate rotations* $\varphi_\alpha = O(\theta)$, $\omega_{\alpha\beta} = O(\theta)$, $\theta_{\alpha\beta} = O(\theta^2)$, and the consistently reduced shell relations are

$$\gamma_{\alpha\beta} = \theta_{\alpha\beta} + \frac{1}{2}\varphi_\alpha\varphi_\beta + \frac{1}{2}\omega^\lambda_{.\alpha}\omega_{\lambda\beta} - \frac{1}{2}\left(\theta^\lambda_\alpha\omega_{\lambda\beta} + \theta^\lambda_\beta\omega_{\lambda\alpha}\right) + O\left(\eta\theta^2\right),$$
$$\kappa_{\alpha\beta} = -\frac{1}{2}\left(\varphi_{\alpha|\beta} + \varphi_{\beta|\alpha} - b^\lambda_\alpha\omega_{\lambda\beta} - b^\lambda_\beta\omega_{\lambda\alpha}\right) + O\left(\frac{\eta\theta}{\lambda}\right), \tag{30}$$

$$\boldsymbol{T}^\alpha = \left\{N^{\alpha\lambda} - \frac{1}{2}\left(b^\alpha_\beta M^{\lambda\beta} + b^\lambda_\beta M^{\alpha\beta}\right) + \frac{1}{2}N^\kappa_\kappa\omega^{\alpha\lambda} - \frac{1}{2}\left(N^\alpha_\beta\omega^{\lambda\beta} + N^\lambda_\beta\omega^{\alpha\beta}\right) + \frac{1}{2}\left(N^\alpha_\beta\theta^{\lambda\beta} - N^\lambda_\beta\theta^{\alpha\beta}\right)\right\}\boldsymbol{a}_\lambda + \left(N^{\alpha\beta}\varphi_\beta + M^{\beta\alpha}|_\beta\right)\boldsymbol{n}, \tag{31}$$

$$\overline{\boldsymbol{n}} = -\varphi_\alpha\boldsymbol{a}^\alpha + \boldsymbol{n}, \quad n_\nu = -\varphi_\nu,$$
$$\boldsymbol{F} = M_{\nu\tau}\boldsymbol{n}, \quad M = M_{\nu\nu}, \tag{32}$$
$$\boldsymbol{F}^* = m^*_\tau\boldsymbol{n}, \quad M^* = m^*_\nu.$$

If additionally the rotation about normal Ω is restricted to be small then also $\omega_{\alpha\beta} = O(\theta^2)$. For such *moderate/small rotation* theory of thin elastic shells the relations (30) and (31) can be considerably simplified to

$$\gamma_{\alpha\beta} = \theta_{\alpha\beta} + \frac{1}{2}\varphi_\alpha\varphi_\beta + O\left(\eta\theta^2\right),$$
$$\kappa_{\alpha\beta} = -\frac{1}{2}\left(\varphi_{\alpha|\beta} + \varphi_{\beta|\alpha}\right) + O\left(\frac{\eta\theta}{\lambda}\right), \tag{33}$$
$$\boldsymbol{T}^\alpha = N^{\alpha\lambda}\boldsymbol{a}_\lambda + \left(N^{\alpha\beta}\varphi_\beta + M^{\beta\alpha}|_\beta\right)\boldsymbol{n}.$$

The nonlinear relations (30) and (31) (or (33)) with (32) and (26), when introduced into the equilibrium conditions (17) and (18), and the surface couples $\boldsymbol{m}$ conventionally omitted, describe the boundary value problem in displacements of the Lagrangian geometrically nonlinear theory of thin elastic shells undergoing moderate (or moderate/small) rotations. This version of shell equations contains as special cases a number of simpler versions of nonlinear shell equations proposed in the literature. A detailed review of those simpler versions was given in Schmidt and Pietraszkiewicz (1981), where also a set of sixteen basic free functionals and several functionals with subsidiary conditions were constructed for conservative dead-load type surface and boundary loadings.

The simplest case of the moderate/small rotation theory is the nonlinear theory of shallow shells proposed by Mushtari (1939) and Marguerre (1939). In this case, one additionally assumes that the tangential surface forces f^α are also small and can be ignored. As a result, the tangential translations can be expected to be one order smaller than the normal ones, $u_\alpha = w \cdot O(\theta)$, so that $\varphi_\alpha = w_{,\alpha}[1 + O(\theta^2)]$ and the surface deformation measures become extremely simple

$$\gamma_{\alpha\beta} \simeq \theta_{\alpha\beta} + \frac{1}{2}w_{,\alpha}w_{,\beta}, \quad \kappa_{\alpha\beta} \simeq -w_{|\alpha\beta}. \tag{34}$$

In the tangential equilibrium equations, the terms $-b^\lambda_\alpha T^\alpha$ are small as compared with $N^{\alpha\lambda}|_\alpha$ and can be omitted. As a result, the equilibrium equations become extremely simple as well,

$$N^{\alpha\beta}|_\alpha = 0,$$
$$M^{\alpha\beta}|_{\alpha\beta} + \left(b_{\alpha\beta} + w_{|\alpha\beta}\right)N^{\alpha\beta} + f = 0. \tag{35}$$

The equilibrium equations (35) together with the constitutive relations (26), the kinematic relations (34) and corresponding boundary conditions form the boundary value problem of the nonlinear theory of shallow elastic shells expressed in terms of translations of $\mathcal{M}$ as the independent variables.

It can be proved that the approximate expression $(34)_2$ for $\kappa_{\alpha\beta}$ satisfies approximately two tangential compatibility conditions, which suggests that within this approximation the order of covariant differentiation is unimportant. This allows one to approximately satisfy $(35)_1$ by $N^{\alpha\beta} = \varepsilon^{\alpha\lambda}\varepsilon^{\beta\mu}\Psi_{|\lambda\mu}$, where Ψ is the stress function. Then $(35)_2$ and the third compatibility condition for $\gamma_{\alpha\beta}$, $\kappa_{\alpha\beta}$ leads to the set of two equations

$$\frac{Eh^3}{12(1-\nu^2)}\, w|^{\alpha\beta}_{\alpha\beta} - \varepsilon^{\alpha\lambda}\varepsilon_{\beta\mu}\left(b^{\beta}_{\alpha} + w^{\beta}_{\alpha}\right)\Psi|^{\mu}_{\lambda} - f = 0,$$
$$\frac{1}{Eh}\Psi|^{\alpha\beta}_{\alpha\beta} + \varepsilon^{\alpha\lambda}\varepsilon_{\beta\mu}\left(b^{\beta}_{\alpha} + \tfrac{1}{2}w^{\beta}_{\alpha}\right) w|^{\mu}_{\lambda} = 0. \tag{36}$$

These two equations usually written in the orthogonal lines of principal curvatures of $\mathcal{M}$, together with corresponding boundary conditions expressed in w, Ψ, are given in many books and papers, for example (Mushtari and Galimov 1961, Brush and Almroth 1975), where also many numerical examples are presented.

The consistent relations of the *large/small rotation* Lagrangian nonlinear theory of shells have been presented in detail in Pietraszkiewicz (1984, 1989). These relations are more involved than those of the moderate rotation theory. As a result, they have been used to solve some engineering shell problems in only limited number of papers.

Cross-References

- Elastic Shells, Resultant Nonlinear Theory
- Junctions in Irregular Shell Structures
- Surface Geometry, Elements
- Thin Elastic Shells, Linear Theory

References

Brush DO, Almroth BO (1975) Buckling of bars, plates and shells. McGraw-Hill, New York

Galimov KZ (1951) On the general theory of plates and shells with finite displacements and deformations (in Russian). Prikl Matem Mekh 15(6):723–742

John F (1965) Estimates for the derivatives of the stresses in a thin shell and interior shell equations. Commun Pure Appl Math 18:235–267

Koiter WT (1960) A consistent first approximation in the general theory of thin elastic shells. In: Proceedings of the IUTAM symposium on the theory of shells. North-Holland, Amsterdam, pp 12–33

Koiter WT (1961) A systematic simplification of the general equations in the linear theory of thin shells. Proc K Ned Akad Wet Ser B 64:612–619

Koiter WT (1966) On the nonlinear theory of thin elastic shells. Proc K Ned Akad Wet Ser B 69(1):1–54

Koiter WT (1980) The intrinsic equations of shell theory with some applications. In: Nemat-Nasser (ed) Mechanics today 5. Pergamon Press, Oxford, pp 139–154

Love AEH (1927) A treatise on the mathematical theory of elasticity, 4th edn. University Press, Cambridge UK

Makowski J, Pietraszkiewicz W (1989) Work-conjugate boundary conditions in the nonlinear theory of thin shells. Trans ASME J Appl Mech 56(2):395–402

Marguerre K (1939) Zur Theorie der gekrümmten Platte grosser Formänderung. In: Proceedings of the 5th international congress for applied mechanics. Cambridge, New York, pp 93–101

Mushtari KM (1939) Some generalizations of the theory of thin shells with applications to the solution of stability problems of elastic equilibrium (in Russian). Prikl Matem Mekh 2(4):439–456

Mushtari KM, Galimov KZ (1961) Non-linear theory of thin elastic shells. The Israel Program for Sci Transl, Jerusalem

Novozhilov VV, Shamina VA (1975) On kinematic boundary conditions in non-linear problems of theory of elasticity (in Russian). Mekh Tverdogo Tela 5: 63–71

Pietraszkiewicz W (1977) An introduction to the non-linear theory of shells. Ruhr-Universität, Mitt Inst für Mech 10, Bochum

Pietraszkiewicz W (1980) Finite rotations in the nonlinear theory of thin shells. In: Olszak W (ed) Thin shell theory: new trends and applications. CISM courses and lectures, no 240. Springer, Wien/New York, pp 154–208

Pietraszkiewicz W (1984) Lagrangian description and incremental formulation in the non-linear theory of thin shells. Int J Non Linear Mech 19(2):115–140

Pietraszkiewicz W (1989) Geometrically nonlinear theories of thin elastic shells. Adv Mech 12(1):51–130

Pietraszkiewicz W (1993) Work-conjugate boundary conditions associated with the total rotation angle of the shell boundary. Trans ASME J Appl Mech 60(3): 785–786

Pietraszkiewicz W (2001) Non-linear theories of shells. In: Woźniak C (ed) Mechanics of elastic plates and shells (in Polish). Wyd Nauk PWN, Warszawa, pp 424–497

Pietraszkiewicz W (2018a) Surface geometry: elements. In: Altenbach H, Öchsner A (eds) Encyclopedia of continuum mechanics, section: shells. Springer, Berlin (in print)

Pietraszkiewicz W (2018b) Thin elastic shells: linear theory. In: Altenbach H, Öchsner A (eds) Encyclopedia of continuum mechanics, section: shells. Springer, Berlin (in print)

Pietraszkiewicz W, Szwabowicz ML (1981) Entirely Lagrangian nonlinear theory of thin shells. Arch Mech 33(2):273–288

Schmidt R, Pietraszkiewicz W (1981) Variational principles in the geometrically non-linear theory of shells undergoing moderate rotations. Ing Arch 50: 187–201

Thin Elastic Shells, Linear Theory

Wojciech Pietraszkiewicz
Faculty of Civil and Environmental Engineering, Department of Mechanics of Materials and Structures, Gdańnsk University of Technology, Gdańnsk, Poland

Synonyms

Classical shell theory; Kirchhoff-Love shell model

Definition

The linear theory of thin elastic shells is a special case of linear theory of elasticity. Here the shell thickness is assumed to be much smaller than the smallest radius of curvature of the shell middle surface. As a result, the shell deformation can approximately be described only by stretching and bending of its middle surface.

Introduction

The linear theory of thin elastic shells belongs to the classical fields within linear elasticity. It was originated by Love (1888), developed subsequently in many thousands of papers and summarized in dozens of monographs. Among the most important books in the field, one might mention Love (1927), Goldenveizer (1961), Novozhilov (1964), Baṣar and Krätzig (1985), and Novozhilov et al. (1991).

Initially, the linear thin shell relations were developed in orthogonal coordinates coinciding with lines of principal curvatures on the shell middle surface. However, such a shape-dependent description was found to be too complex and inefficient due to a large variety of shell shapes appearing in technology and everyday life. Lurie (1940) proposed to describe the linear shell relations in the invariant tensor notation. These relations were valid for any geometry of the shell midsurface. This compact description was then applied in many papers and books, for example, by Green and Zerna (1954), Koiter (1960), Naghdi (1963), Chernykh (1964), Flügge (1972), Baṣar and Krätzig (1985, 2001), and Ciarlet (2000).

In this note, basic relations of the linear theory of thin isotropic elastic shells are briefly derived and discussed. The formulation is based on the following simplifying assumptions:

1. The material elements, which are normal to the shell middle surface in the undeformed placement, remain normal to the deformed shell midsurface and do not change their lengths. This assumption allows one to approximately describe the shell deformation only by stretching and bending of its middle surface.
2. The state of elastic stress in the shell space is approximately plane. This means that the effects of transverse shear stresses and of normal stresses, acting on surfaces parallel to the middle surface, may be neglected in the elastic strain energy density.

To be concise, these assumptions are used to derive the approximate equilibrium equations and boundary conditions from the postulated principle of virtual displacements for the shell midsurface. In deriving the basic shell relations, the tensor notation for description of surface geometry is applied according to Pietraszkiewicz (2018).

Geometry and Small Deformation of a Thin Shell

Let $\mathcal{P}$ be the region of three-dimensional Euclidean point space $\mathcal{E}$ occupied by the shell in the undeformed placement. The position vector of any point $\mathrm{P} \in \mathcal{P}$ relative to a reference point $\mathrm{O} \in \mathcal{E}$ can be given by

$$\mathbf{p}\left(\theta^{\alpha}, \xi\right) = \mathrm{p}^{i}\left(\theta^{\alpha}\right)\mathbf{i}_{i} = \boldsymbol{r}\left(\theta^{\alpha}\right) + \xi \boldsymbol{n}\left(\theta^{\alpha}\right), \quad (1)$$

T

where $\mathbf{i}_i$, $i = 1, 2, 3$, are the three orthonormal vectors, θ^α, $\alpha = 1, 2$, are the curvilinear surface coordinates, $-h/2 \le \xi \le +h/2$ is the distance from the shell middle surface $\mathcal{M}$ defined by the position vector $\boldsymbol{r}(\theta^\alpha)$, $\boldsymbol{n}(\theta^\alpha)$ is the unit normal vector orienting $\mathcal{M}$, and h is the shell thickness. In thin shell theory it is understood that h be constant and small as compared with the smallest radius of curvature R of $\mathcal{M}$, i.e., $h/R \ll 1$, and with linear dimensions of $\mathcal{P}$.

Geometry of the middle surface $\mathcal{M}$ is described by the following fields (Pietraszkiewicz 2018): the natural base vectors $\boldsymbol{a}_\alpha = \partial \boldsymbol{r}/\partial\theta^\alpha \equiv \boldsymbol{r}_{,\alpha}$, the covariant components $a_{\alpha\beta} = \boldsymbol{a}_\alpha \cdot \boldsymbol{a}_\beta$ of the surface metric tensor with determinant $a = \det(a_{\alpha\beta})$, the dual (contravariant) base vectors $\boldsymbol{a}^\beta$ such that $\boldsymbol{a}_\alpha \cdot \boldsymbol{a}^\beta = \delta^\beta_\alpha$, where $\delta^1_1 = \delta^2_2 = 1$, $\delta^1_2 = \delta^2_1 = 0$, the unit normal vector $\boldsymbol{n} = \boldsymbol{a}_1 \times \boldsymbol{a}_2/|\boldsymbol{a}_1 \times \boldsymbol{a}_2|$, and the covariant components $b_{\alpha\beta} = -\boldsymbol{a}_\alpha \cdot \boldsymbol{n}_{,\beta} = -\boldsymbol{n}_{,\alpha} \cdot \boldsymbol{a}_\beta$ of the surface curvature tensor. The contravariant metric components $a^{\alpha\beta} = \boldsymbol{a}^\alpha \cdot \boldsymbol{a}^\beta$ are used to raise indices of surface vectors and tensors, for example, $\boldsymbol{a}^\beta = a^{\beta\alpha}\boldsymbol{a}_\alpha$, $b^\alpha_\beta = a^{\alpha\lambda}b_{\lambda\beta}$, etc.

The boundary contour $\partial\mathcal{M}$ of $\mathcal{M}$ consists of the finite set of piecewise smooth curves $\boldsymbol{r}(s) = \boldsymbol{r}[\theta^\alpha(s)]$, where s is the arc length along $\partial\mathcal{M}$. In each regular point $M \in \partial\mathcal{M}$, two unit vectors are defined: the tangent $\boldsymbol{\tau} = d\boldsymbol{r}/ds \equiv \boldsymbol{r}' = \boldsymbol{a}_\alpha \tau^\alpha$ and the outward normal $\boldsymbol{\nu} = \boldsymbol{\tau} \times \boldsymbol{n} = \boldsymbol{a}_\alpha \nu^\alpha \equiv \boldsymbol{r}_{,\nu}$, $\nu^\alpha = \varepsilon^{\alpha\beta}\tau_\beta$, where $\boldsymbol{r}_{,\nu}$ means the outward normal derivative of $\boldsymbol{r}$ at $\partial\mathcal{M}$ and $\varepsilon^{\alpha\beta}$ are contravariant components of the surface alternation tensor.

The shell midsurface in the deformed placement $\overline{\mathcal{M}}$ is described by the position vector $\overline{\boldsymbol{r}}(\theta^\alpha) = \boldsymbol{r}(\theta^\alpha) + \boldsymbol{u}(\theta^\alpha)$, where θ^α are the surface curvilinear convective coordinates and $\boldsymbol{u} = u_\alpha \boldsymbol{a}^\alpha + w\boldsymbol{n}$ is the surface translation field. The geometric quantities describing $\overline{\mathcal{M}}$ are analogous to those of $\mathcal{M}$, only now they are marked by the overbar, for example, $\overline{\boldsymbol{a}}_\alpha, \overline{\boldsymbol{n}}, \overline{a}_{\alpha\beta}, \overline{b}_{\alpha\beta}$, etc. The barred quantities can be expressed through analogous unbarred ones and the vector $\boldsymbol{u}$. In the linear theory of shells, these relations are approximated by linear functions of $\boldsymbol{u}$. In particular, one has (Koiter 1960, Pietraszkiewicz 1980)

$$\begin{aligned}
&\overline{\boldsymbol{a}}_\alpha = \boldsymbol{a}_\alpha + \boldsymbol{u}_{,\alpha} = (a_{\lambda\alpha} + \theta_{\lambda\alpha} - \omega_{\lambda\alpha})\,\boldsymbol{a}^\lambda + \varphi_\alpha \boldsymbol{n},\\
&\overline{\boldsymbol{n}} = \boldsymbol{n} - \varphi_\alpha \boldsymbol{a}^\alpha,\ \theta_{\alpha\beta} = \tfrac{1}{2}\left(u_{\alpha|\beta} + u_{\beta|\alpha}\right) - b_{\alpha\beta}w,\\
&\omega_{\alpha\beta} = \tfrac{1}{2}\left(u_{\beta|\alpha} - u_{\alpha|\beta}\right), \quad \varphi_\alpha = w_{,\alpha} + b^\lambda_\alpha u_\lambda,
\end{aligned} \tag{2}$$

$$\begin{aligned}
&\overline{a}_{\alpha\beta} = \overline{\boldsymbol{a}}_\alpha \cdot \overline{\boldsymbol{a}}_\beta = a_{\alpha\beta} + 2\theta_{\alpha\beta},\ \overline{b}_{\alpha\beta} = -\overline{\boldsymbol{a}}_\alpha \cdot \overline{\boldsymbol{n}}_{,\beta}\\
&\qquad = b_{\alpha\beta} + \varphi_{\alpha|\beta} + b^\lambda_\beta\,(\theta_{\lambda\alpha} - \omega_{\lambda\alpha}),\\
&\overline{b}_{\alpha\beta} = -\overline{\boldsymbol{a}}_\beta \cdot \overline{\boldsymbol{n}}_{,\alpha} = b_{\alpha\beta} + \varphi_{\beta|\alpha}\\
&\qquad + b^\lambda_\alpha\left(\theta_{\lambda\beta} - \omega_{\lambda\beta}\right),
\end{aligned} \tag{3}$$

where $(.)_{|\alpha}$ denotes the covariant surface differentiation of $(.)$.

In the linear theory of shells, the surface deformation measures are linear functions of the surface translations and their surface derivatives, and are defined by

$$\begin{aligned}
&\gamma_{\alpha\beta} = \frac{1}{2}\left(\overline{a}_{\alpha\beta} - a_{\alpha\beta}\right) = \frac{1}{2}\left(u_{\alpha|\beta} + u_{\beta|\alpha}\right) - b_{\alpha\beta}w,\\
&\kappa_{\alpha\beta} = -\left(\overline{b}_{\alpha\beta} - b_{\alpha\beta}\right) = -w_{|\alpha\beta} - b^\lambda_\alpha u_{\lambda|\beta}\\
&\qquad - b^\lambda_\beta u_{\lambda|\alpha} - b^\lambda_{\alpha|\beta} u_\lambda + b^\lambda_\alpha b_{\lambda\beta} w.
\end{aligned} \tag{4}$$

The components $\gamma_{\alpha\beta}$ describe the linearized surface strains while $\kappa_{\alpha\beta}$ are the linearized surface changes of curvatures (briefly bendings). Both surface deformation measures are symmetric: $\gamma_{\alpha\beta} = \gamma_{\beta\alpha}$, $\kappa_{\alpha\beta} = \kappa_{\beta\alpha}$. Please note that $\kappa_{\alpha\beta}$ are given through the surface translations as well as their first and second surface derivatives.

Equilibrium Conditions

Let the shell base surface $\mathcal{M}$ be loaded by the distributed force field $\boldsymbol{f} = f^\alpha \boldsymbol{a}_\alpha + f\boldsymbol{n}$ per unit area of $\mathcal{M}$, as well as by the boundary force $\boldsymbol{n}^* = n^*_\nu \boldsymbol{\nu} + n^*_\tau \boldsymbol{\tau} + n^* \boldsymbol{n}$ and the boundary couple $\boldsymbol{m}^* = \boldsymbol{n} \times \left(m^*_\nu \boldsymbol{\nu} + m^*_\tau \boldsymbol{\tau}\right)$, both per unit length of the boundary contour $\partial\mathcal{M}_f$. If the shell is to be in equilibrium, then, within the simplifying assumptions of the linear thin shell model, for a virtual

displacement field $\delta\boldsymbol{u} = \delta u_\alpha \boldsymbol{a}^\alpha + \delta w \boldsymbol{n}$ subjected to kinematic constraints the following principle of virtual displacements should be satisfied:

$$\iint_{\mathcal{M}} \left(N^{\alpha\beta}\delta\gamma_{\alpha\beta} + M^{\alpha\beta}\delta\kappa_{\alpha\beta}\right) da = \iint_{\mathcal{M}} \boldsymbol{f}\cdot\delta\boldsymbol{u}\, da + \int_{\partial\mathcal{M}_f} \left(\boldsymbol{n}^*\cdot\delta\boldsymbol{u} + \boldsymbol{m}^*\cdot\delta\boldsymbol{\omega}_\tau\right) ds. \tag{5}$$

Here $N^{\alpha\beta}$ and $M^{\alpha\beta}$ are symmetric components of the internal surface stress and couple resultants, $\partial\mathcal{M}_f$ is that part of $\partial\mathcal{M}$ along which the forces $\boldsymbol{n}^*$ and couples $\boldsymbol{m}^*$ are prescribed, and $\boldsymbol{\omega}_\tau$ is the linearized rotation vector of the shell lateral boundary element.

The first surface integral of (5) indicates the internal virtual work G_{int} performed by $N^{\alpha\beta}$, $M^{\alpha\beta}$ on the respective virtual strains and bendings $\delta\gamma_{\alpha\beta}$, $\delta\kappa_{\alpha\beta}$ given according to (2), (3) and (4) by

$$\begin{aligned}\delta\gamma_{\alpha\beta} &= \frac{1}{2}\left(\delta u_{\alpha|\beta} + \delta u_{\beta|\alpha}\right) - b_{\alpha\beta}\delta w,\\ \delta\kappa_{\alpha\beta} &= -\delta w_{|\alpha\beta} - b^\lambda_\alpha \delta u_{\lambda|\beta} - b^\lambda_\beta \delta u_{\lambda|\alpha}\\ &\quad - b^\lambda_{\alpha|\beta}\delta u_\lambda + b^\lambda_\alpha b_{\lambda\beta}\delta w.\end{aligned} \tag{6}$$

The last two integrals of (5) indicate the external virtual work G_{ext} performed by $\boldsymbol{f}$ on $\delta\boldsymbol{u}$ within $\mathcal{M}$ as well as by $\boldsymbol{n}^*$ and $\boldsymbol{m}^*$ on the corresponding $\delta\boldsymbol{u}$ and $\delta\boldsymbol{\omega}_\tau$ along $\partial\mathcal{M}_f$, respectively. The virtual fields should satisfy the kinematic constraints, that is, $\boldsymbol{\delta u} = \boldsymbol{0}$ and $\boldsymbol{\delta\omega}_\tau = \boldsymbol{0}$ along $\partial\mathcal{M}_d$, where $\partial\mathcal{M} = \partial\mathcal{M}_f \cup \partial\mathcal{M}_d$.

With the help of some tensor identities, the G_{int} in (5) with (6) can be transformed into

$$\begin{aligned}G_{\text{int}} = -\iint_{\mathcal{M}} \Big\{ &\left[\left(N^{\alpha\beta} - b^\beta_\lambda M^{\lambda\alpha}\right)_{|\alpha} - b^\beta_\lambda M^{\lambda\alpha}{}_{|\alpha}\right]\delta u_\beta\\ &+ \left[M^{\alpha\beta}{}_{|\alpha\beta} + b_{\alpha\beta}\left(N^{\alpha\beta} - b^\alpha_\lambda M^{\lambda\beta}\right)\right]\delta w\\ &- \Big[\left(N^{\alpha\beta} - b^\beta_\lambda M^{\lambda\alpha}\right)\delta u_\beta\\ &- M^{\alpha\beta}\left(\delta w_{,\beta} + b^\lambda_\beta \delta u_\lambda\right)\\ &+ M^{\alpha\beta}{}_{|\beta}\delta w\Big]_{|\alpha}\Big\}\, da.\end{aligned} \tag{7}$$

Introducing the vector

$$\boldsymbol{n}^\alpha = \left(N^{\alpha\beta} - b^\beta_\lambda M^{\lambda\alpha}\right)\boldsymbol{a}_\beta + M^{\alpha\beta}{}_{|\beta}\,\boldsymbol{n}, \tag{8}$$

and applying the divergence theorem to the last term of (7) in brackets, relation (7) can be written in the compact form

$$\begin{aligned}G_{\text{int}} = &-\iint_{\mathcal{M}} \boldsymbol{n}^\alpha{}_{|\alpha}\cdot\delta\boldsymbol{u}\, da\\ &+ \int_{\partial\mathcal{M}} \left(\boldsymbol{n}^\alpha\cdot\delta\boldsymbol{u} - M^{\alpha\beta}\delta\varphi_\beta\right)\nu_\alpha\, ds,\end{aligned} \tag{9}$$

where $\delta\varphi_\beta$ are tangential components of variation of the linearized rotation vector of $\mathcal{M}$,

$$\boldsymbol{\phi} = \varepsilon^{\beta\alpha}\left(\varphi_\alpha \boldsymbol{a}_\beta + \frac{1}{2}u_{\alpha|\beta}\boldsymbol{n}\right). \tag{10}$$

Along $\partial\mathcal{M}$, the virtual translations and rotations can be expanded into physical components

$$\begin{aligned}&\delta\boldsymbol{u} = \delta u_\nu \boldsymbol{\nu} + \delta u_\tau \boldsymbol{\tau} + \delta w\boldsymbol{n},\\ &\delta\varphi_\beta = \delta\varphi_\nu \nu_\beta + \delta\varphi_\tau \tau_\beta,\\ &\delta\varphi_\tau = \delta\varphi_\beta\tau^\beta = \tfrac{d}{ds}(\delta w) + \sigma_\tau\delta u_\tau - \tau_\tau\delta u_\nu,\\ &\delta u_\nu = \delta u_\beta\nu^\beta, \quad \delta u_\tau = \delta u_\beta\tau^\beta,\\ &\sigma_\tau = b_{\alpha\beta}\tau^\alpha\tau^\beta, \quad \tau_\tau = -b_{\alpha\beta}\nu^\alpha\tau^\beta.\end{aligned} \tag{11}$$

The first term in $(11)_3$ allows one to integrate by parts the last expressions in the line integral (9) leading to

$$\begin{aligned}&-\textstyle\int_{\partial\mathcal{M}} \left[M_{\nu\nu}\delta\varphi_\nu + M_{\nu\tau}\left(\frac{d}{ds}(\delta w)\right.\right.\\ &\left.\left.+\sigma_\tau\delta u_\tau - \tau_\tau\delta u_\nu\right)\right] ds = \textstyle\int_{\partial\mathcal{M}}\\ &\left[\frac{d}{ds}(M_{\nu\tau}\boldsymbol{n})\cdot\delta\boldsymbol{u} - M_{\nu\nu}\delta\varphi_\nu\right] ds\\ &+\textstyle\sum_{n=1}^{N}\left[M_{\nu\tau}(s_n+0)\right.\\ &\left.-M_{\nu\tau}(s_n-0)\right]\delta w(s_n).\end{aligned} \tag{12}$$

The linearized rotation vector $\boldsymbol{\omega}_\tau$ of the shell lateral boundary element is related to the linearized rotation vector $\boldsymbol{\phi}$ of $\mathcal{M}$ by $\boldsymbol{\omega}_\tau = \boldsymbol{\phi} - \gamma_{\nu\tau}\boldsymbol{n}$ (Chernykh 1964, Pietraszkiewicz 1980). But within the assumptions of the linear

thin shell theory, $\boldsymbol{m}^*$ does not have the normal component, so it is always $\boldsymbol{m}^* \cdot n \equiv 0$. As a result, $\boldsymbol{m}^* \cdot \delta\boldsymbol{\omega}_\tau = \boldsymbol{m}^* \cdot \delta\boldsymbol{\phi}$ and the last term in (5) can be transformed similarly as in (12) leading to

$$\begin{aligned}&\int_{\partial\mathcal{M}_f} \boldsymbol{m}^* \cdot \delta\boldsymbol{\omega}_\tau \, ds \\ &= \int_{\partial\mathcal{M}_f} \left[\tfrac{d}{ds}\left(m_\tau^* \boldsymbol{n}\right) \cdot \delta\boldsymbol{u} - m_\nu^* \delta\varphi_\nu\right] ds \\ &+ \sum_{n=1}^{N} \left[m_\tau^*(s_n+0) - m_\tau^*(s_n-0)\right] \delta w(s_n).\end{aligned} \tag{13}$$

Summarizing, the principle of virtual displacements (5) with (6), (7), (8), (9), (10), (11), (12), and (13) requires the following local relations to be satisfied:

- The equilibrium equations

$$\boldsymbol{n}^\alpha\big|_\alpha + \boldsymbol{f} = \boldsymbol{0} \ \text{ in } \ \mathcal{M}. \tag{14}$$

- The force static boundary conditions

$$\begin{aligned}\boldsymbol{n}^\alpha \nu_\alpha + \frac{d}{ds}\left(M_{\nu\tau}\boldsymbol{n}\right) &= \boldsymbol{n}^* + \frac{d}{ds}\left(m_\tau^* \boldsymbol{n}\right), \\ M_{\nu\nu} &= m_\nu^* \quad \text{along} \ \ \partial\mathcal{M}_f.\end{aligned} \tag{15}$$

- The concentrated forces applied in each singular point $M_n \in \partial\mathcal{M}_f$,

$$\begin{aligned}&\left\{\left[M_{\nu\tau}(s_n+0) - m_\tau^*(s_n+0)\right]\right. \\ &\left. - \left[M_{\nu\tau}(s_n-0) - m_\tau^*(s_n-0)\right]\right\} \boldsymbol{n}(s_n).\end{aligned} \tag{16}$$

- The corresponding work-conjugate displacement boundary conditions are

$$\boldsymbol{u} = \boldsymbol{u}^*, \quad \varphi_\nu = \varphi_\nu^* \quad \text{along} \ \ \partial\mathcal{M}_d. \tag{17}$$

In components, some of these relations are:

- The equilibrium eguations in $\mathcal{M}$,

$$\begin{aligned}T^{\alpha\beta}|_\alpha - b_\lambda^\beta Q^\lambda + f^\beta &= 0, \\ M^{\alpha\beta}|_{\alpha\beta} + b_{\alpha\beta} T^{\alpha\beta} + f &= 0,\end{aligned} \tag{18}$$

where the following abbreviations have been used:

$$T^{\alpha\beta} = N^{\alpha\beta} - b_\lambda^\beta M^{\lambda\alpha}, \quad Q^\lambda = M^{\alpha\lambda}|_\alpha. \tag{19}$$

- The force static boundary conditions along $\partial\mathcal{M}_f$,

$$\begin{aligned}T_{\nu\nu} + \tau_\tau M_{\nu\tau} &= n_\nu^* + \tau_\tau m_\tau^* \ \text{ in direction of } \boldsymbol{\nu}, \\ T_{\nu\tau} - \sigma_\tau M_{\nu\tau} &= n_\tau^* - \sigma_\tau m_\tau^* \ \text{ in direction of } \boldsymbol{\tau}, \\ Q_\nu + \tfrac{d}{ds} M_{\nu\tau} &= n^* + \tfrac{d}{ds} m_\tau^* \ \text{ in direction of } \boldsymbol{n},\end{aligned} \tag{20}$$

where the following abbreviations of the physical components have been used:

$$\begin{aligned}&T_{\nu\nu} = T^{\alpha\beta}\nu_\alpha\nu_\beta, \quad T_{\nu\tau} = T^{\alpha\beta}\nu_\alpha\tau_\beta, \\ &M_{\nu\tau} = M^{\alpha\beta}\nu_\alpha\tau_\beta, \quad Q_\nu = Q^\alpha\nu_\alpha, \\ &M_{\nu\nu} = M^{\alpha\beta}\nu_\alpha\nu_\beta.\end{aligned} \tag{21}$$

Compatibility Conditions

Six components $\gamma_{\alpha\beta}$ and $\kappa_{\alpha\beta}$ are expressed by only three components of $\boldsymbol{u}$ on $\mathcal{M}$. Thus, the surface deformation measures have to satisfy three compatibility conditions.

Two smooth and differentiable vector displacement fields on the regular shell midsurface $\mathcal{M}$ satisfy the obvious identities $\boldsymbol{u}_{,12} = \boldsymbol{u}_{,21}$ and $\boldsymbol{\phi}_{,12} = \boldsymbol{\phi}_{,21}$, which can equivalently be written as

$$\varepsilon^{\alpha\beta}\boldsymbol{u}_{|\alpha\beta} = \boldsymbol{0}, \quad \varepsilon^{\alpha\beta}\boldsymbol{\phi}_{|\alpha\beta} = \boldsymbol{0}. \tag{22}$$

Differentiation of $\boldsymbol{u}$ with the use of (10) leads to

$$\boldsymbol{u}_{,\alpha} = \gamma_{\alpha\lambda}\boldsymbol{a}^\lambda + \boldsymbol{\phi} \times \boldsymbol{a}_\alpha. \tag{23}$$

Differentiating (10), one obtains

$$\begin{aligned}\boldsymbol{\phi}_{,\alpha} &= \varepsilon^{\lambda\mu}\mu_{\alpha\lambda}\boldsymbol{a}_\mu + \zeta_\alpha \boldsymbol{n}, \\ \mu_{\alpha\lambda} &= -\varphi_{\lambda|\alpha} - \varepsilon_{\lambda\rho} b_\alpha^\rho \phi, \\ \zeta_\alpha &= \phi_{,\alpha} + \varepsilon^{\rho\lambda}\varphi_\lambda b_{\alpha\rho}.\end{aligned} \tag{24}$$

Then

$$\begin{aligned}\varepsilon^{\alpha\beta}\boldsymbol{u}_{|\alpha\beta} &= \left(\varepsilon^{\alpha\beta}\gamma_{\alpha\lambda|\beta} + \zeta_\lambda\right)\boldsymbol{a}^\lambda \\ &\quad + \varepsilon^{\alpha\beta}\left(\gamma_{\alpha\lambda}b^\lambda_\beta + \mu_{\alpha\beta}\right)\boldsymbol{n} = \boldsymbol{0}, \\ \varepsilon^{\alpha\beta}\boldsymbol{\phi}_{|\alpha\beta} &= \varepsilon^{\alpha\beta}\left(\varepsilon^{\rho\lambda}\mu_{\alpha\rho|\beta} + b^\lambda_\alpha\zeta_\beta\right)\boldsymbol{a}_\lambda \\ &\quad + \varepsilon^{\alpha\beta}\left(\zeta_{\alpha|\beta} + \varepsilon^{\lambda\rho}\mu_{\alpha\lambda}b_{\beta\rho}\right)\boldsymbol{n} = \boldsymbol{0}.\end{aligned} \tag{25}$$

Using the relations (3) and (4), after some transformations, one obtains

$$\mu_{\alpha\beta} = \kappa_{\alpha\beta} + b^\lambda_\alpha\gamma_{\beta\lambda}. \tag{26}$$

This indicates that the second expression of $(25)_1$ identically vanishes. Then one can solve the first expression in $(25)_1$ for ζ_λ and introduce the result into $(25)_2$. By changing some indices, the remaining three compatibility conditions become

$$\begin{aligned}&\left(\varepsilon^{\alpha\rho}\varepsilon^{\beta\lambda}\mu_{\rho\lambda}\right)|_\alpha - b^\beta_\lambda\left(-\varepsilon^{\alpha\rho}\varepsilon^{\beta\lambda}\gamma_{\rho\lambda}\right)|_\alpha = 0, \\ &\left(-\varepsilon^{\alpha\rho}\varepsilon^{\beta\lambda}\gamma_{\rho\lambda}\right)|_{\alpha\beta} + b_{\alpha\beta}\left(\varepsilon^{\alpha\rho}\varepsilon^{\beta\lambda}\mu_{\rho\lambda}\right) = 0.\end{aligned} \tag{27}$$

Static-Geometric Analogy and Complex Shell Relations

Between the equilibrium equations (18) and the compatibility conditions (27) there exists the following correspondence:

$$\begin{aligned}T^{\alpha\beta} &\Longleftrightarrow \varepsilon^{\alpha\rho}\varepsilon^{\beta\lambda}\mu_{\rho\lambda}, \\ M^{\alpha\beta} &\Longleftrightarrow -\varepsilon^{\alpha\rho}\varepsilon^{\beta\lambda}\gamma_{\rho\lambda}.\end{aligned} \tag{28}$$

When the surface stress measures in (18) are replaced by the surface deformation measures according to (28), the homogeneous equilibrium equations (27) are converted into the compatibility conditions (27). The correspondence is known as the static-geometric analogy in the linear theory of thin shells.

The analogy (28) allows one to introduce three stress functions $\overline{u}_\alpha, \overline{w}$ by the relations

$$\begin{aligned}T^{\alpha\beta} &= T^{\alpha\beta}_* + Ehc\varepsilon^{\alpha\rho}\varepsilon^{\beta\lambda}\overline{\mu}_{\rho\lambda}, \\ M^{\alpha\beta} &= M^{\alpha\beta}_* - Ehc\varepsilon^{\alpha\rho}\varepsilon^{\beta\lambda}\overline{\gamma}_{\rho\lambda}, \\ c &= \frac{h}{\sqrt{12(1-\nu^2)}}.\end{aligned} \tag{29}$$

Here $T^{\alpha\beta}_*$ and $M^{\alpha\beta}_*$ are some particular solutions of the inhomogeneous equilibrium equations (18), and the expressions $\overline{\gamma}_{\rho\lambda}$ and $\overline{\mu}_{\rho\lambda}$ are similar to $(4)_1$ and (26), respectively, only now constructed by corresponding stress functions $\overline{u}_\alpha, \overline{w}$.

With (29), one can introduce the surface complex stress measures

$$\begin{aligned}\tilde{T}^{\alpha\beta} &= T^{\alpha\beta}_* - i\ Ehc\varepsilon^{\alpha\rho}\varepsilon^{\beta\lambda}\tilde{\mu}_{\rho\lambda}, \\ \tilde{M}^{\alpha\beta} &= M^{\alpha\beta}_* + i\ Ehc\varepsilon^{\alpha\rho}\varepsilon^{\beta\lambda}\tilde{\gamma}_{\rho\lambda}, \quad i = \sqrt{-1},\end{aligned} \tag{30}$$

where $\tilde{\gamma}_{\rho\lambda}$ and $\tilde{\mu}_{\rho\lambda}$ are expressions similar to $(4)_1$ and (26) only now constructed by the complex translations $\tilde{u}_\alpha = u_\alpha + i\ \overline{u}_\alpha$, $\tilde{w} = w + i\ \overline{w}$. When the compatibility conditions (27) are multiplied by $i\,Ehc$ and added with the corresponding equilibrium equations (18), this gives the following set of three equations for the complex stress measures:

$$\begin{aligned}&\tilde{T}^{\alpha\beta}|_\alpha - b^\beta_\lambda\tilde{M}^{\alpha\lambda}|_\alpha + f^\beta = 0, \\ &\tilde{M}^{\alpha\beta}|_{\alpha\beta} + b_{\alpha\beta}\tilde{T}^{\alpha\beta} + f = 0.\end{aligned} \tag{31}$$

When expressed in terms of complex translations, the above system of PDEs for the complex independent variables is of the 4th order to be solved in the complex domain, while the system (18) of PDEs for the real translations is of the 8th order in the real domain.

The complex formulation of the linear thin shell theory was used to solve analytically a number of linear shell problems presented, for example, in the books by Novozhilov (1964), Chernykh (1964), and Novozhilov et al. (1991).

Constitutive Equations

When the shell is made of an elastic material, the principle (5) requires the existence of the surface strain energy density $\Sigma(\gamma_{\alpha\beta}, \kappa_{\alpha\beta})$, per unit area of $\mathcal{M}$, such that $N^{\alpha\beta} = \partial\Sigma/\partial\gamma_{\alpha\beta}$ and $M^{\alpha\beta} = \partial\Sigma/\partial\kappa_{\alpha\beta}$. The explicit expression for Σ depends on the shell material properties, but also on the undeformed shell geometry: its thickness, curvatures of $\mathcal{M}$, the internal structure across the thickness, etc.

In case of a homogeneous isotropic shell undergoing small elastic strains, already (Love 1888, 1927) used $\Sigma(\gamma_{\alpha\beta}, \kappa_{\alpha\beta})$ consisting of the sum of two quadratic functions describing stretching and bending energies of the shell. The error of such approximation was analyzed in Novozhilov and Finkel'stein (1943) and in several later papers. In particular, according to Koiter (1960), the consistently approximated strain energy density is given by

$$\begin{aligned}\Sigma &= \tfrac{h}{2} H^{\alpha\beta\lambda\mu}\left(\gamma_{\alpha\beta}\gamma_{\lambda\mu} + \tfrac{h^2}{12}\kappa_{\alpha\beta}\kappa_{\lambda\mu}\right)\\ &\quad + O\left(Eh\eta^2\theta^2\right),\\ H^{\alpha\beta\lambda\mu} &= \tfrac{E}{2(1+\nu)}\\ &\quad \left(a^{\alpha\lambda}a^{\beta\mu} + a^{\alpha\mu}a^{\beta\lambda} + \tfrac{2\nu}{1-\nu}a^{\alpha\beta}a^{\lambda\mu}\right).\end{aligned} \tag{32}$$

Here E is the Young modulus and ν is the Poisson ratio of the linearly elastic isotropic material, while the small parameter θ is defined as $\theta = \max\left(h/L, \sqrt{h/R}, \sqrt{\eta}\right)$, where L is the smallest length of geometric and deformation patterns on $\mathcal{M}$. The form $(32)_1$ of $\Sigma(\gamma_{\alpha\beta}, \kappa_{\alpha\beta})$ was subsequently justified by asymptotic analysis of the equations of 3D linearized elasticity as indeed the consistent first approximation to the 3D strain energy density of the shell (see review by Ciarlet 2000). The material tensor $H^{\alpha\beta\lambda\mu}$ in $(32)_2$ corresponds to the plane stress state in the shell space in accordance with the assumption 2. indicated in Introduction.

With $(32)_1$, the constitutive equations of isotropic elastic shells are given by

$$\begin{aligned}N^{\alpha\beta} &= \tfrac{\partial\Sigma}{\partial\gamma_{\alpha\beta}}\\ &= \tfrac{Eh}{1-\nu^2}\left[(1-\nu)\,\gamma^{\alpha\beta} + \nu a^{\alpha\beta}\gamma_\kappa^\kappa\right]\\ &\quad + O\left(Eh\eta\theta^2\right),\\ M^{\alpha\beta} &= \tfrac{\partial\Sigma}{\partial\kappa_{\alpha\beta}}\\ &= \tfrac{Eh^3}{12(1-\nu^2)}\left[(1-\nu)\,\kappa^{\alpha\beta} + \nu a^{\alpha\beta}\kappa_\kappa^\kappa\right]\\ &\quad + O\left(Eh^2\eta\theta^2\right).\end{aligned} \tag{33}$$

Summarizing, the boundary value equilibrium problem of thin isotropic elastic shells can be formulated in terms of three translations u_α, w of $\mathcal{M}$ as the basic independent field variables. The BVP consists of three scalar equilibrium equations (18) with (19), four natural static (20) and $(15)_2$ and/or four work-conjugate displacement boundary conditions (17), the constitutive equations (33), and the kinematic relations (4).

The error indicated in $(32)_1$ suggests that, within the accuracy of the first approximation to the strain energy function, one can apply various alternative definitions of the bending tensor, provided that they differ from $\kappa_{\alpha\beta}$ by terms of the type $b_\alpha^\lambda\gamma_{\lambda\beta}$. In particular, Koiter (1960) used the bending tensor $\rho_{\alpha\beta} = -\kappa_{\alpha\beta} - 1/2\left(b_\alpha^\lambda\gamma_{\lambda\beta} + b_\beta^\lambda\gamma_{\lambda\alpha}\right)$ and (Budiansky and Sanders 1963) by several additional criteria found it to be the "best" bending tensor for the linear theory of thin elastic shells. Unfortunately, some shell relations compatible with $\rho_{\alpha\beta}$ become more complex and less convenient in general discussions.

According to (26), the nonsymmetric tensor $\mu_{\alpha\beta}$ may also be used as the bending tensor of the linear theory of thin elastic shells. In this case, the constitutive equations $(33)_2$ of an isotropic elastic shell are given by

$$\begin{aligned}M^{\alpha\beta} &= \frac{\partial\Sigma}{\partial\mu_{\alpha\beta}} = \frac{Eh^3}{12\left(1-\nu^2\right)}\\ &\quad \left[(1-\nu)\,\mu^{\alpha\beta} + \nu a^{\alpha\beta}\mu_{\cdot\kappa}^{\kappa}\right] + O\left(Eh^2\eta\theta^2\right).\end{aligned} \tag{34}$$

Conclusions

The limited space for this entry does not allow one to discuss here many other important problems of the linear theory of thin isotropic elastic shells. The literature in the field is numerous and some early important contributions are inaccessible through Internet. The interested reader should consult references given in the books referred to below.

Cross-References

- ▸ Elastic Shells, Resultant Nonlinear Theory
- ▸ Junctions in Irregular Shell Structures
- ▸ Surface Geometry, Elements
- ▸ Thin Elastic Shells, Lagrangian Geometrically Nonlinear Theory

References

Başar Y, Krätzig WB (1985) Mechanik der Flächentragwerke. F. Vieveg & Sohn, Braunschweig

Başar Y, Krätzig WB (2001) Theory of shell structures, 2nd edn. VDI Verlag, Düsseldorf

Budiansky B, Sanders JL (1963) On the "best" first-order linear shell theory. In: Progress in applied mechanics (Prager Anniv Vol). Macmillan, New York, pp 126–140

Chernykh KF (1964) Linear theory of shells, part 2 (in Russian). University Press, Leningrad. English translation: NASA-TT-F-II 562, 1968

Ciarlet PG (2000) Mathematical elasticity, Vol. III: theory of shells. Elsevier, Amsterdam et al

Flügge W (1972) Tensor analysis and continuum mechanics. Springer, Berlin et al

Goldenveizer AL (1961) Theory of elastic thin shells. Pergamon press, Oxford

Green AE, Zerna W (1954) Theoretical elasticity. Clarendon Press, Oxford

Koiter WT (1960) A consistent first approximation in the general theory of thin elastic shells. In: Proceedings of the IUTAM symposium on the theory of thin elastic shells. North-Holland, Amsterdam, pp 139–154

Love AEH (1888) The small free vibrations of a thin elastic shells. Philos Trans R Soc Lond A 179:491–546

Love AEH (1927) A treatise on the mathematical theory of elasticity, 4th edn. University Press, Cambridge UK

Lurie AI (1940) General theory of elastic thin shells (in Russian). Prikl Matem Mekh 4(2):7–34

Naghdi PM (1963) Foundations of elastic shell theory. In: Sneddon IN, Hill R (eds) Progress in solid mechanics IV. North-Holland, Amsterdam, pp 1–90

Novozhilov VV (1964) Thin shell theory. P. Noordhoff, Groningen

Novozhilov VV, Finkel'shtein PM (1943) On the error of Kirchhoff's hypotheses in shell theory (in Russian). Prikl Matem Mekh 7(5):331–340

Novozhilov VV, Chernykh KF, Mikhailovskii EI (1991) The linear theory of thin shells (in Russian). Politekhnika, Leningrad

Pietraszkiewicz W (1980) Finite rotations in the nonlinear theory of thin shells. In: Olszak W (ed) Thin shell theory: new trends and applications. CISM courses and lectures, no 240. Springer, Wien/New York, pp 154–208

Pietraszkiewicz W (2018) Surface geometry, elements. In: Altenbach H, Őchsner A (eds) Encyclopedia of continuum mechanics. Springer, Berlin (in print)

Thin Plate

- ▸ Classical Plate Problems
- ▸ Direct Derivation of Plate Theories

Thin Plates and Shells

- ▸ Thin Bodies Embedded in Fractional Derivative Viscoelastic Medium, Dynamic Response

Thin-Walled Beams of Open Profile

- ▸ Transient Waves in Cosserat Beams: Ray Expansion Approach

Thin-Walled Profiles

- ▸ Pure Torsion of Thin-Walled Cross Sections

Thin-Walled Structures

- ▸ Dynamic Equations, Verification of Hyperbolicity via the Theory of Discontinuities
- ▸ Finite Elements for Plates and Shells

Three-Dimensional (3D) Composites: Through-Thickness Reinforcement

▸ Mechanics of 3D Fibre Reinforced Polymer Composites

Three-Dimensional Derivations of Static Plate Theories

Arthur Lebée and Sébastien Brisard
Laboratoire Navier (UMR 8205), CNRS, ENPC, IFSTTAR, Université Paris-Est, Marne-la-Vallée, France

Synonyms

Dimensional reduction; First-order shear deformation theory; Plate model or theory; Reissner or Hencky or Reissner-Mindlin thick plate theory

Definition

Thin plate model: A model where the only kinematic d.o.f. is the transverse deflection. It neglects the shear energy.

Thick plate model: A model including also two in-plane rotation d.o.f. and including shear deflection.

Introduction

Plates are three-dimensional structures with a small dimension compared to the other two dimensions. Numerous approaches were suggested in order to replace the three-dimensional problem by a two-dimensional problem while guaranteeing the accuracy of the reconstructed three-dimensional fields. Turning the 3D problem into a 2D plate model is known as dimensional reduction.

The approaches for deriving a plate model from 3D elasticity may be separated in two main categories: axiomatic and asymptotic approaches. Axiomatic approaches start with ad hoc assumptions on the 3D field representation of the plate, separating the out-of-plane coordinate from the in-plane coordinates. The limitation of these approaches comes from the educated guess for the 3D field distribution. Asymptotic approaches come often after axiomatic approaches. They are based on the explicit introduction of the plate thickness, which is assumed to go to 0, in the equations of the 3D problem. Following a rather well-established procedure, they enable the derivation of plate models, often justifying a posteriori axiomatic approaches, and are the basis of a convergence result.

The very first and simplest model is the Kirchhoff-Love plate model or thin-plate model (Kirchhoff 1850; Love 1888), where the out-of-plane deflection is the only kinematic degree of freedom. In this model, it is assumed that the fiber normal to the plate mid-surface remains normal during the motion. In order to take into account the influence of shear energy on the deflection, several thick plate models were suggested almost simultaneously (Reissner 1944; Hencky 1947; Bollé 1947). In these models, gathered here under the common denomination Reissner-Hencky models, two in-plane rotations are added to the kinematics. Note that the denomination Reissner-Mindlin is also very common in the literature. It comes from Mindlin's contribution based on dynamic considerations (Mindlin 1951). Whereas all these models were historically derived axiomatically, they also have close relations with asymptotic considerations.

This chapter is dedicated to the case of a homogeneous and linear elastic plate with static loading which was the foundation of many extensions to heterogeneous plates. It recalls in detail the derivation of the thick plate model from Hencky (1947) as well as the one from Reissner (1944). Both approaches are related but yield different plate models. This choice is motivated by the following considerations. First, Reissner-Hencky models are the most widely used plate models in engineering applications. Indeed, their

boundary conditions seem more natural than those of the Kirchhoff-Love plate model. They also relax the higher regularity of the Kirchhoff-Love displacement required for finite elements implementations. Second, the Kirchhoff-Love model may be directly retrieved from these models by means of the Kirchhoff kinematic restriction "Direct Derivation of Plate Theories".

Two modifications are made with respect to the historical contributions. First, the membrane model is also included in the present derivation at very little price. Second, the applied load is a body force uniformly distributed through the thickness instead of a force per unit surface applied only on the upper face of the plate. This choice leads to a more compact derivation and removes a higher-order coupling between the membrane and bending problems widely ignored in the historical literature. Finally, all mathematical developments are purely formal and the reader is referred to ("Mathematical Justifications of Plate Models" and Ciarlet 1997) for rigorous justifications.

The 3D Problem

The plate is the cylindrical body $\Omega = \omega \times \mathcal{T}$ where ω denotes the midplane surface of the plate and $\mathcal{T} = \left[-\frac{h}{2}, \frac{h}{2}\right]$ is the transverse coordinate range. The boundary, $\partial\Omega$, is decomposed into three parts (Fig. 1):

$$\partial\Omega = \partial\Omega_{\text{lat}} \cup \partial\Omega_3^+ \cup \partial\Omega_3^-, \tag{1}$$

with:

$$\partial\Omega_{\text{lat}} = \partial\omega \times \mathcal{T} \text{ and } \partial\Omega_3^{\pm} = \omega \times \left\{\pm\tfrac{h}{2}\right\}. \tag{2}$$

It is assumed that the plate follows a prescribed displacement $\mathbf{u}^d$ on its lateral boundary, $\partial\Omega_{\text{lat}}$, and is subjected to body forces $\mathbf{f(x)}$ in Ω of the form:

$$\mathbf{f} = (f_1(x_1, x_2),\, f_2(x_1, x_2),\, hf_3(x_1, x_2)). \tag{3}$$

In the third component of the body force, the thickness is factored out in order to follow the usual scaling of applied forces when the thickness goes to 0 and will be motivated in the following. It is assumed that the fourth-order stiffness tensor $\mathbf{C}$ characterizing the elastic properties of the constituent material at every point $\mathbf{x} = (x_1, x_2, x_3)$ of Ω is uniform on the whole body. The tensor $\mathbf{C}$ follows the classical minor and major symmetries of linear elasticity and is positive definite. In addition, monoclinic symmetry with respect to a plan of normal $\mathbf{e}_3$ is assumed:

$$C_{3\alpha\beta\gamma} = C_{\alpha 333} = 0, \tag{4}$$

where it is recalled that for Greek indices α, β, $\gamma \ldots = 1, 2$ (in-plane components), while for Latin indices $i, j, k \ldots = 1, 2, 3$ (in-plane and out-of-plane components).

Thus, the constitutive equation writes:

$$\begin{cases} \sigma_{\alpha\beta} = C_{\alpha\beta\gamma\delta}\varepsilon_{\delta\gamma} + C_{\alpha\beta 33}\varepsilon_{33}, \\ \sigma_{\alpha 3} = 2C_{\alpha 3\beta 3}\varepsilon_{3\beta}, \\ \sigma_{33} = C_{33\alpha\beta}\varepsilon_{\beta\alpha} + C_{3333}\sigma_{33}, \end{cases} \tag{5}$$

or conversely,

$$\begin{cases} \varepsilon_{\alpha\beta} = S_{\alpha\beta\gamma\delta}\sigma_{\delta\gamma} + S_{\alpha\beta 33}\sigma_{33}, \\ \varepsilon_{\alpha 3} = 2S_{\alpha 3\beta 3}\sigma_{3\beta}, \\ \varepsilon_{33} = S_{33\alpha\beta}\sigma_{\beta\alpha} + S_{3333}\sigma_{33}, \end{cases} \tag{6}$$

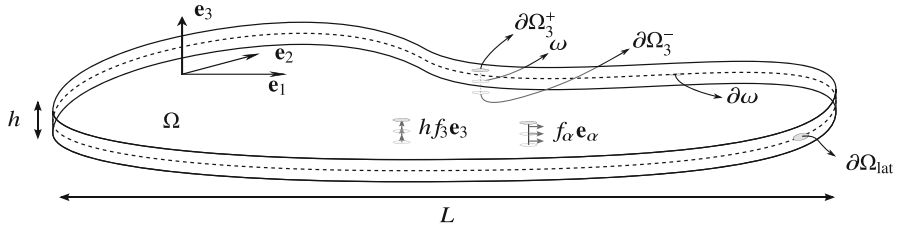

Fig. 1 The 3D problem for a homogeneous plate

where $\sigma = (\sigma_{ij})$ is the stress tensor, $\varepsilon = (\varepsilon_{ij})$ is the strain tensor, and $\mathbf{S}$ is the inverse of $\mathbf{C}$ and has the same properties (4) as the tensor $\mathbf{C}$. In the above equation and in the remainder of this chapter, Einstein's summation convention is used.

The full 3D linear elastic problem, $\mathcal{P}^{3D}$, is to find in Ω a displacement vector field $\mathbf{u}^{3D}$, a strain tensor field ε^{3D}, and a stress tensor field σ^{3D} such that the static conditions:

$$SC^{3D}: \begin{cases} \sigma_{\alpha j,j} + f_\alpha = 0 \ \text{ on } \ \Omega, & (7) \\ \sigma_{3j,j} + hf_3 = 0 \ \text{ on } \ \Omega, & (8) \\ \sigma_{i3} = 0 \ \text{ on } \ \partial\Omega_3^{\pm}, & (9) \end{cases}$$

for regular enough σ, the kinematic conditions:

$$KC^{3D}: \begin{cases} 2\varepsilon_{ij} = u_{i,j} + u_{j,i} \ \text{ on } \ \Omega, & (10) \\ u_i = u_i^d \ \text{ on } \ \partial\Omega_{\text{lat}}, & (11) \end{cases}$$

for regular enough $\mathbf{u}$, and the constitutive law (5) are satisfied.

Kinematic Derivation of Hencky's Plate Model

In this section, the kinematic derivation of a thick plate model from Hencky (1947) and Bollé (1947) is presented. It delivers the correct plate generalized variables. However, the constitutive equations are incorrect. It starts with the assumption of a 3D kinematically compatible displacement field. The plate model is derived from the application of the minimum potential energy principle.

Plate Kinematics

The following 3D kinematics is assumed for the plate:

$$\begin{aligned} u_\alpha^H(x_i) &= U_\alpha(x_\eta) + x_3\phi_\alpha(x_\eta) \quad \text{and} \\ u_3^H(x_i) &= U_3(x_\eta). \end{aligned} \tag{12}$$

Here, U_α is the membrane in-plane displacement, U_3 is the out-of-plane displacement, and ϕ_α is the material inclination of the fiber normal to the midplane of the plate. The corresponding in-plane rotation vector is $\boldsymbol{\theta}$, where $\theta_1 = -\phi_2$ and $\theta_2 = \phi_1$.

With proper scaling, it may be demonstrated that this kinematics is related to the asymptotic expansion of the 3D displacement solution of $\mathcal{P}^{3D}$ with respect to the thickness of the plate h. The membrane displacement and the out-of-plane displacement are the leading-order terms of the expansion. The material rotation is related to the next-order term of the expansion (Ciarlet and Destuynder 1979).

As a consequence of this choice of kinematics, it must be assumed in this section that the prescribed 3D displacement $\mathbf{u}^d$ on the boundary is as follows:

$$\begin{aligned} u_\alpha^d &= U_\alpha^d + x_3\phi_\alpha^d \ \text{and} \\ u_3^d &= U_3^d \ \text{on} \ \partial\Omega_{\text{lat}}, \end{aligned} \tag{13}$$

where U_α^d, ϕ_α^d, and U_3^d are prescribed generalized displacements on the boundary.

The corresponding plate boundary conditions are:

$$\begin{aligned} U_\alpha &= U_\alpha^d, \phi_\alpha = \phi_\alpha^d \ \text{and} \\ U_3 &= U_3^d \ \text{on} \ \partial\omega. \end{aligned} \tag{14}$$

The 3D strain derived from Hencky's kinematics writes as:

$$\begin{aligned} \varepsilon_{\alpha\beta}^H &= E_{\alpha\beta} + x_3\chi_{\alpha\beta}, \\ 2\varepsilon_{\alpha 3}^H &= \gamma_\alpha \ \text{and} \ \varepsilon_{33}^H = 0. \end{aligned} \tag{15}$$

Here the plate generalized strains are defined as follows:

$$\begin{aligned} 2E_{\alpha\beta} &= U_{\alpha,\beta} + U_{\beta,\alpha}, \\ 2\chi_{\alpha\beta} &= \phi_{\alpha,\beta} + \phi_{\beta,\alpha}, \\ \gamma_\alpha &= \phi_\alpha + U_{3,\alpha}. \end{aligned} \tag{16}$$

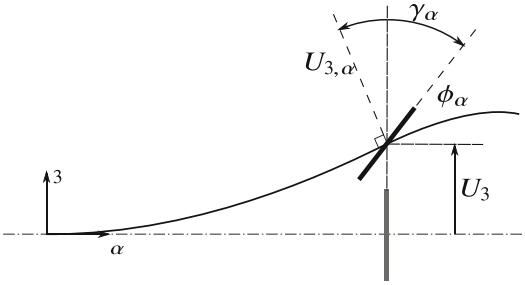

Fig. 2 Hencky's kinematics

The symmetric second-order tensor $E_{\alpha\beta}$ is the membrane strain. The symmetric second-order tensor $\chi_{\alpha\beta}$ is the material curvature. The in-plane vector γ_α is the generalized shear strain. It measures the difference between the normal to the deformed plate mid-surface $U_{3,\alpha}$ and the material inclination ϕ_α (Fig. 2).

Finally the plate kinematically compatible fields are gathered as:

$$KC^{\mathrm{P}} = \{(U_\alpha, \phi_\alpha, U_3) \text{ s.t. (16) and (14)}\}. \quad (17)$$

Formulation of Hencky's Plate Model

Minimum Potential Energy

The minimum potential energy principle states that the strain solution $\varepsilon^{3\mathrm{D}}$ of $\mathcal{P}^{3\mathrm{D}}$ is the one that minimizes the potential energy among all kinematically compatible strain fields:

$$\boldsymbol{\varepsilon}^{3\mathrm{D}} = \underset{\boldsymbol{\varepsilon}\in KC^{3\mathrm{D}}}{\arg\min} \left\{ \int_\Omega \frac{1}{2}\boldsymbol{\varepsilon}:\mathbf{C}:\boldsymbol{\varepsilon} - hf_3u_3 - f_\alpha u_\alpha \, \mathrm{d}\Omega \right\}, \quad (18)$$

The stationarity condition – also known as principle of virtual work – writes for the solution as:

$$\forall \hat{\mathbf{u}} \in KC^{3\mathrm{D},0}, \quad \int_\Omega \boldsymbol{\sigma}\left(\mathbf{u}^{3\mathrm{D}}\right) : \boldsymbol{\varepsilon}(\hat{\mathbf{u}}) - hf_3\hat{\mathbf{u}}_3 - f_\alpha\hat{u}_\alpha \, \mathrm{d}\Omega = 0, \quad (19)$$

where $KC^{3\mathrm{D},0}$ is the set of 3D kinematically compatible fields with vanishing prescribed displacement.

Plate Generalized Stresses

Specifying (19) for Hencky's kinematics yields $\forall \left(\hat{U}_\alpha, \hat{\phi}_\alpha, \hat{U}_3\right) \in KC^{\mathrm{P},0}$

$$\int_\omega \langle\sigma_{\alpha\beta}\rangle\hat{E}_{\alpha\beta} + \langle x_3\sigma_{\alpha\beta}\rangle\hat{\chi}_{\alpha\beta} + \langle\sigma_{\alpha3}\rangle\hat{\gamma}_a - h^2 f_3\hat{U}_3 - hf_\alpha\hat{U}_\alpha \mathrm{d}\omega = 0, \quad (20)$$

where integration through the thickness is denoted: $\langle f(x_3)\rangle = \int_{-\frac{h}{2}}^{\frac{h}{2}} f(x_3)\mathrm{d}x_3$

This suggests the following definition of plate generalized stresses:

$$N_{\alpha\beta} = \langle\sigma_{\alpha\beta}\rangle, \quad M_{\alpha\beta} = \langle x_3\sigma_{\alpha\beta}\rangle, \quad Q_\alpha = \langle\sigma_{\alpha3}\rangle. \quad (21)$$

$N_{\alpha\beta}$ is the membrane stress in duality with the membrane strain $E_{\alpha\beta}$, $M_{\alpha\beta}$ is the bending moment tensor in duality with the material curvature $\chi_{\alpha\beta}$, and Q_α is the shear force in duality with the generalized shear strain γ_α.

Plate Equilibrium

Integrating by parts Eq. (20) over the domain ω and taking into account plate boundary conditions yields:

$$\int_\omega -\left(N_{\alpha\beta,\beta} + hf_\alpha\right)\hat{U}_\alpha - \left(Q_{\alpha,\alpha} + h^2 f_3\right)\hat{U}_3 - \left(M_{\alpha\beta,\beta} - Q_a\right)\hat{\phi}_\alpha \mathrm{d}\omega = 0. \quad (22)$$

This leads to the following plate equilibrium equations:

$$SC^{\mathrm{P}} = \begin{cases} N_{\alpha\beta,\beta} + h f_\alpha = 0 \text{ on } \omega, & (23) \\ Q_\alpha - M_{\alpha\beta,\beta} = 0 \text{ on } \omega, & (24) \\ Q_{\alpha,\alpha} + h^2 f_3 = 0 \text{ on } \omega, & (25) \end{cases}$$

Equation (23) is the in-plane or membrane equilibrium equation. Equation (25) is the out-of-plane equilibrium equation. Equation (24) is the bending equilibrium equation.

These equilibrium equations are almost identical to those obtained from the direct derivation "Direct Derivation of Plate Theories". Here the drilling moment vanishes, and the membrane stress and bending moment tensors are symmetric because the plate is originally assumed as a 3D Cauchy medium.

Natural Scaling of Stresses in Plates

Because the upper and lower face of the plate are actually free of stress, there is a natural scaling of stresses when, for a fixed in-plane dimension L, the thickness h goes to 0.

Indeed, from the out-of-plane part of the 3D equilibrium equation (7), it appears that the normal stress scales like $\sigma_{33} \sim h^2 f_3$ and that the transverse shear stress scales like $\sigma_{\alpha 3} \sim L h f_3$. Furthermore, the bending equilibrium equation (24) ensures the following relation between the in-plane stress and the transverse shear stress: $\sigma_{\alpha 3} \sim \frac{h}{L}\sigma_{\alpha\beta}$. Hence $\sigma_{\alpha\beta} \sim L^2 f_3$ is of order h^0. This is also in agreement with the in-plane equilibrium which yields $\sigma_{\alpha\beta} \sim L f_\alpha$ also of order h^0 and motivates the initial scaling of the load.

Finally, the in-plane stresses are of order h^0, the transverse shear stresses are of order h^1, and the normal stress is of order h^2. A direct consequence of this observation is that at leading order in h, the plate is in a state of plane-*stress*.

Constitutive Equations

Once plate kinematically as well as statically compatible fields are derived, there remains to establish plate constitutive equations. This is usually performed, integrating through the thickness the strain energy related to the approximation of strains (15). However, whereas Hencky's kinematics is correct asymptotically when h goes to 0, the corresponding strain field is not the leading order of the expansion of the 3D solution. Indeed, $\varepsilon^{\mathrm{H}}_{33} = 0$ corresponds to a plane-*strain* state. It is in contradiction with the natural scaling of stresses in the plate and does not satisfy the free boundary conditions on the upper and lower face of the plate. A small out-of-plane displacement is required to release out-of-plane Poisson's effect (see Braess et al. 2010 among others).

In most textbooks, it is arbitrarily assumed at this stage that the correct constitutive equations are those derived in a previous work from Reissner following static considerations and detailed below.

Static Derivation of Reissner Plate Model

In this derivation, Hencky's kinematics relating plate generalized displacements and 3D displacement is dropped and another interpretation of the plate kinematics will be derived. Reissner's model is obtained from the derivation of a statically compatible 3D stress distribution and the application of the minimum complementary energy principle.

Derivation of a Statically Compatible Stress Field

While the out-of-plane components of the strain $\varepsilon^{\mathrm{H}}_{i3}$ are not correct asymptotically, the in-plane components of the strain $\varepsilon^{\mathrm{H}}_{\alpha\beta}$ are correct. They are taken as the starting point for deriving an approximation of the in-plane stress:

$$\varepsilon_{\alpha\beta}(x_1, x_2, x_3) = E_{\alpha\beta}(x_1, x_2) + x_3 \chi_{\alpha\beta}(x_1, x_2), \quad (26)$$

Using plane-*stress* constitutive equation, the in-plane stress writes as:

$$\sigma_{\alpha\beta} = C^{\sigma}_{\alpha\beta\gamma\delta}\left(E_{\delta\gamma} + x_3\chi_{\delta\gamma}\right), \tag{27}$$

where $C^{\sigma}_{\alpha\beta\gamma\delta} = C_{\alpha\beta\gamma\delta} - C_{\alpha\beta 33}C_{33\gamma\delta}/C_{3333} = (S_{\alpha\beta\gamma\delta})^{-1}$ is the plane-stress stiffness tensor.

Computing the membrane stress and the bending moment for this stress distribution leads to the following leading-order relations between generalized stress and strains:

$$\begin{aligned} N_{\alpha\beta} &= \langle\sigma_{\alpha\beta}\rangle = hC^{\sigma}_{\alpha\beta\gamma\delta}E_{\delta\gamma}, \text{ and} \\ M_{\alpha\beta} &= \langle x_3\sigma_{\alpha\beta}\rangle = \frac{h^3}{12}C^{\sigma}_{\alpha\beta\gamma\delta}\chi_{\delta\gamma}. \end{aligned} \tag{28}$$

These equations are leading-order plate constitutive equations. The exact ones will be derived in the following. From these relations and Eq. (27), it is found:

$$\sigma_{\alpha\beta} = \frac{1}{h}N_{\alpha\beta} + \frac{12x_3}{h^3}M_{\alpha\beta}. \tag{29}$$

Note that Reissner (1944) started directly from this in-plane stress distribution. However, (29) would not hold in case the plate is heterogeneous, whereas the in-plane strain distribution (26) remains true at leading order "Homogenization of Thin Periodic Plates".

From this in-plane stress distribution, a complete statically compatible stress distribution is now derived by successively integrating through the thickness of the 3D equilibrium equation (7).

The transverse shear distribution is derived by integrating with respect to x_3 the 3D equilibrium equations $\sigma_{\alpha\beta,\beta} + \sigma_{\alpha 3,3} + f_\alpha = 0$ and by taking into account the free boundary conditions (9) as well as plate equilibrium equations (23) and, (24). This yields:

$$\sigma_{\alpha 3} = \frac{3}{2h}\left(1 - \frac{4x_3^2}{h^2}\right)Q_\alpha. \tag{30}$$

Note that both upper and lower free boundary conditions are satisfied simultaneously.

Similarly, the normal traction σ_{33} is derived by integrating with respect to x_3 the 3D equilibrium equations $\sigma_{\alpha 3,\alpha} + \sigma_{33,3} + hf_3 = 0$ and by taking into account the free boundary conditions (9) as well as the out-of-plane equilibrium equation (25). This yields:

$$\sigma_{33} = f_3\frac{hx_3}{2}\left(1 - \frac{4x_3^2}{h^2}\right). \tag{31}$$

Again, upper and lower free boundary conditions are satisfied simultaneously.

Finally, the following Reissner stress distribution was derived:

$$\boldsymbol{\sigma}^{\mathrm{R}}(\mathbf{N}, \mathbf{M}, \mathbf{Q}; f_3) = \begin{cases} \sigma^{\mathrm{R}}_{\alpha\beta} = \frac{1}{h}N_{\alpha\beta} + \frac{12x_3}{h^3}M_{\alpha\beta}, \\ \sigma^{\mathrm{R}}_{\alpha 3} = \frac{3}{2h}\left(1 - \frac{4x_3^2}{h^2}\right)Q_\alpha, \\ \sigma^{\mathrm{R}}_{33} = f_3\frac{hx_3}{2}\left(1 - \frac{4x_3^2}{h^2}\right). \end{cases} \tag{32}$$

This stress distribution is in the set of 3D statically compatible stress fields $SC^{3\mathrm{D}}$ iff ($\mathbf{N}$, $\mathbf{M}$, $\mathbf{Q}$) satisfy the plate equilibrium equations (23), (24), and (25). It delivers a much better approximation of 3D stress fields than the one obtained from the 3D constitutive equation and the strains (15).

Formulation of the Reissner Plate Model

Minimum of the Complementary Energy

The minimum complementary energy principle states that the stress solution $\sigma^{3\mathrm{D}}$ of the 3D problem $\mathcal{P}^{3\mathrm{D}}$ is the one that minimizes the complementary energy among all statically compatible stress fields:

$$\boldsymbol{\sigma}^{3D} = \underset{\boldsymbol{\sigma}\in SC^{3D}}{\arg\min}\left\{\int_\Omega \frac{1}{2}\boldsymbol{\sigma} : \mathbf{S} : \boldsymbol{\sigma}\ \mathrm{d}\Omega - \int_{\partial\Omega_{\mathrm{lat}}} (\boldsymbol{\sigma}\cdot\mathbf{n})\cdot\mathbf{u}^d \mathrm{d}S\right\} \tag{33}$$

where $\mathbf{n}$ is the outer normal to $\partial\Omega_{\mathrm{lat}}$.

T

Inserting stress distributions of the form (32) following plate equilibrium equations (23), (24), and (25) in the principle of minimum complementary energy yields the following minimization problem:

$$(\mathbf{N}, \mathbf{M}, \mathbf{Q})^{\mathrm{R}} = \underset{(\mathbf{N},\mathbf{M},\mathbf{Q})\in SC^{\mathrm{P}}}{\arg\min} \left\{ P^{*\mathrm{R}}(\mathbf{N}, \mathbf{M}, \mathbf{Q}) \right\}, \tag{34}$$

where the plate complementary energy writes as:

$$P^{*\mathrm{R}}(\mathbf{N}, \mathbf{M}, \mathbf{Q}) = \int_{\omega} w^{*\mathrm{R}}(\mathbf{N}, \mathbf{M}, \mathbf{Q};\, f_3)\, \mathrm{d}S - \int_{\partial\omega} U_\alpha^d N_{\alpha\beta} n_\beta + \phi_\alpha^d M_{\alpha\beta} n_\beta + U_3^d Q_\alpha n_\alpha \, \mathrm{d}s. \tag{35}$$

The generalized stress energy density is:

$$w^{*\mathrm{R}} = \left\langle \frac{1}{2}\boldsymbol{\sigma}^{\mathrm{R}} : \mathbf{S} : \boldsymbol{\sigma}^{\mathrm{R}} \right\rangle, \tag{36}$$

and the generalized displacements on the boundary are defined as:

$$U_\alpha^d = \frac{1}{h}\left\langle u_\alpha^d \right\rangle,\ \phi_\alpha^d = \left\langle \frac{12x_3}{h^3} u_\alpha^d \right\rangle \quad \text{and} \quad U_3^d = \left\langle \frac{3}{2h}\left(1 - \frac{4x_3^2}{h^2}\right) u_3^d \right\rangle \tag{37}$$

This minimization problem fully determines Reissner's plate theory, and the corresponding details may be found in "Direct Derivation of Plate Theories". The plate kinematically compatible and statically compatible fields found from this formulation are the same as those obtained from Hencky's derivation ((23), (24), (25), and (17)). However, the constitutive equations are different and the plate kinematics may be interpreted differently.

Plate Kinematics

The definition of the generalized displacement on the boundary (37) encourages the following interpretation of the plate kinematics as projections of the 3D displacement:

$$U_\alpha \approx \frac{1}{h}\langle u_\alpha \rangle,\ \phi_\alpha \approx \left\langle \frac{12x_3}{h^3} u_\alpha \right\rangle \text{ and } U_3 \approx \left\langle \frac{3}{2h}\left(1 - \frac{4x_3^2}{h^2}\right) u_3 \right\rangle. \tag{38}$$

The membrane displacement U_α is the average through the thickness of the plate of the in-plane displacement. The material inclination ϕ_α is the odd part of the in-plane displacement. Finally, the plate deflection U_3 appears as a weighted average of the out-of-plane displacement.

Remarkably, Hencky's kinematics (12) is in agreement with the projections (38).

Constitutive Equations

From the plate stress energy density (36), the following constitutive equations are derived:

$$E_{\alpha\beta} = \frac{1}{h} S_{\alpha\beta\gamma\delta} N_{\delta\gamma},\quad \chi_{\alpha\beta} = \frac{12}{h^3} S_{\alpha\beta\gamma\delta} M_{\delta\gamma} + p_{\alpha\beta} h f_3,\quad \gamma_\alpha = f_{\alpha\beta} Q_\beta, \tag{39}$$

where the shear force compliance $\mathbf{f}$ is:

$$f_{\alpha\beta} = \frac{6}{5h} 4 S_{\alpha 3 \beta 3}, \tag{40}$$

and $\mathbf{p}$ is a prescribed curvature related to the applied load:

$$p_{\alpha\beta} = -\frac{S_{\alpha\beta 33}}{5}. \tag{41}$$

It must be noted that $\mathbf{p}$ depends on the way the load is applied on the 3D body. Indeed, loading the plate on the upper and lower faces leads to a different value of $\mathbf{p}$.

These equations may be inverted and lead to the following constitutive equations:

$$\mathbf{N}=\mathbf{A}:\mathbf{E}, \quad \mathbf{M}=\mathbf{D}:(\chi-\mathbf{p}h\,f_3) \quad \text{and} \quad \mathbf{Q}=\mathbf{F}\cdot\boldsymbol{\gamma}, \tag{42}$$

where:

$$A_{\alpha\beta\gamma\delta}=hC^{\sigma}_{\alpha\beta\gamma\delta}, \quad D_{\alpha\beta\gamma\delta}=\frac{h^3}{12}C^{\sigma}_{\alpha\beta\gamma\delta} \quad \text{and} \quad F_{\alpha\beta}=\frac{5h}{6}C_{\alpha3\beta3}. \tag{43}$$

Note that the membrane problem for U_α generalized displacements is fully uncoupled from the bending problem for U_3 and ϕ_α generalized displacements. This is because of the monoclinic symmetry assumed in (4) and the mirror symmetry with respect to the midplane of the plate. For heterogeneous plates, this uncoupling is not always true "Anisotropic and Refined Plate Theories".

Finally, the so-called "shear correction factor" 5/6 taking into account the nonuniform distribution of the out-of-plane shear stress was obtained. Note that, when dealing with heterogeneous plates, this definition is meaningless since several shear stiffness moduli may be involved in the shear force constitutive equation.

Static Boundary Conditions

It is also possible to enforce static boundary conditions on the lateral boundary of the plate. However, whereas kinematic boundary conditions are satisfied weakly on the boundary, the static derivation from Reissner requires that static boundary conditions are satisfied strongly on the boundary. Hence, considering the form of the stress approximation (32), only stress distributions through the thickness of the following form:

$$T^d_\alpha=\frac{1}{h}N^d_\alpha+\frac{12x_3}{h^3}M^d_\alpha \quad \text{and} \quad T^d_3=\frac{3}{2h}\left(1-\frac{4x_3^2}{h^2}\right)Q^d, \tag{44}$$

may be enforced on the lateral boundary $\partial\omega^\sigma\times\mathcal{T}$. Here, $\partial\omega^\sigma$ denotes the portion of the boundary where static conditions may apply. They correspond to the following plate static boundary conditions:

$$N_{\alpha\beta}n_\beta=N^d_\alpha, M_{\alpha\beta}n_\beta=M^d_\alpha \quad \text{and} \quad Q_\alpha n_\alpha=Q^d \text{ on } \partial\omega^\sigma, \tag{45}$$

where N^d_α is an in-plane traction, M^d_α is an in-plane couple, and Q^d is a shear force enforced on the boundary. A direct consequence is that traction free boundary conditions are strongly satisfied with Reissner plate model.

Conclusion

The approaches from Hencky and Reissner for deriving a thick plate theory are often confused in the literature. Whereas they are closely related, they actually yield different plate models which suffer from different limitations.

The kinematic derivation from Hencky is probably the most straightforward but leads to incorrect estimates of the local stresses as well as the plate's constitutive equations. The constitutive equations derived by Reissner are commonly used to correct Hencky's model.

The extension of this model to the case of laminated plates was early performed (Yang et al. 1966). This approach is referred to as first-order shear deformation theory and suffers even more critically from the inconsistencies encountered for homogeneous plates. The advantage of this approach is that its kinematics may be extended to large displacements and rotations.

A natural strategy for solving these inconsistencies is to enrich the plate kinematics so that it can accommodate free boundaries at the upper and lower face of the plate. This is the main concept behind hierarchical models

(Babuška and Li 1992; Paumier and Raoult 1997; Alessandrini et al. 1999) where the 3D displacement is assumed as a polynomial of the out-of-plane coordinate and each monomial is multiplied by an in-plane function being a generalized plate displacement. However, this requires more plate kinematic degrees of freedom than those of Reissner-Hencky models.

The static derivation from Reissner leads to a very accurate model in the framework of static linear elasticity and it was observed empirically that it converges faster than Kirchhoff-Love model in some specific configurations (Lebée and Sab 2017b). However, its rigorous extension to laminated plates requires the introduction of numerous additional plate degrees of freedom and is impractical for engineering applications (Lebée and Sab 2017a).

References

Alessandrini SM, Arnold DN, Falk RS, Madureira AL (1999) Derivation and justification of plate models by variational methods. In: Fortin M (ed) Plates and shells, vol 21. American Mathematical Society, Providence, pp 1–21

Babuška I, Li L (1992) The-p-version of the finite-element method in the plate modelling problem. Commun Appl Numer Methods 8(1):17–26

Bollé L (1947) Contribution au problème linéaire de flexion d'une plaque élastique. Bulletin technique de la Suisse romande 73(21):281–285

Braess D, Sauter S, Schwab C (2010) On the justification of plate models. J Elast 103(1):53–71

Ciarlet PG (1997) Mathematical elasticity – volume II: theory of plates. Elsevier Science Bv, Amsterdam

Ciarlet PG, Destuynder P (1979) Justification Of the 2-dimensional linear plate model. Journal de Mecanique 18(2):315–344

Hencky H (1947) Über die Berücksichtigung der Schubverzerrung in ebenen Platten. Ingenieur- Archiv 16(1):72–76

Kirchhoff G (1850) Über das Gleichgewicht und die Bewegung einer elastischen Scheibe. Journal für die reine und angewandte Mathematik (Crelles Journal) 1850(40):51–88

Lebée A, Sab K (2017a) On the generalization of Reissner plate theory to laminated plates, part I: theory. J Elast 126(1):39–66

Lebée A, Sab K (2017b) On the generalization of Reissner plate theory to laminated plates, part II: comparison with the bending-gradient theory. J Elast 126(1):67–94

Love AEH (1888) The small free vibrations and deformation of a thin elastic shell. Philos Trans R Soc Lond A 179:491–546

Mindlin R (1951) Influence of rotatory inertia and shear on flexural motions of isotropic, elastic plates. J Appl Mech 18:31–38

Paumier JC, Raoult A (1997) Asymptotic consistency of the polynomial approximation in the linearized plate theory. Application to the Reissner-Mindlin model. Elast Viscoelast Optim Control 2:203–214

Reissner E (1944) On the theory of bending of elastic plates. J Math Phys 23:184–191

Yang P, Norris CH, Stavsky Y (1966) Elastic wave propagation in heterogeneous plates. Int J Solids Struct 2(4):665–684

Time to Creep Rupture

▸ Creep in Structures

Time-Dependent Behavior of Solids

▸ Viscoelasticity

Time-Dependent Permanent Strain

▸ Creep in Modern Materials

Time-Stepping Algorithms in Nonlinear Resultant Shell Dynamics

Jacek Chróścielewski and Wojciech Witkowski
Faculty of Civil and Environmental Engineering, Gdańsk University of Technology, Gdańsk, Poland

Synonyms

Dynamics in low natural frequency range; Energy conserving algorithms in shell dynamics; Nonlinear dynamics of shells

Definition

Time-stepping algorithms serve as the tool of temporal approximation of evolution equations of dynamical systems. The algorithms are divided into one-step and multistep methods depending on the number of the required preceding time steps. If the sought variable appears as explicit or implicit, the scheme is classified as explicit or implicit, respectively.

Introduction

While formulating the numerical schemes the following three criteria must be taken into account: consistency (relation between the differential equation and its discrete formulation); stability (relation between the computed solution and the exact solution of the discretized equations); convergence (connects the computed solution to the exact solution of the differential equation). In nonlinear dynamics of structures, where the interest is focused on the range of low values of natural frequencies in long time span, often one-step implicit algorithms are used. Such schemes in the nonlinear shell dynamics are additionally required to satisfy the conservation of energy (ECA). In 6-parameter nonlinear shell theory with the drilling rotation, the rotation tensor field $\boldsymbol{Q} \in SO(3)$ requires special nonclassical approach to singular-free approximation procedure both in space and time, since $SO(3)$ does not admit the structure of the linear space. Due to its special properties, the Cayley parameterization of the rotation group plays an important role.

The problem of conservation of energy is an important field of interest in the numerical integration of equations of motion in nonlinear computational mechanics still pursued in the literature, e.g., Campello et al. (2011), Betsch and Janz (2016), and Gebhardt and Rolfes (2017). Graham and Jelenić (2003) classify the conservation of energy and momenta as the features that make the given time integration method successful. This is due to the fact that classical methods of temporal approximation, e.g., Newmark, HHT, or θ-Wilson (Armero 2008), may lead to the unstable behavior when applied directly in nonlinear problems. A lot of research has been devoted to this topic, e.g., Simo and Tarnow (1994), Simo et al. (1995), Romero and Armero (2002), Ibrahimbegović et al. (2000), Chróścielewski and Witkowski (2010). At least three methods may be efficient (Zolghadr Jahromi and Izzuddin 2013) in attempting to preserve the conservation: numerical dissipation, enforced energy conservation, and algorithmic energy control, cf. also e.g. Armero and Romero (2003), Kuhl and Ramm (1996), or Kuhl and Crisfield (1999). As formulated in the latter paper, the sufficient condition for stability of the time integration method in the nonlinear regime is the conservation (or decay) of the total energy within a time step. That is, kinetic K and potential U components of the energy related to work done by external forces G_{ext} at the beginning and the end of the time interval should satisfy the equation

$$K_{n+1} - K_n + U_{n+1} - U_n \leq \Delta G_{ext}. \quad (1)$$

In case of a Hamiltonian system

$$K_{n+1} - K_n + \ U_{n+1} - \ U_n = 0. \quad (2)$$

In the present study the formulation of time integration algorithm is discussed within the framework of 6-parameter nonlinear shell theory with the drilling rotation. The kinematics of the shell theory has features of the Cosserat continuum. Some reference works that may be useful for in-depth formulation are Chróścielewski et al. (1997, 2004b), Witkowski (2009), and Pietraszkiewicz (2017). The exposition of the problem is divided into three parts: the statement of the initial boundary value problem, then extended Newmark time-stepping algorithm is formulated, and finally energy-conserving algorithm is presented. Readers interested in dynamics of the Cosserat rods

Fig. 1 Irregular shell

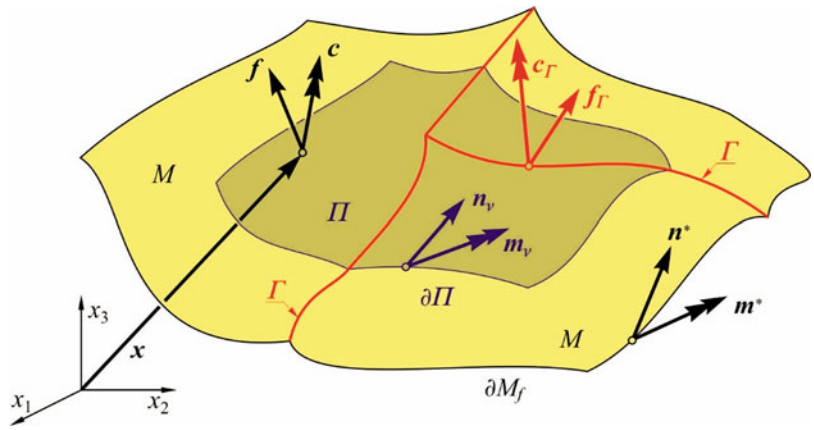

may consult for, e.g., Simo et al. (1995), Ibrahimbegović et al. (2000), or Armero and Romero (2003).

Initial-Boundary Value Problem

Following Chróścielewski et al. (2000) or Lubowiecka and Chróścielewski (2002), an irregular shell as shown in Fig. 1 is considered. The structure is acted upon by the external resultant force and couple vector fields $\boldsymbol{f}(\boldsymbol{x},t)$ and $\boldsymbol{c}(\boldsymbol{x},t)$ on $\boldsymbol{x} \in M\backslash\Gamma$, $\boldsymbol{n}^*(\boldsymbol{x},t)$ and $\boldsymbol{m}^*(\boldsymbol{x},t)$ along ∂M_f, $\boldsymbol{f}_\Gamma(\boldsymbol{x},t)$ and $\boldsymbol{c}_\Gamma(\boldsymbol{x},t)$ along the singular curve $\Gamma \subset M$, and the initial values of translation and rotation fields respectively denoted as $\boldsymbol{u}_0(\boldsymbol{x})$, $\boldsymbol{Q}_0(\boldsymbol{x})$ along with their time derivatives $\dot{\boldsymbol{u}}_0(\boldsymbol{x})$, $\dot{\boldsymbol{Q}}_0(\boldsymbol{x})$ at time $t = 0$.

Define: the translation vector $\boldsymbol{u}(\boldsymbol{x},t) = \boldsymbol{y}(\boldsymbol{x},t) - \boldsymbol{x}$, the linear velocity vector $\boldsymbol{v}(\boldsymbol{x},t) = \dot{\boldsymbol{y}}(\boldsymbol{x},t) = \dot{\boldsymbol{u}}(\boldsymbol{x},t)$, $\boldsymbol{p}(\boldsymbol{x},t)$ and $\boldsymbol{m}(\boldsymbol{x},t)$ as the translational and rotational momenta vectors, $\boldsymbol{n}^\beta(\boldsymbol{x},t)$ and $\boldsymbol{m}^\beta(\boldsymbol{x},t)$ as the internal stress and couple resultant vectors, respectively. Then the IBVP may be stated as follows: find a curve $\mathbf{u}(\boldsymbol{x},t) = (\boldsymbol{u}(\boldsymbol{x},t), \boldsymbol{Q}(\boldsymbol{x},t))$ on the configuration space $C(M, E^3 \times SO(3))$ such that for any continuous, kinematically admissible virtual vector field $\mathbf{w}(\boldsymbol{x}) \equiv (\boldsymbol{v}(\boldsymbol{x}), \boldsymbol{w}(\boldsymbol{x})) \in V_A(M, E^3 \times E^3)$ the following variational statement is satisfied:

$$
\begin{aligned}
G[\mathbf{u},t;\ \mathbf{w}] = &\iint_{M\backslash\Gamma} (\dot{\boldsymbol{p}}\cdot\boldsymbol{v} + (\dot{\boldsymbol{\pi}} + \boldsymbol{v}\times\boldsymbol{p})\cdot\boldsymbol{w})\ \mathrm{d}a + \iint_{M\backslash\Gamma} \left(\boldsymbol{n}^\beta\cdot\left(\boldsymbol{v}_{,\beta} + \boldsymbol{y}_{,\beta}\times\boldsymbol{w}\right) + \boldsymbol{m}^\beta\cdot\boldsymbol{w}_{,\beta}\right)\ \mathrm{d}a \\
&- \iint_{M\backslash\Gamma} (\boldsymbol{f}\cdot\boldsymbol{v} + \boldsymbol{c}\cdot\boldsymbol{w})\ \mathrm{d}a + \int_{\partial M_f} (\boldsymbol{n}^*\cdot\boldsymbol{v} + \boldsymbol{m}^*\cdot\boldsymbol{w})\ \mathrm{d}s + \int_\Gamma \left(\boldsymbol{f}_\Gamma\cdot\boldsymbol{v}_\Gamma + \boldsymbol{c}_\Gamma\cdot\boldsymbol{w}_\Gamma\right)\ \mathrm{d}s = 0.
\end{aligned}
\tag{3}
$$

Here $\boldsymbol{v}_\Gamma = \boldsymbol{v}|_\Gamma$, $\boldsymbol{w}_\Gamma = \boldsymbol{w}|_\Gamma$ denote values of $\mathbf{w}(\boldsymbol{x})$ along $\Gamma \subset M$. In Eq. 3 it is implicitly assumed that the kinematic boundary conditions $\boldsymbol{u}(\boldsymbol{x},t) = \boldsymbol{u}^*(\boldsymbol{x},t)$ and $\boldsymbol{Q}(\boldsymbol{x},t) = \boldsymbol{Q}^*(\boldsymbol{x},t)$ are satisfied on the complementary part $\partial M_d = \partial M\backslash\partial M_f$, and the virtual vector fields are kinematically admissible if $\boldsymbol{v}(\boldsymbol{x}) = \boldsymbol{0}$ and $\boldsymbol{w}(\boldsymbol{x}) = \boldsymbol{0}$ on ∂M_d. The expressions for the momenta $\boldsymbol{p}$ and $\boldsymbol{\pi}$ were suggested by Simmonds (1984):

$$
\begin{aligned}
\boldsymbol{p} &= m_0\boldsymbol{v} = \rho_0 h_0 \boldsymbol{v}, \\
\boldsymbol{\pi} &= I_0\boldsymbol{\omega} = \frac{1}{12}\rho_0\, h_0^3\, \boldsymbol{\omega}, \\
\boldsymbol{\omega}\times\mathbf{1} &= \dot{\boldsymbol{Q}}\ \boldsymbol{Q}^{\mathrm{T}},
\end{aligned}
\tag{4}
$$

where $\rho_0(\boldsymbol{x})$ is the initial mass density, $h_0(\boldsymbol{x})$ is the initial shell thickness, and $\boldsymbol{\omega}(\boldsymbol{x},t)$ is the network spin vector in the spatial representation.

The components of energy in Eq. 1 read

$$
\begin{aligned}
U &= \iint_{M\setminus\Gamma} W \, \mathrm{d}a, \\
K &= \frac{1}{2}\iint_{M\setminus\Gamma} (\boldsymbol{p}\cdot\boldsymbol{v} + \boldsymbol{\pi}\cdot\boldsymbol{\omega}) \, \mathrm{d}a = \frac{1}{2}\iint_{M\setminus\Gamma} (m_0\boldsymbol{v}\cdot\boldsymbol{v} + I_0\boldsymbol{\omega}\cdot\boldsymbol{\omega}) \, \mathrm{d}a, \\
\Delta G_{ext} &= \int_{t_n}^{t_{n+1}} \left\{ \iint_{M\setminus\Gamma} (\boldsymbol{f}\cdot\boldsymbol{v} + \boldsymbol{c}\cdot\boldsymbol{\omega})\mathrm{d}a + \int_{\partial M_f} (\boldsymbol{n}^*\cdot\boldsymbol{v} + \boldsymbol{m}^*\cdot\boldsymbol{\omega})\mathrm{d}s + \int_{\Gamma} (\boldsymbol{f}_\Gamma\cdot\boldsymbol{v}_\Gamma + \boldsymbol{c}_\Gamma\cdot\boldsymbol{\omega}_\Gamma) \, \mathrm{d}s \right\} \mathrm{d}t,
\end{aligned}
\tag{5}
$$

where $W(\boldsymbol{\varepsilon}_\beta, \boldsymbol{\kappa}_\beta;\ \boldsymbol{x})$ is the 2D strain energy function defined by expressions for stretching strains and bending strains given respectively as

$$
\boldsymbol{\varepsilon}_\beta = \boldsymbol{y}_{,\beta} - \ \boldsymbol{Q}\,\boldsymbol{x}_{,\beta},\ \boldsymbol{K}_\beta = \boldsymbol{\kappa}_\beta \times \mathbf{1} = \boldsymbol{Q}_{,\beta}\,\boldsymbol{Q}^{\mathrm{T}}. \tag{6}
$$

For the purposes of this work the constitutive relations of the shell material are given by

$$
\boldsymbol{n}^\beta = \frac{\partial W}{\partial \boldsymbol{\varepsilon}_\beta},\ \boldsymbol{m}^\beta = \frac{\partial W}{\partial \boldsymbol{\kappa}_\beta}. \tag{7}
$$

The temporal approximation of Eq. 3 is based on standard argumentation that the time interval $[0, T]$ is partitioned by a finite number of time instants $0 \equiv t_0 < t_1 < \ldots < t_n < t_{n+1} < \ldots < t_N \equiv T$ such that $[0, T] = \cup_{n=0}^{N-1} [t_n, t_{n+1}]$ and $[t_{n-1}, t_n] \cap [t_n, t_{n+1}] = t_n$ with $\Delta t = t_{n+1} - t_n$ a typical time step. Then, the weak form of the IBVP at the time instant t_{n+1} reads

$$
\begin{gathered}
G_{n+1} \equiv G\,[\mathbf{u}_{n+1}, t_{n+1};\ \ \mathbf{w}_{n+1}] = 0, \\
\forall \mathbf{w}_{n+1} \in T_{\mathbf{u}_{n+1}} C \sim V_A.
\end{gathered}
\tag{8}
$$

With iterative solution of the nonlinear problem with the time-stepping algorithm, the solution of the nonlinear problem (8) is constructed by the incremental-iterative procedure based on the Newton-Kantorovich method (Krasnosel'skii et al. 1972) applied in the configuration space $C(M, E^3 \times SO(3))$. Let an i–th approximation $\mathbf{u}_{n+1}^{(i)}$ to the solution $\mathbf{u}_{n+1} \equiv \mathbf{u}(t_{n+1})$ has been found. In order to calculate the correction $\Delta\mathbf{u}_{n+1}^{(i+1)}$, which yields the successive approximation $\mathbf{u}_{n+1}^{(i+1)}$ to the unknown solution $\mathbf{u}_{n+1}$, Eq. 8 is linearized at the approximation $\mathbf{u}_{n+1}^{(i)}$:

$$
G\left[\mathbf{u}_{n+1}^{(i)}, t_{n+1};\ \ \mathbf{w}_{n+1}^{(i)}\right] + \delta G\left[\mathbf{u}_{n+1}^{(i)}, t_{n+1};\ \ \mathbf{w}_{n+1}^{(i)}, \Delta\mathbf{u}_{n+1}^{(i+1)}\right] = 0,\ \forall \mathbf{w}_{n+1}^{(i)} \in T_{\mathbf{u}_{n+1}^{(i)}} C \sim V_A. \tag{9}
$$

The second term in Eq. 9 denotes a directional derivative of the functional Eq. 8 taken at the point $\mathbf{u}_{n+1}^{(i)} \in C$ in the direction $\Delta\mathbf{u}_{n+1}^{(i+1)} \in T_{\mathbf{u}_{n+1}^{(i)}} C \sim V_A$. This term yields the so-called tangent operator of the nonlinear problem, calculated at the approximation $\mathbf{u}_{n+1}^{(i)}$. The first term in Eq. 9 represents unbalanced forces at the approximation point $\mathbf{u}_{n+1}^{(i)}$.

In the remainder of the paper the variables in spatial representation such as vectors, e.g. ($\boldsymbol{\omega}$, $\boldsymbol{w}$, $\boldsymbol{a}$) and tenors, e.g. ($\boldsymbol{\Omega}$, $\boldsymbol{W}$, $\boldsymbol{A}$) are denoted by boldface italic characters, their counterparts in the material representation are written with boldface font, e.g. ($\boldsymbol{\omega}$, $\mathbf{w}$, $\mathbf{a}$, $\boldsymbol{\Omega}$,$\mathbf{W}$, $\mathbf{A}$).

Extended Newmark Algorithm

The implicit one-step Newmark (1959) formula with the Newton iterations, in which the actual state at time t_{n+1} is calculated from the former state at time t_n alone, is one of the most popular time integration methods. However,

due to the fact that here the configuration space $C(M, E^3 \times SO(3))$ does not have the structure of the linear space, the original approach must be extended to accommodate the rotation group $SO(3)$. In the context of the present shell theory, this issue has been discussed in Chróścielewski et al. (2000) or Lubowiecka and Chróścielewski (2002).

The physical meaning of external loads is well defined only in the spatial representation. Consequently, the generalized momentum balance is formulated in the spatial representation as well. The linearized dynamic equations are written relative to an instantaneous configuration $\mathbf{u}_{n+1}^{(i)}$, that is at the i–th approximation to $\mathbf{u}_{n+1}$, and not relative to $\mathbf{u}_n$. This eliminates the need of applying the transformation relation $\boldsymbol{Y}_n\left(\boldsymbol{Q}_{n+1}^{(i)}\right) : T_{\boldsymbol{Q}_{n+1}^{(i)}} SO(3) \rightarrow T_{\boldsymbol{Q}_n} SO(3)$, compare Cardona and Geradin (1988) or Simo and Vu-Quoc (1988), since in the present case $\boldsymbol{Y}|_{n+1}^{(i)}\left(\boldsymbol{Q}_{n+1}^{(i)}\right) \equiv \mathbf{1}$. Furthermore, as argued by Simo and Wong (1991), the angular velocities and accelerations from different time instants can directly be added only in the material representation. As a result, temporal approximations of these fields are carried out in the material representation. Then the obtained results are transformed into the spatial representation and substituted into the linearized dynamic equations (9).

In the iterative solution of the linearized problem equations (9), it is assumed that the i–th correction of the incremental generalized displacements $\Delta\mathbf{u}_{n+1}^{(i+1)} = \left(\Delta\boldsymbol{u}_{n+1}^{(i+1)}, \Delta\boldsymbol{w}_{n+1}^{(i+1)}\right)$ is known. Here $\Delta\boldsymbol{w}_{n+1}^{(i+1)} \in T_{\boldsymbol{Q}_{n+1}^{(i)}} SO(3)$ ($\Delta\boldsymbol{w} \times \boldsymbol{1} = \Delta\boldsymbol{W} = \Delta\boldsymbol{Q}\boldsymbol{Q}^{\mathrm{T}}$) denotes the i–th correction of the incremental rotation vector in the spatial representation. The part of algorithm associated with the translatory motion $(\boldsymbol{u}, \dot{\boldsymbol{u}}, \ddot{\boldsymbol{u}})$ is standard, see for instance Hughes (2000). The part of algorithm associated with the rotational motion $(\boldsymbol{Q}, \boldsymbol{\omega}, \mathbf{a})$ may be summarized as follows:

1. Update the rotation tensor in the spatial representation

$$\begin{aligned} \boldsymbol{Q}_{n+1}^{(i+1)} &= \exp\left(\Delta\boldsymbol{W}_{n+1}^{(i+1)}\right) \boldsymbol{Q}_{n+1}^{(i)}, \\ \Delta\boldsymbol{W}_{n+1}^{(i+1)} &= \Delta\boldsymbol{w}_{n+1}^{(i+1)} \times \boldsymbol{1}, \\ i &= 0, 1, 2, 3, \ldots, \end{aligned} \tag{10}$$

where $\boldsymbol{Q}_{n+1}^{(0)} \equiv \boldsymbol{Q}_n$, $\Delta\boldsymbol{w}_{n+1}^{(1)} \equiv \Delta\boldsymbol{w}_n^{(1)}$ denote the starting values in iterative correction.

2. Calculate the complete (accumulated) increment of the rotation vector $\Delta\mathbf{w}_n^{(i+1)}$ in the material representation

$$\begin{aligned} \exp\left(\Delta\mathbf{W}_n^{(i+1)}\right) &= \boldsymbol{Q}_n^{\mathrm{T}} \boldsymbol{Q}_{n+1}^{(i+1)}, \\ \Delta\mathbf{W}_n^{(i+1)} &= \Delta\mathbf{w}_n^{(i+1)} \times \mathbf{1}. \end{aligned} \tag{11}$$

3. Calculate angular accelerations and velocities in the material representation according to the extended Newmark scheme

$$\begin{aligned} \mathbf{a}_{n+1}^{(i+1)} &= \frac{1}{\beta(\Delta t)^2}\left[\Delta\mathbf{w}_n^{(i+1)} - \Delta t\ \boldsymbol{\omega}_n \right. \\ &\quad \left. -(\Delta t)^2\left(\frac{1}{2} - \beta\right)\mathbf{a}_n\right], \\ \boldsymbol{\omega}_{n+1}^{(i+1)} &= \frac{\gamma}{\beta\Delta t}\Delta\mathbf{w}_n^{(i+1)} + \left(1 - \frac{\gamma}{\beta}\right)\boldsymbol{\omega}_n \\ &\quad + \Delta t\left(1 - \frac{\gamma}{2\beta}\right)\mathbf{a}_n. \end{aligned} \tag{12}$$

4. Transform the vectors (12) to the spatial representation

$$\begin{aligned} \boldsymbol{\omega}_{n+1}^{(i+1)} &= \boldsymbol{Q}_{n+1}^{(i+1)}\boldsymbol{\omega}_{n+1}^{(i+1)}, \\ \boldsymbol{a}_{n+1}^{(i+1)} &= \boldsymbol{Q}_{n+1}^{(i+1)}\mathbf{a}_{n+1}^{(i+1)}. \end{aligned} \tag{13}$$

5. Formulate the problem linearized equations at the new iteration step $i \rightarrow i+1$ and calculate the new correction of $\Delta\boldsymbol{w}$.

The angular accelerations and velocities are calculated from:

in the material representation

$$\begin{aligned} \boldsymbol{\Omega} &= \boldsymbol{Q}^{\mathrm{T}}\dot{\boldsymbol{Q}} = \boldsymbol{\omega}\times\mathbf{1}, \\ \mathbf{A} &= \dot{\boldsymbol{\Omega}} = \boldsymbol{Q}^{\mathrm{T}}\ddot{\boldsymbol{Q}} - \boldsymbol{\Omega}\boldsymbol{\Omega} = \mathbf{a}\times\mathbf{1} \end{aligned}, \tag{14}$$

or in the spatial representation

$$\begin{aligned} \boldsymbol{\Omega} &= \dot{\boldsymbol{Q}}\boldsymbol{Q}^{\mathrm{T}} = \boldsymbol{\omega}\times\boldsymbol{1}, \\ \boldsymbol{A} &= \dot{\boldsymbol{\Omega}} = \ddot{\boldsymbol{Q}}\boldsymbol{Q}^{\mathrm{T}} - \boldsymbol{\Omega}\boldsymbol{\Omega} = \boldsymbol{a}\times\boldsymbol{1}. \end{aligned} \tag{15}$$

The parameters $0 \le \beta \le \frac{1}{2}$ and $0 \le \gamma \le 1$ in Eq. 12 are free parameters of the Newmark algorithm. Different values of β and γ yield variety of time integration schemes known in E^3 and to various extensions into $E^3 \times SO(3)$.

Energy Conserving Algorithm (ECA)

For the discussed shell theory the energy conserving algorithm has been presented in Chróścielewski et al. (2004a, 2005) and Lubowiecka and Chróścielewski (2005). While the previous algorithm was independent of parameterization of the rotation group, the ECA uses the Cayley parameterization of $\Delta\mathbf{Q} = \mathrm{cay}(\Delta\mathbf{C}) \equiv \mathrm{cay}(\Delta\mathbf{c})$, $\Delta\mathbf{C} = \Delta\mathbf{c}\times\mathbf{1}$ which in the material representation takes the form

$$\begin{aligned} \Delta\mathbf{Q} &= \mathrm{cay}\,(\Delta\mathbf{c}) \\ &= \mathbf{1} + \frac{1}{1+\frac{1}{4}\Delta\mathbf{c}\cdot\Delta\mathbf{c}}\left(\Delta\mathbf{C} + \frac{1}{2}\Delta\mathbf{C}^2\right) \\ &= \left(\mathbf{1} - \frac{1}{2}\Delta\mathbf{C}\right)^{-1}\left(\mathbf{1} + \frac{1}{2}\Delta\mathbf{C}\right) \\ &= \left(\mathbf{1} + \frac{1}{2}\Delta\mathbf{C}\right)\left(\mathbf{1} - \frac{1}{2}\Delta\mathbf{C}\right)^{-1}. \end{aligned} \tag{16}$$

The inversion of Eq. 16 reads

$$\begin{aligned} \Delta\mathbf{C} &= \frac{2}{1+\mathrm{tr}\,\Delta\mathbf{Q}}\left(-\left(\mathrm{tr}\,\Delta\mathbf{Q}\right)\mathbf{1}\right. \\ &\quad \left. + \left(1+\mathrm{tr}\,\Delta\mathbf{Q}\right)\Delta\mathbf{Q} - \Delta\mathbf{Q}^2\right) \\ &= 2\left(\mathbf{1}-\Delta\mathbf{Q}\right)\left(\mathbf{1}+\Delta\mathbf{Q}\right)^{-1} \\ &= 2(\mathbf{1}+\Delta\mathbf{Q})^{-1}\left(\mathbf{1}-\Delta\mathbf{Q}\right). \end{aligned} \tag{17}$$

The Cayley parameterization possesses unique features, not present in other parameterizations, important for ECA (Fig. 2). Namely, for any orthogonal tensor $\boldsymbol{Q} \in SO(3)$ the Cayley transform $\mathrm{cay} : so(3) \to SO(3)$ or equivalently $\mathrm{cay} : E^3 \to SO(3)$, which follows from the isomorphism $so(3) \sim E^3$, the following relations are true:

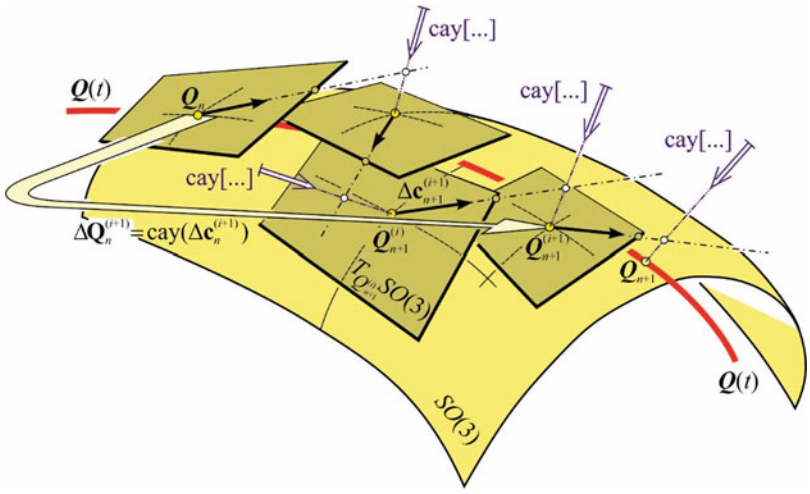

Fig. 2 Concept of overall increment of rotation in the iterative procedure

$$\begin{aligned} \boldsymbol{Q}\ \mathrm{cay}\,(\Delta\mathbf{C})\ \ \boldsymbol{Q}^{\mathrm{T}} &= \ \ \mathrm{cay}\,(\boldsymbol{Q}\ \ \Delta\mathbf{c}) \\ &= \ \ \mathrm{cay}\,(\Delta\boldsymbol{c}) = \Delta\boldsymbol{Q}, \quad (18) \\ \Delta\boldsymbol{c} &= \boldsymbol{Q}\ \Delta\mathbf{c}, \end{aligned}$$

$$\begin{aligned} \mathrm{cay}\,(\Delta\mathbf{C})\ \ \Delta\mathbf{c}\ \ &= \ \ \Delta\mathbf{c}, \\ \mathrm{cay}\,(\Delta\mathbf{C})\ \ \mathrm{cay}\,(-\Delta\mathbf{C}) &= \mathbf{1}. \end{aligned} \quad (19)$$

Here the exponential map plays an auxiliary role

$$\begin{aligned} &\Delta\mathbf{Q} = \exp\,(\Delta\mathbf{W}) = \mathrm{cay}\,(\Delta\mathbf{C})\,, \\ &\Delta\mathbf{c} = 2\ \tan\left(\frac{1}{2}\parallel\Delta\mathbf{w}\parallel\right)\ \mathbf{e},\ \Delta\mathbf{W} = \Delta\mathbf{w}\times\mathbf{1}, \\ &\mathbf{e} = \frac{\Delta\mathbf{c}}{\parallel\Delta\mathbf{c}\parallel} = \frac{\Delta\mathbf{w}}{\parallel\Delta\mathbf{w}\parallel}. \end{aligned} \quad (20)$$

Now, the evolution equations ($[0,T] = \cup_{n=0}^{N-1}\,[t_n, t_{n+1}]$) are introduced as

$$\begin{aligned} &\boldsymbol{y}_{n+1} - \boldsymbol{y}_n = \boldsymbol{u}_{n+1} - \boldsymbol{u}_n = \Delta\boldsymbol{u}, \\ &\boldsymbol{Q}_{n+1} - \boldsymbol{Q}_n = \frac{1}{2}\left(\boldsymbol{Q}_{n+1} + \boldsymbol{Q}_n\right)\ \Delta\mathbf{C} \\ &= \boldsymbol{H}_{n+\frac{1}{2}}\ \Delta\mathbf{C} = \frac{1}{2}\Delta\boldsymbol{C}\ \left(\boldsymbol{Q}_{n+1} + \boldsymbol{Q}_n\right) \\ &= \Delta\boldsymbol{C}\ \boldsymbol{H}_{n+\frac{1}{2}}, \end{aligned} \quad (21)$$

where

$$\begin{aligned} \Delta\boldsymbol{u} &= \frac{1}{2}\Delta t\,(\boldsymbol{v}_{n+1} + \boldsymbol{v}_n)\,, \\ \Delta\mathbf{c} &= \frac{1}{2}\Delta t\,(\boldsymbol{\omega}_{n+1} + \boldsymbol{\omega}_n)\,, \\ \Delta\mathbf{C} &= \Delta\mathbf{c}\times\mathbf{1}, \\ \boldsymbol{H}_{n+\frac{1}{2}} &= \frac{1}{2}\left(\boldsymbol{Q}_{n+1} + \boldsymbol{Q}_n\right). \end{aligned} \quad (22)$$

The increment of the rotation tensor field $\Delta\mathbf{Q}$, together with $\Delta\boldsymbol{Q}$, yields the transformation between the configuration t_n and t_{n+1}:

$$\boldsymbol{Q}_{n+1} = \Delta\boldsymbol{Q}\ \boldsymbol{Q}_n = \boldsymbol{Q}_n\ \Delta\mathbf{Q}. \quad (23)$$

Then from Eq. 23 follows the formula

$$\begin{aligned} \Delta\boldsymbol{Q} &= \mathrm{cay}\,(\Delta\boldsymbol{C}) = \mathrm{cay}\left(\boldsymbol{Q}_n\ \Delta\mathbf{c}\right) \\ &= \boldsymbol{Q}_n\ \mathrm{cay}\,(\Delta\mathbf{C})\ \ \boldsymbol{Q}_n^{\mathrm{T}} = \boldsymbol{Q}_n\ \Delta\mathbf{Q}\ \boldsymbol{Q}_n^{\mathrm{T}}. \end{aligned} \quad (24)$$

The algorithmic approximation of the weak form (3) of the BVP, based for ECA on the mid-point approximation, leads to local relations between the configuration and the velocity fields Eq. 21 within the time interval $[t_n, t_{n+1}]$:

$$\begin{aligned} &\frac{1}{\Delta t}\int\limits_{M\setminus\Gamma}\left(\left(\boldsymbol{p}_{n+1} - \boldsymbol{p}_n\right)\cdot\Delta\boldsymbol{u}\right. \\ &\left.+\left(\boldsymbol{\pi}_{n+1} - \boldsymbol{\pi}_n\right)\cdot\Delta\boldsymbol{c}\right)\,\mathrm{d}a \\ &+\int\limits_{M\setminus\Gamma}\left(\boldsymbol{n}^{\beta}\cdot\left(\Delta\boldsymbol{u}_{,\beta} + \boldsymbol{y}_{n+\frac{1}{2},\beta}\times\Delta\boldsymbol{c}\right)\right. \\ &\left.+\boldsymbol{m}^{\beta}\cdot\Delta\boldsymbol{c}_{,\beta}\right)\,\mathrm{d}a = G_{ext}\,[\mathbf{u}, t;\ \ \mathbf{w}]\,, \end{aligned} \quad (25)$$

where translations and rotations are defined according to the formulae

$$\begin{aligned} \boldsymbol{y}_{n+\frac{1}{2}} &= \frac{1}{2}\left(\boldsymbol{y}_{n+1} + \boldsymbol{y}_n\right), \\ \boldsymbol{H}_{n+\frac{1}{2}} &= \frac{1}{2}\left(\boldsymbol{Q}_{n+1} + \boldsymbol{Q}_n\right), \\ \boldsymbol{H}_{n+\frac{1}{2}} &\notin SO(3), \end{aligned} \quad (26)$$

with the following transformations of the resultant forces

$$\begin{aligned} \mathbf{n}^{\beta} &= \boldsymbol{H}_{n+\frac{1}{2}}^{-1}\ \boldsymbol{n}^{\beta}, \\ \mathbf{m}^{\beta} &= \boldsymbol{H}_{n+\frac{1}{2}}^{*\ -1}\ \boldsymbol{m}^{\beta}, \\ \boldsymbol{H}_{n+\frac{1}{2}}^{*} &= \det\left(\boldsymbol{H}_{n+\frac{1}{2}}\right)\ \boldsymbol{H}_{n+\frac{1}{2}}^{-\mathrm{T}}. \end{aligned} \quad (27)$$

In addition, to satisfy Eq. 2, it is necessary that the constitutive equations must be replaced with the algorithmic constitutive equations in the material representation, i.e.,

$$\begin{aligned} \mathbf{n}^{\beta} &= \mathbf{C}_{\boldsymbol{\varepsilon}\boldsymbol{\varepsilon}}\frac{1}{2}\left(\boldsymbol{\varepsilon}_{\beta n+1} + \boldsymbol{\varepsilon}_{\beta n}\right), \\ \mathbf{m}^{\beta} &= \mathbf{C}_{\boldsymbol{\kappa}\boldsymbol{\kappa}}\frac{1}{2}\left(\boldsymbol{\kappa}_{\beta n+1} + \boldsymbol{\kappa}_{\beta n}\right). \end{aligned} \quad (28)$$

With Eqs. 4 and 22, the increment of the kinetic energy per unit surface Eq. 25 in mid-point approximation takes the form

$$\begin{aligned}\Delta K &= \tfrac{1}{\Delta t}\left[\left(\boldsymbol{p}_{n+1}-\boldsymbol{p}_n\right)\cdot\Delta\boldsymbol{u}+\left(\boldsymbol{\pi}_{n+1}-\boldsymbol{\pi}_n\right)\cdot\Delta\boldsymbol{c}\right]\\ &= \tfrac{1}{\Delta t}\left[m_0\left(\boldsymbol{v}_{n+1}-\boldsymbol{v}_n\right)\cdot\Delta\boldsymbol{u}+I_0\left(\boldsymbol{\omega}_{n+1}-\boldsymbol{\omega}_n\right)\cdot\boldsymbol{Q}_{n+1}\Delta\mathbf{c}\right]\\ &= \tfrac{1}{2}\left[m_0\left(\boldsymbol{v}_{n+1}-\boldsymbol{v}_n\right)\cdot\left(\boldsymbol{v}_{n+1}+\boldsymbol{v}_n\right)+I_0\left(\boldsymbol{\omega}_{n+1}-\boldsymbol{\omega}_n\right)\cdot\boldsymbol{Q}_{n+1}\left(\boldsymbol{\omega}_{n+1}+\boldsymbol{\omega}_n\right)\right]\\ &= \tfrac{1}{2}\left[m_0\boldsymbol{v}_{n+1}\cdot\boldsymbol{v}_{n+1}+I_0\boldsymbol{\omega}_{n+1}\cdot\boldsymbol{\omega}_{n+1}-m_0\boldsymbol{v}_n\cdot\boldsymbol{v}_n-I_0\boldsymbol{\omega}_n\cdot\boldsymbol{\omega}_n\right]\\ &= K_{n+1}-K_n.\end{aligned} \tag{29}$$

Relations (6) and (21) yield the formula for an increase of the internal energy per unit surface in mid-point approximation

$$\Delta U = \boldsymbol{n}^\beta\cdot\left(\Delta\boldsymbol{u},_\beta+\ \boldsymbol{y}_{n+\frac{1}{2}},_\beta\times\Delta\boldsymbol{c}\right)$$

$$+\ \boldsymbol{m}^\beta\cdot\Delta\boldsymbol{c},_\beta=\left(\boldsymbol{\varepsilon}_{\beta\ n+1}-\boldsymbol{\varepsilon}_{\beta\ n}\right)\cdot\mathbf{n}^\beta +\ \left(\boldsymbol{\kappa}_{\beta\ n+1}-\boldsymbol{\kappa}_{\beta\ n}\right)\cdot\mathbf{m}^\beta. \tag{30}$$

The use of $\boldsymbol{\varepsilon}_\beta=\boldsymbol{Q}^{\mathrm{T}}\boldsymbol{\varepsilon}_\beta$ together with Eq. 26, Eq. 21 leads to the following relations

$$\begin{aligned}\boldsymbol{\varepsilon}_{\beta\ n+1}-\boldsymbol{\varepsilon}_{\beta\ n} &= \boldsymbol{Q}^{\mathrm{T}}_{n+1}\boldsymbol{\varepsilon}_{\beta\ n+1}-\boldsymbol{Q}^{\mathrm{T}}_{n}\boldsymbol{\varepsilon}_{\beta\ n}=\boldsymbol{Q}^{\mathrm{T}}_{n+1}\boldsymbol{y}_{n+1},_\beta-\ \boldsymbol{Q}^{\mathrm{T}}_{n}\boldsymbol{y}_{n},_\beta=\\ &= \tfrac{1}{2}\left(\boldsymbol{Q}^{\mathrm{T}}_{n+1}+\boldsymbol{Q}^{\mathrm{T}}_{n}\right)\left(\boldsymbol{y}_{n+1},_\beta-\boldsymbol{y}_{n},_\beta\right)+\left(\boldsymbol{Q}_{n+1}-\boldsymbol{Q}_n\right)^{\mathrm{T}}\tfrac{1}{2}\left(\boldsymbol{y}_{n+1},_\beta+\boldsymbol{y}_{n},_\beta\right)\\ &= \boldsymbol{H}^{\mathrm{T}}_{n+\frac{1}{2}}\left(\boldsymbol{y}_{n+1}-\boldsymbol{y}_n\right),_\beta+\left(\boldsymbol{Q}_{n+1}-\boldsymbol{Q}_n\right)^{\mathrm{T}}\boldsymbol{y}_{n+\frac{1}{2}},_\beta\\ &= \boldsymbol{H}^{\mathrm{T}}_{n+\frac{1}{2}}\Delta\boldsymbol{u},_\beta-\boldsymbol{H}^{\mathrm{T}}_{n+\frac{1}{2}}\Delta\boldsymbol{C}\,\boldsymbol{y}_{n+\frac{1}{2}},_\beta=\boldsymbol{H}^{\mathrm{T}}_{n+\frac{1}{2}}\left(\Delta\boldsymbol{u},_\beta+\boldsymbol{y}_{n+\frac{1}{2}},_\beta\times\Delta\boldsymbol{c}\right).\end{aligned} \tag{31}$$

Since $\boldsymbol{\kappa}_\beta\times\mathbf{1}=\mathbf{K}_\beta=\boldsymbol{Q}^{\mathrm{T}}\boldsymbol{Q},_\beta$, $\mathbf{K}_\beta=\boldsymbol{Q}^{\mathrm{T}}\boldsymbol{K}_\beta\,\boldsymbol{Q}$, $\boldsymbol{\kappa}_\beta=\boldsymbol{Q}^{\mathrm{T}}\boldsymbol{\kappa}_\beta$ and taking into account (21), (26) the expressions entering the kinetic energy read

$$\begin{aligned}\mathbf{K}_{\beta\ n+1}-\mathbf{K}_{\beta\ n} &= \boldsymbol{Q}^{\mathrm{T}}_{n+1}\boldsymbol{Q}_{n+1},_\beta-\ \boldsymbol{Q}^{\mathrm{T}}_{n}\boldsymbol{Q}_{n},_\beta\\ &= \tfrac{1}{2}\left(\boldsymbol{Q}^{\mathrm{T}}_{n+1}+\boldsymbol{Q}^{\mathrm{T}}_{n}\right)\left(\boldsymbol{Q}_{n+1},_\beta-\boldsymbol{Q}_{n},_\beta\right)+\left(\boldsymbol{Q}_{n+1}-\boldsymbol{Q}_n\right)^{\mathrm{T}}\tfrac{1}{2}\left(\boldsymbol{Q}_{n+1}+\boldsymbol{Q}_n\right),_\beta\\ &= \boldsymbol{H}^{\mathrm{T}}_{n+\frac{1}{2}}\left(\boldsymbol{Q}_{n+1}-\boldsymbol{Q}_n\right),_\beta+\ \left(\boldsymbol{Q}_{n+1}-\boldsymbol{Q}_n\right)^{\mathrm{T}}\boldsymbol{H}_{n+\frac{1}{2}},_\beta\\ &= \boldsymbol{H}^{\mathrm{T}}_{n+\frac{1}{2}}\left(\Delta\boldsymbol{C}\,\boldsymbol{H}_{n+\frac{1}{2}}\right),_\beta+\ \left(\Delta\boldsymbol{C}\,\boldsymbol{H}_{n+\frac{1}{2}}\right)^{\mathrm{T}}\boldsymbol{H}_{n+\frac{1}{2}},_\beta\\ &= \boldsymbol{H}^{\mathrm{T}}_{n+\frac{1}{2}}\Delta\boldsymbol{C},_\beta\,\boldsymbol{H}_{n+\frac{1}{2}}+\ \boldsymbol{H}^{\mathrm{T}}_{n+\frac{1}{2}}\Delta\boldsymbol{C}\,\boldsymbol{H}_{n+\frac{1}{2}},_\beta-\ \boldsymbol{H}^{\mathrm{T}}_{n+\frac{1}{2}}\Delta\boldsymbol{C}\,\boldsymbol{H}_{n+\frac{1}{2}},_\beta\\ &= \boldsymbol{H}^{\mathrm{T}}_{n+\frac{1}{2}}\Delta\boldsymbol{C},_\beta\,\boldsymbol{H}_{n+\frac{1}{2}}.\end{aligned} \tag{32}$$

Relation (32), employing an isomorphism between skew-symmetric tensors ($\Delta\boldsymbol{C}$) and their axial vectors ($\Delta\boldsymbol{c}$), can be rephrased as

$$\mathbf{K}_{\beta\ n+1}-\mathbf{K}_{\beta\ n}=\boldsymbol{H}^{\mathrm{T}}_{n+\frac{1}{2}}\Delta\boldsymbol{C},_\beta\,\boldsymbol{H}_{n+\frac{1}{2}}\Rightarrow\boldsymbol{\kappa}_{\beta\ n+1}-\boldsymbol{\kappa}_{\beta\ n}=\boldsymbol{H}^{*\ \mathrm{T}}_{n+\frac{1}{2}}\Delta\boldsymbol{c},_\beta, \tag{33}$$

T

An increase ΔU of the internal energy, following Eqs. 31 and 33 with Eq. 27 and the expressions (28), is described as follows:

$$
\begin{aligned}
\Delta U &= \left(\Delta \boldsymbol{u}_{,\beta} + \boldsymbol{y}_{n+\frac{1}{2},\beta} \times \Delta \boldsymbol{c}\right) \cdot \boldsymbol{n}^{\beta} + \Delta \boldsymbol{c}_{,\beta} \cdot \boldsymbol{m}^{\beta} \\
&= \boldsymbol{H}^{-\mathrm{T}}_{n+\frac{1}{2}} \left(\boldsymbol{\varepsilon}_{\beta\ n+1} - \boldsymbol{\varepsilon}_{\beta\ n}\right) \cdot \boldsymbol{n}^{\beta} + \boldsymbol{H}^{*\ -1}_{n+\frac{1}{2}} \left(\boldsymbol{\kappa}_{\beta\ n+1} - \boldsymbol{\kappa}_{\beta\ n}\right) \cdot \boldsymbol{m}^{\beta} \\
&= \left(\boldsymbol{\varepsilon}_{\beta\ n+1} - \boldsymbol{\varepsilon}_{\beta\ n}\right) \cdot \boldsymbol{H}^{-1}_{n+\frac{1}{2}} \boldsymbol{n}^{\beta} + \left(\boldsymbol{\kappa}_{\beta\ n+1} - \boldsymbol{\kappa}_{\beta\ n}\right) \cdot \boldsymbol{H}^{*\ -1}_{n+\frac{1}{2}} \boldsymbol{m}^{\beta} \\
&= \left(\boldsymbol{\varepsilon}_{\beta\ n+1} - \boldsymbol{\varepsilon}_{\beta\ n}\right) \cdot \mathbf{n}^{\beta} + \left(\boldsymbol{\kappa}_{\beta\ n+1} - \boldsymbol{\kappa}_{\beta\ n}\right) \cdot \mathbf{m}^{\beta} \\
&= \tfrac{1}{2} \left(\boldsymbol{\varepsilon}_{\beta\ n+1} - \boldsymbol{\varepsilon}_{\beta\ n}\right) \cdot \mathbf{C}_{\boldsymbol{\varepsilon}\boldsymbol{\varepsilon}} \left(\boldsymbol{\varepsilon}_{\beta\ n+1} + \boldsymbol{\varepsilon}_{\beta\ n}\right) + \tfrac{1}{2} \left(\boldsymbol{\kappa}_{\beta\ n+1} - \boldsymbol{\kappa}_{\beta\ n}\right) \cdot \mathbf{C}_{\boldsymbol{\kappa}\boldsymbol{\kappa}} \left(\boldsymbol{\kappa}_{\beta\ n+1} + \boldsymbol{\kappa}_{\beta\ n}\right) \\
&= \tfrac{1}{2} \boldsymbol{\varepsilon}_{\beta\ n+1} \cdot \mathbf{C}_{\boldsymbol{\varepsilon}\boldsymbol{\varepsilon}} + \tfrac{1}{2} \boldsymbol{\kappa}_{\beta\ n+1} \cdot \mathbf{C}_{\boldsymbol{\kappa}\boldsymbol{\kappa}} \boldsymbol{\kappa}_{\beta\ n+1} - \tfrac{1}{2} \boldsymbol{\varepsilon}_{\beta\ n} \cdot \mathbf{C}_{\boldsymbol{\varepsilon}\boldsymbol{\varepsilon}} \boldsymbol{\varepsilon}_{\beta\ n} - \tfrac{1}{2} \boldsymbol{\kappa}_{\beta\ n} \cdot \mathbf{C}_{\boldsymbol{\kappa}\boldsymbol{\kappa}} \boldsymbol{\kappa}_{\beta\ n} \\
&= U_{n+1} - U_n .
\end{aligned}
\tag{34}
$$

The results obtained in Eqs. 29 and 34 imply that the discrete approximation of the problem also ensures the energy conservation (2) in the absence of external forces $G_{ext}[\mathbf{u}, t; \ \mathbf{w}] = 0$, cf. for instance, Ibrahimbegović et al. (2000).

Example

Large overall motion of the flexible cylindrical panel with change of the curvature sign, reinforced by an orthogonally placed shell rib, is analyzed (see Fig. 3). Nonlinear static analysis of this example can be found, for instance, in Chróścielewski et al. (1997) and Witkowski (2009). Dimensions and material data are: $L = 2$, $\alpha = 0.4$, $R = 1$, $H = 0.4$, $h_0 = 0.01$, $E = 10^5$, $\nu = 0.25$, $P_{ref} = 1$, $\rho_0 h_0 = 1$. The pair of forces, described by the ramp time function, is initially applied to the structure during a short time period. After 2 s the shell is free from external loading and moves freely in space. Figure 4 depicts the obtained time histories of energy. It is visible that at approximately 4.5 s the time histories obtained with the help of extended Newmark algorithm show sudden break due to energy explosion.

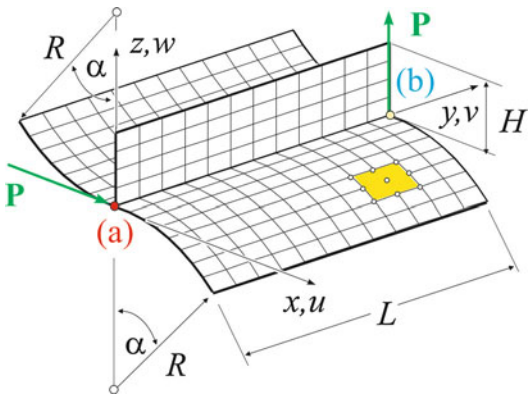

Fig. 3 Flexible cylindrical panel with change of the curvature sign, reinforced by an orthogonally placed shell rib: geometry and loads

Conclusions

In nonlinear dynamics, the use of standard time-stepping algorithms of Newmark type does not guarantee the stability of solution. In Hamiltonian systems, the unstable behavior appears in the course of simulation as the sudden unbounded growth of the total energy of the system (Fig. 4). One of the ways to overcome this problem is the application of the time-stepping algorithm that conserves the energy by assumption in Hamiltonian setup. When the configuration space includes the proper orthogonal rotation group $SO(3)$, the Cayley parameterization of rotation group is crucial in formulation due to its special properties.

Cross-References

- Elastic Shells, Resultant Nonlinear Theory
- Junctions in Irregular Shell Structures
- Surface Geometry, Elements

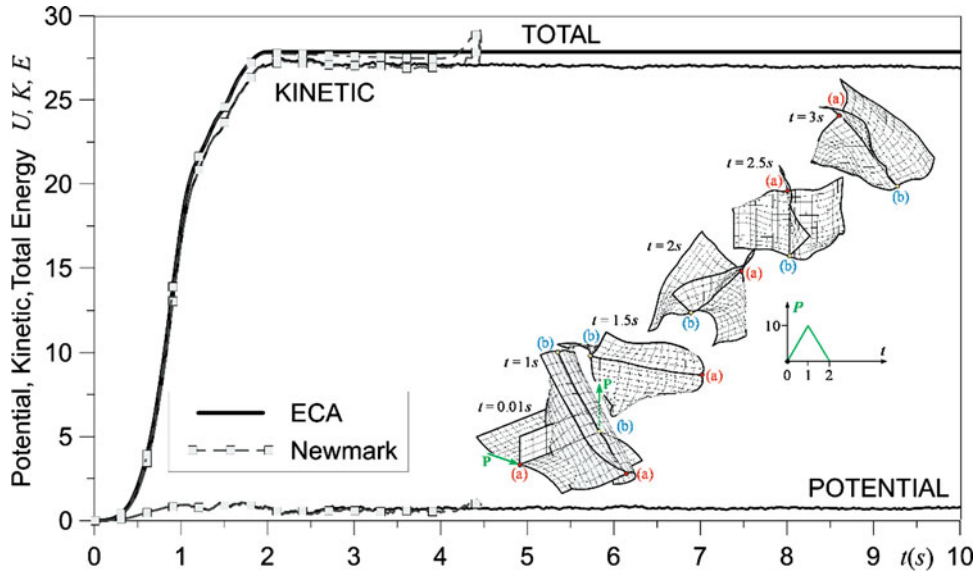

Fig. 4 Flexible cylindrical panel with change of the curvature sign, reinforced by an orthogonally placed shell rib: results

References

Armero F (2008) Assumed strain finite element methods for conserving temporal integrations in non-linear solid dynamics. Int J Numer Methods Eng 74:1795–1847

Armero F, Romero I (2003) Energy-dissipative momentum-conserving time-stepping algorithms for the dynamics of nonlinear Cosserat rods. Comput Mech 31:3–26

Betsch P, Janz A (2016) An energy–momentum consistent method for transient simulations with mixed finite elements developed in the framework of geometrically exact shells. Int J Numer Methods Eng 108: 423–455

Campello EMB, Pimenta PME, Wriggers P (2011) An exact conserving algorithm for nonlinear dynamics with rotational DOFs and general hyperelasticity. Part 2: shells. Comput Mech 48:195–211

Cardona C, Geradin M (1988) A beam finite element nonlinear theory with finite rotations. Int J Numer Methods Eng 26:2403–2438

Chróścielewski J, Witkowski W (2010) Discrepancies of energy values in dynamics of three intersecting plates. Int J Numer Methods Biomed Eng 26:1188–1202

Chróścielewski J, Makowski J, Stumpf H (1997) Finite element analysis of smooth, folded and multi-shell structures. Comput Methods Appl Mech Eng 141: 1–46

Chróścielewski J, Makowski J, Pietraszkiewicz W (2000) Large overall motion of flexible branched shell structures. In: Ambrosio JAC, Kleiber M, (eds) Computational aspects of nonlinear structural systems with large rigid body motion. NATO Advanced Research Workshop, Pułtusk, 2–7 July 2000. pp 201–218

Chróścielewski J, Lubowiecka, Witkowski W (2004a) Energy–conserving integration in six–field shell dynamics. International congress on theoretical and applied mechanics, Warsaw 15–22 Aug

Chróścielewski J, Makowski J, Pietraszkiewicz W (2004b) Statics and dynamics of multi-shells: nonlinear theory and finite element method (in polish). IFTR PASci Press, Warsaw

Chróścielewski J, Lubowiecka I, Witkowski W (2005) Dynamics of six-field shells in the context of energy-conserving scheme, In: Pietraszkiewicz W, Szymczak C (eds) Shell structures: theory and applications. Taylor & Francis/Balkema London, pp 303–307

Gebhardt CR, Rolfes R (2017) On the nonlinear dynamics of shell structures: combining a mixed finite element formulation and a robust integration scheme. Thin-Walled Struct 118:56–72

Graham E, Jelenić G (2003) A general framework for conservative single-step time-integration schemes with higher-order accuracy for a central-force system. Comput Methods Appl Mech Eng 192:3585–3618

Hughes TJR (2000) The finite element method: linear static and dynamics finite element analysis. Dover Publications, New York

Ibrahimbegović A, Mamouri S, Taylor RL, Chen AJ (2000) Finite element method in dynamics of flexible multi-body systems: modeling of holonomic constraints and energy conserving integration schemes. Multibody Sys Dyn 4:195–223

Krasnosel'skii MA, Vainikko GM, Zabreiko PP, Rutitskii YB, Stetsenko VY (1972) Approximate solutions of operator equations. Wolters-Noordhoff Publishers, Groningen

Kuhl D, Crisfield MA (1999) Energy-conserving and decaying algorithms in non-linear structural dynamics. Int J Numer Methods Eng 45:569–599
Kuhl D, Ramm E (1996) Constraint energy momentum algorithm and its application to nonlinear dynamics of shells. Comput Methods Appl Mech Eng 136: 293–315
Lubowiecka I, Chróścielewski J (2002) On dynamics of flexible branched shell structures undergoing large overall motion using finite elements. Comput Struct 80:891–898
Lubowiecka I, Chróścielewski J (2005) Energy-conserving time integration algorithm for six-field irregular shell dynamics. In: ECCOMAS Thematic conference: advances in computational multibody dynamics, Universided Politecnica, Madrid, pp 1–16
Newmark NN (1959) A method of computation for structural dynamics. J Eng Mech Div Proc ASCE 85: 67–94
Pietraszkiewicz W (2017) Elastic shells, resultant nonlinear theory. In: Altenbach H, Őchsner A (eds) Encyclopedia of continuum mechanics, section: shells. Springer, Berlin et al (in print)
Romero I, Armero F (2002) Numerical integration of the stiff dynamics of geometrically exact shells: an energy-dissipative momentum-conserving scheme. Int J Numer Methods Eng 54:1043–1086
Simmonds JG (1984) The nonlinear thermodynamical theory of shells: descent from 3-dimensions without thickness expansion. In: Axelrad EL, Emmerling FA (eds) Flexible shells, theory and applications. Springer, Berlin, pp 1–11
Simo JC, Tarnow N (1994) A new energy and momentum conserving algorithm for non-linear dynamics of shells. Int J Numer Methods Eng 37:2527–2549
Simo JC, Vu-Quoc L (1988) On the dynamics in space of rods undergoing large motions a geometrically exact approach. Comp Meth Appl Mech Eng 66: 125–161
Simo JC, Wong KK (1991) Unconditionally stable algorithms for rigid body dynamics that exactly preserve energy and momentum. Int J Numer Methods Eng 31:19–52
Simo JC, Tarnow N, Doblare M (1995) Non-linear dynamics of three-dimensional rods: exact energy and momentum conserving algorithms. Int J Numer Methods Eng 38:1431–1473
Witkowski W (2009) 4-node combined shell element with semi-EAS-ANS strain interpolations in 6-parameter shell theories with drilling degrees of freedom. Comput Mech 43:307–319
Zolghadr Jahromi H, Izzuddin BA (2013) Energy conserving algorithms for dynamic contact analysis using newmark methods. Comput Struct 118:74–89

Time-Stepping Schemes

► Computational Dynamics

Timoshenko, Stepan Prokofievitch

Isaac Elishakoff
Department of Ocean and Mechanical Engineering, Florida Atlantic University, Boca Raton, FL, USA

Stephan Prokopovych Timoshenko was a world - renown scientist in applied mechanics, who worked in Russia, Ukraine, and United States. He was born in the village Shpotovka in the Chernigov Governorate on December 23, 1878, in Ukraine, then part of the Russian Empire. At every turn, good fortune has found its way to Stephen Timoshenko. The blessings started before his birth. His father was a serf. The nobleman and the landowner fell in love with Timoshenko's aunt, his father's sister, and then married her. As a result, Timoshenko's father became part of the land owner's family, rather than spending his life in serfdom, or near slavery.

Stepan (Stephen) Prokofievich Timoshenko

Russian Empire Period

In 1901, he graduated from the St. Petersburg Institute of Engineers of Ways of Communication. He continued to teach in this same institute during years 1901–1903 as a teaching assistant and then moved to St. Petersburg Polytechnic Institute under Professor Viktor

Kirpichev (1845–1913) where he was employed in years 1903–1906. In 1905, the university was closed due to the first Russian Revolution when czarist troops opened fire on a group of workers marching to the winter palace in St. Petersburg to petition their grievances to Czar Nicolas II. Timoshenko was sympathetic to the workers' cause. Fortuitously, Karl Marx's book *Das Kapital* was "much too heavy" for him, according to his testimony. He then leaves for Germany, where many Russian students pursued postgraduate studies. There he attends lectures by the famous mechanician and author August Föppl (1854–1924) in Munich, as an auditor. He also attends lectures by Ludwig Prandtl (1875–1953) in Göttingen. The city of Göttingen at that time was perhaps the scientific center of the entire world, not unlike present day Cambridge, Massachusetts. There Prandtl assigns him the topic for his dissertation which Timoshenko completes in St. Petersburg and publishes alone.

Victor Kirpichev (1845–1913) played a major role in the life of Timoshenko. Kirpichev greatly appreciated the works of Lord Rayleigh (1842–1919) and recommended engineers to use the methods exposed in his book *Theory of Sound*. Timoshenko eagerly started to study this classic book. Fortunately for S.P. Timoshenko, Kirpichev was the founder and first provost of Kyiv Polytechnic Institute (currently called National Technical University of Ukraine or "Igor Sikorsky Kyiv Polytechnic Institute") that was established in 1898. In 1906, a position opened at Kyiv Polytechnic for the Chairperson of Strength of Materials Department. Timoshenko applied for the job and not without the help of Kirpichev Timoshenko got the position. This was despite the fact that he never, prior to that, served as a lecturer.

Upon recommendation of his teacher Victor Kirpichev, he was appointed the Chairman of Strength of Materials at the Kyiv Polytechnic Institute. In 1909, he was promoted to the deanship. In 1911, he was fired from Kyiv Polytechnic Institute due to "political reasons" as he writes in his essay about his school-time friend Abram Ioffe (1880–1960). In 1911, he returned to St. Petersburg where, luckily, he meets Paul Ehrenfest who came to Russia following his mathematician wife. According to his own testimony in his book on theory of elasticity, they jointly developed the beam theory that incorporates both rotary inertia and shear deformation, published in his 1916 book, in the Russian, as well as in his nearly identical papers in English published in 1920 and 1921, respectively. His joint work with P. Ehrenfest S. P. Timoshenko also mentions in his 1922 paper. Due to S. P. Timoshenko's own testimony of cooperation, it appears that this celebrated theory ought to be called Timoshenko–Ehrenfest beam theory (Elishakoff, 2019a). For detailed discussion of this beam theory in the past century, the interested reader can consult papers by Han et al. (1999) and Elishakoff et al. (2015). In the past one hundred years, thousands of papers appeared on this theory but not even a single book was published. This gap was closed recently by Elishakoff (2019d).

In 1918, after the February and November Revolutions that took place a year earlier in Russia, he returns to Ukraine, which then declared independence. In Kyiv, he participated in the establishment of the Ukraine Academy of Sciences, assisting its first President, Vladimir Ivanovich Vernadsky (1863–1945).

European and American Period

In 1919, Timoshenko moved to Rostov-on-Don. He decided to leave his country and in 1920 arrived, through Constantinople (present-day Istanbul), to the Kingdom of Serbs, Croats, and Slovenes. Luckily for Timoshenko, in Zagreb, the new Polytechnic Institute was established, and Timoshenko was offered professorship. There too, destiny treated him well; students did not protest his lectures being given in the language representing a mixture of Russian and Croatian. Again, he had good fortune: His former student arranged him getting a job at the Vibration Specialty Company in Pittsburgh, United States, in 1922. Later Timoshenko moved to the Westinghouse Electric Corporation from 1923 to 1927, after which he became a professor in the University of Michigan where he created the bachelor's and doctoral programs in engineering mechanics.

It is said that Napoleon Bonaparte had observed that "Ability is of little account without opportunity." The United States offered Timoshenko great opportunities. The University of Michigan offered him a professorship with little time allotted for teaching, primarily for graduate students, at a salary that was double of other faculty members in his position. He was allowed to spend large amounts of time during the day at home, composing his textbooks. In 1936 Timoshenko moved to the Stanford University. In 1938 a special conference was held in his honor as well as book was published dedicated to his 60th birth anniversary (Lessells et al., 1938). In 1957 ASME established a medal named after Stephen Timoshenko; he became its first recipient. In 1964 he moved to Wuppertal, Federal Republic of Germany, to be with his daughter, Anna. He died in 1972; his ashes are buried in Alta Mesa Memorial Park, Palo Alto, California. In 1982 obituary, Soderberg wrote about Timoshenko's "love-hate" relationship with America (See also Elishakoff 2019b, c).

In a tribute written in October 1972, the year of Prof. Timoshenko's death, Prof. Chia-Shun Yih, then Stephen P. Timoshenko Distinguished University Professor of University of Michigan, wrote (see Elishakoff 2019d): "The strong character and inflexible set of values he held sustained him and his work; in regard to America, of which his judgements were severe, they also blinded his vision. To live and work for 42 years in a country, to have tremendous influence there through his work, to be honored there till summer had o'erbrimmed the honeyed cells, and yet not to feel an attachment to it: What would one call it, in point of sentiment? A failure or misfortune? The golden sunset that was his would have had as much warmth as brilliance if he had been able to find joy and solace from the beauty of the wilderness of America, to hold dear the native generosity, kindness, enthusiasm of its inhabitants (as he held the kindness of Germans), and thus to have a feeling of home during those long years." Jacob Peter Den Hartog (1901–1989) wrote about Timoshenko's book *As I Remember*, in *Science* magazine: "There is no question that Timoshenko did much for America. It is an equally obvious truth that America did much for Timoshenko, as it did for millions of other immigrants for all over the world. However, our autobiographer has never admitted as much to his associates and pupils who, like myself often have been painted by his casual statements in conversation. That pain is not diminished by reading these statements on the printed page and one would have wished for a little less acid and a little more human kindness." Soderberg (1982) wrote "... a strange love-hate relationship of his feelings toward America, which never left him and sometimes stood in the way of full utilization of his talents. In reading *As I Remember*, one is astonished at the absence of a single world in grateful recognition of his debt to America, which had awarded him such a rare opportunity."

Truesdell (1984, p. 253), remarked, perhaps overly critically, that Timoshenko was "relying heavily on the scantiness of American engineers' education... although [Timoshenko's] books are almost totally devoid of originality, they served to acquaint American mechanical and civil engineers with theory and history they were otherwise unlikely to encounter."

Timoshenko's Books

The books written by him during his life's American period include:

1. *Applied Elasticity*, with J.M. Lessels, 1925
2. *Vibration Problems in Engineering*, 1928, 1937, 1955 (third edition with D.H. Young)
3. *Strength of Materials*, Parts I and II, 1930, 1940, 1955
4. *Theory of Elasticity*, 1934, 1951 (with J.N. Goodier)
5. *Elements of Strength of Materials*, 1935, 1940, 1949 (with G.H. MacCullough), 1962 (with D.H. Young)
6. *Theory of Elastic Stability*, 1936, 1961 (with J.M. Gere)
7. *Engineering Mechanics* (with D.H. Young), 1937, 1940, 1951, 1956
8. *Theory of Plates and Shells*, 1940, 1959 (with S. Woinowsky-Krieger)
9. *Theory of Structures* (with D.H. Young), 1945, 1965

10. *Advanced Dynamics* (with D.H. Young), 1948
11. *Mechanics of Materials* (with J.M. Gere), 1972

He also wrote a book on history of strength of materials (1953a) as well as a book on engineering education in Russia (1959). His autobiography appeal in several languages (1963, 1968, 1993, 2006, 2014).

Archibald (see Howard, 1967) characterized S. P. Timoshenko on "the patron saint of the American engineering" Laura et al. (1992) designate shear deformable beam vibration theory as 'epoch making.' Soderberg (1982) wrote about S. P. Timoshenko's "highly developed pragmatic skill in using fragments of exact solutions for a variety of approximate solutions to difficult problem in applied mechanics" and "Timoshenko's great influence upon applied science and technology in America."

Cross-References

▸ Föppl, August Otto
▸ Prandtl, Ludwig

References

Den Hartog J (1968) Odyssey of an engineer, Science 160(3832):1102–1103
Elishakoff I (2019a) who developed the so called Timoshenko beam theory? Math Mech Solids, in press
Elishakoff I (2019b) J.P. Den Hartog about S.P. Timoshenko: Fifty years later. Math Mech Solids; 24(5):1340–1348
Elishakoff I (2019c) Stepan Prokofievich Timoshenko and America. Z Angew Math Mech, in press
Elishakoff I (2019d) Handbook on Timoshenko-Ehrenfest Beam and Uflyand-Mindlin plate theories. World Scientific, Singapore
Elishakoff I, Kaplunov J, Nolde E (2015) Celebrating the centenary of Timoshenko's study of effects of shear deformation and rotary inertia. Appl Mech Rev 67(6):060802
Han SM, Benaroya H, Wei T (1999) Dynamics of transversally vibrating beams using four engineering theories. J Sound Vib 325:935–988
Howard TN (ed.) (1967) The Rayleigh archives dedication, Office of Aerospace Research, AFCRL Special Report No 63, United States Air force
Laura PAA, Rossi RE and Maurizi MJ (1992) Vibrating Timoshenko beams, a tribute to the 70th anniversary of the publication of professor S. Timoshenko's epoch making contribution, universidad national del sur, Bahia Balanca, Argentina
Lessells JM et al (eds) (1938) Contributions in the mechanics of solids: dedicated to Stephen Timoshenko by his friends on the occasion of the sixtieth birthday anniversary. Macmillan, New York
Soderberg CR, Stephen P (1982) Timoshenko: December 23, 1878 – May 29, 1972. Biographical Mem 53:323–349
Timoshenko SP (1914) A course in theory of elasticity, Part 1, general theory, bending and torsion of rods. Plane problem. Bodies of revolution. A.E. Collins Publishers, St. Petersburg. (in Russian)
Timoshenko SP (1916) A course of elasticity theory. Part 2: rods and plates. A.E. Collins Publishers, St. Petersburg (in Russian) (2nd edition, Kiev, "Naukova Dumka" Publishers, pp 337–338, 341, 1972)
Timoshenko SP (1920) On the differential equation for the flexural vibrations of prismatical rods. Glasnik Hrvatskoga Prirodaslovnoga Društva (Herald of the Croatian Nature Association) 32(2):55–57
Timoshenko SP 1921 On the correction for shear of the differential equation for transverse vibrations of prismatic bar. Philosophical Magazine Series 6 41/245:744–746
Timoshenko SP (1922) On the transverse vibration of bars of uniform sections, philosophical Magazine, Series 6, 43/125:131.
Timoshenko SP (1953a) History of strength of materials with a brief account of theory and elasticity and theory of structures. McGraw-Hill, New York
Timoshenko SP (1953b) Collected papers. McGraw-Hill, New York
Timoshenko SP (1959) Engineering education in Russia. McGraw-Hill, New York
Timoshenko SP (1963) Remembrances. Paris (in Russian)
Timoshenko SP (1968) As I remember: the autobiography of Stephen P. Timoshenko. Van Nostrand, Princeton
Timoshenko SP (1993) Vospominaniya (Remembrances). "Naukova Dumka" Publishers, Kiev (in Russian)
Timoshenko SP (2006) Errinerungen – eine Autobiographie (translation from Russian by A. Duda). Ernst und Sohn, Berlin (in German)
Timoshenko SP (2014) Vospominaniya (Remembrances). "Vuzovskaya Kniga" Publishers, Moscow (in Russian)
Truesdell CA (1953) Timoshenko's history of strength of materials. Math Rev 14:1050–1053

Topological Derivative

▸ Relation Between Eshelbyan Mechanics and Topological Derivative Concept
▸ Topology Optimization Based on Explicit Geometry Description

Topology Optimization

- Stress-Constrained Topology Optimization for Lattice Materials
- Topology Optimization Based on Explicit Geometry Description

Topology Optimization Based on Explicit Geometry Description

Xu Guo, Weisheng Zhang, and Zongliang Du
State Key Laboratory of Structural Analysis for Industrial Equipment, Department of Engineering Mechanics, International Research Center for Computational Mechanics, Dalian University of Technology, Dalian, China

Synonyms

B-spline curve; Explicit geometry description; Moving Morphable Component (MMC); Moving Morphable Void (MMV); Sensitivity analysis; Topological derivative; Topology optimization

Definition

Topology optimization based on explicit geometry description is defined as a structural topology optimization paradigm where structural topology/geometry is described in an explicit way. The so-called Moving Morphable Components/Voids (MMC/MMV) method, geometry projection method, and B-spline based topological derivative method can all be ascribed to this solution paradigm. Since these methods have the potential to reduce the number of design variables associated with numerical optimization and establish a direct link with the computer aided design/engineering (CAD/CAE) systems, recent years witnessed a growing interest in developing topology optimization methods based on explicit geometry description.

Introduction

Traditional topology optimization approaches, for example, Solid Isotropic Material with Penalization approach (SIMP) (Bendsøe 1989; Zhou and Rozvany 1991) and level set approach (LSM) (Wang et al. 2003; Allaire et al. 2004), are established based on implicit geometry description, where optimized structural topology is *extracted* from a binary pixel/voxel image or the nodal values of a level set function. Although remarkable achievements have been made with these approaches, it is worth noting that the numerical implementation of these approaches often leads to a large number of design variables, and it is not an easy task to establish a seamless link between the optimized results obtained by these methods with CAD/CAE systems. Moreover, it is also not straightforward to consider geometry-related objective/constraint functions in these approaches.

In order to circumvent the aforementioned difficulties, some topology optimization approaches based on explicit geometry description have been proposed recently. The central idea of these approaches is to use some structural components as the basic building blocks of topology optimization and adopt the parameters for describing their geometries as design variables. Figure 1 illustrates the basic idea of the so-called Moving Morphable Component (MMC)-based explicit topology optimization approach (Guo et al. 2014) schematically. In this approach, a set of structural components with explicit geometry description is initially deployed in the design domain, then optimization algorithm is applied to find the optimized sizes, shapes, and layout of the components. Finally, an optimized structural topology can be obtained through the deforming, overlapping, and merging of these components. Besides components made of solid materials, void can also be viewed as a specific type of structural component and the so-called Moving Morphable Void (MMV)-based explicit topology optimization approach, where a set of voids is used as the basic building blocks of topology optimization, had also been developed in the literature (Zhang et al. 2017c). Besides the MMC/MMV approaches mentioned above, the readers are

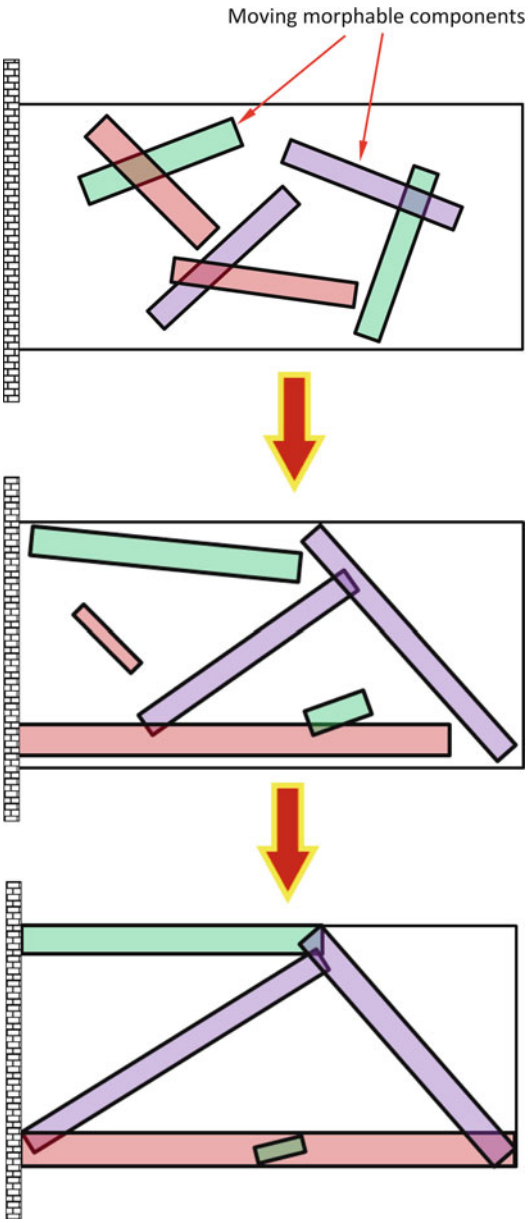

Fig. 1 The basic idea of the MMC-based topology optimization approach

referred to Norato et al. (2015) and Hur et al. (2017) for other forms of explicit geometry-based topology optimization approaches.

Compared with the implicit geometry-based topology optimization framework, the explicit geometry-based solution framework has the following advantages: (1) Direct link with the computer aided design (CAD) modeling systems, since the geometries of the whole structural topology are described explicitly by a set of parameters. (2) Capability of integrating shape, size, and topology optimization or even structural type optimization in a unified framework. (3) Great potential to share the merits of both Lagrangian and Eulerian topology optimization approaches. (4) The optimized structures obtained are pure black-and-white and there is no need to introduce special techniques to eliminate numerical instabilities such as checkerboard phenomenon and mesh-dependent solutions. (5) Great potential to reduce the computational efforts associated with topology optimization.

These distinct advantages over other topology optimization approaches based on implicit geometry description render the MMC/MMV-based explicit topology optimization approaches become a hot topic in topology optimization field. Nowadays, numerous MMC/MMV-based methods have been developed to solve topology optimization problems based on explicit geometry description.

Theory

In this section, the theoretical aspects of the MMC approach, which is a representative explicit geometry-based topology optimization approach, will be introduced.

Geometry Description

In the MMC-based approach, the material distribution of a structure can be descripted in the following form:

$$\begin{cases} \chi^{\mathrm{s}}(\boldsymbol{x}) > 0, & \text{if } \boldsymbol{x} \in \Omega^{\mathrm{s}}, \\ \chi^{\mathrm{s}}(\boldsymbol{x}) = 0, & \text{if } \boldsymbol{x} \in \partial\Omega^{\mathrm{s}}, \\ \chi^{\mathrm{s}}(\boldsymbol{x}) < 0, & \text{if } \boldsymbol{x} \in \mathrm{D}\backslash(\Omega^{\mathrm{s}} \cup \partial\Omega^{\mathrm{s}}), \end{cases} \tag{1}$$

respectively. In the above equations, D represents a prescribed design domain. $\Omega^{\mathrm{s}} \subset \mathrm{D}$ is a subset of D comprised by n components made of solid material. As shown in Guo et al. (2014), $\chi^{\mathrm{s}}(\boldsymbol{x}) = \max(\chi_1(\boldsymbol{x}), \ldots, \chi_n(\boldsymbol{x}))$ with $\chi_i(\boldsymbol{x})$ denoting the topology description function (TDF) of the i-th component. For two-dimensional (2D) case, the function $\chi_i(\boldsymbol{x})$ can be adopted as:

T

$$\chi_i(x, y) = 1 - \left(\frac{x'}{a_i}\right)^p - \left(\frac{y'}{b_i(x')}\right)^p, \quad (2)$$

with

$$\begin{Bmatrix} x' \\ y' \end{Bmatrix} = \begin{bmatrix} \cos\theta_i & \sin\theta_i \\ -\sin\theta_i & \cos\theta_i \end{bmatrix} \begin{Bmatrix} x - x_{0i} \\ y - y_{0i} \end{Bmatrix} \quad (3)$$

and p is a relatively large even integer number ($p = 6$ is often adopted in the MMC approach). In the above equations, the symbols (x_{0i}, y_{0i}), a_i, $b_i(x')$ and θ_i denote the coordinate of the center, the half-length, the variable half width, and the inclined angle (measured from the horizontal axis anticlockwisely) of the i-th component. It should be noted that the variation of the width of the component $b_i(x')$ is measured with respect to local coordinate system and can take different forms (Guo et al. 2016), such as the linearly varying thicknesses as follows:

$$b_i(x') = \frac{t_i^1 + t_i^2}{2} + \frac{t_i^2 - t_i^1}{2a_i}x', \quad (4)$$

where t_i^1 and t_i^2 are parameters used to describe the thicknesses of the component.

For three-dimensional (3D) case, the following TDF can be used to characterize the region occupied by the i-th component:

$$\chi_i(x, y, z) = 1 - \left(\frac{x'}{L_i^1}\right)^p - \left(\frac{y'}{g_i(x')}\right)^p - \left(\frac{z'}{f_i(x', y')}\right)^p \quad (5)$$

with

$$\begin{Bmatrix} x' \\ y' \\ z' \end{Bmatrix} = \begin{bmatrix} R_{11} & R_{12} & R_{13} \\ R_{21} & R_{22} & R_{23} \\ R_{31} & R_{32} & R_{33} \end{bmatrix} \begin{Bmatrix} x - x_{0i} \\ y - y_{0i} \\ z - z_{0i} \end{Bmatrix} \quad (6)$$

and

$$\begin{bmatrix} R_{11} & R_{12} & R_{13} \\ R_{21} & R_{22} & R_{23} \\ R_{31} & R_{32} & R_{33} \end{bmatrix} = \begin{bmatrix} c_b \cdot c_t & -c_b \cdot s_t & s_b \\ s_a \cdot s_b \cdot c_t + c_a \cdot s_t & -s_a \cdot s_b \cdot s_t + c_a \cdot c_t & -s_a \cdot c_b \\ -c_a \cdot s_b \cdot c_t + s_a \cdot s_t & c_a \cdot s_b \cdot s_t + s_a \cdot c_t & c_a \cdot c_b \end{bmatrix}, \quad (7)$$

respectively. In the above equations, $s_a = \sin\alpha$, $s_b = \sin\beta$, $s_t = \sin\theta$, $c_a = \sqrt{1 - s_a^2}$, $c_b = \sqrt{1 - s_b^2}$ and $c_t = \sqrt{1 - s_t^2}$ with α, β, and θ denoting the rotation angles of the component from a global coordinate system $Oxyz$ to the local coordinate system $O'x'y'z'$, respectively. The central coordinate and the half-length of the component are represented by the coordinate (x_{0i}, y_{0i}, z_{0i}) and L_i^1, respectively. Furthermore, the functions $g_i(x')$ and $f_i(x', y')$ in the above equation are used to describe the thickness profiles of the component in y' and z' directions, respectively. The functions $g_i(x')$ and $f_i(x', y')$ can be simply chosen as

$$g_i(x') = L_i^2, \quad f_i(x', y') = L_i^3. \quad (8)$$

The readers are referred to Fig. 2 for the reference of the above components descriptions.

With use of the above expressions, the region Ω_i^s occupied by the i-th component (composed of solid material) can be described as:

$$\begin{cases} \chi_i(\boldsymbol{x}) > 0, & \text{if } \boldsymbol{x} \in \Omega_i^s, \\ \chi_i(\boldsymbol{x}) = 0, & \text{if } \boldsymbol{x} \in \partial\Omega_i^s, \\ \chi_i(\boldsymbol{x}) < 0, & \text{if } \boldsymbol{x} \in \mathrm{D} \backslash \left(\Omega_i^s \cup \partial\Omega_i^s\right). \end{cases} \quad (9)$$

Optimization Formulation

Under the above geometry representation scheme, the layout of a structure can be solely determined by a design vector $\boldsymbol{D} = ((\boldsymbol{D}^1)^\mathsf{T}, \ldots, (\boldsymbol{D}^i)^\mathsf{T}, \ldots, (\boldsymbol{D}^n)^\mathsf{T})^\mathsf{T}$, where $\boldsymbol{D}^i$ contains the design variables associated with the i-th component. It can be observed that under the MMC-based solution framework, a topology optimization problem, which intends to seek the optimal

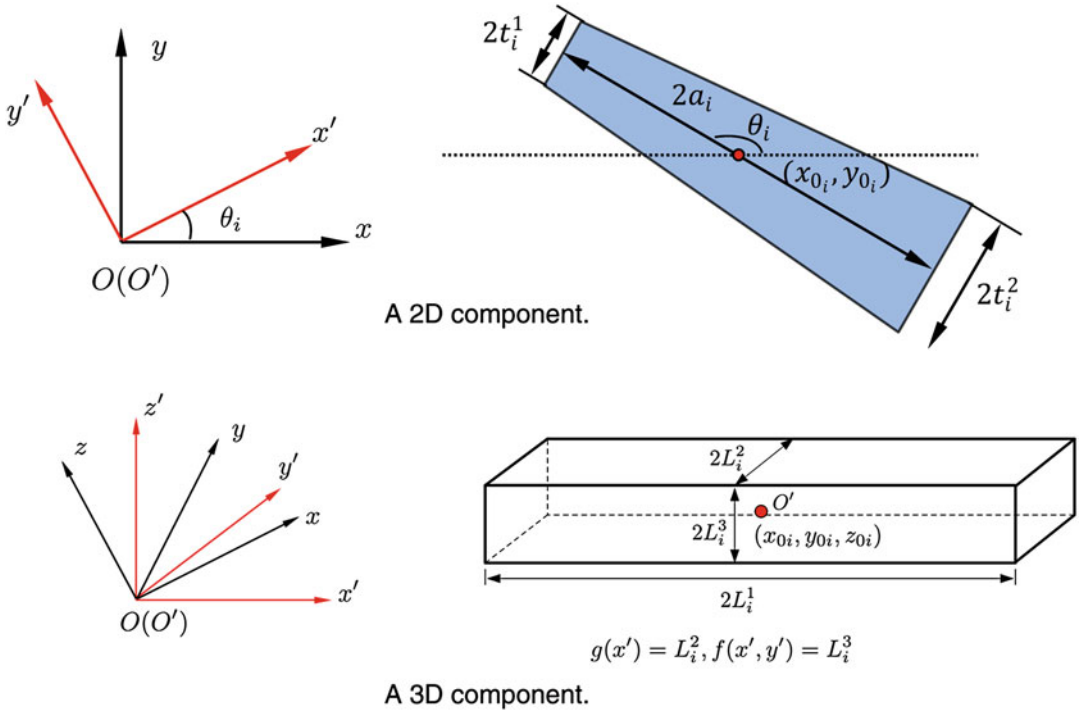

Fig. 2 The geometry description of a structural component

material distribution in a prescribed design domain, is transformed to a shape optimization problem.

Under the MMC-based solution framework, a typical topology optimization problem can be formulated as follows:

$$\begin{aligned}
&\text{Find}\quad \boldsymbol{D}=\left(\left(\boldsymbol{D}^1\right)^{\mathrm{T}},\ldots,\left(\boldsymbol{D}^i\right)^{\mathrm{T}},\ldots,\left(\boldsymbol{D}^n\right)^{\mathrm{T}}\right)^{\mathrm{T}}\\
&\text{Minimize}\quad I=I\left(\boldsymbol{D}\right)\\
&\text{S.t.}\\
&g_k\left(\boldsymbol{D}\right)\leq 0,\quad k=1\ldots,m,\\
&\boldsymbol{D}\subset \boldsymbol{U}_{\boldsymbol{D}},
\end{aligned}\tag{10}$$

where $I(\boldsymbol{D})$, g_k, $k=1,\ldots,m$ are the objective function/functional and constraint functions/functionals. $\mathbf{U}_{\boldsymbol{D}}$ is the admissible set of $\boldsymbol{D}$. For example, if structures are designed to minimize the structural compliance under the volume constraint of available solid material, the corresponding problem formulation can be specified as:

$$\begin{aligned}
&\text{Find}\quad \boldsymbol{D}=\left(\left(\boldsymbol{D}^1\right)^{\mathrm{T}},\ldots,\left(\boldsymbol{D}^i\right)^{\mathrm{T}},\ldots,\left(\boldsymbol{D}^n\right)^{\mathrm{T}}\right)^{\mathrm{T}},\\
&\quad \boldsymbol{u}(x)\in \boldsymbol{H}^1\left(\Omega^{\mathrm{s}}\right)\\
&\text{Minimize}\quad C=\int_{\mathrm{D}} H\left(\chi^{\mathrm{s}}\left(\boldsymbol{x};\boldsymbol{D}\right)\right)\boldsymbol{f}\cdot\boldsymbol{u}\mathrm{dV}\\
&\qquad\qquad +\int_{\Gamma_t}\boldsymbol{t}\cdot\boldsymbol{u}\mathrm{dS}\\
&\text{S.t.}\\
&\int_{D} H\left(\chi^{\mathrm{s}}\left(\boldsymbol{x};\boldsymbol{D}\right)\right)\boldsymbol{\varepsilon}\left(\boldsymbol{u}\right):\mathbb{E}:\boldsymbol{\varepsilon}\left(\boldsymbol{v}\right)\mathrm{dV}\\
&\qquad=\int_{D} H\left(\chi^{\mathrm{s}}\left(\boldsymbol{x};\boldsymbol{D}\right)\right)\boldsymbol{f}\cdot\boldsymbol{v}\mathrm{dV}+\int_{\Gamma_t}\boldsymbol{t}\cdot\boldsymbol{v}\mathrm{dS},\\
&\qquad\forall\boldsymbol{v}\in U_{\mathrm{ad}}\\
&\int_{\mathrm{D}} H\left(\chi^{\mathrm{s}}\left(\boldsymbol{x};\boldsymbol{D}\right)\right)\mathrm{dV}\leq\overline{V},\\
&\boldsymbol{D}\subset U_{\boldsymbol{D}},\\
&\boldsymbol{u}=\overline{\boldsymbol{u}},\quad \text{on}\ \Gamma_u,
\end{aligned}\tag{11}$$

where D, $\boldsymbol{f}$, $\boldsymbol{t}$, $\boldsymbol{u}$, $\boldsymbol{\varepsilon} = \text{sym}(\nabla \boldsymbol{u})$ and $\overline{\boldsymbol{u}}$ are the design domain, the body force density, the prescribed surface traction on Neumann boundary Γ_u, the displacement field, the linear strain tensor, and the prescribed displacement on Dirichlet boundary Γ_t, respectively. The symbol $H = H(s)$ denotes the Heaviside function with $H = 1$ if $s > 0$ and $H = 0$ otherwise. $\mathbb{E} = E^s/(1+\nu)[\mathbb{I} + \nu^s/(1-2\nu^s)\boldsymbol{\delta} \otimes \boldsymbol{\delta}]$ is the fourth order elasticity tensor of the isotropic solid material with E^s, ν^s, $\mathbb{I}$, and $\boldsymbol{\delta}$ denoting the Young's modulus as well as the Poisson's ratio of the solid material, symmetric part of the fourth order identity tensor, and the second order identity tensor, respectively. The symbol $U_{ad} = \left\{\boldsymbol{v} | \boldsymbol{v} \in \boldsymbol{H}^1(\Omega^s),\ \boldsymbol{v} = \boldsymbol{0} \text{ on } \Gamma_u\right\}$ represents the admissible set of virtual displacement vector $\boldsymbol{v}$ and $\overline{V}$ is the upper limit of the volume of the available solid material.

Sensitivity Analysis

In the section, the sensitivity analysis of the objective and constraint functions/functionals under the MMC-based solution framework will be discussed. Generally speaking, the well-established adjoint approach can be used to obtain the corresponding sensitivity information. The sensitivity of a general structural shape-related functional $I = I(\boldsymbol{D})$ with respect to a design variable a associated with χ_i (i.e., the TDF of the i-th component) can be written as

$$\frac{\partial I}{\partial a} = \int_{\mathrm{D}} f(\boldsymbol{u}, \boldsymbol{w}) \frac{\partial H_\varepsilon(\chi_i)}{\partial a} \mathrm{dV}, \quad i = 1, \ldots, n, \tag{12}$$

where $\boldsymbol{u}$ and $\boldsymbol{w}$ are the primary and adjoint displacement fields, $H_\varepsilon(x)$ is the regularized Heaviside function (Zhang et al. 2016b), respectively. When I is the structural compliance, it yields that $f(\boldsymbol{u}, \boldsymbol{w}) = \mathbb{E}{:}\boldsymbol{\varepsilon}(\boldsymbol{u}) : \boldsymbol{\varepsilon}(\boldsymbol{w})$ with $\boldsymbol{w} = -\boldsymbol{u}$ while $f(\boldsymbol{u}, \boldsymbol{w}) = 1$ when I is the volume of the structure. Furthermore

$$\frac{\partial H_\varepsilon(\chi_i)}{\partial a} = \delta_\varepsilon^i(\chi^s) \frac{\partial \chi_i}{\partial a} \tag{13}$$

with $\delta_\varepsilon(s) = \mathrm{d}H_\varepsilon(s)/\mathrm{d}s$ denoting the regularized Dirac delta function and $\delta_\varepsilon^i(\chi^s) = \min(\delta_\varepsilon(\chi_i), \delta_\varepsilon(\chi^s))$. The expressions of the sensitivities of χ_i with respect to each design variable are trivial and will not be repeated here. The readers are referred to Guo et al. (2014) and Zhang et al. (2016b) for the details.

Examples

In order to illustrate the effectiveness of the MMC-based method for topology optimization, a torsion beam example shown in Fig. 3 is considered. The geometry of the design domain, the boundary condition, and the external load are all depicted in Fig. 3. Four loads are imposed on four vertices of the right side of the design domain, respectively. The goal of this problem is to minimize the structural compliance considering the volume constraint (it is assumed $V \leq 0.15 \times |\mathrm{D}| = 28.8$ in this example).

The initial designs of the problem shown in Fig. 4 consist of 128 components. The total number of design variables in the MMC is only 1152, while there are about 98,304 design variables in traditional methods (if the design domain is discretized by $96 \times 32 \times 32$ meshes). Figure 5 plots the corresponding optimized structures obtained with use of MMC-based method. It is worth noting that the optimized structures obtained with MMC-based approach are actually pure black-and-white and contain no grey elements which are unavoidable in traditional approaches especially for 3D problems. Furthermore, since the optimized structures are described by a set of parameters of

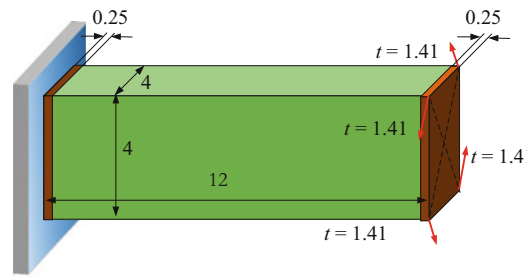

Fig. 3 The torsion beam example

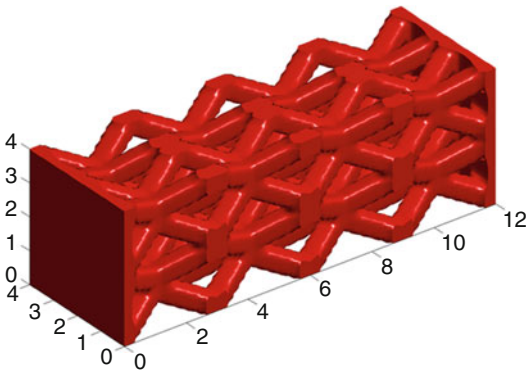

Fig. 4 The initial design for the torsion beam example by the MMC approach

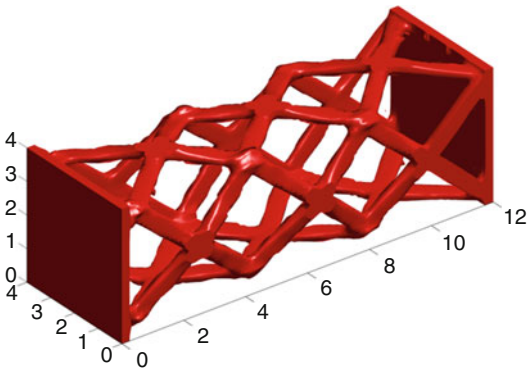

Fig. 5 Optimized structure for the torsion beam example obtained by the MMC approach

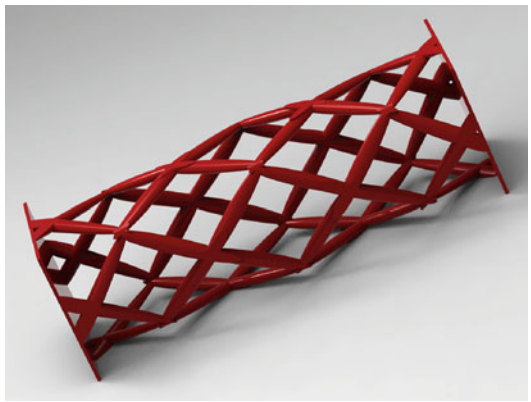

Fig. 6 Optimized structure obtained by the MMC approach plotted in CAD system

geometric meanings, the final results can import to CAD system directly as shown in Fig. 6.

Some Extensions

Topology optimization based on explicit geometry description has received more and more attention since the MMC approach was proposed by Guo et al. (2014). As a dual method of MMC, the MMV method was also developed by Zhang et al. (2017c). Takalloozadeh and Yoon (2017) proposed a topological derivative based method under the MMC-based solution framework. Due to the big potential in reducing the computational cost and providing explicit geometry information, MMC and MMV methods had also been extended to solve 3D topology optimization problems in Zhang et al. (2017a, b). Bujny et al. (2018) proposed to solve the crashing problem under the MMC framework with use of evolutionary algorithms. Zhang et al. (2016a), Hoang and Jang (2017), and Guo et al. (2017) solved the length scale control problem and the overhang angle control problem in additive manufacturing by the MMC/MMV methods, respectively. A successfully generalization of the MMC method was proposed by Sun et al. (2018a, b). In these works, the authors took the full advantages of the MMC method to solve topology optimization problems in flexible multibody systems. Inspired by the MMC method, Deng and Chen (2016) developed a connected morphable components (CMC) method to design flexible structures. Recently, Hou et al. (2017) introduced the isogeometric analysis scheme into the MMC-based solution framework to obtain higher accuracy structural response analysis. Zhang et al. (2018b) proposed a MMC-based method for solving the topology optimization problem with multiple materials. Topology optimization problem considering stress constraints was also discussed under the MMV-based framework in Zhang et al. (2018a).

Conclusions

Compared with the traditional SIMP and LSM approaches for structural topology optimization where a *fixed* ground structure is adopted, the MMC/MMV-based explicit topology optimization approaches actually represent a

new type of paradigm for structural topology optimization using *adaptive* ground structures. These approaches, in some sense, revival the classical shape optimization since in principle we can now use Lagrangian description-based shape optimization methods to solve topology optimization problems under the MMC/MMV-based solution framework. Possible future directions for developing explicit topology optimizations can be summarized as follows: (1) Topology optimization considering uncertainty. Since one has explicit boundary description in the MMC/MMV approaches, it is straightforward to consider the perturbation of structural boundary (possibly due to manufacturing error) by simply allowing the uncertainty of shape parameters describing the profiles of the components/voids. It is also more natural to considered fail-safe design (Zhou and Fleury 2016) in the MMC-based solution framework. (2) Data driven topology optimization. Since in the MMC/MMV-based solution framework the number of design variables is relatively small, the computational time associated with supervised learning or network construction can also be saved substantially as shown in Lei et al. (2019). (3) Topology optimization via hybrid explicit/implicit approaches. As demonstrated in Liu et al. (2018), the explicit MMC-based approach can be degenerated into the classical SIMP approach if multidomain strategy is employed. Therefore, it is highly promising to develop some hybrid approaches which can take both advantages of the explicit and implicit geometry description-based solution frameworks.

References

Allaire G, Jouve F, Toader AM (2004) Structural optimization using sensitivity analysis and a level-set method. J Comput Phys 194(1):363–393

Bendsøe MP (1989) Optimal shape design as a material distribution problem. Struct Optim 1(4):193–202

Bujny M, Aulig N, Olhofer M, Duddeck F (2018) Identification of optimal topologies for crashworthiness with the evolutionary level set method. Int J Crashworthiness 23(4):395–416

Deng JD, Chen W (2016) Design for structural flexibility using connected morphable components based topology optimization. Sci China Technol Sci 59(6): 839–851

Guo X, Zhang WS, Zhong WL (2014) Doing topology optimization explicitly and geometrically—a new moving morphable components based framework. Am Soc Mech Eng 81:081009-1–081009-12

Guo X, Zhang WS, Zhang J, Yuan J (2016) Explicit structural topology optimization based on moving morphable components (MMC) with curved skeletons. Comput Methods Appl Mech Eng 310:711–748

Guo X, Zhou JH, Zhang WS, Du ZL, Liu C, Liu Y (2017) Self-supporting structure design in additive manufacturing through explicit topology optimization. Comput Methods Appl Mech Eng 323:27–63

Hoang VN, Jang GW (2017) Topology optimization using moving morphable bars for versatile thickness control. Comput Methods Appl Mech Eng 317:153–173

Hou WB, Gai YD, Zhu XF, Wang X, Zhao C, Xu LK, Jiang K, Hu P (2017) Explicit isogeometric topology optimization using moving morphable components. Comput Methods Appl Mech Eng 326:694–712

Hur J, Kang P, Youn SK (2017) Topology optimization based on spline-based meshfree method using topological derivatives. J Mech Sci Technol 31:2423–2431

Lei X, Liu C, Du ZL, Zhang WS, Guo X (2019) Machine learning-driven real-time topology optimization under moving morphable component-based framework. Am Soc Mech Eng 86:011004-1–011004-9

Liu C, Zhu YC, Sun Z, Li DD, Du ZL, Zhang WS, Guo X (2018) An efficient moving morphable component (MMC)-based approach for multi-resolution topology optimization. Struct Multidiscip Optim 58(6): 2455–2479

Norato JA, Bell BK, Tortorelli DA (2015) A geometry projection method for continuum-based topology optimization with discrete elements. Comput Methods Appl Mech Eng 293:306–327

Sun JL, Tian Q, Hu HY (2018a) Topology optimization of a three-dimensional flexible multibody system via moving morphable components. J Comput Nonlinear Dyn 13(2):021010-1–021010-11

Sun JL, Tian Q, Hu HY, Pedersen NL (2018b) Topology optimization of a flexible multibody system with variable-length bodies described by ALE–ANCF. Nonlinear Dyn 93(2):413–441

Takalloozadeh M, Yoon GH (2017) Implementation of topological derivative in the moving morphable components approach. Finite Elem Anal Des 134: 16–26

Wang MY, Wang X, Guo D (2003) A level set method for structural topology optimization. Comput Methods Appl Mech Eng 192(1–2):227–246

Zhang WS, Li D, Zhang J, Guo X (2016a) Minimum length scale control in structural topology optimization based on the moving morphable components (MMC)

approach. Comput Methods Appl Mech Eng 311: 327–355
Zhang WS, Yuan J, Zhang J, Guo X (2016b) A new topology optimization approach based on moving morphable components (MMC) and the ersatz material model. Struct Multidiscip Optim 53(6):1243–1260
Zhang WS, Li D, Yuan J, Song JF, Guo X (2017a) A new three-dimensional topology optimization method based on moving morphable components (MMCs). Comput Mech 59:647–665
Zhang WS, Chen JS, Zhu XF, Zhou JH, Xue DC, Lei X, Guo X (2017b) Explicit three dimensional topology optimization via moving morphable void (MMV) approach. Comput Methods Appl Mech Eng 322: 590–614
Zhang WS, Yang WY, Zhou JH, Li D, Guo X (2017c) Structural topology optimization through explicit boundary evolution. Am Soc Mech Eng 84:011011-1–011011-10
Zhang WS, Li D, Zhou JH, Du ZL, Li BJ, Guo X (2018a) A moving morphable void (MMV)-based explicit approach for topology optimization considering stress constraints. Comput Methods Appl Mech Eng 334:381–413
Zhang WS, Song JF, Zhou JH, Du ZL, Zhu YC, Sun Z, Guo X (2018b) Topology optimization with multiple materials via moving morphable component (MMC) method. Int J Numer Methods Eng 113(11):1653–1675
Zhou M, Fleury R (2016) Fail-safe topology optimization. Struct Multidiscip Optim 54(5):1225–1243
Zhou M, Rozvany GIN (1991) The COC algorithm. Part II: topological, geometrical and generalized shape optimization. Comput Methods Appl Mech Eng 89(1–3):309–336

Transient Surface Waves of Strong and Weak Discontinuity

▸ Surface Wave Propagation in 3D Medium

Transient Wave Propagation

▸ Dynamic Equations, Verification of Hyperbolicity via the Theory of Discontinuities

Transient Waves in Cosserat Beams: Ray Expansion Approach

Yury A. Rossikhin and Marina V. Shitikova
Research Center on Dynamics of Solids and Structures, Voronezh State Technical University, Voronezh, Russia
Research Center for Wave Dynamics of Solids and Structures, Voronezh State Technical University, Voronezh, Russia

Synonyms

Micropolar elasticity; Pseudo-continuum Cosserat; Thin-walled beams of open profile

Definition

The theory of propagation of transient waves (surfaces of strong discontinuity) in thin-walled beams of open profiles with Cosserat-type microstructure is presented, resulting in the data comparable with those corresponding to transient wave propagation in the three-dimensional Cosserat continuum.

Backgrounds and Some Historical Remarks

It is well known that in order to generalize the Bernoulli-Euler beam model, Stephen Timoshenko in his Russian publication (Timoshenko 1916), which is more known worldwide by its English publication (Timoshenko 1921), introduced into consideration two independent functions, namely, the displacement of the center of gravity of the cross section and the rotation of the cross section with respect to the longitudinal central axis, i.e., he suggested to consider the angle of transverse shear as an

Yury A. Rossikhin: deceased.

independent variable. It was a starting point for deduction of two hyperbolic differential equations describing the dynamic behavior of a beam. As a result, two transient waves propagate in the Timoshenko beam with finite velocities: the longitudinal wave with the velocity $G_L = \sqrt{E/\rho}$ and the wave of transverse shear with the velocity $G_T = \sqrt{k\mu/\rho}$, where E and μ are elastic moduli, ρ is the density, and k is the so-called shear coefficient, which, generally speaking, depends on the geometry of the beam's cross section and could not be determined experimentally. In the Bernoulli-Euler beam, the wave of transverse shear does not propagate.

Since there are a lot of difficulties in the coefficient k experimental measurement, then different researchers accepted different magnitudes of this value (Grigoluk and Selezov 1973). Thus, Reissner (1944) and Ambartsumyan (1967) used the magnitude of 5/6, Timoshenko (1916, 1921) accepted 2/3 or 8/9, Uflyand (1948) utilized 2/3, Mindlin (1951) suggested to vary the coefficient k from 0.76 to 0.91 with the variation of Poisson's ratio from 0 to 0.5, some researchers prefer to use the value of $k = \pi^2/12$, and so on.

The secret of persistence of S.P. Timoshenko ideas lies in the fact that in engineering practice, it is often necessary to face with dynamic processes occurring in thin bodies which are dealing with the propagation of transient strain waves. The matter in question is the strain initiated by the impact response or by other means in some domain of a thin body and then transmitted in different directions along the medium surface. In these problems it is very important to consider the influence of transverse forces, the transmission of which occurs by virtue of waves of transverse shear. These waves are absent in classical models describing the dynamic response of thin bodies.

All enumerated above nonclassical theories (Grigoluk and Selezov 1973) involve the shear coefficient k, which is not determined experimentally, but this coefficient allows one to define the velocity of the transient wave of transverse shear. An engineer could bear with one uncertain coefficient and one shear wave. But when Korbut and Lazarev (1974) decided to extend the ideas of S.P. Timoshenko on thin-walled beams of open profile, then their attempts resulted in the generation of three types of transient shear waves propagating with different velocities depending on geometric characteristics of cross sections of thin-walled beams. Then the question arises of whether such a theory is practical. It significantly complexifies the solution of engineering problems. As for the experimental verification of this theory, then it occurs to be intricate due to the presence of three types of transient shear waves, the velocities of which depend on the choice of the beam's cross section. Note that, despite of shear waves, in a thin-walled beam of open profile, there exists only one longitudinal wave, which is a longitudinal-flexural-warping wave propagating with the velocity $\sqrt{E/\rho}$ independent on the geometry of the beam's cross section.

Contradictions brought to light in Korbut-Lazarev approach (Korbut and Lazarev 1974), as well as in approaches by other researchers, the detailed analysis of which is presented in Chap. 2 of Rossikhin and Shitikova (2011), point out their inconsistency. The critical review of different approaches for constructing hyperbolic equations for thin-walled beams of open cross section has been done in Rossikhin and Shitikova (2011), wherein a simple method of checking the correctness of equations for different dynamic systems was suggested for the first time using the theory of discontinuities.

This brings up a question: whether it is possible to develop such a theory of dynamic behavior of thin-walled beams of open profile which admits the propagation instead of three shear waves only of one rotational-shear wave propagating with the velocity $\sqrt{\mu/\rho}$ independent on the geometric characteristics of the beam's cross section, as in the case of the longitudinal-flexural-warping wave.

Such a theory considering the rotary inertia and transverse shear deformations, as well as variations in the width of a beam, has being carried out since 2009 by Rossikhin and Shitikova. Contrary to the approaches based on the Timoshenko ideas, this new theory of thin-walled beams is based only on physical and mechanical constants of the material, from which the beam is made of, and it is not burdened by additional "artificial" coefficients. The results were published in the SpringerBrief Series (Rossikhin and

Shitikova 2011). In 2012 it has been generalized for the dynamic response of a thermoelastic spatially curved thin-walled beam of an open profile with coupled strain and temperature fields (Rossikhin and Shitikova 2012).

The authors of the new theory started from the three-dimensional theory of linear elasticity, but unlike the classical approach, wherein the solution is represented as a sum of infinite power series in terms of a coordinate measured along the normal to the middle surface, they utilized the theory of discontinuities and the ray series constructed behind the fronts of transient waves (surfaces of strong discontinuities). In order to determine the ray series coefficients for thin-walled bodies, the recurrent sets of first-order differential equations with respect to derivatives along the rays were deduced with the help of the modified Hadamard-Thomas conditions of compatibility (Rossikhin and Shitikova 1995). Arbitrary functions obtained during integration of recurrent equations and involved in the coefficients of the ray series are determined by initial and boundary conditions. The developed approach allows one to solve boundary-value problems dealing with nonstationary excitations on thin bodies, such as impacts, different kinds of force and velocity excitations, and so on.

The creation of a simple calculating scheme for the strength analysis of thin bodies and first of all of thin-walled beams of open profile under transient dynamic loads is a serious problem, which is under consideration by researchers over a century. Since in our daily life we are surrounded by structures involving thin bodies as elements, overlapping plates, train metals, suspension bridges and roofs, and different types of bridges and viaducts as examples, then the study of their dynamic response and development of a calculating procedure for their strength analysis is of fundamental importance.

In the present entry, a new wave theory of thin-walled beams of open profile with Cosserat-type microstructure is presented based on the approach proposed in Rossikhin and Shitikova (2011) for prestressed spatially curved elastic thin-walled beams of open profile. The aim is to create the theory of propagation of transient waves (surfaces of strong discontinuity) in thin-walled beams of open profile, which should be quite different from Timoshenko-like theories, resulting in the data comparable with those corresponding to transient wave propagation in the three-dimensional Cosserat continuum.

Problem Formulation

The dynamical behavior of a three-dimensional Cosserat continuum is described by the following set of equations (Nowacki 1962, 1986):

$$\sigma_{ij} = \lambda u_{k,k}\delta_{ij} + \mu(u_{i,j} + u_{j,i}) + \alpha(u_{i,j} - u_{j,i} - 2\in_{kij}\psi_k), \quad (1)$$

$$\mu_{ij} = \beta\psi_{k,k}\delta_{ij} + \gamma(\psi_{i,j} + \psi_{j,i}) + \varepsilon(\psi_{i,j} - \psi_{j,i}), \quad (2)$$

$$\sigma_{ij,j} = \rho\dot{v}_i, \quad (3)$$

$$\mu_{ij,j} + \in_{ijk}\sigma_{jk} = J\dot{\omega}_i, \quad (4)$$

where σ_{ij} is the stress tensor; μ_{ij} is the moment stress tensor; $\in_{kij}$ are the Levi-Civita tensor components; u_i is the displacement vector; $v_i = \dot{u}_i$ is the velocity vector; a dot denotes a time derivative; an index after a coma labels a derivative with respect to the corresponding coordinate; ψ_i is the angular rotation vector; $\omega_i = \dot{\psi}_i$ is the angular velocity vector; ρ is the density; δ_{ij} is Kronecker's symbol; J is the moment of inertia; λ, μ, α, β, γ, and ε are material constants; and x_i ($i = 1, 2, 3$) are Cartesian coordinates.

Suppose now that a wave surface of strong discontinuity propagates with a normal velocity G in a thin-walled beam of open profile with a Cosserat-type microstructure (Fig. 1), i.e., the wave surface at each instant of moment is normal to the axial line of the beam.

For the ease of further treatment, let us introduce two sets of coordinates: λ , τ, ξ with the unit vectors $\boldsymbol{\lambda}\{\lambda_i\}$, $\boldsymbol{\tau}\{\tau_i\}$, and $\boldsymbol{\xi}\{\xi_i\}$ and λ, x, y with the unit vectors $\boldsymbol{\lambda}$, $\mathbf{k}\{k_i\}$, and $\mathbf{s}\{s_i\}$. The axes λ, τ, ξ are the natural axes for the curved axis of the beam; in so doing the λ-axis is the tangent to the beam's axis, the τ-axis is its binormal, the ξ-axis is its main normal, and s is the arc

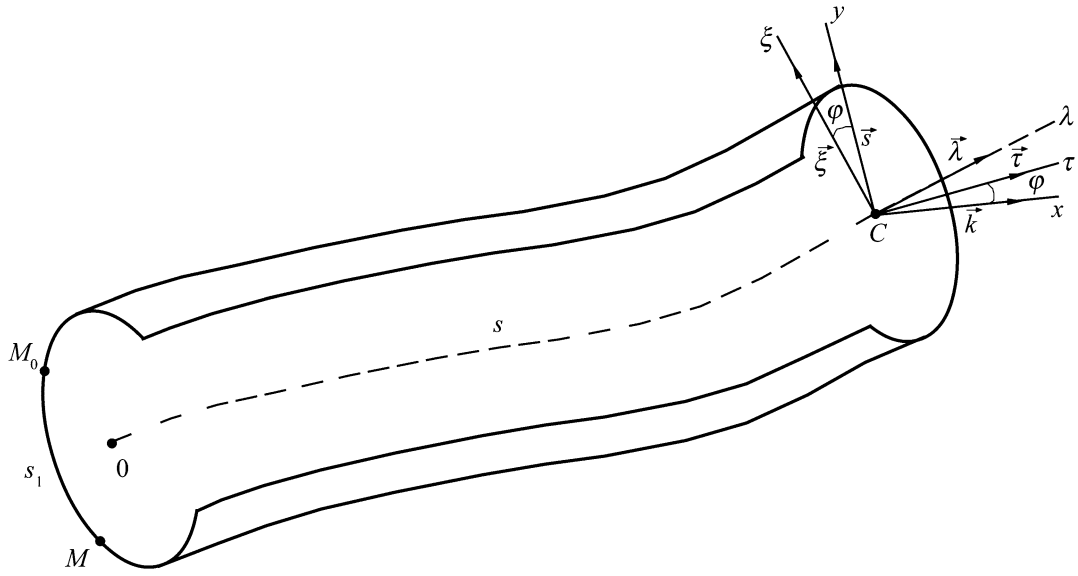

Fig. 1 Scheme of a spatially curved thin-walled beam of open profile of arbitrary cross section

length calculated from a certain point with the coordinate s_0 along the beam axis (Fig. 1), while the $x-$ and $y-$axes are the main central axes of the beam's normal section, and $\varphi(s)$ is the angle between the x- and τ-axes (y- and ξ-axes).

In order to obtain the dynamic condition of compatibility, it is necessary to use equations of motion (3) and (4), as well as the conditions of compatibility of the mixed type which are derived from the geometric conditions of compatibility (Thomas 1961)

$$[Z_{,i}] = B\lambda_i + \frac{\partial [Z]}{\partial x} k_i + \frac{\partial [Z]}{\partial y} s_i, \qquad (5)$$

and kinematic conditions of compatibility (Thomas 1961)

$$[\dot{Z}] = -BG + \frac{\delta [Z]}{\delta t}, \qquad (6)$$

where Z is the desired value, $[Z] = Z^+ - Z^-$, "+" and "−" denote that the given value is calculated ahead of and behind the surface of discontinuity, respectively, $B = [Z_{,i}]\lambda_i$, λ_i are components of the unit vector normal to the wave surface, k_j and s_j are components of the unit vectors tangential to the wave surface (Fig. 1), and $\delta/\delta t$ is the Thomas δ-derivative (Thomas 1961) which could be represented as follows:

$$\frac{\delta [Z]}{\delta t} = G \frac{d[Z]}{ds}.$$

After eliminating B from (5) and (6), the condition of compatibility of the "mixed" type could be obtained (Rossikhin and Shitikova 1995):

$$[Z_{,i}] = -G^{-1} [\dot{Z}] \lambda_i + \frac{d[Z]}{ds} \lambda_i + \frac{\partial [Z]}{\partial x} k_i + \frac{\partial [Z]}{\partial y} s_i. \qquad (7)$$

Substituting the value Z in formula (7) with the values σ_{ij}, μ_{ij}, u_i, and $u_{i,j}$ yields

$$[\sigma_{ij,l}] = -G^{-1} [\dot{\sigma}_{ij}] \lambda_l + \frac{d[\sigma_{ij}]}{ds} \lambda_l + \frac{\partial [\sigma_{ij}]}{\partial x} k_l + \frac{\partial [\sigma_{ij}]}{\partial y} s_l, \qquad (8)$$

$$[\mu_{ij,l}] = -G^{-1} [\dot{\mu}_{ij}] \lambda_l + \frac{d[\mu_{ij}]}{ds} \lambda_l + \frac{\partial [\mu_{ij}]}{\partial x} k_l + \frac{\partial [\mu_{ij}]}{\partial y} s_l, \qquad (9)$$

$$[e_{il}] = \left[u_{i,l}\right] = -G^{-1}\,[\dot{u}_i]\,\lambda_l + \frac{d\,[u_i]}{ds}\,\lambda_l + \frac{\partial\,[u_i]}{\partial x}\,k_l + \frac{\partial\,[u_i]}{\partial y}\,s_l, \tag{10}$$

$$\left[e_{il,j}\right] = \left[u_{i,lj}\right] = -G^{-1}\,[\dot{e}_{il}]\,\lambda_j + \frac{d[e_{il}]}{ds}\,\lambda_j + \frac{\partial\,[e_{il}]}{\partial x}\,k_j + \frac{\partial\,[e_{il}]}{\partial y}\,s_j. \tag{11}$$

Determination of Transient Wave Velocities Propagating in Thin-Walled Beams with Cosserat-Type Microstructure

Since the dynamic stability of thin-walled beams is often studied with respect to nonstationary excitations and particularly under impact loads which originate transient waves (surfaces of strong discontinuity), then in the further treatment, it is convenient to interpret the wave surface as a layer of small width δ, inside which the desired values Z change monotonically and continuously from the magnitudes Z^- to magnitudes Z^+.

Further it is assumed that the forward front of the shock layer arrives at the fixed point M with the coordinate s at the moment t while the back front at the moment $t+\Delta t$. Then with due account for (8), (9), (10), and (11), Eqs. (3) and (4) take the form

$$-G^{-1}\dot{\sigma}_{ij}\lambda_j + \frac{d\sigma_{ij}}{ds}\,\lambda_j + \frac{\partial\sigma_{ij}}{\partial x}\,k_j + \frac{\partial\sigma_{ij}}{\partial y}\,s_j = \rho\dot{v}_i, \tag{12}$$

$$-G^{-1}\dot{\mu}_{ij}\lambda_j + \frac{d\mu_{ij}}{ds}\,\lambda_j + \frac{\partial\mu_{ij}}{\partial x}\,k_j + \frac{\partial\mu_{ij}}{\partial y}\,s_j + \varepsilon_{kji}\sigma_{jk} = J\dot{\omega}_i. \tag{13}$$

Equations (12) and (13) have been derived considering that Rossikhin and Shitikova (2011)

$$\frac{d\lambda_i}{ds} = -k_i æ \sin\varphi(s) + s_i æ \cos\varphi(s), \tag{14}$$

$$\frac{dk_i}{ds} = -s_i(K+\tau) + æ\lambda_i \sin\varphi(s), \tag{15}$$

$$\frac{ds_i}{ds} = k_i(K+\tau) - æ\lambda_i \cos\varphi(s), \tag{16}$$

where $K = d\varphi/ds$, $æ(s)$ and $\tau(s)$ are the curvature and the torsion of the beam's axis, respectively.

In order to obtain relationships (14), (15), and (16), it is sufficient to differentiate with respect to s the relationships coupling the vector components ξ_i, τ_i with k_i, s_i:

$$\xi_i = -k_i \sin\varphi + s_i \cos\varphi, \tag{17}$$

$$\tau_i = k_i \cos\varphi + s_i \sin\varphi, \tag{18}$$

and to consider the Frenet formulas (Rossikhin and Shitikova 2011):

$$\frac{d\xi_i}{ds} = \tau\tau_i - æ\lambda_i, \quad \frac{d\tau_i}{ds} = -\tau\xi_i, \quad \frac{d\lambda_i}{ds} = æ\xi_i. \tag{19}$$

Integrating Eqs. (12) and (13) over t from t to $t+\Delta t$, tending then $\Delta \to 0$ and considering that

$$[u_i] = 0, \tag{20}$$

it could be found that

$$[\sigma_{ij}]\lambda_j = -\rho G[v_i], \tag{21}$$

$$[\mu_{ij}]\lambda_j = -JG[\omega_i]. \tag{22}$$

Now let us add components of the force and moment stresses to dynamic conditions of compatibility utilizing the following conditions of compatibility involving the terms considering transverse deformations resulting in changes in the thickness of a thin body (which could be named as the compatibility conditions for thin bodies) (Rossikhin and Shitikova 2011, 2007):

$$\left[u_{i,j}\right] = -G^{-1}\,[v_i]\,\lambda_j + \left[\frac{\partial u_i k_j}{\partial x}\right] + \left[\frac{\partial u_i s_j}{\partial y}\right], \tag{23}$$

T

$$\left[\psi_{i,j}\right] = -G^{-1}\left[\omega_i\right]\lambda_j + \left[\frac{\partial \psi_i k_j}{\partial x}\right] + \left[\frac{\partial \psi_i s_j}{\partial y}\right], \tag{24}$$

which are distinct from the Hadamard conditions of compatibility:

$$\left[u_{i,j}\right] = -G^{-1}\left[v_i\right]\lambda_j, \tag{25}$$

$$\left[\psi_{i,j}\right] = -G^{-1}\left[\omega_i\right]\lambda_j. \tag{26}$$

The difference between the Hadamard compatibility conditions (25) and (26) and the compatibility conditions (23) and (24) has the principal character depending on an object under investigation. In the first case, a transient wave propagates in a three-dimensional unbounded medium. In the second case, a transient wave propagates in a thin body, wherein longitudinal deformations could generate transverse deformations, resulting in changes in the thickness of the thin body. Allowance for the transverse deformations is carried out by the new additional terms in (23) and (24) as compared with (25) and (26).

As a result of utilization of (23) and (24) in Eqs. (1) and (2), it is found

$$\begin{aligned}
[\sigma_{ij}] = {} & -\lambda G^{-1}\zeta\delta_{ij} - \mu G^{-1}\left([v_i]\lambda_j + [v_j]\lambda_i\right) \\
& + \alpha G^{-1}\left([v_j]\lambda_i - [v_i]\lambda_j\right) \\
& + \mu\left(\left[\frac{\partial u_i k_j}{\partial x}\right]\left[\frac{\partial u_j k_i}{\partial x}\right] \right. \\
& \left. + \left[\frac{\partial u_i s_j}{\partial y}\right] + \left[\frac{\partial u_j s_i}{\partial y}\right]\right) \\
& + \lambda\left([E_x] + [E_y]\right)\delta_{ij} \\
& + \alpha\left(\left[\frac{\partial u_i k_j}{\partial x}\right] - \left[\frac{\partial u_j k_i}{\partial x}\right] \right. \\
& \left. + \left[\frac{\partial u_i s_j}{\partial y}\right] - \left[\frac{\partial u_j s_i}{\partial y}\right]\right), \qquad (27) \\
[\mu_{ij}] = {} & -\beta G^{-1}\omega_\lambda\delta_{ij} - \gamma G^{-1}\left([\omega_i]\lambda_j + [\omega_j]\lambda_i\right) \\
& + \varepsilon G^{-1}\left([\omega_j]\lambda_i - [\omega_i]\lambda_j\right) \\
& + \gamma\left(\left[\frac{\partial \psi_i k_j}{\partial x}\right] + \left[\frac{\partial \psi_j k_i}{\partial x}\right] \right. \\
& \left. + \left[\frac{\partial \psi_i s_j}{\partial y}\right] + \left[\frac{\partial \psi_j s_i}{\partial y}\right]\right) \\
& + \beta\left([e_x] + [e_y]\right)\delta_{ij} \\
& + \varepsilon\left(\left[\frac{\partial \psi_i k_j}{\partial x}\right] - \left[\frac{\partial \psi_j k_i}{\partial x}\right] \right. \\
& \left. + \left[\frac{\partial \psi_i s_j}{\partial y}\right] - \left[\frac{\partial \psi_j s_i}{\partial y}\right]\right), \qquad (28)
\end{aligned}$$

where $\zeta = [v_i]\lambda_i$, $\omega_\lambda = [\omega_i]\lambda_i$,

$$[E_x] = \left[\frac{\partial u_i k_i}{\partial x}\right] = \left[\frac{\partial u_x}{\partial x}\right],$$

$$[E_y] = \left[\frac{\partial u_i s_i}{\partial y}\right] = \left[\frac{\partial u_y}{\partial y}\right],$$

$$[e_x] = \left[\frac{\partial \psi_i k_i}{\partial x}\right] = \left[\frac{\partial \psi_x}{\partial x}\right],$$

$$[e_y] = \left[\frac{\partial \psi_i s_i}{\partial y}\right] = \left[\frac{\partial \psi_y}{\partial y}\right].$$

Assume that the lateral surface of a thin-walled beam of open profile is free from stresses and moment stresses. In this case, the following relationships are valid:

$$[\sigma_{ij}]k_i k_j = [\sigma_{ij}]s_i s_j = [\sigma_{ij}]s_i k_j = 0, \tag{29}$$

$$[\mu_{ij}]k_i k_j = [\mu_{ij}]s_i s_j = [\mu_{ij}]s_i k_j = 0. \tag{30}$$

From relationships (29), it could be obtained

$$(\lambda + 2\mu)[E_x] + \lambda[E_y] = \lambda G^{-1}\zeta, \tag{31}$$

$$\lambda[E_x] + (\lambda + 2\mu)[E_y] = \lambda G^{-1}\zeta, \tag{32}$$

$$\left[\frac{\partial u_i s_i}{\partial x}\right] = \left[\frac{\partial u_y}{\partial x}\right] = 0,$$

$$\left[\frac{\partial u_i k_i}{\partial y}\right] = \left[\frac{\partial u_x}{\partial y}\right] = 0. \tag{33}$$

The solution of Eqs. (31) and (32) has the form

$$[E_x] = [E_y] = G^{-1}\frac{\lambda}{2(\lambda + \mu)}\zeta. \tag{34}$$

From relationships (30), it could be found

$$(\beta + 2\gamma)[e_x] + \beta[e_y] = \beta G^{-1}\,\omega_\lambda, \tag{35}$$

$$\beta[e_x] + (\beta + 2\gamma)[e_y] = \beta G^{-1}\,\omega_\lambda, \tag{36}$$

$$\left[\frac{\partial \psi_i s_i}{\partial x}\right] = \left[\frac{\partial \psi_y}{\partial x}\right] = 0,$$
$$\left[\frac{\partial \psi_i k_i}{\partial y}\right] = \left[\frac{\partial \psi_x}{\partial y}\right] = 0. \tag{37}$$

The solution of the set of Eqs. (35) and (36) has the form

$$[e_x] = [e_y] = G^{-1}\,\frac{\beta}{2(\beta+\gamma)}\,\omega_\lambda. \tag{38}$$

Substituting (34) in Eq. (27) and then multiplying by $\lambda_i\lambda_j$ yield

$$\left[\sigma_{ij}\right]\lambda_i\lambda_j = -\frac{\mu(3\lambda+2\mu)}{\lambda+\mu}\,G^{-1}\zeta,$$

or

$$\left[\sigma_{ij}\right]\lambda_i\lambda_j = -E\,G^{-1}\zeta. \tag{39}$$

From the dynamic condition of compatibility (21), it follows that

$$G\left[\sigma_{ij}\right]\lambda_i\lambda_j = -\rho G^2\zeta. \tag{40}$$

From relationships (39) and (40), the velocity of the first wave could be obtained:

$$G_1 = \sqrt{\frac{E}{\rho}}, \quad \zeta = [v_i]\,\lambda_i \neq 0, \tag{41}$$

where E is the elastic modulus.

Multiplying Eq. (27) sequentially by $\lambda_j k_i$ and $\lambda_j s_i$ and multiplying the dynamic condition of compatibility (21) sequentially k_i and s_i with due account for (34) and (38), the following equations could be derived:

$$\left[\sigma_{ij}\right]\lambda_j k_i = -(\mu+\alpha)\,G^{-1}\xi, \tag{42}$$

$$G\left[\sigma_{ij}\right]\lambda_j k_i = -\rho G^2\xi, \tag{43}$$

$$\left[\sigma_{ij}\right]\lambda_j s_i = -(\mu+\alpha)\,G^{-1}\eta, \tag{44}$$

$$G\left[\sigma_{ij}\right]\lambda_j s_i = -\rho G^2\eta, \tag{45}$$

whence it follows that

$$G_2 = \sqrt{\frac{\mu+\alpha}{\rho}}, \quad \xi = [v_i]\,k_i \neq 0,$$
$$\eta = [v_i]\,s_i \neq 0. \tag{46}$$

Substituting (38) in Eq. (28) and then multiplying by $\lambda_i\lambda_j$ yield

$$\left[\mu_{ij}\right]\lambda_i\lambda_j = -\frac{\gamma(3\beta+2\gamma)}{\beta+\gamma}\,G^{-1}\omega_\lambda$$

or

$$\left[\mu_{ij}\right]\lambda_i\lambda_j = -e\,G^{-1}\omega_\lambda, \quad e = \frac{\gamma(3\beta+2\gamma)}{\beta+\gamma}. \tag{47}$$

From the dynamic condition of compatibility (22), it follows that

$$G\left[\mu_{ij}\right]\lambda_i\lambda_j = -J\,G^2\omega_\lambda. \tag{48}$$

From relationships (47) and (48), it could be finally obtained the velocity of the third wave:

$$G_3 = \sqrt{\frac{e}{J}}, \quad \omega_\lambda = [\omega_i]\,\lambda_i \neq 0. \tag{49}$$

Multiplying Eq. (28) sequentially by $\lambda_j k_i$ and $\lambda_j s_i$ and multiplying the dynamic condition of compatibility (22) sequentially k_i and s_i with due account for (34) and (38) yield the following equations:

$$\left[\mu_{ij}\right]\lambda_j k_i = -(\gamma+\varepsilon)\,G^{-1}\omega_x, \tag{50}$$

$$G\left[\mu_{ij}\right]\lambda_j k_i = -J\,G^2\omega_x, \tag{51}$$

$$\left[\mu_{ij}\right]\lambda_j s_i = -(\gamma+\varepsilon)\,G^{-1}\omega_y, \tag{52}$$

$$G\left[\mu_{ij}\right]\lambda_j s_i = -J\,G^2\omega_y, \tag{53}$$

whence it follows that

$$G_4 = \sqrt{\frac{\gamma + \varepsilon}{J}}, \quad \omega_x = [\omega_i]\, k_i \neq 0,$$
$$\omega_y = [\omega_i]\, s_i \neq 0. \tag{54}$$

Thus, the four types of waves, the characteristics of which are defined by relationships (41), (46), (49), and (54), have been found. The first wave propagating with the velocity G_1 is a quasi-longitudinal wave, the second is a quasi-shear wave propagating with the velocity G_2, and the third is a quasi-rotational wave travelling with the velocity G_3, while the fourth one is a quasi-flexural wave propagating with the velocity G_4. The prefix "quasi-" in the name of the wave points to the fact that the enumerated waves are the waves of the "mixed" type, i.e., along to the main components characterizing the type of the wave, other admixed components could be distinct from zero; however, they are at least of the higher order than the main components.

Note that for an elastic thin-walled beam of open profile, the coefficients α, β, γ, and ε are equal to zero, and thus from four waves only two waves remain, i.e.,

$$G_1 = \sqrt{\frac{E}{\rho}}, \qquad G_2 = \sqrt{\frac{\mu}{\rho}},$$

with which two transient waves propagate, namely, the quasi-longitudinal-flexural-warping wave wherein the values ζ, ω_x, and ω_y are nonzero and the quasi-shear-rotational wave on which the values ξ, η, and ω_λ are nonzero (Rossikhin and Shitikova 2011).

Determination of Transient Wave Velocities Propagating in a Cosserat Continuum

In Rossikhin and Shitikova (2015), it has been shown that velocities of the four transient waves propagating in the Cosserat continuum (1), (2), (3,) and (4) could be found using the same procedure which has been described above, but in this case with the help of the Hadamard conditions of compatibility (25) and (26):
For the quasi-longitudinal wave

$$G_1 = \sqrt{(\lambda + 2\mu)/\rho}, \quad [v_\lambda] \neq 0, \tag{55}$$
$$[v_x] = [v_y] = [\omega_\lambda] = [\omega_x] = [\omega_y] = 0;$$

For the quasi-shear wave

$$G_2 = \sqrt{(\mu + \alpha)/\rho}, \quad [v_x] \neq 0, \quad [v_y] \neq 0, \tag{56}$$
$$[v_\lambda] = [\omega_\lambda] = [\omega_x] = [\omega_y] = 0;$$

For the quasi-rotational wave

$$G_3 = \sqrt{(\beta + 2\gamma)/J}, \quad [\omega_\lambda] \neq 0, \tag{57}$$
$$[v_x] = [v_y] = [v_\lambda] = [\omega_x] = [\omega_y] = 0;$$

For the quasi-flexural wave

$$G_4 = \sqrt{(\gamma + \varepsilon)/J}, \quad [\omega_x] \neq 0, \quad [\omega_y] \neq 0, \tag{58}$$
$$[v_\lambda] = [\omega_\lambda] = [v_x] = [v_y] = 0.$$

From the comparison of velocities of transient waves propagating in thin-walled spatially curved beams of open profile and in the Cosserat continuum, it is seen that velocities G_2 and G_4 in both cases are the same, while velocities G_1 and G_3 are different.

Travelling waves in a three-dimensional Cosserat continuum were studied in Pal'mov (1964), wherein phase velocities were found. Asymptotic magnitudes of the phase velocities were defined for small and large magnitudes of the frequency. It has been shown that when the frequency tends to infinity, four waves propagate with the velocities of transient waves (55), (56), (57) and (58).

Table 1 Magnitudes of transient wave velocities in the Cosserat 3D continuum and Cosserat-type thin-walled structures

3D Cosserat continuum (Pal'mov 1964; Rossikhin and Shitikova 2015)	Thin-walled Cosserat shells (Rossikhin and Shitikova 2018)	Thin-walled Cosserat beams of open profile (Rossikhin and Shitikova 2015)
Quasi-longitudinal wave $G_1 = \sqrt{\frac{\lambda+2\mu}{\rho}}$	Quasi-longitudinal wave $G_1 = \sqrt{\frac{4\mu(\lambda+\mu)}{\rho(\lambda+2\mu)}} = \sqrt{\frac{E'}{\rho}}$	Quasi – longitudinal – flexural – warping wave $G_1 = \sqrt{\frac{E}{\rho}}$
Quasi-shear wave $G_2 = \sqrt{\frac{\mu+\alpha}{\rho}}$	Quasi-shear wave $G_2 = \sqrt{\frac{\mu+\alpha}{\rho}}$	Quasi-shear-rotational wave $G_2 = \sqrt{\frac{\mu+\alpha}{\rho}}$
Quasi-torsional wave due to microstructure $G_3 = \sqrt{\frac{\beta+2\gamma}{J}}$	Quasi-torsional wave due to microstructure $G_3 = \sqrt{\frac{4\gamma(\beta+\gamma)}{J(\beta+2\gamma)}} = \sqrt{\frac{e'}{J}}$	Quasi-torsional wave due to microstructure $G_3 = \sqrt{\frac{e}{J}}$
Quasi-flexural wave due to microstructure $G_4 = \sqrt{\frac{\gamma+\varepsilon}{J}}$	Quasi-flexural wave due to microstructure $G_4 = \sqrt{\frac{\gamma+\varepsilon}{J}}$	Quasi-flexural wave due to microstructure $G_4 = \sqrt{\frac{\gamma+\varepsilon}{J}}$

Conclusion

A new theory of thin-walled beams of open profile with Cosserat-type microstructure has been suggested based on the approach proposed in Rossikhin and Shitikova (2011) for prestressed spatially curved elastic thin-walled beam of open profile. The aim to create the theory of propagation of transient waves (surfaces of strong discontinuity) in thin-walled beams of open profile, which should be quite different from Timoshenko-like theories, resulting in the data comparable with those corresponding to transient wave propagation in the three-dimensional Cosserat continuum, has been achieved. The advantage of the developed approach lies in the fact that the found wave velocities depend only on material constants and are independent of any additional coefficients involving the geometry of thin bodies.

This conclusion is supported by Table 1, wherein the velocities of the transient waves propagating in the three-dimensional Cosserat continuum (Pal'mov 1964; Rossikhin and Shitikova 2015), in the Cosserat-type shell (Rossikhin and Shitikova 2018), and in thin-walled beams of open profile made of Cosserat-type materials (Rossikhin and Shitikova 2015, 2017) are presented. From Table 1 it is seen that all velocities depend only on material constants. Note that the micropolar longitudinal modulus $e = \frac{\gamma(3\beta+2\gamma)}{\beta+\gamma}$ was suggested in Rossikhin and Shitikova (2017) as the analog of the elastic longitudinal modulus $E = \frac{\mu(3\lambda+2\mu)}{\lambda+\mu}$, and the reduced micropolar modulus $e' = \frac{4\gamma(\beta+\gamma)}{\beta+2\gamma}$ was introduced in Rossikhin and Shitikova (2018) as the analog of the reduced modulus $E' = \frac{E}{1-\nu^2} = \frac{4\mu(\lambda+\mu)}{\lambda+2\mu}$ frequently used in the theory of elastic shells.

From the comparison of velocities of transient waves propagating in Cosserat-type thin shells and thin-walled spatially curved beams with those in the Cosserat continuum, it is seen that velocities G_2 and G_4 in all cases are the same, while velocities G_1 and G_3 are different. The same situation takes place for the case of the transient wave velocities in elastic shells and beams, which could be obtained from the corresponding magnitudes presented in Table 1 by vanishing to zero all additional Cosserat constants except Láme constants.

The knowledge of the velocities of transient waves in thin-walled beams of open profile made of Cosserat-type material will allow one to solve boundary-value transient dynamic problems resulting in the propagation of surfaces of strong and weak discontinuity. This could be carried out by the utilization of the theory of discontinuities

and further construction of the ray series behind the fronts of transient waves (surfaces of strong discontinuities). In order to determine the ray series coefficients for thin-walled bodies, the recurrent sets of first-order differential equations with respect to derivatives along the rays could be deduced with the help of the modified Hadamard-Thomas conditions of compatibility. Arbitrary functions obtained during integration of recurrent equations and involved in the coefficients of the ray series could be determined from initial and boundary conditions. The developed approach will allow one to solve boundary-value problems dealing with nonstationary excitations on thin bodies, such as impacts (Rossikhin and Shitikova 2017), different kinds of force and velocity excitations, and so on.

Cross-References

- ▸ Bernoulli, Daniel
- ▸ Cosserat, Eugène and François
- ▸ Euler, Leonhard
- ▸ Ray Expansion Theory
- ▸ Timoshenko, Stepan Prokofievitch

References

Ambartsumyan SA (1967) Theory of anisotropic plates (in Russian). Fizmatlit, Moscow

Grigoluk EI, Selezov IT (1973) Nonclassical theories of vibrations of rods, plates and shells (in Russian). Outputs in science and technology, series of mechanics of deformable solids, vol 5. VINITI, Moscow

Korbut VA, Lazarev VI (1974) Equations of flexural-torsional waves in thin-walled bars of open cross section. Sov Appl Mech 10(6):640–644

Mindlin RD (1951) Influence of rotary inertia and shear on flexural motions of isotropic, elastic plates. J Appl Mech 18(1):31–38

Nowacki W (1962) Theory of elasticity (in Polish). Państwowe Wydawnictwo Naukowe, Warszawa

Nowacki W (1986) Theory of asymmetric elasticity. Pergamon Press, Oxford

Pal'mov VA (1964) Fundamental equations of the theory of asymmetric elasticity. J Appl Math Mech 28(3): 496–505

Reissner E (1944) On the theory of bending of elastic plates. J Math Phys 23(4):184–191

Rossikhin YA, Shitikova MV (1995) Ray method for solving dynamic problems connected with propagation of wave surfaces of strong and weak discontinuities. Appl Mech Rev 48(1):1–39

Rossikhin YA, Shitikova MV (2007) The method of ray expansions for investigating transient wave processes in thin elastic plates and shells. Acta Mech 189: 87–121

Rossikhin YA, Shitikova MV (2011) Dynamic response of pre-stressed spatially curved thin-walled beams of open profile. Springer briefs in applied sciences and technology. Springer, Netherlands

Rossikhin YA, Shitikova MV (2012) Dynamic response of spatially curved thermoelastic thin-walled beams of generic open profile subjected to thermal shock. J Therm Stresses 35:205–234

Rossikhin YA, Shitikova MV (2015) Transient wave velocities in pre-stressed thin-walled beams of open profile with Cosserat-type micro-structure. Compos Part B Eng 83:323–332

Rossikhin YA, Shitikova MV (2017) A new approach for studying the transient response of thin-walled beams of open profile with Cosserat-type micro-structure. Comp Struct 169:153–166

Rossikhin YA, Shitikova MV (2018) Analysis of transient waves in Cosserat-type shells (in Russian). Uchenye Zapiski Komsomol'skogo-na-Amure Gosudarstvennogo Tehnicheskogo Universiteta 2(4)

Thomas TY (1961) Plastic flow and fracture in solids. Academic, New York

Timoshenko SP (1916) Course of theory of elasticity (in Russian). Part II. A.E. Kollins Publishing House, Petrograd

Timoshenko SP (1921) On the correction for shear of the differential equation for transverse vibrations of prismatic bar. Phil Mag Ser 6 41(245):744–746

Uflyand YaS (1948) Wave propagation under transverse vibrations of rods and plates (in Russian). Prikl Mat Mech 12(3):287–300

Transport Coefficients

- ▸ Kinetic Theory and Thermodynamics, Non-equilibrium Reacting Gas Flows

Trescas Solids

- ▸ Planar Ideal Plastic Flows

Truesdell, Clifford Ambrose III

Holm Altenbach[1] and Otto T. Bruhns[2]
[1]Lehrstuhl Technische Mechanik, Institut für Mechanik, Fakultät für Maschinenbau, Otto-von-Guericke-Universität Magdeburg, Magdeburg, Germany
[2]Institute of Mechanics, Ruhr-University Bochum, Bochum, Germany

Clifford Ambrose Truesdell III (*February 18th, 1919 in Los Angeles, CA, USA; †January 14th, 2000 in Baltimore, MD, USA) was a mathematician, natural philosopher, and historian of science.

Clifford Ambrose Truesdell III

Education

After high school, Truesdell spent 2 years in Europe learning French, German, and Italian and improving his Latin and Greek. At Caltech he was deeply influenced by the teaching of Harry Bateman. In particular, a course in partial differential equations "taught me the difference between an ordinary good teacher and a great mathematician, and after that I never cared what grade I got in anything" (Truesdell 1984). He obtained a B.Sc. in mathematics and physics in 1941 and a M.Sc. in mathematics in 1942. In 1943, he completed a Ph.D. in mathematics at Princeton University. For the rest of the decade, the US Navy employed him to do mechanics research.

Professional Career

Truesdell taught at Indiana University from 1950 to 1961, where his students included James Serrin, Jerald LaVerne Ericksen, and Walter Noll. From 1961 until his retirement in 1989, he was professor of rational mechanics at Johns Hopkins University.

Scientific Achievements and Honors

Truesdell and Noll contributed to foundational rational mechanics and thermodynamics, whose aim is to construct a mathematical model for treating continuous mechanical phenomena (Noll 2003). Truesdell was the founder and editor-in-chief of the journals *Archive for Rational Mechanics and Analysis* and *Archive for History of Exact Sciences*, which were unusual in several ways. Following Truesdell's criticisms of awkward style in scientific writing (Truesdell 1984), the journals accepted papers in English, French, German, and Latin.

In addition to his original work in mechanics, Truesdell was a major historian of science and mathematics, editing or coediting six volumes of the collected works of Leonhard Euler.

During his life, Truesdell liked to criticize and thus was criticized by others. He became, e.g., famous for his attacks on Onsager and related scientists. As Ingo Müller (2007) reported: "Truesdell's outspoken partisanship of rational thermodynamics and his flamboyant style fuelled some lively controversies between adherents of TIP (thermodynamics of irreversible processes) and the protagonists of rational thermodynamics, chiefly Truesdell himself. His attacks on Onsagerism were advanced with much satirical verve, that makes them fun to read for those who were not targeted. However, the defenders of TIP tried their best to pay Truesdell back in his own coin." And Ronald Samuel Rivlin (1915–2005)

delighted a worldwide audience with a frequently repeated humorous lecture under the title: "On red herrings and other sundry unidentified fish in modern continuum mechanics".

Truesdell obtained the following awards:

- Euler Medal of the USSR Academy of Sciences, 1958 and 1983;
- Bingham Medal of the Society of Rheology, 1963;
- Birkhoff Prize of the American Mathematical Society and Society for Industrial and Applied Mathematics, 1978;
- Honorary doctorate from the Faculty of Mathematics and Science at Uppsala University, Sweden 1979;
- Theodore von Kármán Medal, 1996

Further Reading

The article is based partly on Ball and James (2002).

Cross-References

- ▸ Bingham, Eugene Cook
- ▸ Euler, Leonhard
- ▸ Noll, Walter
- ▸ History of Plasticity
- ▸ Kármán, Theodore von

References

Ball JM, James RD (2002) The Scientific Life and Influence of Clifford Ambrose Truesdell III. Arch Rat Mech Anal 161:1–26

Müller I (2007) A History of Thermodynamics: the Doctrine of Energy and Entropy. Springer, Heidelberg/New York

Noll W (2003) The Genesis of Truesdell's nonlinear field theories of mechanics. J Elast 70:23–30

Truesdell CA (1984) An idiot's fugitive essays on science: methods, criticism, training, circumstances. Springer, New York

Truesdell's and Zhilin's Approaches: Derivation of Constitutive Equations

Elena A. Ivanova[1,2] and
Elena N. Vilchevskaya[1,2,3]
[1]Department of Theoretical Mechanics, Peter the Great Saint Petersburg Polytechnic University, Saint Petersburg, Russia
[2]Institute for Problems in Mechanical Engineering of Russian Academy of Sciences, Saint Petersburg, Russia
[3]Peter the Great Saint Petersburg Polytechnic University, Saint Petersburg, Russia

Synonyms

Constitutive equations; Coleman-Noll procedure; Entropy production; Reduced equation of energy balance; Second law of thermodynamics; Temperature and entropy introduction

Definition

Truesdell's method of entropy and temperature introduction is based on the second law of thermodynamics in a form of Clausius-Duhem inequality and starts with choosing a subset of independent variables in which constitutive equations are formulated. In Zhilin's approach the independent variables emerge from the reduced equation of energy balance; the second law represents the set of Fourier and Planck inequalities that impose restrictions on the heat flux and dissipative part of stress tensors correspondingly.

Introduction

There are many different ways of entropy introduction and constitutive equation formulation. Truesdell's and Zhilin's approaches are among them. Although these methods show many similarities, they also exhibit a number of

distinctions. In order to provide a comparative analysis of these approaches, an inelastic micropolar continuum is considered. Note that in inelastic processes, the neighboring particles can separate and travel significant distances from one another. It means that it is more preferable to use a spatial description, since, in contrast to the material description, it does not impose strict constraints on the motion of material points.

Balance Equations for the Micropolar Continuum

Within the spatial description, motion is described by focusing on a specific location of space $\mathbf{r}$ through which the matter moves as time passes on. It is assumed that an elementary particle of the matter is a body point that occupies zero volume and has both translational and angular degrees of freedom. The angular velocity field $\boldsymbol{\omega}(\mathbf{r}, t)$ is independent of the linear velocity field $\mathbf{v}(\mathbf{r}, t)$ in a micropolar body, and, in addition to the momentum balance, the balance of angular momentum has to be taken into account. Due to the presence of traction couples or body couples, the stress tensor becomes an antisymmetric one. Further the balance equations for a micropolar continuum within the spatial description are formulated.

The control volume V fixed in the inertial reference system and containing some amount of body points is observed.

The local form of the mass conservation law is

$$\frac{\delta\rho}{\delta t} + \rho\,\nabla\cdot\mathbf{v} = 0. \tag{1}$$

Here $\delta/\delta t$ is the material derivative (see Ivanova et al. 2016), $\rho(\mathbf{r}, t)$ is a mass density, and ∇ denotes the independent on time nabla operator.

For a micropolar medium, it is natural to postulate the existence of the kinetic energy, K, as an additive function of mass:

$$K = \int\limits_V \rho\kappa\,\mathrm{d}V. \tag{2}$$

The specific kinetic energy density κ serves as a potential for the specific linear momentum $\boldsymbol{\mathcal{K}}_1$ and for the dynamic spin $\boldsymbol{\mathcal{L}}$:

$$\kappa = \frac{1}{2}\mathbf{v}\cdot\mathbf{v} + \frac{1}{2}\boldsymbol{\omega}\cdot\mathbf{J}\cdot\boldsymbol{\omega}, \quad \boldsymbol{\mathcal{K}}_1 = \frac{\partial\kappa}{\partial\mathbf{v}} = \mathbf{v},$$
$$\boldsymbol{\mathcal{L}} = \frac{\partial\kappa}{\partial\boldsymbol{\omega}} = \mathbf{J}\cdot\boldsymbol{\omega} \tag{3}$$

where $\mathbf{J}$ is the mass density of the inertia tensor of the body point.

Euler's first dynamical law (the momentum balance equation) for the control volume V bounded by smooth surface Σ is

$$\frac{\mathrm{d}}{\mathrm{d}t}\int\limits_V \rho\mathbf{v}\,\mathrm{d}V = \int\limits_V \rho\mathbf{f}\,\mathrm{d}V + \int\limits_\Sigma (\mathbf{T}_n - \rho\mathbf{n}\cdot\mathbf{vv})\,\mathrm{d}\Sigma, \tag{4}$$

where $\mathrm{d}/\mathrm{d}t$ is the total time derivative, $\mathbf{f}$ is an external force per unit mass, $\mathbf{T}_n$ is a stress vector acting upon an elementary surface, and $\mathbf{n}$ is the surface normal.

The local form of Euler's first dynamical law is

$$\rho\,\frac{\delta}{\delta t}\mathbf{v} = \nabla\cdot\mathbf{T} + \rho\mathbf{f}, \tag{5}$$

where $\mathbf{T}$ is the Cauchy stress tensor ($\mathbf{T}_n = \mathbf{n}\cdot\mathbf{T}$).

Euler's second dynamical law (the equation for balance of the angular momentum) with respect to the origin is

$$\frac{\mathrm{d}}{\mathrm{d}t}\int\limits_V \rho(\mathbf{r}\times\mathbf{v} + \boldsymbol{\mathcal{L}})\,\mathrm{d}V = \int\limits_V \rho\,(\mathbf{r}\times\mathbf{f} + \mathbf{m})\,\mathrm{d}V + \int\limits_\Sigma (\mathbf{r}\times\mathbf{T}_n + \mathbf{M}_n - \rho\mathbf{n}\cdot\mathbf{v}(\mathbf{r}\times\mathbf{v} + \boldsymbol{\mathcal{L}}))\,\mathrm{d}\Sigma, \tag{6}$$

where $\mathbf{m}$ is an external moment per unit mass and $\mathbf{M}_n$ is a moment acting upon a surface with the normal $\mathbf{n}$.

Owing to Euler's first law and the mass balance, the local form for Euler's second dynamical law for a generalized continuum has the form

$$\rho\,\frac{\delta}{\delta t}(\mathbf{J}\cdot\boldsymbol{\omega}) = \nabla\cdot\mathbf{M} + \mathbf{T}_\times + \rho\mathbf{m}, \tag{7}$$

where $\mathbf{M}$ is the couple-stress tensor introduced by analogy with the stress tensor ($\mathbf{M}_n = \mathbf{n} \cdot \mathbf{M}$) and $\mathbf{T}_\times$ is a vector invariant of a second rank tensor. For a dyad it is defined by $(\mathbf{ab})_\times = \mathbf{a} \times \mathbf{b}$.

The first law of thermodynamics (the energy balance equation) states that there is a function of state U (called internal energy) satisfying the equation

$$\frac{\mathrm{d}}{\mathrm{d}t}(K + U) = N + Q, \tag{8}$$

where N is the mechanical power or total rate of working of the mechanical actions upon the matter within the volume and Q is a rate of energy supply to the control volume.

For a continuum the mechanical power N is the rate of working of the assigned forces and couples within the body plus the rate of working of the stress vector and the couple stress on the boundary:

$$N = \int_V \rho \left(\mathbf{f} \cdot \mathbf{v} + \mathbf{m} \cdot \boldsymbol{\omega}\right) \mathrm{d}V + \int_\Sigma \left(\mathbf{T}_n \cdot \mathbf{v} + \mathbf{M}_n \cdot \boldsymbol{\omega}\right) \mathrm{d}\Sigma \tag{9}$$

The energy supply per unit time, $\mathbf{Q}$, is determined by the adding (or removing) of new particles to the control volume and by the rate of nonmechanical transfer of energy from external sources which is expressed in terms of a flux of energy $\mathbf{h}$ through the boundary and a supply of energy q within the volume:

$$Q = \int_V \rho q \, \mathrm{d}V - \int_\Sigma \mathbf{n} \cdot \mathbf{h} \, \mathrm{d}\Sigma - \int_\Sigma \mathbf{n} \cdot \mathbf{v} (\rho\kappa + \rho u) \mathrm{d}\Sigma. \tag{10}$$

Being an additive set function, the internal energy may be expressed in terms of a specific internal energy. Generally, in chemical thermodynamics or studies involving structure transformations, the internal energy is an additive function of the number of particles (e.g., Prigogine 1955; Müller and Ruggeri 1998; Zhilin 2003), https://meteor.springer.com/chapter/contribute.jsf?id=108543. However, if the number of particles is not changing, then the density of particle distribution is proportional to the mass density, and the internal energy becomes an additive function of the mass as it is usually assumed in most continuum mechanics applications (see, e.g., Truesdell and Toupin 1960; Truesdell 1965; Müller and Müller 2009). Thus it is accepted that

$$U = \int_V \rho u \, \mathrm{d}V, \tag{11}$$

where u is the specific internal energy per unit mass.

Taking into account Gauss' theorem, balance laws (1), (5), and (7), the local form of energy balance equation can be written as

$$\rho \frac{\delta u}{\delta t} = N_{ex} + Q_{ex}, \tag{12}$$

$$N_{ex} = \mathbf{T}^T \cdot\cdot \left(\nabla \mathbf{v} + \mathbf{I} \times \boldsymbol{\omega}\right) + \mathbf{M}^T \cdot\cdot \nabla \boldsymbol{\omega}, \qquad Q_{ex} = -\nabla \cdot \mathbf{h} + \rho q,$$

where $\mathbf{I}$ is a unit tensor and the double dot product is defined by $(\mathbf{ab}) \cdot\cdot (\mathbf{cd}) = (\mathbf{b} \cdot \mathbf{c})(\mathbf{a} \cdot \mathbf{d})$.

To proceed further it is necessary to introduce the notions of temperature and entropy, obtain the heat conduction equation, and perform the so-called closure which equalizes the number of variables with the number of equations. The latter is done in the form of constitu-

tive relations which limit the applicability of the model.

Temperature and Entropy Introduction

Truesdell's Approach

In Truesdell and Toupin (1960), the temperature and entropy introduction starts with choosing parameters $\boldsymbol{\upsilon} = \upsilon_1 \dots \upsilon_N$ which are regarded as influencing the internal energy. The assignment of these parameters is made a priori; their totality is the thermodynamic substate. Then the basic assumption of thermodynamics is the substate plus a single scalar parameter suffices to determine the internal energy. Thus

$$u = u(\boldsymbol{\upsilon}, \eta). \tag{13}$$

The parameter η is called the specific entropy. Here it is assumed that the entropy, like the internal energy, is a continuous function of mass. Thus the role of entropy is that of a specifying parameter.

The temperature θ and the thermodynamic tensions τ_α are defined from (13) by

$$\theta = \frac{\partial u}{\partial \eta}, \qquad \tau_\alpha = \frac{\partial u}{\partial \upsilon_\alpha}. \tag{14}$$

Thus the temperature measures the sensitivity of energy to changes in entropy and the tensions to changes in the corresponding parameters.

As a result the balance of the internal energy can be written in the form

$$\begin{aligned} \rho \frac{\delta u}{\delta t} &= N_i + Q_i, \\ N_i &= \rho \sum_{\alpha=1}^{N} \tau_\alpha \frac{\delta \upsilon_\alpha}{\delta t}, \\ Q_i &= \rho\theta \frac{\delta \eta}{\delta t}. \end{aligned} \tag{15}$$

Index "i" stays for internal. Elimination of $\delta u/\delta t$ between (15) and (12) yields

$$N_{ex} - N_i + Q_{ex} - Q_i = 0, \tag{16}$$

an equation stating that the difference of external and internal working cancels the difference of external and internal supplies of nonmechanical energy.

Taking into account the definition of the internal nonmechanical supply of energy $(15)_3$, Eq. (16) can be rewritten in a form of equation for production of specific entropy:

$$\rho\theta \frac{\delta \eta}{\delta t} = N_{ex} - N_i + Q_{ex} \tag{17}$$

The work done by the thermodynamic tensions is said to be recoverable, so only the dissipative parts of the stress and moment tensors contribute to the entropy. The further transformation of the (17) depends on the choice of the parameters $\boldsymbol{\upsilon}$.

Zhilin's Approach

In some way Zhilin's approach is similar to the one before. It results in obtaining the reduced equation of the energy balance and starts with Eq. (12). The right-hand side of this equation contains the power of forces and moments. A part of this power leads to the change of the internal energy. The remaining part of the power is partly conserved within the body as heat and is partly emanated into the external medium. In order to separate these parts, the following decomposition is introduced:

$$\begin{aligned} \mathbf{T} &= -(p_e + p_f)\mathbf{I} + \boldsymbol{\tau}_e + \boldsymbol{\tau}_f, \\ \mathbf{M} &= \mathbf{M}_e + \mathbf{M}_f, \\ \operatorname{tr} \boldsymbol{\tau}_e &= \operatorname{tr} \boldsymbol{\tau}_f = 0, \end{aligned} \tag{18}$$

where the quantities with the index "e" are independent of rates. These quantities always affect the internal energy. The quantities with the index "f" account for an internal friction. These quantities may have an influence on the internal energy but, as we shall see, only by means of additional parameters like entropy. In view of (18), the energy balance equation has the form

$$\rho\frac{\delta u}{\delta t} = -p_e\nabla\cdot\mathbf{v} + \boldsymbol{\tau}_e^T \cdot\cdot (\nabla\mathbf{v} + \mathbf{I}\times\boldsymbol{\omega}) + \mathbf{M}_e^T \cdot\cdot \nabla\boldsymbol{\omega} + \rho q - \nabla\cdot\mathbf{h} - p_f\nabla\cdot\mathbf{v} + \boldsymbol{\tau}_f^T \cdot\cdot (\nabla\mathbf{v} + \mathbf{I}\times\boldsymbol{\omega}) + \mathbf{M}_f^T \cdot\cdot \nabla\boldsymbol{\omega}. \tag{19}$$

Note that the left-hand side of this equation consists of a material differential. Hence the right-hand side should also have this property and consist of terms showing material differentials of the state variables the internal energy density depends upon. Some of these terms are straightforward to obtain formally, as follows. The part of the power of forces and moments, which does not depend on rates, can be represented as

$$\boldsymbol{\tau}_e^T \cdot\cdot (\nabla\mathbf{v} + \mathbf{I}\times\boldsymbol{\omega}) + \mathbf{M}_e^T \cdot\cdot \nabla\boldsymbol{\omega} = -\left(\mathbf{g}^{-1}\cdot\boldsymbol{\tau}_e^T + \mathbf{g}^{-1}\cdot\boldsymbol{\Gamma}\cdot\mathbf{M}_e^T\right) \cdot\cdot \frac{\delta\mathbf{g}}{\delta t} + \mathbf{M}_e^T \cdot\cdot \frac{\delta\boldsymbol{\Gamma}}{\delta t} + \frac{1}{2}\left[(\mathbf{M}_e^T\cdot\boldsymbol{\Gamma} - \boldsymbol{\tau}_e)_\times \times \mathbf{Q}\right]^T \cdot\cdot \frac{\delta\mathbf{Q}}{\delta t}. \tag{20}$$

Here the strain measure $\boldsymbol{\Gamma}$ and the spatial deformation gradient $\mathbf{g}$ are determined by

$$\nabla\mathbf{Q} = \boldsymbol{\Gamma}\times\mathbf{Q}, \qquad \mathbf{g} = \mathbf{I} - \nabla\mathbf{u} \tag{21}$$

where $\mathbf{u}$ is a displacement field and $\mathbf{Q}$ is a rotational tensor. In view of Eqs. (1) and (19), the energy balance equation takes the form

$$\rho\frac{\delta u}{\delta t} = \frac{p_e}{\rho}\frac{\delta\rho}{\delta t} - \left(\mathbf{g}^{-1}\cdot\boldsymbol{\tau}_e^T + \mathbf{g}^{-1}\cdot\boldsymbol{\Gamma}\cdot\mathbf{M}_e^T\right) \cdot\cdot \frac{\delta\mathbf{g}}{\delta t} + \mathbf{M}_e^T \cdot\cdot \frac{\delta\boldsymbol{\Gamma}}{\delta t} + \frac{1}{2}\left[(\mathbf{M}_e^T\cdot\boldsymbol{\Gamma} - \boldsymbol{\tau}_e)_\times \times \mathbf{Q}\right]^T \cdot\cdot \frac{\delta\mathbf{Q}}{\delta t} + \rho q - \nabla\cdot\mathbf{h} - p_f\nabla\cdot\mathbf{v} + \boldsymbol{\tau}_f^T \cdot\cdot (\nabla\mathbf{v} + \mathbf{I}\times\boldsymbol{\omega}) + \mathbf{M}_f^T \cdot\cdot \nabla\boldsymbol{\omega}. \tag{22}$$

Obviously the underlined terms do not show the desired form of material derivatives yet, a form which was referred to as reduced equation of the energy balance by Zhilin. In order to reach this state, the concepts of temperature and entropy have to be defined. In Zhilin (2001, 2002, 2003, 2004, 2006, 2012) and Altenbach et al. (2003), the temperature $\theta(\mathbf{r}, t)$ and entropy $\eta(\mathbf{r}, t)$ are introduced by the following equation, which in fact formally coincides with (17) for a certain choice of the thermodynamical substate:

$$\rho\theta\frac{\delta\eta}{\delta t} = \rho q - \nabla\cdot\mathbf{h} - p_f\nabla\cdot\mathbf{v} + \boldsymbol{\tau}_f^T \cdot\cdot (\nabla\mathbf{v} + \mathbf{I}\times\boldsymbol{\omega}) + \mathbf{M}_f^T \cdot\cdot \nabla\boldsymbol{\omega}. \tag{23}$$

Here the (theoretical) temperature θ is considered to be some characteristic of the medium, which is assigned as an experimental temperature through a thermometer. Moreover, the specific entropy density η is introduced as a quantity conjugate to theoretical temperature. The function η has to

be defined by means of constitutive equations in such a manner that the theoretical and experimental temperatures coincide. From this it follows that entropy itself is not the meaning of an objective (measurable) quantity. If the meaning of temperature is changed, then the meaning of entropy will change as well. Also note that this definition of temperature and entropy is consistent with the introduction of these quantities for equilibrium processes even though Eq. (23), being the heat conduction equation, describes nonequilibrium processes.

Because of (23) the reduced energy balance equation now takes the form

$$\rho\frac{\delta u}{\delta t}=\frac{p_e}{\rho}\frac{\delta\rho}{\delta t}-\left(\mathbf{g}^{-1}\cdot\boldsymbol{\tau}_e^T+\mathbf{g}^{-1}\cdot\boldsymbol{\Gamma}\cdot\mathbf{M}_e^T\right)\cdot\cdot\,\frac{\delta\mathbf{g}}{\delta t}+\mathbf{M}_e^T\cdot\cdot\,\frac{\delta\boldsymbol{\Gamma}}{\delta t}+\frac{1}{2}\left[(\mathbf{M}_e^T\cdot\boldsymbol{\Gamma}-\boldsymbol{\tau}_e)_\times\times\mathbf{Q}\right]^T\cdot\cdot\,\frac{\delta\mathbf{Q}}{\delta t}+\rho\theta\,\frac{\delta\eta}{\delta t} \tag{24}$$

Thus the internal energy is a function of the following independent arguments:

$$u=u(\rho,\eta,\mathbf{g},\boldsymbol{\Gamma},\mathbf{Q}). \tag{25}$$

Note that the definition of temperature and entropy (23) is also a definition of the internal energy since it determines on what variables the internal energy depends. Different variants of the introduction of variables within Zhilin's approach can be found in https://meteor.springer.com/chapter/contribute.jsf?id=108543. As a result, the constitutive equations for the elastic part of the stress and couple-stress tensors and the temperature can be obtained from (24) as

$$\begin{aligned}p_e&=\rho^2\frac{\partial u}{\partial\rho},\\ \boldsymbol{\tau}_e&=-\rho\frac{\partial u}{\partial\mathbf{g}}\cdot\mathbf{g}^T-\rho\frac{\partial u}{\partial\boldsymbol{\Gamma}}\cdot\boldsymbol{\Gamma}^T,\\ \mathbf{M}_e&=\rho\frac{\partial u}{\partial\boldsymbol{\Gamma}},\\ \theta&=\frac{\partial u}{\partial\eta}\end{aligned} \tag{26}$$

with the following constraints for the internal energy:

$$\left(\frac{\partial u}{\partial\mathbf{g}}\right)^T\cdot\cdot\,\mathbf{g}+\left(\frac{\partial u}{\partial\boldsymbol{\Gamma}}\right)^T\cdot\cdot\,\boldsymbol{\Gamma}=0, \tag{27}$$

$$\left(\frac{\partial u}{\partial\mathbf{g}}\right)^T\cdot\cdot\,(\mathbf{A}\cdot\mathbf{g})+\left(\frac{\partial u}{\partial\mathbf{Q}}\right)^T\cdot\cdot\,(\mathbf{A}\cdot\mathbf{Q})+\left(\frac{\partial u}{\partial\boldsymbol{\Gamma}}\right)^T\cdot\cdot\,(\mathbf{A}\cdot\boldsymbol{\Gamma}-\boldsymbol{\Gamma}\cdot\mathbf{A})=0,$$

where $\mathbf{A}$ is an arbitrary antisymmetric tensor. These constraints follow from the fact that the rotational tensor has to be related to the angular velocity by means of the so-called Poisson relation:

$$\frac{\delta\mathbf{Q}}{\delta t}=\boldsymbol{\omega}\times\mathbf{Q} \tag{28}$$

In conclusion of this section, note that the introduction of temperature and entropy by means of Eq. (23) is always possible from a mathematical point of view. However, it can happen that the theory based on (23) fails to describe a particular experimental data. It means that the introduction of one entropy is not enough and some other variables have to be introduced.

Second Law of Thermodynamics

In general there are almost as many "second laws" as there are different thermodynamics.

Here only Truesdell's approach resulting in the Clausius-Duhem inequality and Zhilin's point of view are considered.

Derivation of the Clausius-Duhem inequality starts with introduction of the internal dissipation $\tilde{\delta}$, which is defined as being the amount by which the increase of entropy multiplied by the temperature exceeds the local rate of the energy supply (see Truesdell 1984):

$$\tilde{\delta} = \theta \frac{\delta \eta}{\delta t} - \frac{1}{\rho} \left(-\nabla \cdot \mathbf{h} + \rho q \right). \tag{29}$$

The equation of energy balance (12) permits to interpret (29) also as the amount by which the increase of entropy times temperature exceeds the increase of energy not produced by working or taking into account (16) as the difference of external and internal working

$$\rho \tilde{\delta} = N_e - N_i. \tag{30}$$

It is said that the internal dissipation cannot be negative:

$$\tilde{\delta} \geq 0. \tag{31}$$

It is called the Planck inequality and it is not considered as an axiom.

In the classical theory of Fourier, heat conduction is associated with differences of temperature. Heat is said to flow from hot to cold, and the classical a priori inequality, which is also called the Fourier inequality, is

$$\mathbf{h} \cdot \nabla \theta \leq 0. \tag{32}$$

If both the Planck and the Fourier inequalities hold, then

$$\rho \tilde{\delta} - \frac{1}{\theta} \mathbf{h} \cdot \nabla \theta \geq 0. \tag{33}$$

That by (29) is equivalent to

$$\rho \frac{\delta \eta}{\delta t} + \nabla \cdot \left(\frac{\mathbf{h}}{\theta} \right) - \frac{\rho q}{\theta} \geq 0 \tag{34}$$

Integrating this inequality over the control volume yields to the condition

$$\int_V \rho \frac{\delta \eta}{\delta t} \, dV \geq - \int_\Sigma \mathbf{n} \cdot \left(\frac{\mathbf{h}}{\theta} \right) d\Sigma + \int_V \frac{\rho q}{\theta} \, dV, \tag{35}$$

which is called in Truesdell (1984) the Clausius-Duhem inequality. The derivation of the Clausius-Duhem inequality makes it clear that it is equivalent to the local inequality (33) and, conversely, the Planck inequality and the Fourier inequality do not follow from it in general. That is, heat can flow from cold to hot, if the process is accompanied with a significant internal dissipation.

Then the energy balance Eq. (12) can be used to eliminate the quantities associated with temperature and heat from (34). It leads to the so-called reduced dissipation inequality:

$$\rho\theta \frac{\delta \eta}{\delta t} - \rho \frac{\delta u}{\delta t} + \mathbf{T}^T \cdot\cdot (\nabla \mathbf{v} + \mathbf{I} \times \boldsymbol{\omega}) + \mathbf{M}^T \cdot\cdot \nabla \boldsymbol{\omega} - \frac{\mathbf{h} \cdot \nabla \theta}{\theta} \geq 0. \tag{36}$$

Using the decomposition

$$\mathbf{T} = -p\mathbf{I} + \boldsymbol{\tau}, \quad \operatorname{tr} \boldsymbol{\tau} = 0 \tag{37}$$

together with Eq. (19), the dissipation inequality (36) reduces to the form

$$\rho\theta \frac{\delta \eta}{\delta t} - \rho \frac{\delta u}{\delta t} + \frac{p}{\rho} \frac{\delta \rho}{\delta t} - \left(\mathbf{g}^{-1} \cdot \boldsymbol{\tau}^T + \mathbf{g}^{-1} \cdot \boldsymbol{\Gamma} \cdot \mathbf{M}^T \right) \cdot\cdot \frac{\delta \mathbf{g}}{\delta t} + \mathbf{M}^T \cdot\cdot \frac{\delta \boldsymbol{\Gamma}}{\delta t} + \frac{1}{2} \left[(\mathbf{M}^T \cdot \boldsymbol{\Gamma} - \boldsymbol{\tau})_\times \times \mathbf{Q} \right]^T \cdot\cdot \frac{\delta \mathbf{Q}}{\delta t} - \frac{\mathbf{h} \cdot \nabla \theta}{\theta} \geq 0, \tag{38}$$

where the strain measures are given by Eq. (21).

If the chosen thermodynamical substate coincides with the independent variables determined by (25), inserting (25) into (38) and making use of the chain rule for $\delta u/\delta t$ yields

$$\rho\left(\theta-\frac{\delta u}{\delta \eta}\right)\frac{\delta \eta}{\delta t}+\rho\left(\frac{p}{\rho^2}-\frac{\delta u}{\delta \rho}\right)\frac{\delta \rho}{\delta \rho} \tag{39}$$
$$-\left(\mathbf{g}^{-1}\cdot\boldsymbol{\tau}^T+\mathbf{g}^{-1}\cdot\boldsymbol{\Gamma}\cdot\mathbf{M}^T+\rho\left(\frac{\delta u}{\delta \mathbf{g}}\right)^T\right)\cdot\cdot\,\frac{\delta \mathbf{g}}{\delta t}+\left(\mathbf{M}^T-\rho\left(\frac{\delta u}{\delta \boldsymbol{\Gamma}}\right)^T\right)\cdot\cdot\,\frac{\delta \boldsymbol{\Gamma}}{\delta t}$$
$$+\left(\frac{1}{2}\left[(\mathbf{M}^T\cdot\boldsymbol{\Gamma}-\boldsymbol{\tau})_\times\times\mathbf{Q}\right]^T-\rho\left(\frac{\delta u}{\delta \mathbf{Q}}\right)^T\right)\cdot\cdot\,\frac{\delta \mathbf{Q}}{\delta t}-\frac{\mathbf{h}\cdot\nabla\theta}{\theta}\geq 0.$$

Equation (39) must hold for every admissible thermodynamic process. In a case when the factor in front of the rate of the independent variable does not depend on this rate (e.g., the thermoelastic material), then it is necessary and sufficient that the constitutive equations for the elastic part of the stress tensors and the temperature fulfill (26) and $\mathbf{h}$ satisfies the thermal conduction inequality (32).

The internal dissipation of a thermoelastic material is always zero. Thus (29) becomes the heat conduction equation:

$$\rho\theta\,\frac{\delta \eta}{\delta t}=\rho q-\nabla\cdot\mathbf{h}, \tag{40}$$

which together with (26) and a constitutive equation for the heat flux, say in a form of linear Fourier law (see Fourier 1822), forms a closed system of equations.

If a medium possesses inelastic properties, then the reduced dissipation inequality (39) does not allow to obtain the constitutive equations in the formal way without additional assumptions even for the elastic parts of the stress tensors and only makes it possible to eliminate those constitutive equations which contradict the second law of thermodynamics in the form of the Clausius-Duhem inequality. Moreover, in that case, the form of the heat conduction equation remains an open question.

Zhilin's formulation of the second law of thermodynamics represents the set of the Fourier and Planck inequalities (see Zhilin 2003, 2012), which in the problem under consideration have the forms

$$\mathbf{h}\cdot\nabla\theta\leq 0,\quad -p_f\nabla\cdot\mathbf{v}+\boldsymbol{\tau}_f^T\cdot\cdot\,(\nabla\mathbf{v}+\mathbf{I}\times\boldsymbol{\omega})$$
$$+\mathbf{M}_f^T\cdot\cdot\,\nabla\boldsymbol{\omega}\geq 0, \tag{41}$$

The first one imposes a restriction on the constitutive equation for the heat flux, and the second one is associated with the statement that the dissipative forces and moments cannot perform positive work and imposes a restriction of the constitutive equations for the dissipative components of stress tensors. Note that within Zhilin's approach, the constitutive relations for the elastic parts of stress tensors (26) are obtained independently of the second law of thermodynamics. In addition, (23) is the heat conduction equation independently of the medium's rheology. Thus, in order to have a closed system of equations, constitutive equations for the heat flux and dissipative components of stress tensor have to be proposed.

Constitutive Equations for Inelastic Components of the Stress Tensors

According to Altenbach et al. (2003) and Zhilin (2001, 2002, 2003, 2004, 2006, 2012) for micropolar media, the components of stress tensors connected with inelastic behavior and internal dissipation can be related to antisymmetric ten-

sors. Some examples of constitutive equations for the dissipative stress tensor components are given below.

To describe the inelastic behavior of solids, for example, plasticity and dynamics of granular media, Zhilin (2001, 2002, 2003, 2004, 2006, 2012) proposed the following constitutive equations:

$$\begin{aligned} p_f &= 0, \\ \boldsymbol{\tau}_f &= \mathbf{I} \times \mathbf{t}, \\ \mathbf{M}_f &= \mathbf{0}, \end{aligned} \tag{42}$$

where vector $\mathbf{t}$ is determined by analogy with the Coulomb dry friction and takes the form

$$\mathbf{t} = k\,|\mathbf{n}\cdot\boldsymbol{\tau}_e\cdot\mathbf{n}|\,\sigma(\mathbf{n}\cdot\boldsymbol{\tau}_e\cdot\mathbf{n})\,\frac{2\boldsymbol{\omega}-\nabla\times\mathbf{v}}{|2\boldsymbol{\omega}-\nabla\times\mathbf{v}|},$$
$$\boldsymbol{\omega} \neq \frac{1}{2}\,\nabla\times\mathbf{v}. \tag{43}$$

Here $k > 0$ is the parameter of friction, and the function $\sigma(\mathbf{n}\cdot\boldsymbol{\tau}_e\cdot\mathbf{n})$ is

$$\sigma(\mathbf{n}\cdot\boldsymbol{\tau}_e\cdot\mathbf{n}) = \begin{cases} 1, & \mathbf{n}\cdot\boldsymbol{\tau}_e\cdot\mathbf{n} < 0, \\ 0, & \mathbf{n}\cdot\boldsymbol{\tau}_e\cdot\mathbf{n} \geq 0. \end{cases} \tag{44}$$

The unit vector $\mathbf{n}$ in Eq. (43) depends on $\boldsymbol{\tau}_e$ and is determined by the conditions

$$\begin{aligned} &\mathbf{n}\cdot\boldsymbol{\tau}_e\cdot\mathbf{m} = \max, \\ \forall\ \mathbf{n},\mathbf{m}: \quad &|\mathbf{n}| = |\mathbf{m}| = 1, \\ &\mathbf{n}\cdot\mathbf{m} = 0. \end{aligned} \tag{45}$$

The uniqueness of the solution of (45) was proved in Zhilin (2001, 2012).

It is easy to see that the constitutive Eqs. (42) and (43) satisfy the second law of thermodynamics in the form of Eq. $(41)_2$. Indeed,

$$\boldsymbol{\tau}_f^T\cdot\cdot\,(\nabla\mathbf{v}+\mathbf{I}\times\boldsymbol{\omega}) \equiv 2\mathbf{t}\cdot\left(\boldsymbol{\omega}-\frac{1}{2}\nabla\times\mathbf{v}\right). \tag{46}$$

Hence, in view of Eqs. (43) and (44) and the fact that $k > 0$ it follows:

$$\boldsymbol{\tau}_f^T\cdot\cdot\,(\nabla\mathbf{v}+\mathbf{I}\times\boldsymbol{\omega}) = k\,|\mathbf{n}\cdot\boldsymbol{\tau}_e\cdot\mathbf{n}|$$
$$\sigma(\mathbf{n}\cdot\boldsymbol{\tau}_e\cdot\mathbf{n})\ |2\boldsymbol{\omega}-\nabla\times\mathbf{v}| \geq 0. \tag{47}$$

All aforesaid relates to sliding. In the absence of sliding, i.e., if the condition $2\boldsymbol{\omega} = \nabla\times\mathbf{v}$ holds, the vector $\mathbf{t}$ is found from the equation of the angular momentum balance. Note that if there is no sliding, the friction force is conservative and there is no energy dissipation. In this case the constitutive Eqs. (42) also satisfy the second law of thermodynamics in the form of Eq. $(41)_2$.

Also Zhilin (2003, 2012) noted that in many cases Coulomb dry friction can be replaced by viscous friction, i.e., instead of Eq. (43), the constitutive equation

$$\mathbf{t} = k\left(\boldsymbol{\omega}-\frac{1}{2}\nabla\times\mathbf{v}\right), \tag{48}$$

can be used. Here $k > 0$ is the coefficient of viscous friction.

To describe the behavior of a two-component micropolar medium consisting of fluid particles (liquid constituent) and immersed particles-fibers (solid-liquid constituent), Zhilin (2006, 2012) and Altenbach et al. (2003) proposed the constitutive equations for inelastic components of stress tensors containing both symmetric and antisymmetric parts.

The constitutive equations for the fluid component are

$$p'_f = 0, \qquad \boldsymbol{\tau}'_f = 2\boldsymbol{\mu}\cdot\cdot\,\mathbf{D}+\mathbf{t}'\times\mathbf{I}, \qquad \mathbf{M}'_f = \mathbf{0}, \tag{49}$$

where

$$\mathbf{D} = \frac{1}{2}\left(\nabla\mathbf{v}_1+\nabla\mathbf{v}_1^T-\frac{2}{3}(\nabla\cdot\mathbf{v}_1)\mathbf{I}\right). \tag{50}$$

Vector $\mathbf{t}'$ characterizes the viscous friction between the solid particles and the fluid and depends on the particle distribution density of the solid-liquid component n_2:

$$\mathbf{t}' = n_2\boldsymbol{\mu}_1\cdot\left(\boldsymbol{\omega}-\frac{1}{2}\nabla\times\mathbf{v}_1\right). \tag{51}$$

The first term in Eq. (49) is a standard term for a viscous fluid; the second term characterizes friction due to the presence of a solid-liquid component.

The constitutive equations for the viscous stresses in the solid-liquid component are

$$p''_f = 0, \qquad \boldsymbol{\tau}''_f = \mathbf{t}'' \times \mathbf{I}, \qquad \mathbf{M}''_f = \mathbf{m}'' \times \mathbf{I}, \tag{52}$$

where vectors $\mathbf{t}''$ and $\mathbf{m}''$ are

$$\mathbf{t}'' = n_2 \boldsymbol{\mu}_2 \cdot \left(\boldsymbol{\omega} - \frac{1}{2} \nabla \times \mathbf{v}_2 \right),$$
$$\mathbf{m} = -n_2 \mu_3 \left(\nabla \times \boldsymbol{\omega} \right). \tag{53}$$

The tensors of viscous friction coefficients must satisfy the restrictions

$$\forall\, \mathbf{a}, \mathbf{b}, \mathbf{c} \text{ with } \mathbf{c} = -\mathbf{c}^T : \quad \mathbf{a} \cdot\cdot\, \boldsymbol{\mu} \cdot\cdot\, \mathbf{a} \geq 0,$$
$$\mathbf{b} \cdot \boldsymbol{\mu}_1 \cdot \mathbf{b} \geq 0, \quad \mu_3 \geq 0, \quad \mathbf{a} \cdot\cdot\, \boldsymbol{\mu} = \boldsymbol{\mu} \cdot\cdot\, \mathbf{a},$$
$$\mathbf{c} \cdot\cdot\, \boldsymbol{\mu} = \mathbf{0}, \quad \mathbf{I} \cdot\cdot\, \boldsymbol{\mu} = \mathbf{0}, \quad \mathbf{b} \cdot \boldsymbol{\mu}_1 = \boldsymbol{\mu}_1 \cdot \mathbf{b}. \tag{54}$$

Besides, if the particle density n_2 vanishes, then the vector $\mathbf{t}'$ must be zero.

Thus in accordance with Zhilin's constitutive equations, the transfer of energy into heat is associated with the motion by rotational degrees of freedom, i.e., by degrees of freedom with inelastic interactions.

Summary and Comparison

In Truesdell's approach all state variables need to be defined a priori, and entropy, introduced as a primitive quantity, is one of them. This set of state variables is required to determine the internal energy, which then serves as a potential for temperature.

In Zhilin's approach the state variables emerge from rewriting the energy balance such that material derivatives of them appear successively. To do that quantities are additively decomposed into rate-independent and rate-dependent ones. Rewriting the energy balance in terms of material derivatives is possible up to a remaining part, which is then defined as the product of (theoretical) temperature and material derivative of entropy. By imposing the constraint that an experimentally measured temperature has to agree with the theoretical one, entropy must be redefined accordingly.

As far as the second law of thermodynamics is concerned, Zhilin's arguments are based on two, namely, the Fourier and the Planck inequality. Both can be combined to result in the Clausius-Duhem inequality, which forms the basis for Truesdell's constraint arguments. In general, however, the former two do not follow from the latter one. At the same time, Zhilin does not consider the second law of thermodynamics as a fundamental law. The inequalities (41) are based on experimental observations and practical experiences on a macro level and can be violated, say, on a micro level or for nonlocal materials.

In Zhilin's approach, these two inequalities (the second law) impose restrictions on the heat flux and the dissipative part of stress tensors, while the constitutive equations for the rate-independent parts of the stress tensors follow from the material derivative character of the internal energy. Truesdell believes that Clausius-Duhem inequality is the correct mathematical form of the second law of thermodynamics. The later theory of Coleman and Noll states that the constitutive equations, which characterize the material properties of continuous media, must be assigned in such a way that the Clausius-Duhem inequality holds for all thermodynamic processes. Thus, the Clausius-Duhem inequality becomes a restriction on all constitutive relations.

Cross-References

- Coleman-Noll Procedure for Classical and Generalized Continuum Theories
- Cosserat Media
- Truesdell, Clifford Ambrose III
- Zhilin, Pavel Andreevich
- Zhilin's Method and Its Modifications

References

Altenbach H, Naumenko K, Zhilin P (2003) A micropolar theory for binary media with application to phase-transitional flow of fiber suspensions. Contin Mech Thermodyn 15(6):539–570

Fourier J (1822) Thèorie analytique de la chaleur. Firmin Didot Père et Fils, Paris

Ivanova E, Vilchevskaya E, Müller W (2016) Time derivatives in material and spatial description – what are the differences and why do they concern us? In: Naumenko K, Aßmus M (eds) Advanced methods of continuum mechanics for materials and structures, vol 20. Springer, Singapore

Müller I, Müller W (2009) Fundamentals of thermodynamics and applications: with historical annotations and many citations from Avogadro to Zermelo. Springer, Berlin

Müller I, Ruggeri T (1998) Rational extended thermodynamics. Springer, New York

Prigogine I (1955) Introduction to thermodynamics of irreversible processes. Charles C. Thomas Publishers, Sprindfield

Truesdell C (1965) The elements of continuum mechanics. Springer, New York

Truesdell C (1984) Rational thermodynamics, 2nd enlarged edn. Springer, New York

Truesdell C, Toupin R (1960) The classical field theories. In: Flügge S (ed) Encyclopedia of phycics, vol III/1. Springer, Heidelberg

Zhilin PA (2001, in Russian) Basic equations of the theory of non-elastic media. In: Proceedings of the XXVIII summer school "Actual Problems in Mechanics", pp 14–18

Zhilin PA (2002) Phase transitions and general theory of elasto-plastic bodies. In: Proceedings of XXIX summer school – conference "Advanced Problems in Mechanics", pp 36–48

Zhilin P (2003, in Russian) Mathematical theory of non-elastic media. Uspehi mechaniki (Advances in mechanics) 2(4):3–36

Zhilin PA (2004) On the general theory of non-elastic media. In: Mechanics of materials and strength of constructions. Proceedings of St. Petersburg State Polytechnical University, vol 489, pp 8–27

Zhilin PA (2006) Advanced problems in mechanics, vol 2. Institute for Problems in Mechanical Engineering, St. Petersburg

Zhilin PA (2012, in Russian) Racional'naya mekhanika sploshnykh sred (Rational Continuum Mecanics). Politechnic University Publishing House, St. Petersburg

Two Dimensional Structural Models

▸ Axiomatic/Asymptotic Method and Best Theory Diagram for Composite Plates and Shells

Two Dimensional Elastic Materials with Microstructure

▸ Negative Poissons Ratio in Plane Elasticity